INFORMATION TO USERS

This manuscript has been reproduced from the microfilm master. UMI

films the text directly from the original or copy submitted. Thus, some

thesis and dissertation copies are in typewriter face, while others may be

from any type of computer printer.

The quality of this reproduction is dependent upon the quality of the

copy submitted. Broken or indistinct print, colored or poor quality

illustrations and photographs, print bleedthrough, substandard margins,

and improper alignment can adversely affect reproduction.

In the unlikely event that the author did not send UMI a complete

manuscript and there are missing pages, these will be noted. Also, if

unauthorized copyright material had to be removed, a note will indicate

the deletion.

Oversize materials (e.g., maps, drawings, charts) are reproduced by

sectioning the original, beginning at the upper left-hand corner and

continuing from left to right in equal sections with small overlaps. Each

original is also photographed in one exposure and is included in reduced

form at the back of the book.

Photographs included in the original manuscript have been reproduced

xerographically in this copy. Higher quality 6" x 9" black and white

photographic prints are available for any photographs or illustrations

appearing in this copy for an additional charge. Contact UMI directly to

order.

UMI

A Bell & Howell Information Company
300 North Zeeb Road, Ann Arbor MI 48106-1346 USA
313/761-4700 800/521-0600

NOTE TO USERS

The original manuscript recieved by UMI contains pages with indistinct and slanted print exceeding margin guidelines. Pages were microfilmed as received.

This reproduction is the best copy available

IIMI

PHARMACOKINETIC MODELING OF POLLUTANT FLUXES BY LIMNOPLANKTON

YUAN HUA WEN

Department of Biology

McGill University, Montreal

A thesis submitted to the Faculty of Graduate Studies and Research in partial fulfilment of the requirements for the degree of Doctor of Philosophy.



National Library of Canada

Acquisitions and Bibliographic Services

395 Wellington Street Ottawa ON K1A 0N4 Canada Bibliothèque nationale du Canada

Acquisitions et services bibliographiques

395, rue Wellington Ottawa ON K1A 0N4 Canada

Your file Votre référence

Our file Notre référence

The author has granted a nonexclusive licence allowing the National Library of Canada to reproduce, loan, distribute or sell copies of this thesis in microform, paper or electronic formats.

The author retains ownership of the copyright in this thesis. Neither the thesis nor substantial extracts from it may be printed or otherwise reproduced without the author's permission.

L'auteur a accordé une licence non exclusive permettant à la Bibliothèque nationale du Canada de reproduire, prêter, distribuer ou vendre des copies de cette thèse sous la forme de microfiche/film, de reproduction sur papier ou sur format électronique.

L'auteur conserve la propriété du droit d'auteur qui protège cette thèse. Ni la thèse ni des extraits substantiels de celle-ci ne doivent être imprimés ou autrement reproduits sans son autorisation.

0-612-30415-9



DEDICATION

I dedicate this thesis to the memory of Dr. Robert Henry Peters, a scientist, an educator and a philosopher. He taught me what is good science and how to do good science. His dedication, creativity and intellect have always been my inspiration. His influence on my life is more than any words can express. I will remember you forever, Rob.

Suggested short title: Modeling Pollutant Fluxes.

ABSTRACT

The objective of this thesis was to construct general models to predict pollutant fluxes in limnoplankton by incorporating characteristics of the organism and the structures of the chemical. A two-compartmental pharmacokinetic model was used to quantify the pollutant uptake, depuration and intercompartmental exchanges. The model pollutants were phosphorus and 22 organic chemicals.

The rate constants of phosphorus uptake, excretion and intercompartmental changes by algae and cladocerans decreased with cell volume or body size raised to a power close to -0.25, except the intercompartmental exchanges for cladocerans which showed more negative slopes. In contrast, uptake, excretion and internal exchange rates per individual increased with cell size or body weight to a power similar to 0.75 with a similar exception for the cladoceran intercompartmental exchanges, which had slopes < 0.75.

Bioconcentration factors, rate constants and flux rates of uptake and intercompartmental exchange from metabolic pool to structural pool of 22 ¹⁴C-labelled organic toxicants by <u>Chlorella pyrenoidosa</u> and <u>Daphnia magna</u> were positively correlated with the octanol/water partition coefficient, molecular weight, parachor, connectivity index, boiling point and melting point, and negatively with aqueous solubility. However, those of elimination and internal transfer from structural pool to metabolic pool showed opposite changes. Comparisons of pharmacokinetic parameters between <u>Daphnia</u> and <u>Chlorella</u> demonstrated that, although all kinetic parameters displayed similar patterns, the relative magnitudes of each corresponding parameters were significantly different between two species.

Résumé

Cette thèse avait comme objectif de produire des modèles généraux pouvant prédire les flux de polluants dans le limnoplancton à partir de caractéristiques de l'organisme et de la structure du produit chimique. Un modèle pharmacocinétique à deux compartiments fut employé pour quantifier les taux d'absorbtion, de dépuration et d'échanges entre compartiments des polluants. Les taux de flux du phosphore ainsi que de 22 substances organiques ont été modélisés.

Chez les algues et les cladocères, les taux d'absorption, d'excrétion et de transfert entre compartiments du phosphore diminuaient en fonction du volume cellulaire ou taille de l'organisme selon une relation de puissance ayant un exposant de -0.25. La seule exception concernait les échanges entre compartiments chez les cladocères, qui avaient des relations aux pentes plus négatives. Par contre, les taux spécifiques d'absorption, d'excrétion et des échanges internes par individu augmentaient en fonction de la taille des organismes selon une relation de puissance avec exposant 0.75. Encore une fois, l'exception était les échanges internes chez les cladocères, qui avaient des relations avec des pentes plus faibles que 0.75.

Les facteurs de bioconcentration, les constantes et les taux d'absorption et de transfert du compartiment 1 vers le compartiment 2 de 22 produits chimiques organiques marqués au ¹⁴C ont été mesurées chez <u>Chlorella pyrenoidosa</u> et <u>Daphnia magna</u>. Il y avait des corrélations positives entre tous ces paramètres et le coefficient de séparation octanol/eau, la masse moléculaire, le parachor, l'indice de connectivité, le point de congélation et le point de fusion, mais les corrélations avec la solubilité aqueuse étaient négatives. Cependant, les paramètres d'élimination et de transfert du compartiment 2 vers le compartiment 1 démontraient des tendances opposées. Bien que les patrons généraux étaient semblables pour les deux

organismes, une comparaison des paramètres pharmacocinétiques démontre que les grandeurs relatives de ces paramètres sont significativement différents entre <u>Daphnia</u> et <u>Chlorella</u>. Il faudra tenir compte des ces différences lors de l'utilisation des relations quantitatives entre la structure et la pharmacocinétique (QSPRs) pour prédire les flux pharmacocinétiques des substances toxiques chez le plancton lacustre.

ACKNOWLEDGMENTS

I would like to express my sincere gratitude to my research supervisor Dr. R. H. Peters for his constant support, advice, help and encouragement for making this work possible. I am especially grateful for his patience in correcting my last two chapters when he was seriously ill in the hospital.

Grateful acknowledgments are given to my committee advisors, Dr. J. Kalff and Dr. N. Price for their invaluable suggestion and constructive criticisms, to Dr. J. Rasmussen for his commenting and criticising my results and to A. Vézina for giving me his unpublished data.

I thank M. Peters, D. Klimuk and E. P. Y. Tang for their laboratory assistance. Thanks are also due to A. Cimbleris, P. del Giorgio, R. Lehmann, J. Meeuwig, A. V. Pawlisz for their help and friendship.

Special thanks are given to my parents, parents-in-law, sister-in-law and brother-in-law for their understanding, encouragement and support. My great gratitude goes to my wife, Dr. W. Wang for her support, encouragement and love. Thanks are also extended to my daughter, Karen and son Jason.

I am grateful to the financial support from Dr. R. H. Peters, Studentship from FCAR of Quebec government (1992-1995).

TABLE OF CONTENTS

Short title \ldots i
Abstract ii
Résumé iii
Acknowledgments
Table of Contents
List of Figures
List of Tables
Statement of originality xxiii
Statement of thesis office xxvi
Statement of authorship xxvii
GENERAL INTRODUCTION
ABSTRACT 2
INTRODUCTION 3
1. Individual-based Pharmacokinetic Models 6
1.1. Compartmental Pharmacokinetic Models 6
1.1.1. One-compartment models
1.1.2. Multi-compartment models
1.2. Physiologically Based Pharmacokinetic Models
1.3. Non-compartmental Pharmacokinetic Models
2. Population-based Pharmacokinetic Models

3. Two new-generation Pharmacokinetic Models	. 3
3.1. Allometric Pharmacokinetic Models	. 3
3.2. Quantitative Structure-Pharmacokinetic Models	. 34
4. Validation of Pharmacokinetic Models	. 38
4.1. Evaluation of Absolute Performance	. 39
4.2. Evaluation of Relative Performance	. 4
5. A Philosophical View of Pharmacokinetic Modeling	. 43
6. CONCLUSIONS	. 50
7. OBJECTIVES	. 53
REFERENCES	. 55
CHAPTER I.	
CHAPTER I. ALLOMETRIC SCALING OF COMPARTMENTAL	
	. 63
ALLOMETRIC SCALING OF COMPARTMENTAL	
ALLOMETRIC SCALING OF COMPARTMENTAL FLUXES OF PHOSPHORUS IN FRESHWATER ALGAE	. 64
ALLOMETRIC SCALING OF COMPARTMENTAL FLUXES OF PHOSPHORUS IN FRESHWATER ALGAE. ABSTRACT	. 64 . 65
ALLOMETRIC SCALING OF COMPARTMENTAL FLUXES OF PHOSPHORUS IN FRESHWATER ALGAE. ABSTRACT INTRODUCTION	. 64 . 65
ALLOMETRIC SCALING OF COMPARTMENTAL FLUXES OF PHOSPHORUS IN FRESHWATER ALGAE. ABSTRACT INTRODUCTION MATERIALS AND METHODS	. 64 . 65 . 67
ALLOMETRIC SCALING OF COMPARTMENTAL FLUXES OF PHOSPHORUS IN FRESHWATER ALGAE. ABSTRACT INTRODUCTION MATERIALS AND METHODS Reagents and glassware	. 64 . 65 . 67 . 68
ALLOMETRIC SCALING OF COMPARTMENTAL FLUXES OF PHOSPHORUS IN FRESHWATER ALGAE. ABSTRACT INTRODUCTION MATERIALS AND METHODS Reagents and glassware Algal cultures	. 64 . 65 . 67 . 68
ALLOMETRIC SCALING OF COMPARTMENTAL FLUXES OF PHOSPHORUS IN FRESHWATER ALGAE. ABSTRACT INTRODUCTION MATERIALS AND METHODS Reagents and glassware Algal cultures Growth monitoring	. 64 . 65 . 67 . 68 . 69

Literature data conection and analysis
RESULTS 7
Cell P content-alga size relationship
P uptake
P excretion
P fluxes 85
Net P uptake
Comparison to Michaelis-Menten Model 89
DISCUSSION
ACKNOWLEDGMENTS
REFERENCES 100
CHAPTER II.
PHOSPHORUS FLUXES IN LIMNETIC CLADOCERANS: THE
COUPLING OF ALLOMETRY AND COMPARTMENTAL ANALYSIS 107
ABSTRACT 108
INTRODUCTION 109
THE TWO-COMPARTMENT MODEL
MATERIALS AND METHODS
Animal culture, sizing and body P determinations
Radioactivity counting
Isotope-labelling of yeast
P ingestion

P release	117
P assimilation	120
Allometric statistics	120
RESULTS AND DISCUSSIONS	121
Body dry weight and P content	121
Homogeneity of yeast labelling	121
P ingestion	122
P release	123
P assimilation	132
GENERAL DISCUSSION	132
Compartmental modeling of P fluxes	132
The validity of the feeding and flux allometries	136
ACKNOWLEDGMENTS	142
REFERENCES	143
СНАРТЕК ІП.	
QUANTITATIVE STRUCTURE-PHARMACOKINETIC	
RELATIONSHIPS FOR ORGANIC TOXICANT FLUXES	
IN CHLORELLA PYRENOIDOSA	148
ABSTRACT	149
INTRODUCTION	150
MATERIALS AND METHODS	152
Reagents and Labware	152

Test Organisms and Culture Conditions	154
Uptake Experiments	155
Elimination Experiments	156
Pharmacokinetic Modeling	157
Uptake	157
Elimination	158
Intercompartmental Fluxes	160
Curve Fitting	161
QSPR Analysis and Statistics	161
RESULTS	166
Pharmacokinetics	166
Uptake	166
Elimination	166
K _{ow} Based QSPRs	168
Rate Constants	168
Relative Pool Sizes	171
Flux Rates	171
Bioconcentration	172
Validation of the Kow Based Accumulation Model	172
Bioconcentration Factors	175
Other Structure-based QSPRs	175
DISCUSSION	170

Pharmacokinetic Fluxes	179
Bioconcentration factors	181
QSPR Models	183
ACKNOWLEDGMENTS	187
REFERENCES	188
CHAPTER IV.	
STRUCTURAL DEPENDENCY OF PHARMACOKINETIC	
FLUXES OF ORGANIC TOXICANTS BY CRUSTACEAN	
DAPHNIA MAGNA, WITH COMPARISONS OF THE QSPRS	
OF DAPHNIA AND OF THE ALGA CHLORELLA PYRENOIDOSA	192
ABSTRACT	193
INTRODUCTION	194
MATERIALS AND METHODS	196
Organisms	196
Chemicals	196
Uptake	197
Aqueous uptake	197
Dietary uptake	198
Elimination	199
Pharmacokinetic modeling and QSPR analysis	200
Estimation of morphometric properties and metabolic rates	

of <u>Chlorella</u> and <u>Daphnia</u>	200
RESULTS	201
Pharmacokinetic Parameters	201
Uptake	201
Elimination	202
K _{ow} Based QSPRs	206
Uptake	206
Elimination and Intercompartmental Exchanges	208
Bioaccumulation	211
Bioconcentration Factors	212
Other Structure Based QSPRs	212
Inter-specific Comparison of Pharmacokinetic Parameters	215
DISCUSSION	221
Pharmacokinetic Parameters	221
Bioconcentration Factors	223
Structure-Pharmacokinetic Relationships	224
Interspecies Comparison of QSPRs	227
ACKNOWLEDGMENTS	233
REFERENCES	234
CHAPTER V.	
GENERAL CONCLUSIONS	188

APPENDIX I.

EMPIRICAL MODELS OF PHOSPHORUS AND

NITROGEN EXCRETION BY ZOOPLANKTON	248
ACKNOWLEDGMENTS	249
ABSTRACT	250
INTRODUCTION	251
METHODS	252
Data Base	252
Data Analysis	253
RESULTS	254
Description of the Data Base	254
Regression Models	258
Effects of Taxonomy	263
DISCUSSION	266
REFERENCES	277

LIST OF FIGURES

Figure 1. Schematic representation of one-compartment models	. 8
Figure 2. Possible variants of two-compartment models	11
Figure 3. An assortment of three-compartment models	13
Figure 4. Conceptual representation of a physiologically	
based pharmacokinetic model	21
Figure 5. Physical structure for a noncompartment model	28
CHAPTER I.	
Figure 1. Schematic representation of a two-compartment model with first	
order uptake and excretion of P	74
Figure 2. Time courses of uptake of P in nine species of freshwater algae	
following exposure to ³² PO ₄ -spiked culture medium	78
Figure 3. Allometric relations between kinetic parameters of P uptake	
and algal cell volume	81
Figure 4. Relationship of uptake rate of P to algal cell volume	82
Figure 5. Excretion of P from ³² P-exposed algae as a function of time	
after being transferred to nonradioactive water.	84
Figure 6. Correlations between P flux kinetic data for excretion or	
intercompartmental turnover rates and algal cell volume	87

Figure 7. Size dependency of P flux rates for excretion and internal
flows in ten algal species
Figure 8. Comparison of predictions by the allometric compartment model
and the Michaelis-Menten-type enzyme function for P uptake
by algae with data from the literature 91
CHAPTER II.
Figure 1. Diagrammatic representation of the two-compartment
model of ³² P kinetics in cladocerans
Figure 2. Changes of body ³² P activity in individual groups of
cladocerans after transfer from non-radioactive to
radioactive yeast suspension
Figure 3. The allometric relations describing the size dependence of P
ingestion rate in cladocerans feeding on a radio-labelled
yeast suspension
Figure 4. Experimentally observed and model-fitted time-course
curves of ³² P excreted by initially fully labelled
individual groups of cladocerans feeding on nonradioactive
food at various time-intervals
Figure 5. The allometric relations describing the size dependence
of inter-compartmental release and fractional turnover rates 131
Figure 6. The allometric relations describing the size-dependence of

intercompartmental exchange and exit flux rates
CHAPTER III.
Figure 1. Schematic representation of two-compartment model 159
Figure 2. The relationships between rate constants of uptake,
elimination, and intercompartmental exchanges of organic
chemicals and octanol-water partition coefficient
in <u>C. pyrenoidosa</u>
Figure 3. The relationships between flux rates of uptake, elimination,
and intercompartmental exchanges of organic chemicals
and octanol-water partition coefficient in $\underline{\mathbf{C}}$. $\underline{\mathbf{pyrenoidosa}}$ 173
Figure 4. Comparison of predicted and experimentally-determined
concentration of contaminant in the algal cell
Figure 5. The relationships between bioconcentration factors of
organic chemicals and octanol-water partition coefficient
in <u>C. pyrenoidosa</u>
CHAPTER IV.
Figure 1. The relationships between rate constants of uptake
(uptake from water and uptake from food), and flux
rates of uptake (uptake from water and uptake from
food) of organic chemicals and their octanol-water
or organic enemients and men ocumor-water

partition coefficient in D. magna	207
Figure 2. The relationships between elimination and intercompartmental	
exchanges of organic chemicals and their octanol-water	
partition coefficient in <u>D. magna</u>	209
Figure 3. The relationship between bioconcentration factors of organic	
chemicals and their octanol-water partition coefficient	
in <u>D. magna</u>	213
Figure 4. Comparison of rate constants of aqueous uptake, elimination and	
intercompartmental exchanges of organic chemicals	
between C. pyrenoidosa and D. magna	216
Figure 5. Comparison of flux rates of aqueous uptake, elimination and	
intercompartmental exchanges of organic chemicals	
between C. pyrenoidosa and D. magna	219
Figure 6. Comparison of bioconcentration factors of organic chemicals	
between C. pyrenoidosa and D. magna	220
Figure 7. Logarithms of observed vs predicted accumulation from water	
of various organic chemicals in D. magna	228
Figure 8. Logarithms of observed vs predicted accumulation from food	
of various organic chemicals in D. magna	229
Figure 9. Comparison of surface area/volume ratio, metabolic rates,	
metabolic rate/volume, and metabolic rate/weight	
between Chlorella and Daphnia	231

APPENDIX I.

Figure 1. The relationship between P excretion rates and N excretion	
rates in freshwater and marine zooplankton	259
Figure 2. The relationship between P excretion rates or N excretion	
rates and respiration rates in freshwater and	
marine zooplankton	260
Figure 3. The relationship between (A) P excretion rates or (B) N	
excretion rates and animal body size in freshwater and	
marine zooplankton	261

LIST OF TABLES

Table 1. C	Cell volume (V), cell density (D), and biphasic P uptake
co	onstants for nine algal species
Table 2. A	algal cell or colony volume (V), cell density (D), biexponential
P	excretion constants and relative pool size of compartment 1
(Ç	Q ₁ %) for ten freshwater species
СНАРТЕ	R II.
Table 1. L	ist of major symbols used, and their meanings and dimensions 113
Table 2. T	he time course of specific activity of TCA extractable fraction,
to	tal specific activity of the yeast suspension, TCSA/TSA,
to	tal phosphorus and total radioactivity of the yeast cells
Table 3. V	alues of model parameters deduced from computer-curve fitting
a o	double exponential equation to excreted 32P activity data
an	d the relative pool sizes of two compartments in the different
sp	ecies of cladocerans studied
Table 4. Co	omparison of size-specific P release rates of limnetic
zo	oplankton measured by different techniques
Table 5. Ti	he results of a simulation to show the effects of incubation
ti	me and number of compartments on the cladoceran P excretion rates . 140

CHAPTER III.

Table 1. Test compounds	153
Table 2. Structural parameters of the tested chemical compounds	162
Table 3. Matrix of the correlation coefficients	164
Table 4. Biphasic uptake constants and model-fitting statistics	
for C. pyrenoidosa	167
Table 5. C. pyrenoidosa cell density (D), biexponential excretion	
constants and model- fitting statistics for 22 organic compounds	170
Table 6. Simple regression equations relating BCF and rate constants of	
C. pyrenoidosa to other chemical structural properties	177
Table 7. Simple regression equations relating flux parameters of	
C. pyrenoidosa to other chemical structural properties	178
Table 8. Comparisons of relationships between BCFs and physical-chemical	
properties of the chemicals for limnoplankton	182
CHAPTER IV.	
Table 1. Pharmacokinetic model parameters and model-fitting statistics	
for D. magna exposed to radiolabelled green water	203
Table 2. Pharmacokinetic model parameters and model-fitting statistics	
for D. magna feeding on radiolabelled water	204
Table 3. Biexponential excretion constants and model-fitting statistics	
for D. magna	205

Table 4. Simple regression equations relating BCF and rate constants	
of <u>D</u> . <u>magna</u> to chemical structural properties	214
Table 5. Simple regression equations relating pharmacokinetic flux	
parameters of D. magna to chemical structural properties	217
Table 6. Comparisons of relationships between BCFs and physical-chemical	
properties of the chemicals for <u>Daphnia</u>	225
APPENDIX I.	
Table 1. Mean phosphorus excretion rates, nitrogen excretion rates,	
respiration rates, body size, water temperature, container	
volume, duration of experiment for the whole data set and	
for Crustacea	255
Table 2. Correlation matrix of variables used in the analyses	257
Table 3. Simple regression equations relating zooplankton P or N	
excretion rates to excretion rate of another element,	
respiration rate and body size	262
Table 4. Multivariate regression equations for predicting total	
zooplankton P or N excretion rates from body size,	
excretion rate of other element, respiration rate,	
temperature, container volume and experimental duration	264
Table 5. As Table 4. but for crustacean zooplankton	265

Table 6. Residual means around the multivariate equations in	
Table 4 for total zooplankton.	267
Table 7. As Table 6, but for the multivariate equations in	
Table 5 for crustaceans	268

STATEMENT OF ORIGINALITY

This thesis is the first effort to use two-compartmental pharmacokinetic models to predict the rate constants and flux rates of phosphorus and organic toxicants by algae and zooplankton. It examines a broad range of chemicals with diverse structural properties, and a variety of physiological and biological factors that interact to determine the pharmacokinetic behaviors, such as uptake, excretion, distribution and metabolism. In addition, Instead of focusing on a single pharmacokinetic model, the thesis has taken an integrated experimental approach that incorporates pharmacokinetics with allometry or quantitative structure-activity relationship. The following aspects described in this thesis are considered contributions to original knowledge.

General Introduction. This chapter provides the first critical review of most pharmacokinetic models. The theory, principles and data requirements are critically discussed. The fundamental differences among various pharmacokinetic models were compared and contrasted. The techniques and philosophy for model validation were discussed and illustrated. The implications of these models for the environmental risk assessments were described.

Chapter 1. This chapter contains the experimental results of allometric scaling of the pharmacokinetic fluxes of phosphorus by freshwater algae. This

is the first investigation that applies both allometry and pharmacokinetics to describe the uptake, excretion and intercompartmental exchanges of phosphorus by the primary producers. The results suggest that the phosphorus flux rates at ambient limiting concentrations increase proportionately to the 3/4 power of the cell volume.

Chapter 2. This chapter tests the generality of the allometric pharmacokinetic model for describing phosphorus uptake, excretion and intercompartmental exchanges by cladocerans. By employing the similar experimental approach developed in Chapter 2, various pharmacokinetic parameters for phosphorus fluxes were, for the first time, allometrically determined. From the experimental results, the allometric models of assimilation rates and assimilation efficiency of phosphorus by cladocerans were established.

Chapter 3. This chapter develops the relationships between physico-chemical properties and pharmacokinetic parameters of uptake, elimination and intercompartmental transfers, and bioconcentration factor of up to 22 organic contaminants by green alga Chlorella pyrenoidosa. By regression analysis, the structural properties, including partition coefficient, aqueous solubility, connectivity index, parachor, molecular weight, melting point, boiling point and density, were used to predict the time courses of contaminant uptake, elimination and internal exchanges. This is the first study to use the chemical structural properties to predict the pharmacokinetic fluxes of organic contaminants by algae.

Chapter 4. This chapter examines the validity of the quantitative structure-pharmacokinetic relationships established in Chapter 4 by applying this model to the description of organic contaminant fluxes by <u>Daphnia magna</u>. The experiments were conducted on the same chemical compounds under the same laboratory conditions. This is the first experimental design to establish an approach permitting the comparisons of inter-species and inter-compound flux responses by aquatic organisms.

Appendix I. This appendix presents an empirical approach to the predictions of phosphorus and nitrogen excretion rates by zooplankton from body weight, respiration rates, water temperature, container volume and duration of the experiment. The predictive models were developed from the literature data, and validation of the models were tested by the difference between residual means of observed and predicted data. This thorough empirical analysis of phosphorus and nitrogen excretion rates by zooplankton has never been performed previously.

THESIS OFFICE STATEMENT

In accordance with the regulation of the Faculty of Graduate Studies and Research of McGill University, the following is included in this thesis.

"Candidates have the option, subject to the approval of their Department, of including, as part of their thesis, copies of the text of a paper(s) submitted for publication, or the clearly-duplicated text of a published paper(s), provided that these copies are bound as an integral part of the thesis.

If this option is chosen, connecting texts, providing logical bridges between the different papers are mandatory.

The thesis must still conform to all other requirements of the "Guidelines Concerning Thesis Preparation" and should be in a literary form that is more than a mere collection of manuscripts published or to be published. The thesis must include, as separate chapters or sections: (1) a table of contents, (2) a general abstract in English and French, (3) an introduction which clearly states the rationale and objective of the study, (4) a comprehensive general review of the background literature to the subject of the thesis, when this review is appropriate, and (5) a final overall conclusion and/or summary.

Additional material (procedural and design data, as well as descriptions of equipment used) must be provided where appropriate and in sufficient detail (eg. in appendices) to allow a clear and precise judgement to be made of the importance and originality of the research reported in the thesis.

In the case of manuscripts co-authored by the candidate and others, the candidate is required to make an explicit statement in the thesis of who contributed to such work and to what extent; supervisor must attest to the accuracy of such claims at the Ph. D. Oral Defense. Since the task of the examiners is made more difficult in these cases, it is in the candidate's interest to make perfectly clear the responsibilities of the different authors of co-authored papers.

STATEMENT OF AUTHORSHIP

This thesis consists of six manuscripts in the format of peer-reviewed, scholarly journals. General Introduction has been submitted to Aquatic Toxicology as a review paper under the title "Pharmacokinetic modeling in toxicology, a critical perspective". Chapter 1 is in press in Limnology and Oceanography. Chapter 2 has been published in Canadian Journal of Fisheries and Aquatic Sciences (51: 1055-1064, 1994). Chapters 3 and 4 have been submitted to Environmental Toxicology and Chemistry. Appendix I has been published in Limnology and Oceanography (39: 1669-1680, 1994). Chapters 1, 2, 3, 4 and Appendix I were coauthored with my supervisor, Dr. Robert H. Peters. Dr. Peters provided financial resources for the laboratory work and advice for this study, and correction of the manuscripts. Dr. A. Vézina was the third author on Chapters 1 and 2 for his contribution of unpublished data. I am responsible for the experimental design, execution, data analysis and texts of the manuscripts.

General Introduction*

* Submitted to Aquatic Toxicology under the title: "Pharmacokinetic Modeling in Toxicology: A Critical Perspective".

Abstract

Pharmacokinetic models provide novel approaches for evaluating toxicological problems. For example, pharmacokinetic parameters play an important and even determinant role in risk assessment and policy making. The present contribution reviews most basic pharmacokinetic models, their development and their applications in toxicology. The theory, principles and data requirements are critically discussed. The fundamental differences among various pharmacokinetic models are compared and contrasted. The techniques and philosophy for model validation are discussed and illustrated.

Introduction

Pharmacokinetics is the study of the time course of drug absorption, distribution, metabolism, and elimination (Gibaldi and Perrier 1982). Pharmacokinetic modelling is the process of developing mathematical descriptions for these critical fluxes. Due to their quantitative nature, pharmacokinetic models have long been used in the prediction of amounts and concentrations of drug in the body as function of time and dosing. The blend of pharmacology with toxicology provides a firm foundation for environmental health research.

The number of xenobiotic industrial chemicals produced commercially is large. More than 10 million chemicals have been identified and manufactured; at least 76,000 chemicals are currently in common use, and new chemicals increase at a rate of about 200 to 1000 every year (Moriarity 1985; Cairns and Mount 1990: Cockerham and Shane 1994). The presence of many of these chemicals in the environment is a serious public health problem. For environmental scientists, the major challenge is to devise diagnostic tools for impact assessment, to restore environments, and to prevent toxicological risks. To undertake these tasks, it is very important to know the toxicological fate of these chemicals in the environment. However, due to the large number of chemicals and the complexity of the natural environment, gathering this information will be labour intensive, time consuming, and expensive (Peters

1991). Our human and material resources are far insufficient to measure the toxicity data experimentally for all compounds and organisms. It becomes imperative that reliable predictive models be developed to facilitate accurate and rapid assessment of the environmental risks of a variety of chemical classes for different biological species and environmental conditions, thus providing a basis for decision making and policy implementation by regulatory agencies. Consequently "toxicokinetics" has been increasingly used to provide non-specific description of toxicants and their kinetics at various doses (Renwick 1994). Because this blend is only the application of pharmacokinetic principles to toxicological problems, pharmacokinetics still remains the semantically correct term.

Pharmacokinetic models have applied widely to predict the kinetics of chemical residues in the environment, to solve pollution problems, and to help understand and interpret toxicological findings. As a consequence, several types of predictive models exist, e.g., compartmental and noncompartmental models, physiologically based pharmacokinetic models, population pharmacokinetic models, etc. Such models have had good success in risk assessment, describing contaminant distribution in test organisms under various toxicological conditions and doses and monitoring contaminant transfer rates in ecosystems (Spacie and Hamelink 1982; Karara and Hayton 1984; Barron et al. 1990; Landrum et al. 1992).

Pharmacokinetic modelling is currently a very "hot" area of research in

environmental science (Clark and Smith 1984). The applications of pharmacokinetic models have been extensive, scientifically precise and accurate. More vigorous utilization of these models is on the way. Several relevant review articles on the subject have focused primarily on the development of models (Barron et al. 1990) and the application of these modelling techniques to toxicological testing (Landrum et al. 1992). However, most of these reviews do not critically scrutinize the pharmacokinetic models they discuss. They tend simply to accept any working hypotheses that relate exposure of a specific hazard to a toxicological result without carefully examining the susceptibility of the subject exposed and other important determinants of the response. This approach restricts the data needs, but also risk assessment capabilities.

In this review, general pharmacokinetic models are critically discussed in terms of their concepts, mechanisms and applicabilities. The advantages and limitations of the models, some future remedies and alternative models that make better predictions are presented. This review concentrates upon the most frequently used pharmacokinetic models, including conventional compartmental models and physiologically based pharmacokinetic models, and suggests future avenues for research. It is not the purpose of this paper to compile examples of pharmacokinetics already published in the literature or to provide a detailed description of the whole field. The detailed mathematical aspects of pharmacokinetics are also beyond scope of this review, but others

have dealt in depth with these materials (Gibaldi and Perrier 1982; Jacquez 1985).

1. Individual-based Pharmacokinetic Models

1.1. Compartmental Pharmacokinetic Models

The most widely used models in pharmacokinetics are compartmental models with first order exchange of contaminants between compartments. A compartment is considered to be a kinetically homogeneous and well-mixed hypothetical volume which interacts with other compartments by exchanging contaminants (Jacquze 1985). For example, the animal body may be viewed as an assortment of compartments each made up of identical molecules. Generally a compartment has no physiological counterpart, but might be regarded as an anatomic region where tissue groups are kinetically related (such as plasma, tissue). Nevertheless, in principle, such compartments do not physically exist and therefore are not easily visualized. Compartmental modelling is based on the assumption that specific compartments can be kinetically identified so that discharge of contaminants therefrom can be described by exponential equations. Considerable knowledge and judgement are needed to justify the correct use of these equations. Otherwise, compartment models may be meaningless to the real system being modelled.

Compartment models can be divided in terms of model configuration into one-compartment and multi-compartment models.

1.1.1. One-compartment models

The simplest model is the one-compartment model which treats the whole body as a single, kinetically homogenous unit. The plasma or serum is usually considered as the anatomical reference compartment. If a contaminant is quickly distributed through the body and equilibrium is rapidly established, then a one-compartment model can be developed to predict concentrations of contaminants in readily accessible media, such as blood and excreta. Of the two possible one-compartment models (Fig. 1) that with both uptake and elimination (Fig. 1B) is more common. The rates of uptake and clearance of contaminants for this model can be quantified by the following equations:

for uptake:
$$C_t = C_0 (1 - \exp(-k_1 t))$$

for clearance:
$$C_t = C_0 \exp(-k_2 t)$$

where C_t is the internal body concentration at any time t, C_0 is the initial internal body concentration, k_1 is the uptake rate constant, k_2 is the elimination rate constant, and t is the time elapsed after the administration of the dose.

The advantage of this model is simplicity. Its parameters do not require complex mathematical procedures, but are instead readily determined from a

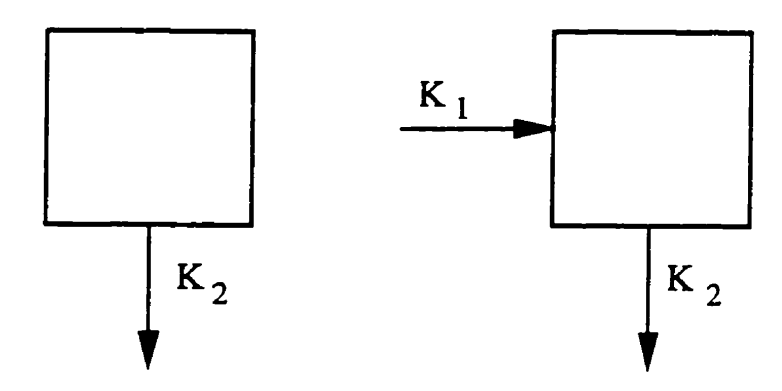


Fig. 1. Schematic representation of one-compartment models: A: with elimination; B: with uptake and elimination.

semilogarithmic plot of contaminant concentration (logarithmic scale) versus time (linear scale) or by the non-linear fitting, for example, by the NLIN procedure of the SAS program (SAS Institute Inc. 1983). However, this model can produce substantial errors and misleading calculations, because a pure single-compartment is only a crude approximation to most physiological systems. All organisms are better described as the sum of a network of compartments. When many interconnecting pools are treated as a single compartment, compartments having relatively slow interchanges or markedly disparate sizes may be very poorly represented. The one-compartment model is useful only when the contaminants are distributed throughout the body so fast that the concentration of a contaminant in various fluid spaces and tissues can reach an equilibrium almost simultaneously (Jacquze 1985). Unfortunately, most contaminants do not exhibit this kinetic property.

1.1.2. Multi-compartment models

The error inherent in treating multiple-compartments as one pool is considerable and consequently one compartment models have limited usage. As a result, multi-compartment models have become increasingly common in pharmacokinetic studies (Segre 1982). As the number of the compartments increases, the computation for the rate parameters becomes more complex and the components in the curve become numerous so that both graphic curve

fitting and computer programming become impractical or difficult. These problems can be, more or less, rounded off by lumping several interchanging compartments into one common "homogeneous" unit generally referred to as the central or peripheral compartment. The contaminant elimination in multicompartment systems is still assumed to be a first-order process, but more than one exponential terms are required to characterize the declining function of contaminant concentration with time. The number of exponentials necessary to describe the kinetics adequately depends on the quality of the data. The mostly commonly used multi-compartment models have two and three compartments, since it is usually difficult to identify more than three exponents in a multi-exponential equation. Models with four or more compartments are less frequent.

In a two-compartment model, the administration and elimination of contaminant may be assumed to occur from the central compartment, from the peripheral compartment or from both compartments simultaneously (Shipley and Clark 1972; Wagner 1975). The central compartment is generally considered to be blood, extracelluar space and tissues which kinetically appear to achieve spontaneous equilibrium with blood (e.g., liver, heart, lung), while the peripheral compartment is represented by poorly perfused organs and tissues (e.g., fat, bones, skin). There are nine possible two-compartment models (Fig. 2), and they are mathematically indistinguishable. The most commonly used two-compartment model is the open model with elimination from the

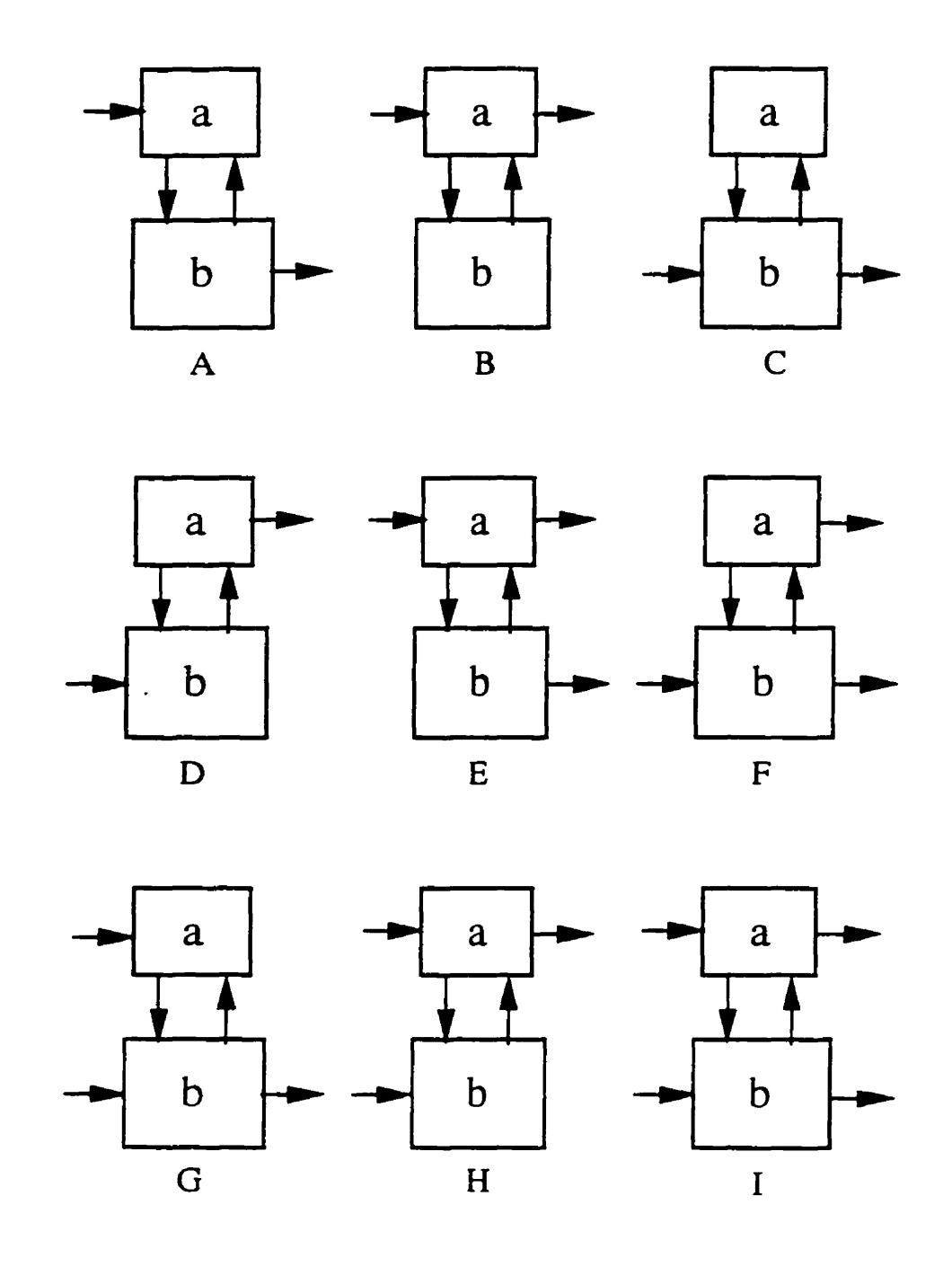


Fig. 2. Possible variants of two-compartment models (modified from Shipley and Clark 1972).

central compartment (type B). In this model, the inward and outward rate constants can be estimated by the following equations:

For uptake:
$$A_t = A_1 [1-exp(-b_1t)] + A_2 [1-exp(-b_2t)]$$

For clearance:
$$C_t = C_1 \exp(-k_1 t) + C_2 \exp(-k_2 t)$$

where A_t is the total concentration of contaminant in the body at time t; C_t is the total contaminant concentration of the washout at time t; A_1 and A_2 are the maximal activities and C_1 and C_2 are the maximal concentrations incorporated in two compartments; b_1 and b_2 are uptake rate constants and k_1 and k_2 are clearance rate constants for two compartments.

Although two-compartment models can significantly improve the estimation of contaminant flux rates in biota, they do not provide any information regarding the time course for either contaminant or their metabolite in a specific organ. In addition, injudicious lumping of numerous compartments into a working model with only two compartments can introduce errors for reasons similar to those described for one-compartment models. To reduce this error to some extent, a second peripheral compartment may be added to the two existing pools. These three compartments are interrelated and there is at least one elimination pathway. There are eleven possible, kinetically equivalent, three-compartment models (Fig. 3). The most common model is that with elimination from the central compartment (type F). Three-

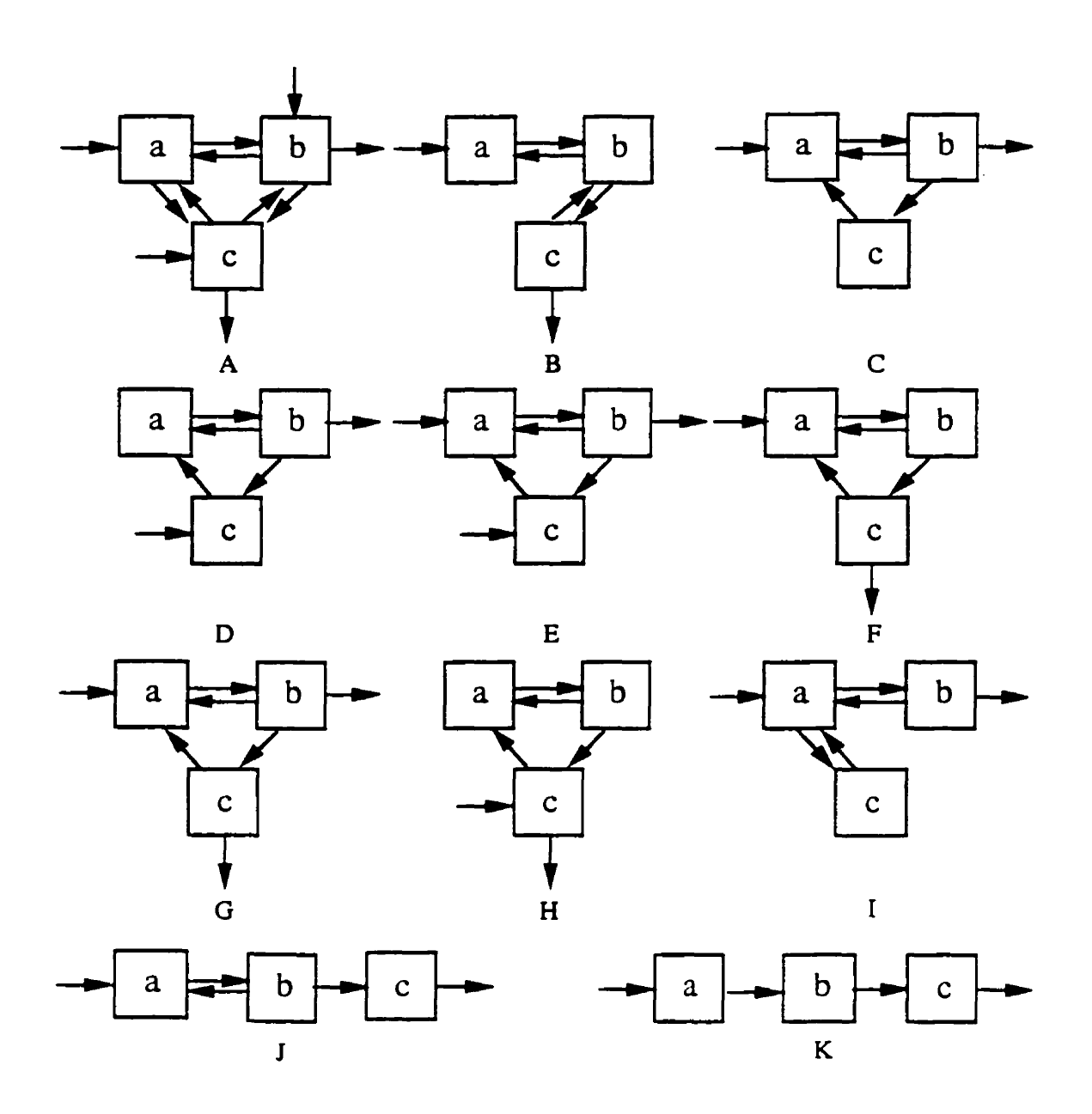


Fig. 3. An assortment of three-compartment models (modified from Shipley and Clark 1972).

compartment models also suffer from the limitations of the two-compartment models, and further increase in number of compartments does not alter this situation.

There is some controversy in the literature concerning the selection of the most appropriate model, because each has advantages and disadvantages. DiStefano and Landaw (1984) pointed out that three factors predominate in determining the number of compartments in a model: 1) the physiological (structural) knowledge base, 2) the number and identity of directly measurable compartments, and 3), the number of exponentials that fit the data best. However, because there is no analytical answer to questions about how much a model can be reduced and still provide satisfactory fit to the observations, and therefore no objective criteria for selection of the number of compartments, the choice of an appropriate model is usually an arbitrary selection from kinetically equivalent models (Wagner 1975).

Here only the method of curve fitting is assessed, because the question can be approached analytically, and its solution will apply to most often empirical questions arisen in model selection. Two techniques commonly employed are graphical and computer curve fitting.

A. Graphical method of curve peeling (back-projection or stripping)

Curve peeling is a traditional method used to estimate the components of exponential decay curves (Riggs 1963). The number of compartments needed to describe the tracer behavior is mathematically resolved into decaying

exponential terms to account for the curvature of the data. The number of exponential terms corresponds to the number of compartments in the model. Compartmentalization by this method is a rather abstract mathematical construct which deemphasize physiological relevance.

A good criterion of how well the "peeling" technique has been applied to a given set of data is to consider the sum of squared deviations (Σ dev²) of the data from the model:

$$\sum dev^2 = \sum [\hat{C}_i(t) - C_i(t)]^2$$

where $\hat{C}(t)$ is estimated concentration at time t, C(t) is the observed concentration at the time t. By definition, the better peeling technique produces the smaller value of Σ dev².

The number of compartments that may be distinguished reflects the interactions between the components. Since one can take only a finite number of samples, the sampling schedule can affect the range of decay components that will be detectable. In practice, if there are more than three components, it is rarely possible to estimate the components with much accuracy because the errors in estimating parameters propagate into the subsequent estimates of the remaining parameters (Jacquez 1985). This method also has a severe problem in that terms with closely similar values for the exponential constants may not be adequately separated by subtracting a single straight-line asymptote (Zierler 1981). In addition, this method is prone to the greatest degree of subjectivity (DiStefano and Elloit 1984) and therefore varies from

user to user.

B. Computer curve fitting

Currently many computer programs are available for curve fitting (Buffington et al. 1993). Most of the programs estimate the parameters for a wide variety of nonlinear functions by least squares using a modified Gauss-Newton algorithm (Dixon 1988). The goodness-of-fit is judged by two statistical criteria:

(1) The F statistic. The sums of weighted squared deviations between the data and the predictions should be minimized by the method of least squares. To justify an additional compartment, the F-ratio test may be used to decide whether the last added compartment significantly reduces the residual variance (Boxenbaum et al. 1974):

$$F = [(WSS_i - WSS_k)/WSS_k] \times [df_k/(df_i - df_k)]$$

where WSS_j is the weighted sums of squared deviations obtained with the j-th set of parameters, WSS_k is the weighted sums of squared deviations obtained with the k-th set of parameters, and df is the degrees of freedom which is equal to the number of data points used to fit the curve(s) minus the number of parameters fitted $(df_j > df_k)$. The F value will be compared to the critical value of F at the required degree of confidence and corresponding degrees of freedom (df). If the calculated F value is less than the critical value, the last added exponent did not significantly reduce the residual variance, indicating this compartment should be deleted from the model.

(2) Residual analysis. Residual analysis may be used to examine the difference between the observed and predicted values of a response. The residuals should have a zero mean and a homogeneous variance. Therefore, the scatter of observed data points about the modelled curves should be randomly distributed if the model is adequate. The sum of squared weighted residuals (the residual sum of the squares, RSS) can be estimated by:

RSS =
$$\sum W_j (y_j - \hat{y}_j)^2$$

where y_j is the observed value of the dependent variable in case j, and \hat{y}_j is the predicted value from the function, and W_j is the weighting. The sum of the squared weighted residuals is the quantity minimized in a least-squares analysis.

In addition, a plot of residuals against time is a useful visual aid to identify any lack-of-fit. Apparent systematic variation in the residuals suggests a lack of fit of the equation chosen and in that case, the data might be better fit by higher orders of compartmental functions. Plots of residuals or squared residuals against predicted values are also useful to detect model inadequacy and assess outliers. A normal probability plot of the weighted residuals or a detrended normal probability plot of the weighted residuals can also indicate systematic lack of fit of the function. In the former case, if the residuals are from a normal distribution, they will have a linear trend. In the latter case, the residuals should cluster around zero with little apparent pattern (Dixon 1988).

Other methods, such as maximum likelihood estimation, Bayes estimation,

optimization methods, etc., are also used to give a "best fit" of the data to the model (Metzler 1981; Jacquez 1985). Due to the computational difficulties and other limitations, these methods have not yet received wide applications (Metzler 1981).

In compartmental analysis, equations which sum a series of exponential functions are frequently fitted to data. Recent improvements in computational algorithms and hardware allow numerical solutions of large sets of simultaneous linear and nonlinear differential equations rapidly with arbitrary accuracy. The more parameters used, the better should be the fit we obtain. Increasing the number of exponential terms in the fitted equation may reduce the sum of the weighted squared deviations but the model that results may be unnecessarily complicated and/or the parameters may be very difficult to interpret biologically. Therefore the goodness-of-fit is not the only basis for judging what model is "best". The number of compartments should also be selected on the criterion that the equation provides a good interpretation of the experiment or adds to the body of knowledge in that field. For biological systems, other information, such as anatomical structure, biochemistry and physiology, should be used in conjunction with tracer experiments. Thus the choice for the number of compartments rests on both biological and mathematical considerations. The selection of a pharmacokinetic model also depends very much on the proposed use (Boxenbaum et al. 1974).

Multi-compartmental models have several advantages. They are

moderately simple in terms of both data collection and computation. They can provide reasonably accurate estimations of model parameters and describe the available data effectively. An attractive feature of these models is that they are sufficiently general that they apply to unicells and invertebrates. For example, Wen et. al. (1994, 1996) scaled a two-compartment model for phosphorus flux through freshwater algae and cladocerans in terms of cell volume or body size. Another important advantage of these models is their usefulness in directing further research with other related contaminants once the models are fairly well established with a representative contaminant.

Two- and three-compartment models have serious limitations. The most obvious is that the basic information that they provide regarding distribution and elimination is intrinsically limited. Because these models are typically based on the curve fitting of multi-exponential model equations to plasma-concentration time data, they do not explicitly describe the physiological system that determines the pharmacokinetic behaviour, and do not provide information on tissue-to-tissue concentration differences (Segre 1984). Therefore, transfer rate constants calculated from these models have a high degree of uncertainty (Shipley and Clark 1972). Furthermore, compartment volumes and transfer rate constants derived from these models have no anatomical or physiological reality, so these models can not predict the concentration-time course of a contaminant at the particular target site other than the plasma. Consequently, this class of pharmacokinetic models can be

only employed for interpolation, and not for extrapolation outside the range of doses, dose routes and species studied (Krishnan and Andersen 1994). The model compartmentalization is only an abstract mathematical construct, and lacks actual anatomical, physiological and biochemical relevance (Leung 1991). Because of their substantial differences in tissue-to-plasma contaminant concentrations between animals and humans, these models can not easily be used in direct quantitative scale-up.

1.2. Physiologically Based Pharmacokinetic Models

Physiologically based pharmacokinetic (PBPK) models utilize basic physiological and biochemical information to describe and quantify the pharmacokinetic processes affecting the contaminant distribution and disposition. These models separate the organism's body into a series of biologically relevant anatomical compartments of defined volumes. The tissues of interest are then arranged in anatomical order based on blood circulation to form an integrated model (Fig. 4). The transfer of contaminants between compartments is thus governed by actual blood flow rates and tissue solubilities (partition coefficients). Each compartment can have several subcompartments consisting of a vascular section, an interstitial space, and a cellular space (Gerlowski and Jain 1983). These models permit the prediction of contaminant concentrations from the time it is absorbed to its interaction

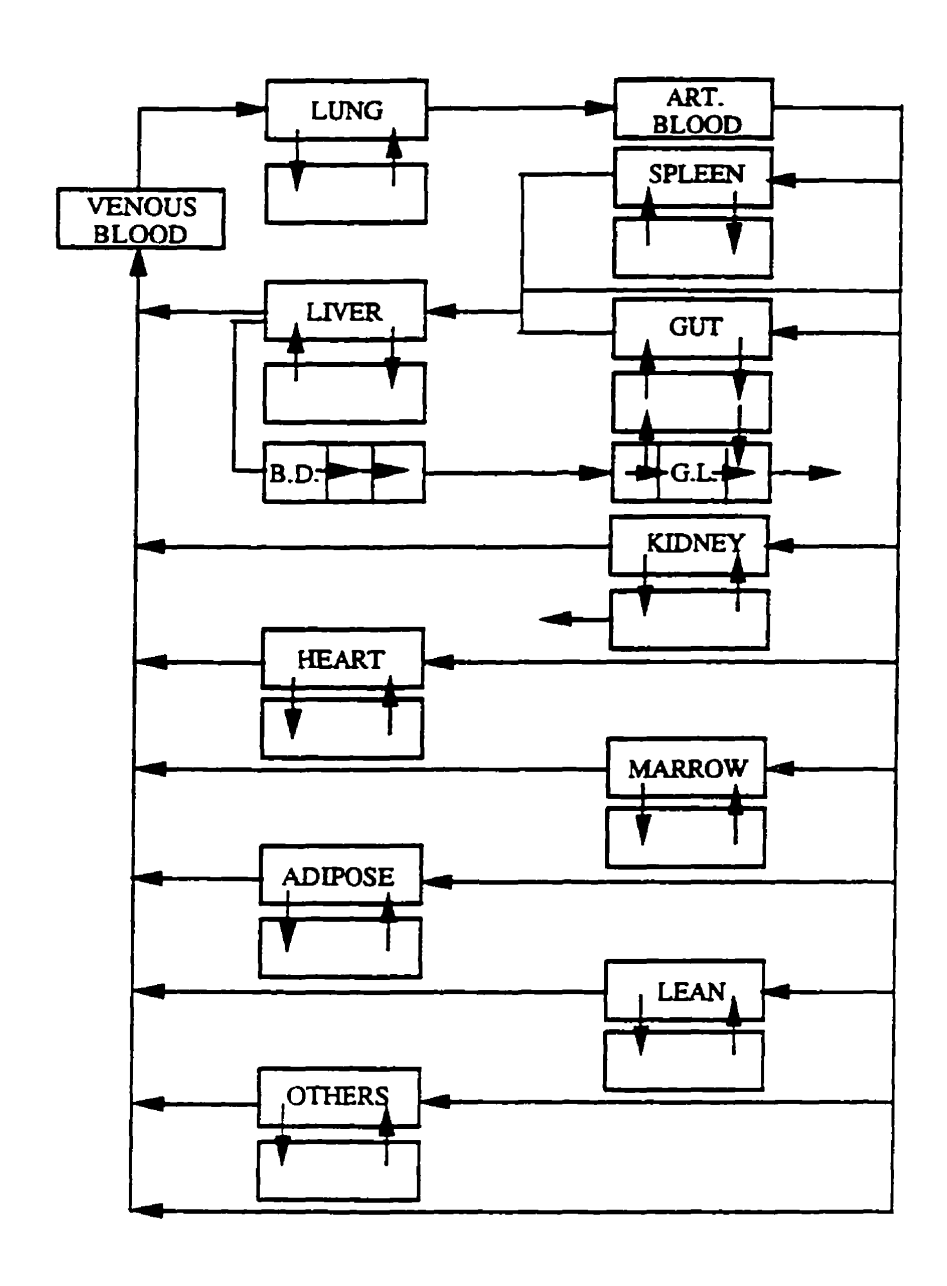


Fig. 4. Conceptual representation of a physiologically based pharmacokinetic model (adapted from Himmelstein and Lutz 1979).

with various body tissues, and may provide considerable information about the internal contaminant dynamics. To examine the transport mechanisms, binding, excretion, and metabolism of the contaminants being considered, Himmelstein and Lutz (1979) proposed that four kinds of information are potentially important in the model structure: anatomical (e.g. organ volumes and tissue sizes), physiological (e.g., blood flow rates, vascular perfusion), thermodynamic (e.g., binding isotherms) and transport (e.g., permeability of the tissue membrane). Consequently the events occurring in each organ, tissue, or group of kinetically related tissues, are all expressed explicitly (Rowland 1985). Because these models are usually based on all available knowledge about the underlying mass transport and physiology, they are considered to be the most comprehensive and phenomenologically based models (Himmelstein and Lutz 1979; Rowland 1984).

PBPK models have been extensively employed to make a priori predictions of the contaminant distributions in various tissues (Menzel 1987). They simulate the uptake and disposition of the contaminant by performing numerical integration of mass balance equations on each organ and tissue on the assumption that organs and tissues with similar behaviour can be lumped together into compartments (Krishnan and Anderson 1994). The mass balance for the sum of the processes occurring in each compartment can be described by a set of differential equations, which contain terms for inflow, outflow, accumulation, and elimination of the contaminant and its metabolites as given

in the following equation:

$$dA/dt = A_{in} - A_{out} - A_{elim} + A_{syn}$$

where dA/dt is the rate of change of contaminant concentration, $A_{\rm in}$ rate of entry, $A_{\rm out}$ the rate of exit, $A_{\rm elim}$ the rate of metabolic breakdown or elimination, and $A_{\rm syn}$ the rate of synthesis in the tissue or compartments. The equations are then solved simultaneously by numerical integration or other appropriate algorithms to find solutions over time. Values for the various constants can be obtained from the literature, from in vitro experiments or from interspecies allometric extrapolations (Chappell and Mordenti 1991). The accuracy of the models depends on the blood and tissue solubilities, metabolism and protein binding characteristics in various tissues, and the physiology of the organisms.

Because PBPK model describes the quantitative interrelationships among the toxicologically important determinants for the uptake and disposition of chemicals, the models assume (1) that each tissue acts as a well-mixed compartment, therefore the efferent blood has the same concentration as the vascular space; (2) that intercompartmental exchange occurs by blood flow, that contaminant crosses the capillary wall and diffuses into the interstitial phase, and then it moves from the interstitial fluid across the cellular membrane into the cell; (3) that the distribution of contaminant is a blood-limited and linear process. The validity of these assumptions should be tested. It is essential to examine the uncertainty, sensitivity, and variability of the

model parameters in the model validation and testing stages (Krishnan and Andersen 1994).

The PBPK models have very important applications in toxicology. Because the tissue compartments in these models are interpretable in terms of the general biology of the organism, and because of the similarities in the anatomy and physiology in mammalian species, PBPK models can be used to make interspecies extrapolations of pharmacokinetic data. After the values of target tissue dose in the animal model have been estimated and validated, the data can then be scaled to humans to predict the target organ dose (i.e., animal scale-up or -down; Dedrick 1973; Boxenbaum and D'souza 1990; Ings 1990) and they should be exploited to the fullest extent in planning experiments, interpreting data and developing protocols (Chappell and Mordenti 1991). Because this class of models can be parameterized independently of exposure information, they allow for incorporation of complex dosing scenarios, different routes of exposure and varying conditions of exposure in risk assessment (Krishnan and Andersen 1994).

There are some barriers to the progress of PBPK modelling. First, the models are still in their early development. They need to incorporate the factors influencing contaminant distribution and elimination, such as perfusion, binding, pH, etc. Second, many chemical reactions within the animal body are very complicated, and often little understood. It is difficult to ensure that the contaminant metabolism in vitro or in the model can quantitatively

and accurately predict that <u>in vivo</u>. Consequently the utility of the PBPK models depends on how realistically they describe the sizes of organ compartments, partitioning of test material between blood and tissues, flow of blood and gases through the organs, and rates of metabolic transformation of the test chemical (Gibaldi and Perrier 1982). Furthermore, for many contaminants, binding to plasma proteins and tissue constituents varies considerably among contaminants, animals and environments, so the animal scale-up could be difficult.

PBPK models have some serious limitations and shortcomings. Firstly, although the PBPK models are essentially mechanistic, they neither provide an explanation of what mechanisms underlie the pharmacokinetic fluxes nor allow for differential sensitivity of one target organ over another or one species over another. Secondly, because these models separate an organism into a series of anatomical compartments, they are very difficult to apply to unicells, invertebrates and plants, where homologous organs or tissues are hard to identify or study. In the pharmacokinetic literature, most PBPK model configurations are limited to vertebrates, especially mammals and humans. Thirdly, because the models involve complex sets of algebraic and mass balance differential equations for important compartments, large amounts of data are necessary to run or test the model. Because most of these data are usually unavailable, particularly in humans, the acquisition of these data often represent an unrealistically demanding task. The alternative is to use data

from in vitro studies or to aggregate information gained from different species (Balant and Gex-Fabry 1990). Therefore, PBPK models are far more expensive and time-consuming than the classic compartmental models described previously. Fourthly, due to the difficulties of analyzing various tissues for contaminant concentrations, it is uncertain exactly how many body regions or compartments are needed to model the contaminant distribution. The initial choice is based on the knowledge of physicochemical properties (binding, lipid solubility, ionization) and pharmacological properties (mechanism of the transport, sites of action) of the contaminant (Himmelstein and Lutz 1979). Fifthly, in this class of models, if too many parameters are applied to data that are limited in both quantity and quality, computational problems become serious. Consequently there have been few systematic attempts to establish a statistical approach to the estimation of the parameter values within the model and to optimize experimental design (Roland 1984). Its ability to predict contaminant flux rates depends on the precision of the parameter estimates used and the model chosen. Finally because these models are sophisticated, they should be used by people with enough experience to avoid misinterpretations. This complexity may limit their routine application in toxicological studies.

1.3. Noncompartmental Pharmacokinetic Models

To overcome the disadvantages of compartmental analysis, noncompartmental pharmacokinetic models have recently been used to predict bioavailability, excretion and apparent volume of distribution after a single dose of a contaminant or metabolite. The physical structure of the noncompartmental model is illustrated in Fig. 5. In addition to the direct influx of contaminant into a central pool, there is an indirect entry from a noncentral pool. The contaminant or metabolite is removed or eliminated from either central or noncentral pool. The model parameters are estimated according to statistical moment theory which estimates the area under the curve (AUC) and the moment curve (AUMC) by the following equations (Gabaldi and Perrier 1982):

$$AUC = \int_0^\infty C dt$$

$$MRT = \frac{\int_0^\infty tC dt}{\int_0^\infty C dt} = \frac{AUMC}{AUC}$$

$$VRT = \frac{\int_0^\infty t^2C dt}{\int_0^\infty C dt} = \frac{\int_0^\infty (t - MRT)^2 C dt}{AUC}$$

where t is the last sampling time, MRT the mean residence time, VRT the variance of the mean residence time of a contaminant in the body, AUC, MRT, and VRT are the zero, first, and second moment, respectively, of the contaminant concentration-time curve.

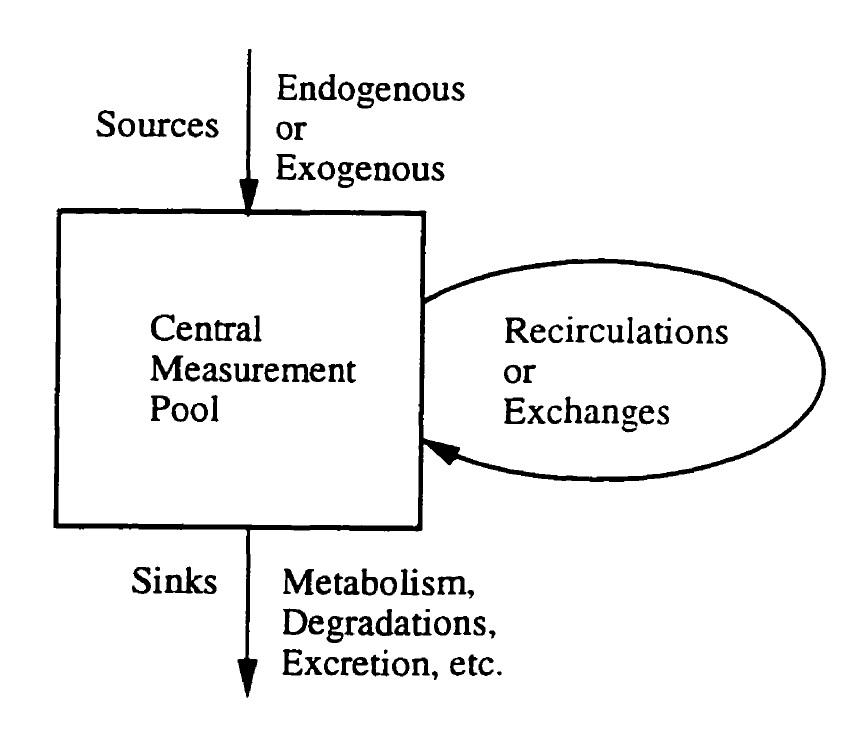


Fig. 5. Physical structure for a noncompartmental model (adapted from DiStefano, III and Landaw 1984).

The most significant advantages of non-compartmental models are that they do not assume specific compartments for contaminant or metabolite. Any number of recirculations or exchanges can occur, with any number of noncentral pools, none of which has to be identified with any physiological structure (DiStefano and Landaw 1984). In addition, because noncompartment modeling does not involve fitting a particular model to data, the model assumptions are minimized, and the moments are completely model-independent measures and can be easily calculated. One of the severe disadvantages is that, the higher order of moments can lead to unacceptable levels of computation errors (Nüesch 1984). Consequently noncompartmental analysis received only limited application in toxicology.

2. Population-based Pharmacokinetic Models

Population pharmacokinetics describe the typical relationships between physiology and pharmacokinetics, the inter-individual variability in these relationships and their residual intra-individual variability (Sheiner 1984). To construct the model, the time-course data are pooled from more than one individual and these data are then used to predict the pharmacokinetic parameters in other individuals. Thus the modelling can be carried out with data arising from different subjects, such as different groups of age, weight, gender, state of health, etc. The derived population pharmacokinetic

parameters actually represent population mean kinetics. These data can consequently be used to modify dosage appropriately in response to observed contaminant levels, to make rational decisions regarding the regulatory process and to examine some research problems in pharmacokinetics (Sheiner 1984). The other advantages include the flexibility of sampling times, the capability of using different toxicological information, the possibility of measuring the interindividual variability and residual variability (Sheiner 1984). In addition, these models require fewer design criteria than other methods and have few or no statistical design restrictions (Powers 1993).

The shortcomings of this class of models are mainly associated with the use of nonhomogenerous data. First, choosing the subjects can produce problems. Because the number of study subjects is usually relatively small, estimated population parameters deviate substantially from the true population values, because of the random (e.g. individual response to the contaminant) and fixed (e.g., inter-individual variability) effects and measurement errors. Second, the naive pooled data approach ignores individual differences, therefore the method can not differentiate random inter- from intra-individual variability. Finally because of the relatively large number of samples needed, the modelling effort is highly costly.

3. Two new-generation pharmacokinetic models

All classic pharmacokinetic models described above have important drawbacks and limitations. Their major difficulty lies in the number of parameters they contain and the difficulty of estimating them (Conover and Francis 1973; DiStefano and Landaw 1984). Furthermore, the validity of most models has not been tested using different biological species, body sizes and chemicals (Landrum et al. 1992). Therefore, to obtain more accurate predictions and easier assessments, the capacity of both established and new models to predict changes in contaminant concentrations resulting from absorption, distribution, metabolism and elimination needs to be established. There are two types of promising and fruitful hybrid pharmacokinetic models: allometric models and structure-pharmacokinetic relations.

3. 1. Allometric pharmacokinetic models

Allometry, the empirical examination of relationships between size and its consequences, may be an effective tool for predicting physiological rates (Peters 1983). It is assumed that the relevant measure of metabolic activity is a power function of body mass, the coefficient and an exponent of which are empirically determined. In pharmacokinetic analysis, a regression of the logarithm of the pharmacokinetic parameter (Y) on the logarithm of the body weight (W) of

animal also follows a linear function, and so enables information from one or more species to be used to predict the pharmacokinetic parameters of the contaminant in another untested species, usually humans (Chappel 1992), by the simple power equation:

$$Y = aW^b$$

where b is the allometric exponent, and a is the allometric coefficient. Several patterns in the allometric exponent have emerged. Biological frequencies tend to have an exponent of -0.25, biological times tend to have an exponent of 0.25, surface area tends to have an exponent of 0.67, clearance and physiological flow rates tend to have an exponent of 0.75, and volumes tend to have an exponent of 1.0 (Weiß et al. 1977; Peters 1983; Mordenti 1986; Mordenti and Chappell 1989). Major differences between contaminants are indicated by the magnitude of the scalar coefficient a. Basic biological similarities, such as similar anatomy, physiology, biochemistry, and fine cellular structure, are presumably the basis for this pharmacokinetic scaling.

There are two approaches to inter-species pharmacokinetic modelling: allometric and physiological. The allometric approach is based on the formulation of allometric equations which represent individual pharmacokinetic parameters (Mordenti 1986). This empirical approach is the method of choice when there is no need to determine the detailed organ distribution of the contaminant or to give physiological meanings to pharmacokinetic parameters. This approach is easy and fast, and potentially

useful because it uses data which are routinely collected and because the calculations are relatively simple.

The allometric pharmacokinetic scaling technique has drawbacks. The models assume first order pharmacokinetics in each species, linear similarity in the percentage of protein binding over the concentration range of interest, and enough data for linear regression to achieve statistical significance (Mordenti 1986). These assumptions are frequently not met in practice. Because these allometric regressions are empirically determined, they apply only to sizes with the ranges of the original data (Peters 1983). In addition, this approach can not give physiological meaning to pharmacokinetic parameters.

Numerous examples in the literature show the suitability of allometric pharmacokinetic models for organic contaminants (Peters 1983, Mordenti and Chappell 1989) and metals (Newman and Heagler 1991). Wen et al. (1994) related the measurements of overall pharmacokinetic parameters, such as uptake, excretion and intercompartmental exchange rates of phosphorus to body size in cladocerans. However, fundamental allometric pharmacokinetic models have not yet been established for most environmental contaminants. In particular, few empirical allometric equations scale pharmacokinetic parameters, such as absorption, distribution, metabolism and excretion, to organism size. Therefore there is a need to further define this potential technique by establishing empirical bases and developing toxicological

applications.

The physiological approach is based on the scale-up of physiologically based models. Physiological parameters such as tissue volume, etc, are scalable from species to species by a proportionality constant times body weight to some power. Once these studies are conducted, it may be possible to estimate the risk of toxicity in humans or other animals exposed to the same contaminant. This reductionistic approach should be used when the detailed contaminant distribution is the major focus, when the central compartment is not the action site, when the contaminant is highly soluble and extensively metabolized, when the protein binding is strong and/or nonlinear, and when pharmacokinetic values can be derived from only one animal species (Mordenti 1986). Using this approach, the models would be anatomically, physiologically, thermodynamically, and biochemically realistic, and the behavior of the contaminant under different conditions, such as dose route, disease state or animal species, would be predictable. Because of the complexity of the technique, however, this approach demands more resources and the interim models produced will fail more frequently.

3. 2. Quantitative structure-pharmacokinetic models

Mathematical models that relate some chemical, biological or environmental activity of interest to some quantitative descriptor of chemical

structure or physico-chemical property are collectively known as quantitative structure-activity relationships (QSARs). QSARs are usually developed for structural congeners. The primary objective in creating QASRs is to predict the activities of untested congeners, and also to understand better the mechanisms of action of structure under study (Kaiser 1983). Recent attempts have been made at defining the overall relationships between molecular structure and pharmacokinetics by the multiple regression equation:

$$\log P = a_0 + a_1 x_1 + a_2 x_2 + ... a_n x_n$$

where P is a pharmacokinetic parameter, a_0 , a_1 , ..., a_n are coefficients determined by a least squares analysis, x_1 , x_2 , ..., x_n are physicochemical descriptors. These models form a new branch of the QSAR paradigm referred to as quantitative structure-pharmacokinetic relationships (QSPRs; Seydel and Schaper 1982).

In QSPRs, some usual key pharmacokinetic parameters are rates of absorption, distribution, or elimination (biotransformation and excretion). The potential structural descriptors used in these studies include the number of carbon atoms, saturated vapor pressure, molecular volume, alkyl side-chain length, solubility, molecular weight, boiling point, reversed-phase thin layer chromatographic R_m value, and partition coefficient (Mailhot 1987, Mailhot and Peters 1988). Model complexity is of crucial importance in the predictor selection. On the one hand, the model should include all the state variables and the processes necessary for the problem in focus; on the other hand, the

model should not be more complex than the data set would bear.

The QSPR models are of special importance in predicting pharmacokinetic behaviour. Some promising results have emerged in drug design, toxicity testing, in understanding the mechanisms of actions of sets of congeners, in selecting and screening candidate pharmaceutical compounds in congeneric series, and in predicting biological activities quantitatively. Seydel and Schaper (1982) pointed out that several pharmacokinetic parameters varied with the chemical structure, including (1) rate of absorption, (2) apparent volume of distribution, (3) rate and type of metabolism, (4) protein binding and (5) rate and type of elimination. Because most previous studies of QSARs used only small numbers of compounds, heterogenous series of data taken from a heterogenous literature, these relationships should be used with caution. Pharmacokinetic descriptors also depend on sex, age, race, physical condition, etc. (Mayer and Waterbeemd 1985).

There are a number of pitfalls and difficulties in using QSPRs and consequently corresponding remedies are required. Firstly, because all of physicochemical parameters tend to be co-linear and most pharmacokinetic parameters are strongly correlated with lipophilicity (log octanol/water partition coefficient), collinearity between the variables are highly possible. This will increase chance correlations and decrease the dependency of some pharmacokinetic parameters on structure (Moulton 1988). Therefore, $r^2 = 0.40$ is suggested to be the minimum acceptable level of chance correlation (Chu

1979). Moreover, a large sample size is required. To test 5 independent variables requires at least 30 observations, to test 10 requires at least 40, 20 requires 65, and 30 requires 85 (Chu 1979). The principle of parsimony should be always used, i.e. all things being equal, the simplest equation is best. Secondly, even if a linear correlation is found, this relationship may only hold true in the parameter ranges studied. Extrapolation may produce errors due to non-linear relationships. Therefore, the equation should be tested outside its original data domain to establish generality and predictive utility. The multiple regression coefficient, r², which is proportional to the amount of variance explained by the equation, should be maximized, and the standard deviation should be minimized. To select the "best equation", the F-test, a measure of the probability that the results could be derived by chance, should be used. In this case, stepwise regression methods, like forward or backward elimination, are efficient tools. Thirdly, the pharmacokinetic data are often limited, for example, only plasma or urine data are generally available, which makes high statistical significance in correlations and regressions unlikely. In most literature reports, less than 60% of the observed variation was explained by the regression. Therefore, if the regression is to be biologically meaningful, experimental data should be chosen for the model development. Even if the pharmacokinetic data are quite variable (i.e., when the standard deviation is high), the determination of the structural dependence might still be possible using other statistical approaches, such as discriminant analysis, pattern

recognition or principal component analysis (Seydel and Schaper 1982). Finally, even though the QSPR analysis may produce a statistically sound equation relating structure to effect, it is often difficult to interpret the relationship biologically or biochemically. To ensure that meaningful QSPRs are obtained, it is essential that the physical-chemical data used to generate these relationships be accurate and consistent. This may be aided by the development of high performance computer technology, such as developing integrated computer programs and large data bases, applying expert systems to QSPR model construction, and the establishment of consistent sets of structural parameters and standardized surrogate testing procedures for data collection and analysis. With these precautions, it should be possible to predict model parameters with reasonable accuracy.

Despite their limitations, the QSPR modelling appears to be a promising approach to understanding and predicting the influence of chemical structure on pharmacokinetics. More reliable data on contaminant flux rates and a better understanding of the mechanism and the rate-determining steps are required if QSARs for toxicology are to be more than a "black box" tool.

4. Validation of pharmacokinetic models

The goal of pharmacokinetic modelling is prediction. Model validation is a necessary step to ensure the predictive accuracy. A model can never be proven

valid, only invalid (Peters 1991). Therefore, we need techniques and statistics for comparing validation data with model predictions. The standard statistical techniques frequently used for the validation of models include tests of means and variances, analysis of variance, goodness-of-fit testing, regression and correlation analysis, confidence interval comparisons, the chi-squared test, the Kolmogorov-Smirnov test, factor analysis and a variety of non-parametric tests (Gad and Weil 1994).

There are no absolute criteria for model correctness. In practice, the overall goodness of fit is examined by an F-test, by the scatter of the actual data points around the fitted function and by the plot of residuals against the regressor (time). The adequacy of a model is assessed by achieving a minimal sum of squared residuals, the lowest possible standard deviations of the parameter estimates, and unbiased distribution patterns of residuals in plots of observed versus predicted values. In addition, several sensitivity tests are used to detect errors in model outputs, to assess how well the predictions match measured values and to increase the degree of confidence that the events inferred by a model will in fact occur.

4.1. Evaluation of absolute performance.

In pharmacokinetic modelling, a simple measure of the accuracy of a prediction is the difference between the prediction and the measured value. If

a particular observation is represented by X_i , the actual value by T_i , and error by e_i ,

$$e_i = X_i - T_i$$

where e_i may take either positive or negative values. Then we can estimate the mean squared error (MSE) of the prediction or the root of the mean squared error (RMSE) of predictions using the following formulas:

$$MSE = 1/N \sum (e_i)^2$$

$$RMSE = \sqrt{MSE}$$

there is an ambiguity involved when the domain of the deviation between predicted and observed values is high. For example, suppose in one case the predicted and observed values are 7 and 4, respectively, and in another case they are 85 and 82. In both instances, the MSE is 9, but the prediction in later case is obviously better than the former since the percentage error is relatively small.

In regression analysis, model inaccuracy (e_i) is referred as a residual. The residual can be viewed as the deviation between the data and model predictions, and consequently is a measure of the variability not explained by the regression model. The adequacy of the model can be assessed as described earlier in fitting compartmental analysis. Therefore, analysis of residuals is an effective method for discovering the model deficiencies. Residual plots are usually used to visually diagnose the predictability of a model. To check the

normality assumption, the residuals are plotted on normal probability paper and the resulting plots should approximate a straight line. The plots of residuals against \hat{y}_i or each regressor x_i are also useful for detecting departures from normality, outliers, inequality of variance, and adequate functional specification for a regressor (Montgomery and Peck 1982).

The predictions can be also regressed on measured values. If there is significant correlation between prediction and observation, the model could be partially correct. Therefore, models should also be tested for systematic bias in the predicted values. One approach to testing this is the graphic representation of the measured values of the predicted variable and the modeled values to determine if the 1:1 line bisects the data. This approach still suffers from uncertainty since the data points may be equally distributed about the 1:1 line but still be biased. Another approach is to test whether the regression slope significantly differs from 1 and the intercept significantly differ from 0. It is better to conduct both tests (Roff 1992).

4. 2. Evaluation of relative performance

A better approach to assess the utility of a predictive model is to measure the relative performance of the predictor. This can be determined by examining the percent prediction error (%PE; Roff 1983):

%PE = (Observation - Prediction)/Observation x 100%

In this equation, the percent prediction error scales the prediction error to the measured value, and is consequently the normalized residual describing the difference between measured and predicted values. A negative prediction error indicates that the predicted value is greater than the measured value, and that the model overpredicts. A positive prediction error indicates that the predicted value is smaller than the measured value, and that the model underpredicts.

Bias is an indication of the systematic over- or underestimation of the predicted value. The estimated bias is calculated as:

Bias =
$$1/n \sum E_i$$

where n is the number of measurements, and E_i is the i-th prediction error. The directional bias is indicated by the negative or positive sign of the prediction error and, thus, does not provide information about the average size of the prediction error if there are both over- (negative) and under- (positive) predictions. The influence of the sign can be avoided by using the mean absolute prediction error (APE) as follows:

$$APE = 1/n \sum |E_i|$$

where $|E_i|$ is the absolute value of each prediction error. The mean absolute prediction error is not influenced by the positive or negative sign of the prediction error and thus represents the typical magnitude of the prediction error. Parametric (e.g. t test) or nonparametric tests (e.g. sign test) are used to test whether the mean bias is different from zero. The mean bias should approximate zero if the predictive equation is unbiased. If the data

distributions are asymmetrical, the median prediction error, the median absolute prediction error, and 10th, 50th and 90th percentiles of the E_i's will be calculated. The hypothesis that the median prediction error differs from zero can be tested using statistics such as the Wilcoxon signed rank test.

In regression analysis, the performance of a predictive equation is often evaluated by an index of goodness of fit (r) and confidence intervals. The correlation coefficient (r) describes the strength of the association between the two sets of data. However, r alone can be quite misleading, as it does not assess actual closeness of the predictions to true values. If there is a systematic over- or underprediction, the correlation between prediction and true values would be perfect. However, the predictions would not predict effectively (Peters 1983). Moreover, no correlation provides insight in the underlying mechanisms or functional relationships (Peters 1991).

Confidence limits give a plausible range for the true values of certain measures of predictive ability. However, the confidence limits may be very large if sample size is small or the deviations from the regression are substantial (Peters 1983). This will increase the probability of a type II error or in extreme cases make the prediction practically meaningless.

5. A philosophical view of pharmacokinetic modelling

Due to the urgent challenges of environmental management and protection,

the predictive approach has gained growing attention (Peters 1986). The interrelatedness of environmental problems requires a modelling philosophy which can deal with dynamic and complex phenomena and meet the coming needs for decision support about environmental issues. Some pharmacokinetic phenomena are predictable from current theory (Boxenbaum 1992). However, at present, most predictive models in general, and pharmacokinetic models in particular, have not been evaluated as predictive devices, but only as self consistent mathematical systems (Peters 1991). The purpose of this section is to show the relations between the mathematical formalism and philosophical knowledge, and to indicate the potential problems of pharmacokinetic modelling for gaining knowledge in toxicology.

Any part of the nature is unique: it has its specific characteristics. If we want to forecast the future events, we need to generalize and abstract these singular aspects of reality. The forms of abstraction determine which aspects of nature we find to be important. In this process, the degree of abstraction introduces error and bias. Because of the difference between reality and our perception of it, the determination of actual states (i.e. the size of a variable) can only be performed with limited precision, leaving a certain degree of uncertainty (Sattler 1986), and a model can be only the oversimplification of reality. This is especially so in pharmacokinetics. Since most pharmacokinetic variables are quantitative (in terms of data), our interpretation of the distinction between subject and object, between an inner mental world and an

outside reality will change with our understanding of the natural processes. Although pharmacokinetic models may finally reach a reasonably satisfying coincidence between a real process and its abstract representation, whether this process of abstraction has led to suitable results with respect to reality is open to question. In most studies in the pharmacokinetic modelling literature, predictive validation is ignored. Therefore we rely on philosophical criteria to examine the performance of pharmacokinetic models.

Statistical validation is a necessary step for model acceptance (Mayer and Butller 1993). This process measures the agreement between observed and simulated values to compare the model's predictions with the real world and to determine whether the model is suitable for its intended purpose. The greater the commonality between the simulated and experimental data, the higher the level of confidence for using the model in decision making. A lack of fit constitutes strong grounds for rejecting or at least amending the model. A wide variety of techniques have been employed to assess models. Among visual techniques, observed vs. predicted plots have good diagnostic capabilities. Among the statistical tests, some simple statistics, such as tests of means and variances, analysis of variance, goodness-of-fit testing, regression and correlation analysis, confidence interval construction, etc., can provide most of the required information. There are no absolute criteria to measure model adequacy. They vary with the potential applications and users of the models.

Good statistical power merely establishes the fact that there is no reason to reject the model on the basis of data in hand. In fact, no amount of data can ever prove a model; all that we can hope is that they do not disprove it (Power 1993). This is because (1) a range of potential errors and problems exists and weakens the overall process of validation; (2) type I and type II statistical errors, nonlinearities and the stochasticity of nature make correct predictions less likely; (3) important variables may be overlooked or ignored, and measurements can be biased; (4) correlations can arise for spurious or accidental reasons, and (5) regression analysis can be affected by multiple causality or multicollinearity. Moreover, the choice of regression model and predictor variables depends more upon the modeller rather than on specifically defined pharmacokinetic laws. Nowadays, powerful computers and sophisticated programs are available for fitting data rapidly to many mathematical functions with an arbitrary accuracy. This being so, high descriptive power does not necessarily confer a high degree of confidence that the events inferred by a model will in fact occur. For instance, adding a sufficient number of arbitrary parameters to multicompartment models or PBPK models will produce good fits quite independant of representing reality.

Another important check on the validity of a pharmacokinetic model is to see if the model's prediction is consistent with current theory. Because theory is a hypothesis or a set of hypotheses that has presumably stood the test of a wide range of experimental attempts to falsify it, passed several reviews and modifications and gained a certain level of acceptability, theory embodies more generality than a specific model, in particular with respect to explanation. If a theory can be translated into a model, the model can then be used for some specific, often practical, purposes, and can serve to synthesize current knowledge about some concrete objects (Fagerstrom 1987).

All theories remain open to doubt because they are mental constructions and cover only limited areas of the universe. If the theory changes, the model may become invalid. In addition, it is often difficult to derive predictive models from theory, because there are so many theories and we do not know how to choose which ones are "correct" (i.e., work in prediction) and which ones are not (Peters 1980). Some theories that are demonstrably wrong are still retained, because they have dominated thinking for a long time or are useful in practice. For instance, although one-compartment models have been demonstrated to cause error in kinetic analysis numerous times (Shipley and Clark 1972; Conover and Francis 1973, Wen et al. 1994), they are still common in the pharmacokinetic literature. Consequently, we have to tighten the link between the application of the theory and the testing of that theory in model assessment.

It is also a common practice to test a model's validity by comparison with empirical data (Peters 1986). Data may be thought to be clean and pure; they are seen as "hard facts" and considered as the objective basis for knowledge. However, this view is untenable for two main reasons. Methodologically

because data are produced with the aid of scientific tools which rely on pieces of scientific theory, they are as uncertain as the combined contribution of uncertainty from the theories used to produce those tools. As a consequence, they are open to reinterpretation within the constraints set by the accuracy of these aids. Psychologically because the act of perception is guided and constrained by the limitations of our minds, we do not report what we would see with mindless eyes, but we report rather what we think we have seen. What we think is easily influenced by predominant theory, prejudices, previous experience, moral and ideological streams (Sattler 1986). Although these uncertainties can be minimized, they can not be eliminated. Consequently new techniques, such as semantical networks, fuzzy set systems, expert systems and the development of methods to combine different techniques, should be used to help us to work with errors and uncertainties. At the same time, we have to recognize the limit of model predictability. Dedrick (1973) pointed out that some physiological processes in animals such as chemical reactions or active transport are fundamentally unpredictable. If we ignore this limitation, we may spend our whole lives falsifying hypotheses and only to learn nothing about nature in the end.

Pharmacokinetic models can not predict anything that was not built into them. The only task a model can do is to forecast the full range of possibilities set by formal assumptions (Lehman 1986). It can not provide any clue where to look for unpredicted results. For example, physiologically based

pharmacokinetic models can accurately predict contaminant distributions in the tissues studied, but they can not foretell the contaminant distribution in the tissues not included in the model. Clearly in the predictive enterprise, models should be checked against their biological entities. However, it is also necessary to take the limits of predictive power into consideration. The biological object is very complicated and highly variable from individual to individual, because many internal and external factors are working interactively thereby influencing the outcome or response.

Progress in pharmacokinetic modelling does not only involve improved fits to equations, but also holistic understanding of the whole body system (Boxenbaum 1992). Because of the complexity of an organism, it is unlikely that we can find system properties by connecting a series of component processes or models. This restriction is especially strong in compartment models and physiologically based pharmacokinetic models, which simulate the whole system through an appreciation of its component parts. Holistic properties are more likely to be found by directly investigating the organism itself as a whole. Our way of looking at the whole system behaviour can be entirely different from the way we look at the components. Thus we need an holistic, hierarchial, dynamic approach to evaluate the utility of pharmacokinetic models in the context of the appropriate biological systems. The network of interactions has to be understood as a whole if we want to describe the chains of effects which are responsible for the behaviour of whole

organisms. By doing so, we may gain a better understanding of the underlying pattern and model-observation correspondence, and we may uncover new processes, previously unknown relationships and "hidden" variables which will lead to new hypothesis, more studies and different models. The future of pharmacokinetic modelling may be expected to combine different approaches to compensate for the limitation of each individual approach.

6. Conclusions

Pharmacokinetic models have increasingly served as valuable tools for prediction of the time-course of contaminant concentration in specific tissues of interest, and provide a basis for comparison of kinetic data across species. The most promising pharmacokinetic models are two- and three-compartment models in which the body is represented as an interconnected network of a small number of kinetic compartments. Such models can describe the dynamics of the various contaminants reasonably well and are widely used in analyzing toxicological fate of environmental contaminants. However, these models have no anatomical boundaries or physiological characteristics and so provide no a priori basis for interspecies scaling. The choice of number of compartments depends usually on the type of contaminant, its physio-chemical properties, the purpose of the model and the accuracy expected. The use of different models will produce considerable differences in the numerical values of the kinetic

parameters.

Physiologically based pharmacokinetic models are constructed to conform to anatomical reality. They define an organism in terms of its anatomy, physiology and biochemistry, and can be used to predict contaminant accumulation in blood and tissues. The advantages of these models are their capacities to explain observations, to make reasonable predictions and to extrapolate experimental data across species, doses and routes of administration in risk assessments. Such models are highly desirable for toxicology. However, these models are highly complex, the experimental data for the model fitting are difficult to acquire, and the operation of the models are more time consuming and costly than traditional compartmental models.

Two new generations of models appear to be promising: the allometric pharmacokinetic models and quantitative structure-pharmacokinetic models. In allometric pharmacokinetic models, two approaches are currently used: one empirical and holistic, and other reductionistic and mechanistic. The empirical approach regresses the logarithm of the pharmacokinetic parameter on the logarithm of body weight of the animal. The resultant model can be used to make a priori predictions of pharmacokinetic parameters in any animal species from body weight. The reductionistic approach examines individual subcomponents which interrelate to produce the characteristics of the whole system extrapolating from one species to another. Both approaches permit us to extrapolate outside the range of data with some confidence, if the

mechanisms of transport are well known.

Quantitative structure-pharmacokinetic relationships (QSPRs) enable the pharmacokinetic parameters, such as contaminant absorption, distribution and elimination, to be predicted from physicochemical properties of the contaminant. The most commonly used method of developing such relations is linear multiple regression analysis. Therefore QSPRs suffer from all the shortcomings of regression analysis. These models are of considerable interest to toxicologists, because this quantitative approach may contribute to the development of real predictive toxicology.

Validation of the predictive capability of pharmacokinetic models is a significant step toward model acceptance. Quantifying error is an important component of the model description and first stage in validation. Several validation techniques assess the closeness of predictions to measured values. Statistical techniques provide us with the means to assess the utility of a model and provide guidance as to which parameters and modelling assumptions may be in error and therefore need further investigation. Examination of model sensitivity is of enormous importance for the quality of pharmacokinetic models as well. Among available measures, the mean squared prediction error and the mean prediction error provide widely used bases for evaluation of predictive performance. In addition, visual techniques, such as observed vs. predicted plots, have superior diagnostic capabilities.

All the abbreviations and symbols are summerized in Talbe 1.

Table 1, Abbreviations and symbols used to describe the pharmacokinetic model.

Symbol	Definition
а	Scaling equation constant
ь	Scaling equation power constant
W	Body weight
C_0	Initial chemical concentration after disposition started (one-compartment model)
$\mathbf{C_t}$	Chemical concentration at time t during elimination phase (one-compartment model)
A ₁ , A ₂	Compartment size for compartment 1, 2 during uptake
$\mathbf{C_1}$, $\mathbf{C_2}$	Compartment size for compartment 1, 2 during release
$\mathbf{k}_{\mathbf{up}}$	Uptake rate constant (one-compartment model)
\mathbf{k}_{el}	Release rate constant (one-compartment model)
$\mathbf{k_1}$	Rate constant for compartment 1
k_2	Rate constant for compartment 2
k_{01}	Uptake rate constant
k ₁₂	Flux rate constant from compartment 1 to compartment 2
k_{21}	Flux rate constant from compartment 2 to compartment 1
k ₁₀	Elimination rate constant
F_{01}	Uptake rate
F ₁₂	Flux rate from compartment 1 to compartment 2
F_{21}	Flux rate from compartment 2 to compartment 1
F ₁₀	Elimination rate
K _{ow}	Partition coefficient

7. Objectives

The overall objective of present thesis is to use allometric pharmacokinetic modelling and Quantitative Structure-Pharmacokinetic Relationships to predict pollutant flux rates in limnoplankton. To achieve this goal, I chose phytoplankton and zooplankton as model species to demonstrate the predictability of these ecologically important processes in aquatic ecosystems. Plankton was used because it is a point of entry of pollutants into the food web of aquatic ecosystems and the biosphere (Mailhot 1987; Mailhot and Peters 1991; Richer and Peters 1993), and also because their small size and rapid kinetics facilitates study within a limited time frame. The main model pollutants I studied were phosphorus and 22 organic chemicals. Phosphorus was chosen because it is ecologically important as the nutrient that most commonly drives the lake eutrophication (Rigler 1973). The organic chemicals were studied because they are now globally distributed in the environment, considered as priority pollutants and of particular environmental concern. Therefore they provide a contrast with phosphorus. The specific aims of this study were twofold: to establish an allometric pharmacokinetic model to predict uptake, distribution and excretion of phosphorus by phyto- and zooplankton; and to develop quantitative structure-pharmacokinetic relationships to predict the uptake and excretion rates of organic pollutants by an alga Chlorella pyrenoidosa and a crustacean Daphnia magna.

References

- Balant, L. P., and M. Gex-Fabry. 1990. Physiological pharmacokinetic modelling. Xenobiotica 20: 1241-1257.
- Barron, M. G., G. R. Stehly, and W. L. Hayton. 1990. Pharmacokinetic modelling in aquatic animals. I. Models and concepts. Aquat. Toxicol. 18:61-86.
- Boxenbaum, H. 1992. Pharmacokinetics: philosophy of modelling. Drug Metab.

 Rev. 24: 89-120.
- Boxenbaum, H. G., and R. W. D'souza. 1990. Interspecies pharmacokinetic scaling, biological design and neoteny. Adv. Drug Res. 19: 139-196.
- Boxenbaum, H. G., S. Riegelman, and R. M. Elashoff. 1974. Statistical estimations in pharmacokinetics. J. Pharmacokin. Biopharm. 2: 123-148.
- Buffington, D. E., V. Lampasona, and M. H. H. Chaudler. 1993. Computers in pharmacokinetics. Clin. Pharmacokinet. 25: 205-216.
- Cairns, J., Jr., and D. I. Mount. 1990. Aquatic toxicology: Part 2 of a four-part series. Environ. Sci. Technol. 24: 154-161.
- Chappell, W. R. 1992. Scaling toxicity data across species. Environ. Geochem.

 Health 14: 71-80.
- Chappell, W. R., and J. Mordenti. 1991. Extrapolation of toxicological and pharmacological data from animals to humans. Adv. Drug Res. 20: 1-116.

- Chu, K. C. 1979. The quantitative analysis of structure-activity relationships.

 In The basis of medicinal chemistry, 4th ed. Ed by M. E. Wolff. pp 393-418. John Wiley, N.Y.
- Clark, B.and D.A. Smith, 1984. Pharmacokinetics and toxicity testing. CRC Crit. Rev. Toxicol. 12, 343-385.
- Cockerham, L. G., and B. S. Shane. 1994. Basic Environmental Toxicology.

 CRC Press, Boca Raton, FL. 627 p.
- Conover, R. J., and V. Francis. 1973. The use of radioactive isotopes to measure the transfer of materials in aquatic food chains. Mar. Biol. 18: 272-283.
- Dedrick, R.L., 1973. Animal Scale-up. J. Pharmacok. Biopharm. 1, 434-461.
- DiStefano, J. J. III., and E. M. Landaw. 1984. Multiexponential, multicompartmental, and noncompartmental modeling. I. Methodological limitations and physiological interpretations. II. data analysis and statistical considerations. Am. J. Physiol. 246, R651-664, R665-677.
- Dixon, W. J. 1988. BMDP Software Manual. Berkeley: University of California Press.
- Fagerstrom, T. 1987. On theory, data and mathematics in ecology. Oikos 50: 258-261.
- Gad, S. C., and C. S. Weil. 1994. Statistics for toxicologists. p221-274. In Principles and methods of toxicology. 3rd ed, A. W. Hayes (ed.). Raven Press, ltd. New York.

- Gerlowski, L. E., and R. K. Jain. 1983. Physiologically based pharmacokinetic modeling: principles and applications. J. Pharm. Sci. 72: 1103-1127.
- Gibaldi, M., and D. Perrier. 1982. Pharmacokinetics, 2nd ed. Marcel Dekker,
 Inc. New York/Basel.
- Himmelstein, K.J. and R.J. Lutz, 1979. A review of the applications of physiologically based pharmacokinetic models. J. Pharmacok. Biopharm. 7:127-145.
- Ings, R. M. J. 1990. Interspecies scaling and comparisons in drug development and toxicokinetics. Xenobiotica 20: 1201-1231.
- Jacquez, J. A. 1985. Compartmental Analysis in Biology and Medicine. 2nd ed.

 Thse University of Michigan Press, Ann Arbor.
- Kaiser, K. L. E. 1983. QSAR in environmental toxicology. D. Reidel Publishing Company.
- Karara, A. H., and W. L. Hayton. 1984. Pharmacokinetic model for the uptake and distribution of di-2-ethylhexyl phthalate in sheepshead minnows

 Cyprinodon variegatus. Aquat. Toxicol. 5: 181-195.
- Krishnan, K, and Andersen, M. E. 1994. Physiologically based pharmacokinetic modeling in toxicology. p 143-188. In Principles and methods of toxicology. 3rd ed, A. W. Hayes (ed.). Raven Press, ltd. New York.
- Landrum, P. F., H. Lee II., and M. J. Lydy. 1992. Toxicokinetics in aquatic systems: Model comparisons and use in hazard assessment. Environ.

 Toxicol. Chem. 11: 1709-1725.

- Lehman, J. T. 1986. The goal of understanding in limnology. Limnol. Oceanogr. 31: 1160-1168.
- Leung, H-W. 1991. Development and utilization of physiologically based pharmacokinetic models for toxicological applications. J. Toxicol. Environ. Health. 32: 247-267.
- Mailhot, H. 1986. The use of some physico-chemical properties to predict algal uptake of organic compounds. M. Sc. thesis. McGill University, Montreal, Quebec, Canada.
- Mailhot, H., and R. H. Peters. 1991. Short-term sorption of chlorinated benzenes by concentrated seston. Verh. Internat. Verein. Limnol. 24: 2302-2306.
- Mayer, D. G., and D. G. Butller 1993. Statistical validation. Ecol. Modelling 68:21-32.
- Mayer, J. M., and H. Waterbeemd. 1985. Development of quantitative structure-pharmacokinetic relationships. Environ. Health Perspect. 61: 295-308.
- Menzel, D. B. 1987. Physiological pharmacokinetic modeling: second of a fivepart series on cancer risk assessment. Environ. Sci. Technol. 21: 944-950.
- Metzler, C. M. 1981. Estimation of pharmacokinetic parameters: statistical considerations. Pharmac. Ther. 13: 543-556.
- Montgomery, D. C., and E. A. Peck. 1982. Introduction to linear regression

- analysis. John Wiley & Sons, N.Y..
- Mordenti, J. 1986. Man versus beast: pharmacokinetic scaling in mammals. J. Pharm. Sci. 75: 1028-1040.
- Mordenti, J., and W. Chappell. 1989. The use of interspecies scaling in toxicokinetics. p42-96. In Toxicokinetics and new drug development, Yacobi, Y., J. Skelly, and V. Batra, (eds). Pergamon Press, New York.
- Moriarity, F. 1985. Ecotoxicology. The Study of Pollutants in Ecosystems, 3rd ed. Academic Press, San Diego, California.
- Moulton, M. P. 1988. Regression analysis in QSAR: potential pitfalls in modeling polar narcotic phenols. in: Turner, J. E., M. W. England, T. W.
- Schultz, and N. J. Kwaak. (eds.), QSAR88, Proceedings of the Third

 International Workshop on Qantitative structure-Activity Relationships
 in Environmental Toxicology, Oak Ridge TN 1988, pp. 1-9.
- Newman, M. C., and M. G. Heagler. 1991. Allometry of metal bioaccumulation and toxicity. p91-130. In: Metal ecotoxicology, concept and applications,
- Newman, M. C., and A. W. McIntosh, (eds). Lewis Publishers, Michigan.
- Nüesch, E. A. 1984. Noncompartmental approach in pharmacokinetics using moments. Drug Metab. Rev. 15: 103-131.
- Peters, R. H. 1980. Useful concepts for predictive ecology. p215-227. In Conceptual issues in ecology. E. Saarinen (ed.). D. Reidel, Dordrecht.
- Peters, R. H. 1983. Ecological implications of body size. Cambridge University Press, Cambridge.

- Peters, R. H. 1986. The role of prediction in limnology. Limnol. Oceanogr. 31: 1143-1159.
- Peters, R. H. 1991. A Critique for Ecology. Cambridge University Press,

 Cambridge.
- Power, M. 1993. The predictive validation of ecological and environmental models. Ecol. Modelling 68: 33-50.
- Powers, J. D. 1993. Statistical considerations in pharmacokinetic study design.

 Clin. Pharmacokinet 24: 380-387.
- Renwick, A. G. 1994. Toxicokinetics Pharmacokinetics in toxicology. p 101-147. In Principles and methods of toxicology. 3rd ed, A. W. Hayes (ed.).

 Raven Press, ltd. New York.
- Riggs, D. S. 1963. The mathematical approach to physiological problems.

 Wilkins.
- Roff, D. A. 1983. Analysis of catch/effort data: a comparison of three methods.

 Can. J. Fish. Aquat. Sci. 40: 1496-1506.
- Roff, D. A. 1992. The Evolution of Life Histories: Theory and Analysis.

 Chapman & Hall, New York.
- Rowland, M. 1984. Physiologic pharmacokinetic models: relevance, experience, and future trends. Drug Metab. Rev. 15: 55-74.
- Rowland, M. 1985. Physiologic pharmacokinetic models and interanimal species scaling. Pharmac. Ther. 29: 49-68.
- SAS Institute Inc. 1983. SAS/STAT User's Guide. Release 6.03 edition. Cary,

- NC: SAS Institute.
- Sattler, R. 1986. Biophilosophy: Analytic and Holistic Perspectives. Berlin: Springer-Verlag.
- Segre, G. 1982. Pharmacokinetics-compartmental representation. Pharmac.

 Ther. 17: 111-127.
- Segre, G. 1984. Relevance, experiences, and trends in the use of compartmental models. Drug. Metab. Rev. 15: 7-53.
- Seydel, J. K., and K.-J. Schaper. 1982. Quantitative structure-pharmacokinetic relationship and drug design. Pharmac. Ther. 15: 131-182.
- Sheiner, L. B. 1984. The population approach to pharmacokinetic data analysis: rationale and standard data analysis methods. Drug Metab. Revs. 15: 153-171.
- Shipley, R. A., and R. E. Clark. 1972. Tracer methods for in vivo kinetics: theory and applications. Academic Press, New York and London.
- Spacie, A., and J. L. Hamelink. 1982. Alternative models for describing the bioconcentration of organics in fish. Environ. Toxicol. Chem. 1: 309-320.
- Wagner, J. G. 1975. Fundamentals of clinical pharmacokinetics. Drug
 Intelligence Publications. Hamilton, III. IL.
- Weiβ, M., W. Sziegoleit and W. Forster. 1977. Dependence of pharmacokinetic parameters on the body weight. Int. J. Clin. Pharmacol. 15: 572-575.
- Wen, Y. H., A. Vézina, and R. H. Peters. 1994. Phosphorus fluxes in limnetic cladocerans: coupling of allometry and compartmental analysis. Can. J.

- Fish. Aquat. Sci. 51: 1055-1064.
- Wen, Y. H., A. Vézina, and R. H. Peters. 1996. Allometric scaling of phosphorus flux in freshwater algae. Limnol. Oceanogr. (in press).
- Zierler, K. 1981. A critique of compartmental analysis. Annu. Rev. Biophys. Bioeng. 10: 531-562.

CHAPTER I

Allometric Scaling of Compartmental

Fluxes of Phosphorus in Freshwater Algae*

^{*} In press in Limnology and Oceanography

Abstract

The time courses of uptake, distribution and excretion of radioactive PO4 were determined for eleven species of freshwater algae. Uptake of PO₄ by algae was rapid, reaching a steady state asymptote within an hour and maintaining that maximum for at least 10 h. Uptake could be described as a biphasic exponential function. The rate constants for uptake decreased with cell volume raised to a power close to -0.25, while the uptake rates per cell increased with cell size to a power similar to 0.75, suggesting that small cells were much more efficient at sequestering PO₄. Excretion of PO₄ by algae was fast over the first 10 to 20 min; thereafter there was a slower prolonged loss for the remaining period of experiments. A two-compartment model could be convincingly fitted directly to the excretion time-course data. Both rate constants and flux rates of PO₄ excretion and intercompartmental exchanges showed a similar size dependency to those of PO_4 uptake. The net uptake of PO_4 by algae increased proportionately to cell volume raised to a normalized power of 0.75. The allometric compartment model yielded estimates for net PO_4 uptake rates one order of magnitude higher than the Michaelis-Menten model.

Introduction

Phosphate (PO₄) uptake is thought to be the principal pathway of phosphorus (P) accumulation by algae (Lean 1973). Because ${\rm PO_4}$ uptake is mediated by an algal enzyme system, the rate parameters are traditionally estimated by the Michaelis-Menten equation. Since this model describes the PO4 uptake velocity as a function of external substrate concentrations, it requires steady state conditions in which PO₄ concentrations do not change significantly over the course of incubation (Dodds 1995; Istvánovics and Herodek 1995). Many more recent studies have demonstrated that actual PO_4 uptake kinetics deviate considerably from this formalism (Brown et al. 1978; Li 1983; Tarapchak and Herche 1986), probably because PO₄ uptake is multiphasic, and ceases when the external phosphate concentration falls below some threshold level, so PO4 uptake does not follow the rectangular hyperbolic relationship described by Michaelis-Menten equation. Methodological difficulties in measuring low ambient substrate concentrations (Bentzen et al. 1992; Nürnberg and Peters 1984) also seriously affect the reliability of the results. Moreover, some of the kinetic parameters for this model may be difficult to estimate (Dodds 1995) and their accuracy and precision can be markedly influenced by the fitting techniques, data transformation, experimental design (Currie 1982; Bentzen and Taylor 1991) and algal size (Suttle and Harrison 1988; Suttle et al. 1988, 1991). Auer and Canale (1982)

further pointed out that the magnitude of the kinetic parameters for PO_4 uptake varied among algal species, and with their physiological state. As a consequence, the parameter values for algal PO_4 uptake kinetics using simulated, laboratory and in situ data are rather paradoxical, varying 1000-fold for K_m and 10000-fold for V_{max} (Cembella et al. 1984). It becomes imperative that alternative models be pursued (Istvánovics and Herodek 1995).

Algae could excrete as much as 20% of P assimilated from the ambient waters (Kuenzler 1970). The excretory product, which is mostly PO₄ (Lean 1973), is readily available to the plankton. Therefore, an estimate of PO₄ excretion by algae can provide quantitative information on both net P accumulation in algae and algal contributions of P to aquatic food webs. However, our knowledge of both PO₄ excretion by algae and the relative importance of this P release to other organisms remains rather fragmentary. Hence there is a decades-long controversy about the relative contributions of bacterioplankton, phytoplankton and zooplankton to total P flux.

Statistical description has proven a useful tool for quantifying many aspects of metabolism for many organisms. The most efficient empirical relation is often a power function of body size: rate = $a(\text{size})^b$. The exponents (b-values or slopes) for allometric models of metabolic rates tend toward 0.75 (Peters 1983). Because phytoplankton span a 10^8 -fold weight range (Vézina 1986), a general description of the size-dependent relationships of PO₄ uptake and excretion kinetics should be possible. However, the exponents of size

dependence of PO₄ uptake and excretion by algae have not yet been extensively defined (Smith and Kalff 1982; Vézina 1986).

In a previous study (Wen et al. 1994), we demonstrated that a two-compartment, first order equilibrium model (Fig. 1) would satisfactorily describe PO₄ uptake, distribution and excretion in cladocerans, and derived a series of significant size-dependent models for the underlying kinetic parameters. This technique has not been applied to phytoplankton. In this study, our primary motivation is to further explore the applicability of that approach to algal PO₄ uptake and excretion rates and so to establish its greater generality. We measured algal PO₄ uptake and excretion in a series of laboratory experiments involving ³²P-PO₄ flux to and from freshwater algae, spanning a wide range in cell size. These data were fit by compartmental analysis of each algal species, and the rate parameters were then scaled to organism size. By comparing the allometric relations, we hoped to test the wider applicability of the zooplankton P flux models and their descriptions of the size dependence of P uptake and excretion in other lake organisms.

Materials and methods

Reagents and glassware - Carrier-free ³²P-PO₄ was purchased from New England Nuclear (specific activity = 60 Ci mMol⁻¹). Distilled-deionized water was used in preparing stock solutions and culture media, and all chemicals

used for preparation of stock solution met ACS standards of chemical purity. Glassware used in all chemical analyses was washed with phosphate-free detergent, rinsed three times in distilled, deionized water, and oven-dried before use. All glassware, fittings and media used for algal cultivation were sterilized by autoclaving.

Algal cultures - Eleven strains of freshwater algae (Anabaena flos-aquae, Ankistrodesmus falcatus, Carteria olivieri, Chlamydomonas Sp., Chlamydomonas moewusii, Chlorella vulgaris, Closterium Eremosphaera viridis, Golenkinia minutus, Scenedesmus quadricauda, Staurastrum gracile), with cell or colony volumes varying from 59 to 2x10⁷ um³, were originally obtained from the Carolina Biological Supply Co. (Burlington, N.C.). Stock cultures of all species were maintained in cottonstoppered 250-mL flasks with Alga-gro medium in a thermally controlled incubator (20 °C), illuminated by cool-white fluorescent lights (100 µEinst m ²S⁻¹) set to cycle from 18 h light to 6 h darkness. To ensure that algae rapidly take up PO4 and that the experimental conditions more closely approach natural environments, we used P-limited batch cultures for algal PO_4 uptake and excretion experiments. Three or 4-mL portions of dense stock culture were centrifuged, washed twice with P-free growth medium, resuspended in a small volume of culture medium, inoculated into 500 mL flasks of newly sterilized, low phosphate (0.323 µM), synthetic medium (Morgan 1976), and incubated under the same light and temperature conditions in which the stock culture

was grown.

Growth monitoring - The growth of the monoalgal cultures was monitored by daily haemocytometer cell counts or in vivo chlorophyll concentrations until stationary phase was reached. During the exponential phase of growth, three 5-mL subsamples were withdrawn from the flasks to measure cell density and volume, chlorophyll-a concentration, particulate P content and cell P content. Small species, such as G. minutus and A. falcatus, were counted with an improved Neubauer haemocytometer under a Zeiss binocular microscope. For large species, such as A. flos-aquae and E. viridis, three 1-mL aliqots of the batch culture were filtered onto 47-mm 0.45-µm HA Millipore filters. The filters were subsequently cleared with immersion oil and the algae were counted under a microscope. Cell size or volume (V, $\mu\text{m}^3)$ was calculated from the geometrical formula: $V = 4/3 \pi LW^2$, where L is half of the average maximum length and W is half of average maximum width measured with an ocular micrometer (n = 20 - 30). Chlorophyll a concentration was measured with a Turner Design fluorometer (primary filter #5543 and secondary filter #2408). P concentrations of the culture medium filtered through a 0.3-um Nuclepore membrane filter and those of the total culture were determined by the ascorbic acid modification of the molybdenum blue technique (Strickland and Parsons 1968) after digestion with potassium persulfate under pressure (Menzel and Corwin 1965). Algal P content was calculated by subtracting the P concentration of filtrate from that of the total culture. Cellular P content was

estimated as the algal P content + mean cell density.

Periodic checks for bacterial and fungal contamination of the cultures were made by inoculating sterile medium with algal culture. Contaminated cultures were discarded.

P uptake - Time-course measurements of PO4 uptake by algae were conducted using a ³²P tracer incorporation method. Prior to culture harvest, 50-mL replicates of batch culture in exponential phase were dispensed into 125-mL Erlenmeyer flasks. The final density of algal cells was adjusted with culture medium to between 25 and 6.8×10^5 cells ml⁻¹ to maintain roughly constant total biovolumes. Each flask was then aseptically spiked with ca. 100 KBq of ³²P-PO₄ radioactive tracer, and mixed briefly with a magnetic bar stirrer. These flasks were incubated under the same light conditions and temperature as the batch cultures. Duplicate 1-mL aliquots of radioactive culture were withdrawn by pipet and filtered through 25-mm 3-µm Nuclepore filters immediately and then at geometrically increasing time intervals. The algae-laden filters and the aqueous samples were transferred into plastic counting vials, mixed with a 10-mL Aquasol scintillation cocktail (New England Nuclear), capped and assayed for ³²P activity in a Beckman Model LS-150 or LKB Wallac liquid scintillation counter. In all cases, counting error was maintained to ±2%. No correction for quenching was made because of its tiny quantity.

The resulting cellular ³²P activities were plotted against time for each

species. The time-course of the algal radioactivities was then fit to a two-compartment uptake model:

$$A_t = A_1 [1-\exp(-b_1 t)] + A_2 [1-\exp(-b_2 t)]$$
 (1)

where A_t is the radioactivity measured in algal cells at time t, A_1 and A_2 are the maximal activities incorporated in "metabolic" and "structural" compartments (cpm mL⁻¹), and b_1 and b_2 are rate constants (per min) of the two compartments. Because in our model, PO_4 is taken up by the metabolic compartment, the uptake rates of PO_4 (v_{gross} , μ M cell⁻¹ min⁻¹) can be estimated by the equation of Lean and Nalewajko (1976):

$$v_{gross} = [PO_{4 \text{ solution}}] \times b_1$$
 (2)

Where $[PO_{4 \text{ solution}}]$ is the PO_{4} concentration in the culture medium (μM) prior to the addition of the tracer.

Because phosphate at low concentration in the culture medium can not be reliably measured (Bentzen et al. 1992), a plausible estimation of PO₄ concentration in the medium is necessary. Lean and Nalewajko (1976) indicated that PO₄ was rapidly exchanged between algal cells and culture medium and could be approximately estimated by

$$[PO_{4 \text{ solution}}] = [P_{added}] \times (^{32}P-PO_{4}/Total ^{32}P)$$
 (3)

where $[P_{added}]$ is the initial phosphorus concentration added in the culture medium, and $^{32}P-PO_4/Total$ ^{32}P is the phosphate equilibrium ratio. In the laboratory cultures, they demonstrated that, on average about 0.61% of the total ^{32}P added existed as $^{32}PO_4$ in the culture medium after the asymptote

level was reached. This percentage was adopted in our calculation of PO_4 uptake rates.

P excretion - Algae used for excretion were counted, sized and exposed to \$\$^{32}PO_4\$-spiked culture medium. Subsequently, at intervals, two 5-mL aliquots of the cell suspension were collected to analyze the uniformity of \$^{32}P\$ label in two major compartments. One of the aliquots was directly measured for total P (TP) and radioactivity, and the other was centrifuged at 2000 g for 15 min. The supernatant liquid was discarded. The pellets were resuspended in 5-mL of ice-cold 10% trichloroacetic acid (TCA), centrifuged for 10 min and the supernatant analyzed for TP and radioactivity as well. The \$^{32}P^{-31}P equilibrium of the algal cells was assessed by comparing the total activity of the whole cells with that of the last supernatant. When algae were completely labelled, the specific activity of the whole cells should equal that of the TCA extracts. The results indicated that cells were fully labelled after one day exposure, but all our cultures were labelled for at least 3-5 days before excretion rates were measured to ensure complete labelling.

To determine the excretion rate, a suspension of homogeneously labelled algal cells was injected into a 25-mm diameter flow-through excretion chamber. The cells were retained without apparent mechanical damage in the column (Phamacia Fine Chemicals) with 3-µm screens fitted to the adapter. The experiment began by pumping unlabelled sterile culture medium at a rate of 1-mL min⁻¹ into the top of the column with a Buchler peristaltic pump, and

draining the labelled solution from the bottom of the column. The eluent was fractionated at set intervals and collected with an LKB automatic fraction collector. ³²P radioactivity was measured by Cerenkov liquid scintillation spectrometry as previously described (Wen et al. 1994). The efficiency of Cerenkov counting relative to that determined with Aquasol was 30.8±0.8%.

The release curves were constructed from the time courses of radioactivities in the washout. The first-order two-compartment open model (Fig. 1) was fit to the ³²P release data:

$$C_t = C_1 \exp(-k_1 t) + C_2 \exp(-k_2 t)$$
 (4)

where C_t is the total radioactivity of the washout at each sampling; C_1 is the initial radioactivity in compartment 1 (metabolic compartment); C_2 the initial radioactivity in compartment 2 (structural compartment), and k_1 and k_2 are the rate constants for two compartments. The rate constants for transfer between the two compartments (k_{12} and k_{21}), and for excretion (k_{10}) were determined from the equations of Wen et al. (1994):

$$k_{21} = (C_1k_2 + C_2k_1)/(C_1 + C_2)$$
 (5)

$$k_{10} = k_1 k_2 / k_{21} \tag{6}$$

$$k_{12} = k_{21} (Q_0/Q_1)$$
 (7)

where Q_1 and Q_2 are the compartment sizes of the metabolic and structural pools, respectively, which were estimated as the product of relative pool size and algal cell P content. The relative pool size for each compartment was calculated from the rate constants and time-zero intercepts as previously

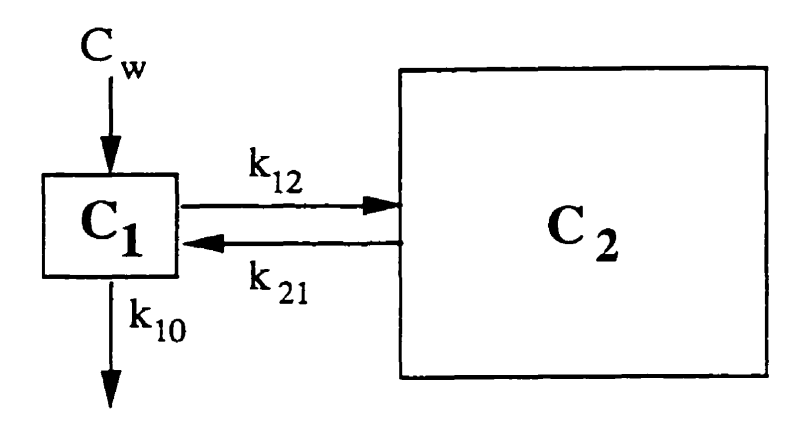


Fig. 1. Schematic representation of a two-compartment model with first order uptake and excretion of P. C_w , P concentration in water; C_1 , P concentration in compartment 1 (metabolic compartment); C_2 , P concentration in compartment 2 (structural compartment); and k_{10} , k_{12} and k_{21} , rate constants.

described (Wen et al. 1994). The internal fluxes and efflux rates were estimated by multiplying the compartment size by the corresponding rate constant.

Curve fitting and allometric statistics - For both uptake and excretion data analyses, the sampling times (independent variable) were assumed to be without error. The kinetic constants estimated by fitting the data to the model were reported as mean ± asymptotic standard error. ³²P uptake data were fitted to eqn 4 with the Marquardt least square fit of nonlinear regression by NLIN procedure of the Statistical Analysis System (SAS 1983). The overall goodness of fit was examined by an F-test, by the scatter of the actual data points around the fitted function and by the plot of residuals against the regressor (t). Eqn 2 was fitted to the ³²P excretion data using the 3R program of the Biomedical Statistics Package (BMDP, Dixon 1988). The "best model" was identified as that with a minimal sum of squared residuals, the lowest possible standard deviations of the parameter estimates, and unbiased distribution patterns of residuals of estimates of observed versus predicted radioactivities. An F-test was used to select the most appropriate number of compartments (Boxenbaum et al. 1974).

All values for allometric analysis were logarithmically transformed to obtain homogeneity of variances. The empirical constants a and b of the power function $(Y = aV^b)$ were estimated by least-squares linear regression on the transformed variables with the General Linear Models procedure (PROC GLM)

of SAS. Model I regression was performed because the average variance in the estimation of cell volume was much smaller than the taxonomic variations in cell size. The significance of linear correlation coefficients was determined by examination of a table of critical values in Zar (1984). The strength of the relationship was further evaluated by r^2 and $S_{y,x}$. Slopes of the regression lines were determined to be significant by comparison to zero (Student's t test). Statistical probabilities less than 0.05 were considered significant. Standard errors are presented throughout the text unless otherwise indicated.

Literature data collection and analysis - Algal Net P uptake rate is usually described by the Michaelis-Menten-type (M-M) hyperbolic function with two defined model parameters: the maximum uptake rate (V_{max}) and the half saturation constant (K_m). Because different kinetic parameters were measured in this study, a direct comparison of our parameters with those descriptions is not possible. To yield comparable results, we compiled the literature data on algal V_{max} and K_m for P uptake. To achieve uniformity of the data set, cell volume was calculated from cell quota and Shuter's (1978) quota:size relationship or, if quota was not specified from cell dry weight, from the equation in Peters (1983). Maximum uptake rates (V_{max}) were expressed as μM cell⁻¹ min⁻¹, and half-saturation constant (k_m) as μM . Median values were used when several data points were presented for the same species. The complete literature data set is available from the authors or from the Depository of Unpublished Data (CISTI, National Research Council of Canada,

Ottawa, Ontario K1A 0S2). Uptake rates were calculated by substituting the culture medium P concentration into the M-M equation ($v = (V_{max}[PO_4]/(k_m + [PO_4])$). All rate parameters were then logarithmically transformed to conform with the requirements of linear regression analysis. The uptake rates were subsequently regressed against algal cell volume. Because the M-M model predicts a net uptake, this can be compared directly to the prediction of net P uptake from our allometric model over the same size regime.

Results

Cell P content - algal size relationship - There was a significant relationship between unialgal P content and cell volume in the species studied. The overall relationship fits a power function:

$$Q = 5.09 \times 10^{-10} \text{ V}^{0.78 \pm 0.07} \quad n = 23, r^2 = 0.84, S_{v,x} = 0.51$$
 (8)

where Q is the cell P content (μ M), V is cell volume (μ m³), and 0.78±0.07 is the size-scaling exponent. On average, the P content of algal species investigated was 0.185 x 10⁻⁹ μ M μ m⁻³.

P uptake - ³²P uptake by all algae followed similar biphasic time courses over the periods of exposure (Fig. 2). Expressed as total radioactivity counts incorporated per mL, ³²P uptake was much more rapid in the first 3 - 20 min of incubation. Algae attained apparent steady state values after 20 to 50 min,

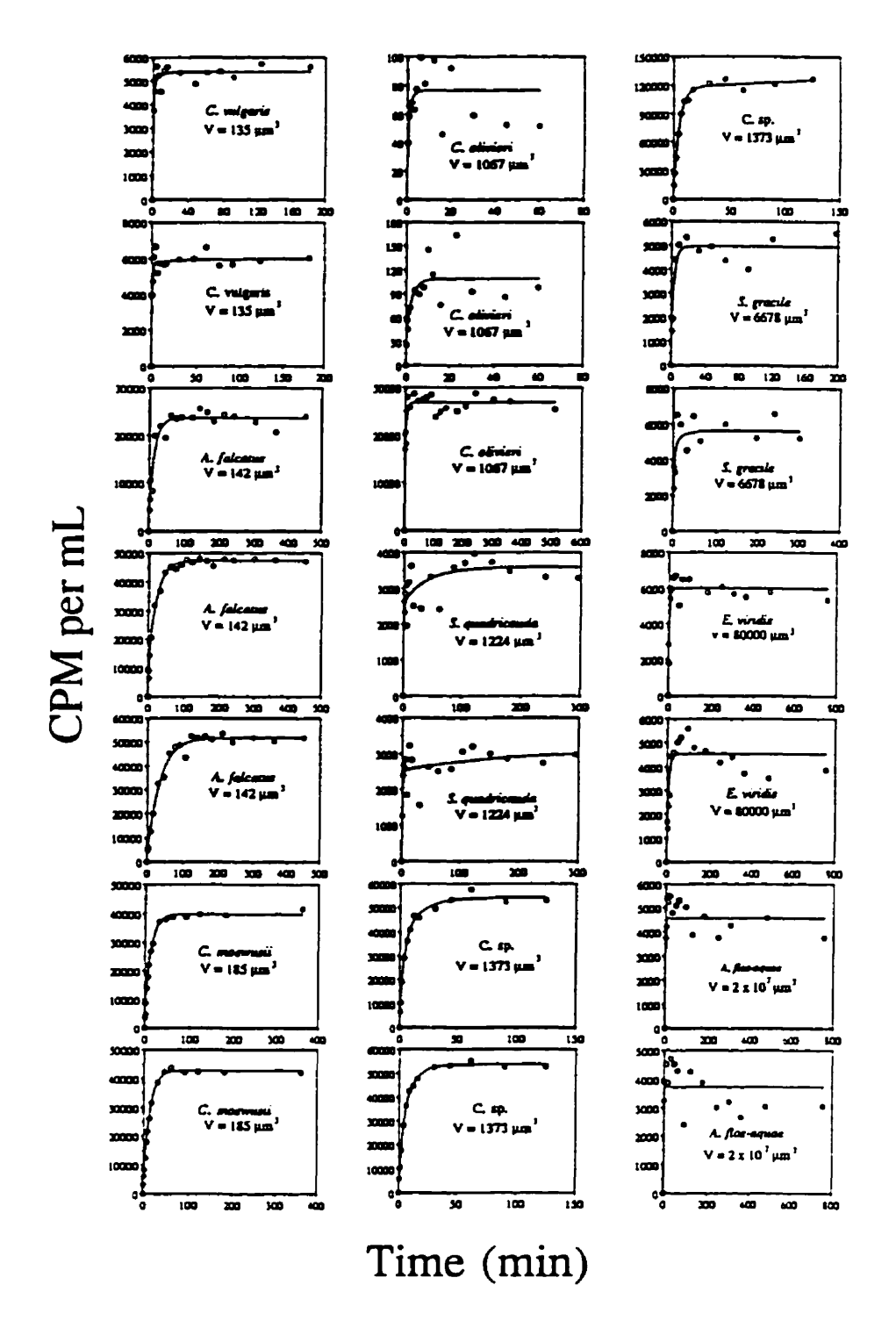


Fig. 2. Time courses of uptake of P in nine species of freshwater algae following exposure to $^{32}\mathrm{PO_4}$ -spiked culture medium. Symbols represent observed data and lines show model-predicted values.

depending on species. Thereafter, no significant increase in uptake of radioactivity was observed until the termination of the exposure at over 12 h. The amount of radioactivity taken up varied considerably among the experimental runs.

A two-compartment uptake function provided an adequate model for the observed trend. Uptake rate constants (b_1 and b_2) were estimated by fitting the radioactivity-time data to eqn 1 (Table 1). The b_1 values were about 1.2 -1.4 fold greater than b_2 values. Linear regression analysis of the uptake rate constants (b, min⁻¹) and time-zero intercepts (A, cpm cell⁻¹) against algal cell volume (Fig. 3) yielded the following relationships (p < 0.01, p = 21):

$$b_1 = 7.52 \text{ V}^{-0.27 \pm 0.06} \text{ (r}^2 = 0.54, S_{v,x} = 0.39)$$
 (9)

$$b_2 = 1.03 \text{ V}^{-0.32 \pm 0.08} \text{ (r}^2 = 0.43, S_{y,x} = 0.58)$$
 (10)

$$A_1 = 4.29 \times 10^{-8} \text{ V}^{1.02 \pm 0.15} \text{ (r}^2 = 0.72, S_{y,x} = 0.99)$$
 (11)

$$A_2 = 1.04 \times 10^{-7} \text{ V}^{0.93 \pm 0.17} \text{ (r}^2 = 0.62, S_{v,x} = 1.13)$$
 (12)

Both uptake rate constants (b_1 and b_2) decreased with cell volume with slopes which were not statistically different from -0.25 (t-test, p > 0.05). In contrast, A_1 and A_2 representing the equilibrium distributions of tracer labels increased with increasing cell volume at slopes which did not significantly differ from unity (t-test, p > 0.05). This implies that the relative sizes of A_1 and A_2 were unaffected by changes in cell size.

There was a significant allometric relationship between gross PO_4 uptake rate (v_{gross} , μM cell⁻¹ min⁻¹) and algal cell volume (Fig. 4). The predictive

Table 1. Cell volume (V), cell density (D), and biphasic P uptake constants for nine algal species. Data are a mean \pm SD. N is the number of experiments.

Species	N	٧	D	A ₁	b ₁	A ₂	b ₂
		μm ³	cells mL ⁻¹	cpm mL·1	min ⁻¹	cpm mL ⁻¹	min ⁻¹
Anabaena flos-aquae	2	2x10 ⁷	4	10390	0.096	3592	0.0017
				±1460	±0.010	±1057	±0.0004
Ankistrodesmus	3	142	657000	5254	1.767	35596	0.1367
falcatus				±3037	±1.123	±12303	±0.1332
Carteria olivieri	3	1067	170000	4842	3.423	4140	0.4100
				±6781	±0.974	±5790	±0.1700
Chlamydomonas sp.	3	1373	114000	50245	0.500	67632	0.3633
				±47782	±0.309	±67780	±0.5006
Chlamydomonas	2	185	675000	2875	2.320	38277	0.0800
moewusii				±557	±1.120	±2087	±0.0000
Chlorella vulgaris	2	135	925000	5370	2.340	291	0.1350
				±387	±0.250	±107	±0.0071
Eremosphaera viridis	2	80000	18450	1085	0.330	4179	0.1747
			±350	±372	±0.020	±362	±0.2338
Scenedesmus	2	1224	77100	2557	3.595	778	0.4000
quadricauda			±3900	±38	±1.815	±217	±0.2828
Staurastrum gracile	2	6678	13100	11889	0.270	15572	0.2900
			±2200	±10298	±0.100	±12211	±0.0800

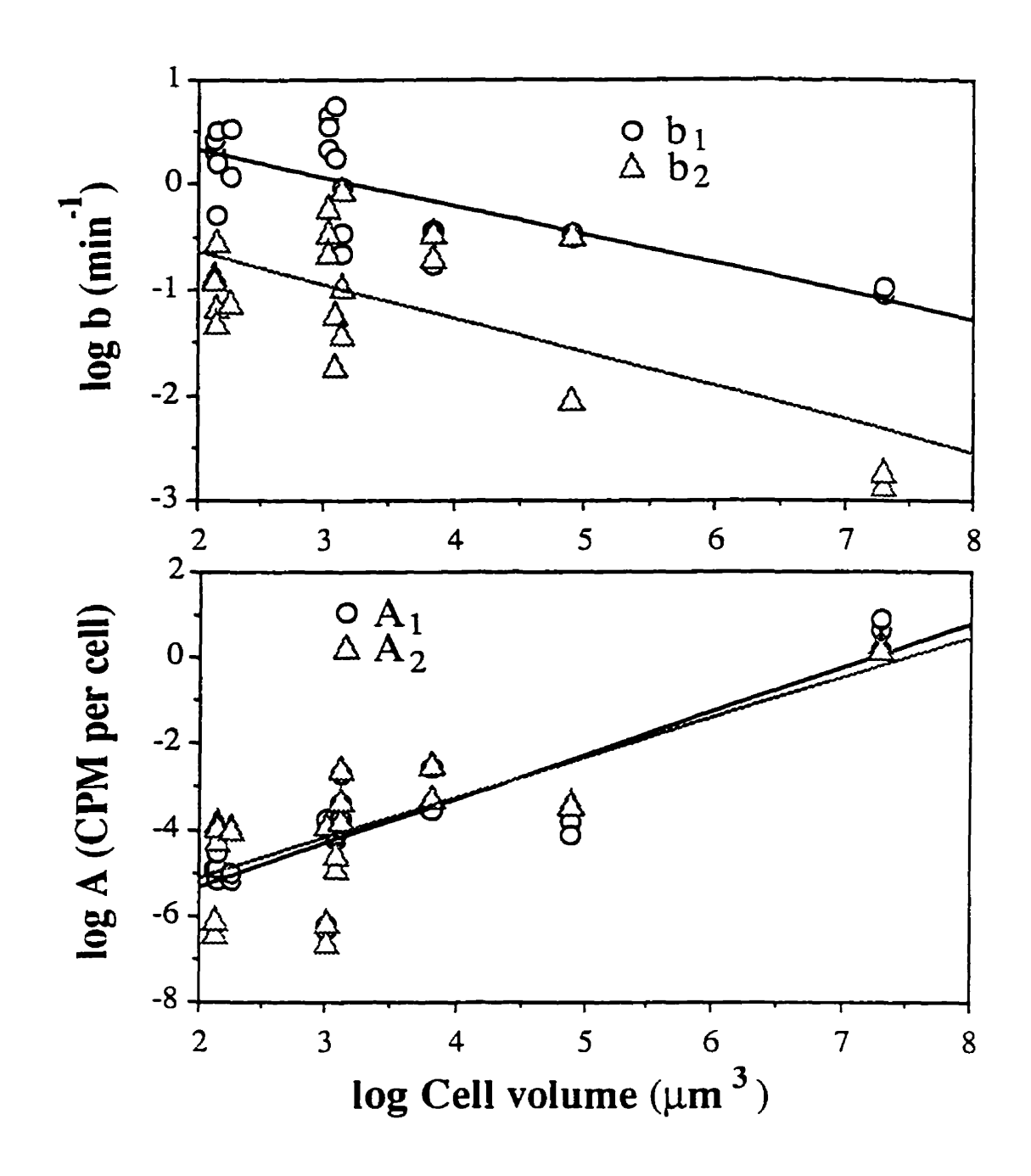


Fig. 3. Allometric relations between kinetic parameters of P uptake and algal cell volume.

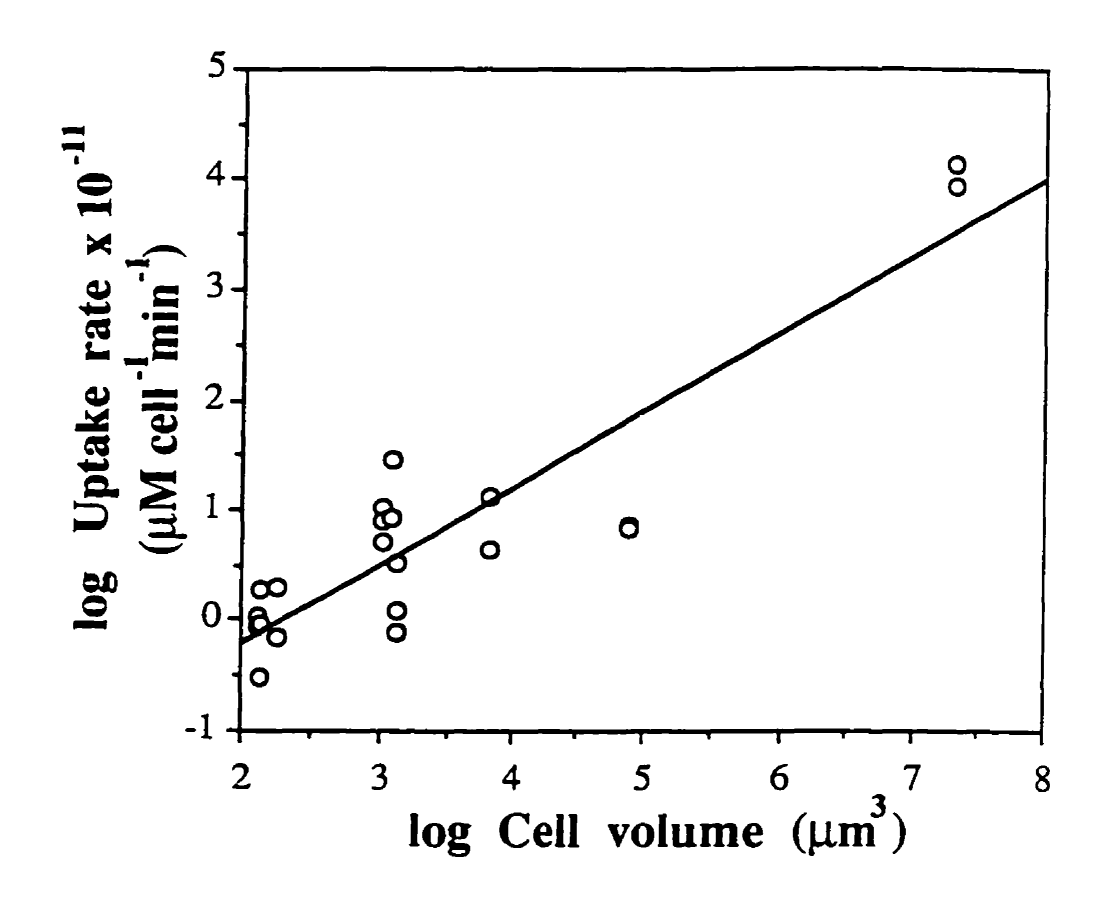


Fig. 4. Relationship of uptake rate of P to algal cell volume.

relation is (n = 21):

$$v_{gross} = 2.54 \times 10^{-13} \text{ V}^{0.70 \pm 0.08} \text{ (r}^2 = 0.81, S_{y,x} = 0.53, p < 0.01)}$$
 (13)

The allometric constant (0.70) did not deviate significantly from 0.75, as expected from general allometry (t-test, p > 0.05).

P excretion - Excretion of ³²P total radioactivity showed a biphasic decline (Fig. 5). The initial excretion of ³²P was very rapid, and 70 -80% of the absorbed radioactivity was eliminated within 0.5 - 2 h. The rates dropped to a plateau in 1 - 5 h after which a further 10 to 23% of the total accumulated counts were lost. With few exceptions, this plateau was maintained until the end of the experiments. The remaining species, A. falcatus, C. acerosum, C. olivieri, and S. gracile, lacked the final plateau and instead showed a steady, slow decline in excretion rates until the end of the experiments.

Most radioactivity-time relations conformed to a two-compartment model. For <u>Chlamydomonas</u> sp., <u>A. falcatus</u> and <u>S. quadricauda</u>, however, almost one third of the algal species tested did not conform to a two compartment model. The fits of these data are presented in Table 2. The k_1 values were 7 - 113 times greater than k_2 values, and small algae tended to have larger k_1 values than large algae ($r^2 = 0.63$, n = 13, P < 0.01). There was however no significant relationship between algal size and excretion rate constants (k_2) for the slow compartment ($r^2 = 0.14$, n = 13, p > 0.05).

The intercompartmental exchange rate constants calculated using equations 5 and 7 differed by one order of magnitude, and the rate constants

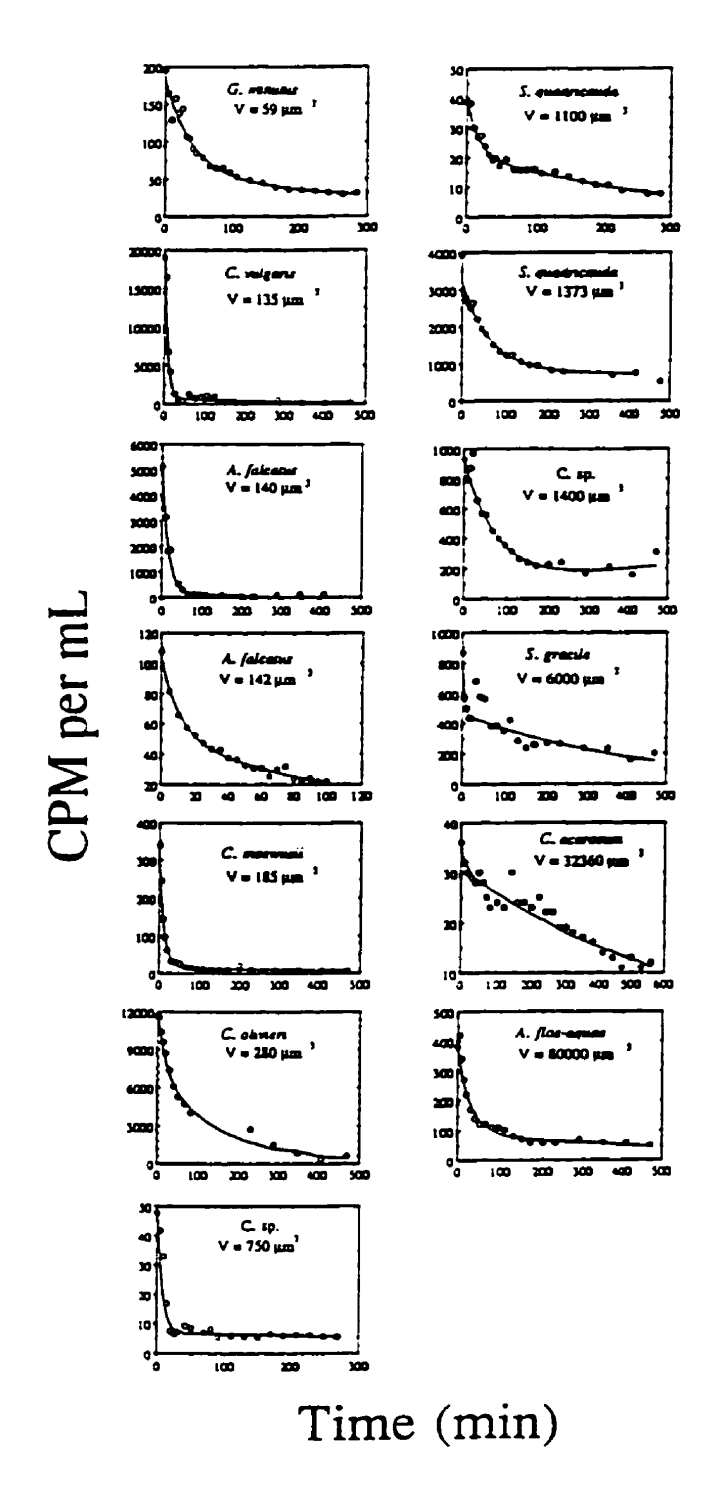


Fig. 5. Excretion of P from ³²P-exposed algae as a function of time after being transferred to nonradioactive water. Symbols represent observed radioactivity and lines are the model-predicted values for each experimental run.

for excretion were lower than those for internal exchanges. There were significant negative allometric relationships for the rate constants of both excretion and intercompartmental exchanges (Fig. 6, n=13, p<0.01):

$$k_{12} = 5.315 \text{ V}^{-0.31 \pm 0.10} \text{ (r}^2 = 0.45, S_{v,x} = 0.36)$$
 (14)

$$k_{21} = 0.166 \text{ V}^{-0.29 \pm 0.08} (r^2 = 0.54, S_{v,x} = 0.27, p < 0.01)$$
 (15)

$$k_{10} = 0.021 \text{ V}^{-0.23 \pm 0.07} \text{ (r}^2 = 0.48, S_{y,x} = 0.24, p < 0.01)}$$
 (16)

The slopes of all above allometric functions do not significantly differ from - 0.25 (t-test, p > 0.05) as expected. The time-zero intercepts (C_1 , C_2 in eqn 4) expressed per cell were not correlated with cell volume ($r^2 < 0.2$, p > 0.05).

P fluxes - The relative pool size of the dominant compartment $(Q_2\%)$ was much bigger than that of the minor one $(Q_1\%)$. The dominant compartment always contained 95-98% of the total cellular P (Table 2). There was no statistically significant relationship between the relative pool size and algal cell volume (r^2 <0.001, $S_{y,x}$ = 1.34, n = 13, p > 0.05).

Small algae had generally lower flux rates per cell than large cells (Fig. 7), and slopes of allometric equations were not significantly different from 0.75 (test, p > 0.05). The allometric relations for P fluxes were represented by the following equations (n = 13, p < 0.01):

$$F_{12} = F_{21} = 2.89 \times 10^{-11} \text{ V}^{0.71 \pm 0.08} (r^2 = 0.88, S_{y,x} = 0.27)$$
 (17)

$$F_{10} = 1.12 \times 10^{-13} \text{ V}^{0.80 \pm 0.09} \text{ (r}^2 = 0.89, S_{y,x} = 0.30)}$$
 (18)

Net P uptake - Since the allometric exponents for PO_4 uptake (0.79 ± 0.22) and PO_4 excretion (0.80 ± 0.09) differ significantly neither from each other nor

Table 2. Algal cell or colony volume (V), cell density (D), biexponential P excretion constants and relative pool size of compartment 1 (Q_1 %) for ten freshwater species. Data are a mean \pm SD. N is the number of experiments.

Species	N	V µm ³	D x10 ⁵ mL ⁻¹	C ₁ cpm mL ⁻¹	K ₁	C ₂ cpm mL ⁻¹	k ₂ min ⁻¹	Q ₁ %
Anabaena flos-aquae	1	80000	0.18	61.23	0.0179	83.84	0.0012	4.7
Closterium acerosum	1	32360	0.14	4.50	0.0118	30.92	0.0018	2.2
Chlamydomon as moewusii	1	185	6.75	300.76	0.0821	131.10	0.0014	3.8
Carteria olivieri	1	280	1.75	1557.30	0.0489	7043.46	0.0062	2.7
Chlorella vulgaris	1	135	6.25	1325.16	0.1466	718.89	0.0036	4.3
Golenkinia minutus	1	59	9.50	128.30	0.2600	55.51	0.0023	2.0
Staurastrum gracile	1	6000	0.11	208.37	0.0232	457.76	0.0024	4.5
Ankistrodesm us falcatus	2	141 ±1	6.50	288.08 ±255.82	0.0819 ±0.0147	542.44 ±489.57	0.0062 ±0.0031	3.9 ±1.6
Chlamydomon as sp.	2	1075 ±325	1.15	56.89 ±14.86	0.0778 ±0.0640	62.56 ±55.56	0.0010 ±0.0003	4.3 ±1.1
Scenedesmus quadricauda	2	1237 ±137	0.75	1070.93 ±1052.82	0.0422 ±0.0256	419.38 ±398.35	0.0020 ±0.0016	4.8 ±0.0

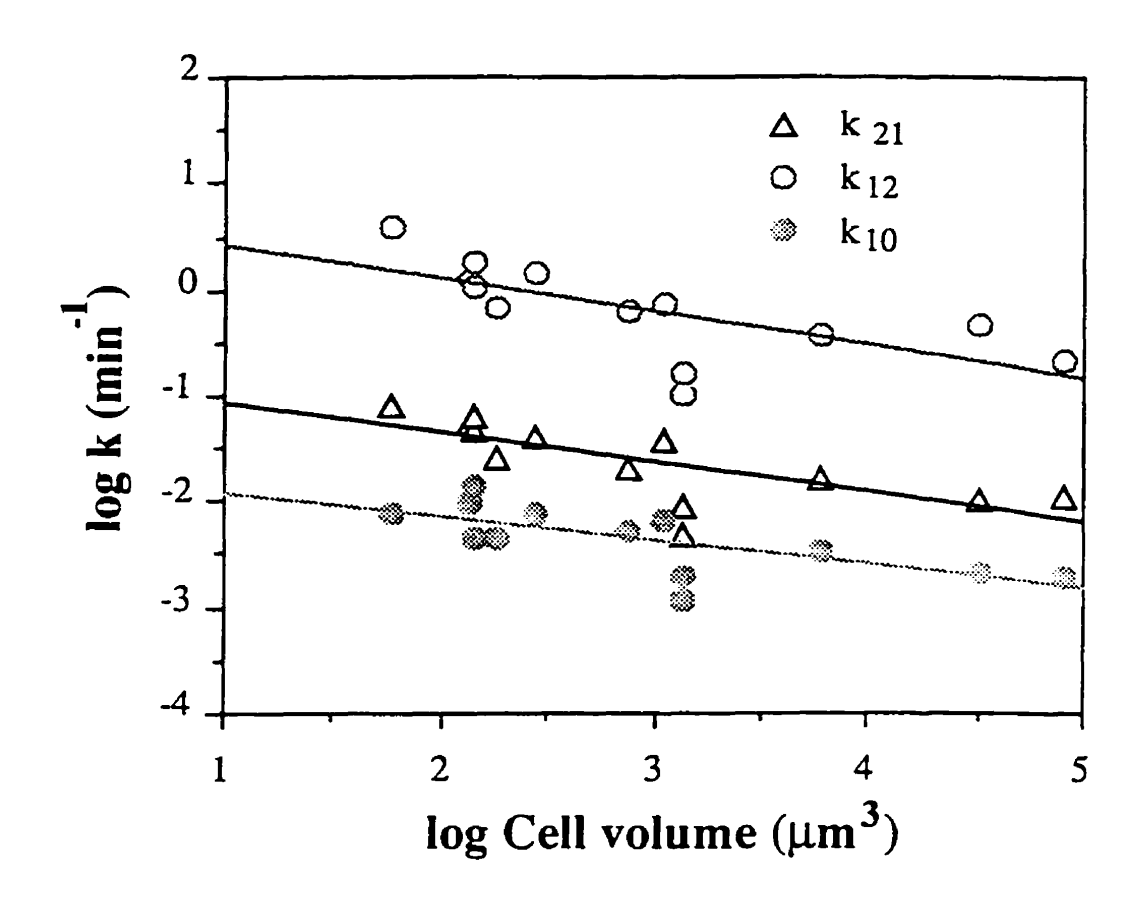


Fig. 6. Correlations between P flux kinetic data for excretion or intercompartmental turnover rates and algal cell volume.

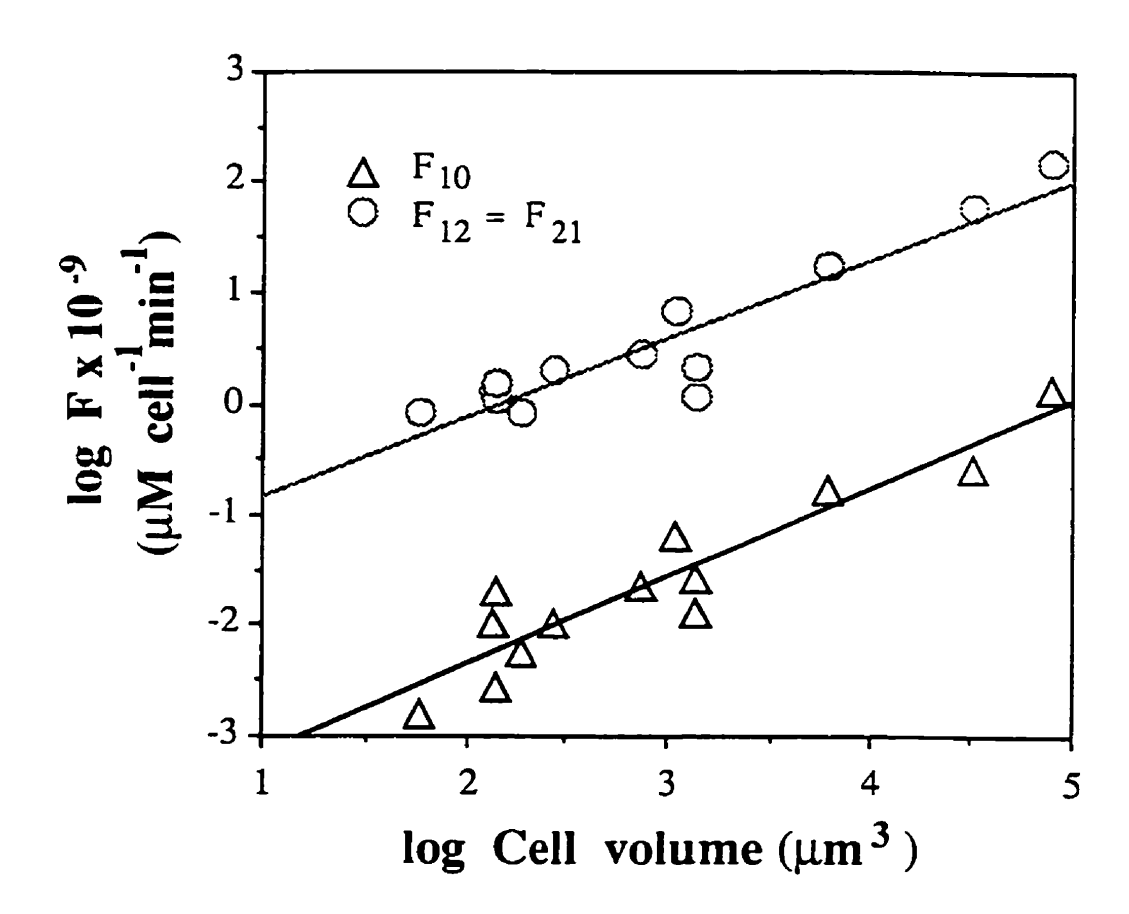


Fig. 7. Size dependency of P flux rates for excretion and internal flows in ten algal species.

from the expected value of 0.75, both equations were intentionally standardized to this common slope. This normalization has very little effect on value of the intercept or on the residual error of the original relationship. The net P uptake $(v_{net}, \mu M \text{ cell}^{-1} \text{ min}^{-1})$ was then calculated from the normalized equations and yielded the following allometric relation:

 $v_{net} = v_{gross}$ ' - $F'_{10} = 2.54 \times 10^{-13} \ V^{0.75}$ - $1.12 \times 10^{-13} \ V^{0.75} = 1.42 \times 10^{-13} \ V^{0.75}$ (19) where v_{gross} ' and F'_{10} are the normalized equations for PO_4 uptake and excretion, respectively. The net uptake of PO_4 by algae increases with increasing cell volume with a normalized slope of 0.75.

The gross/net uptake ratio could be further estimated as:

Gross/Net ratio =
$$v_{gross}$$
'/ v_{net} = 2.54x10⁻¹³ V^{0.75}/1.42x10⁻¹³ V^{0.75} = 1.79 (20)
The ratio of gross uptake : net uptake is independent of algal cell size.

Comparison to Michaelis-Menten Model - A total of 57 data entries were collected, representing 37 different species. Algal cell volume ranged from 0.4 to $3.0 \times 10^5 \ \mu\text{m}^3$, V_{max} ranged from 1×10^{-4} to 257 μM cell⁻¹ min⁻¹, and K_{m} ranged from 0.03 to 28.0 μM . Algal cell volume is a significant predictor for V_{max} , K_{m} , and $V_{\text{max}}/K_{\text{m}}$ (p < 0.01, n = 57):

$$V_{\text{max}} = 3.48 \times 10^{-11} V^{0.70 \pm 0.10} (r^2 = 0.45, S_{y,x} = 1.80)$$
 (21)

$$K_{\rm m} = 4.05 \text{ V}^{-0.28 \pm 0.06} \text{ (r}^2 = 0.29, S_{\rm v,x} = 0.62)$$
 (22)

$$V_{\text{max}}/K_{\text{m}} = 4.45 \times 10^{-11} \text{ V}^{0.68 \pm 0.08} (\text{r}^2 = 0.56, S_{\text{v.x}} = 0.85)$$
 (23)

 V_{max} and V_{max}/K_m were both positively correlated with cell volume, while K_m decreased with increasing cell volume across the entire algal size range.

By substituting the external phosphate concentration into the M-M model, we further calculated the PO_4 uptake rates. These estimated PO_4 uptake rates were also significantly correlated to algal cell volume and can be represented by the following allometric equation (p < 0.01, n = 50):

$$v_{M-M} = 1.73 \times 10^{-14} \text{ V}^{0.89 \pm 0.11} (r^2 = 0.56, S_{y,x} = 1.11)$$
 (24)

The M-M model predicts net PO_4 uptake rates for algae one order magnitude lower compared to the allometric compartment model. In addition, these models also differ in that the M-M model gave a steeper slope, suggesting that the net PO_4 uptake rates increase with increasing algal cell volume somewhat faster than those predicted by our allometric model. However, given the variation in individual uptake rates, it is apparent that both models describe mean trends that are consistent with observation (Fig. 8).

Discussion

In this study, some credible allometric compartment models were formulated to provide a basis for predicting the fluxes of P in freshwater algae. The proposed mathematical representations of the relationships between kinetic parameters and algal size provide a quantitative framework to assess the P accumulation in aquatic organisms. This assessment provides some insight into P bioaccumulation in algae.

Our results have demonstrated that PO₄ uptake by freshwater algae is

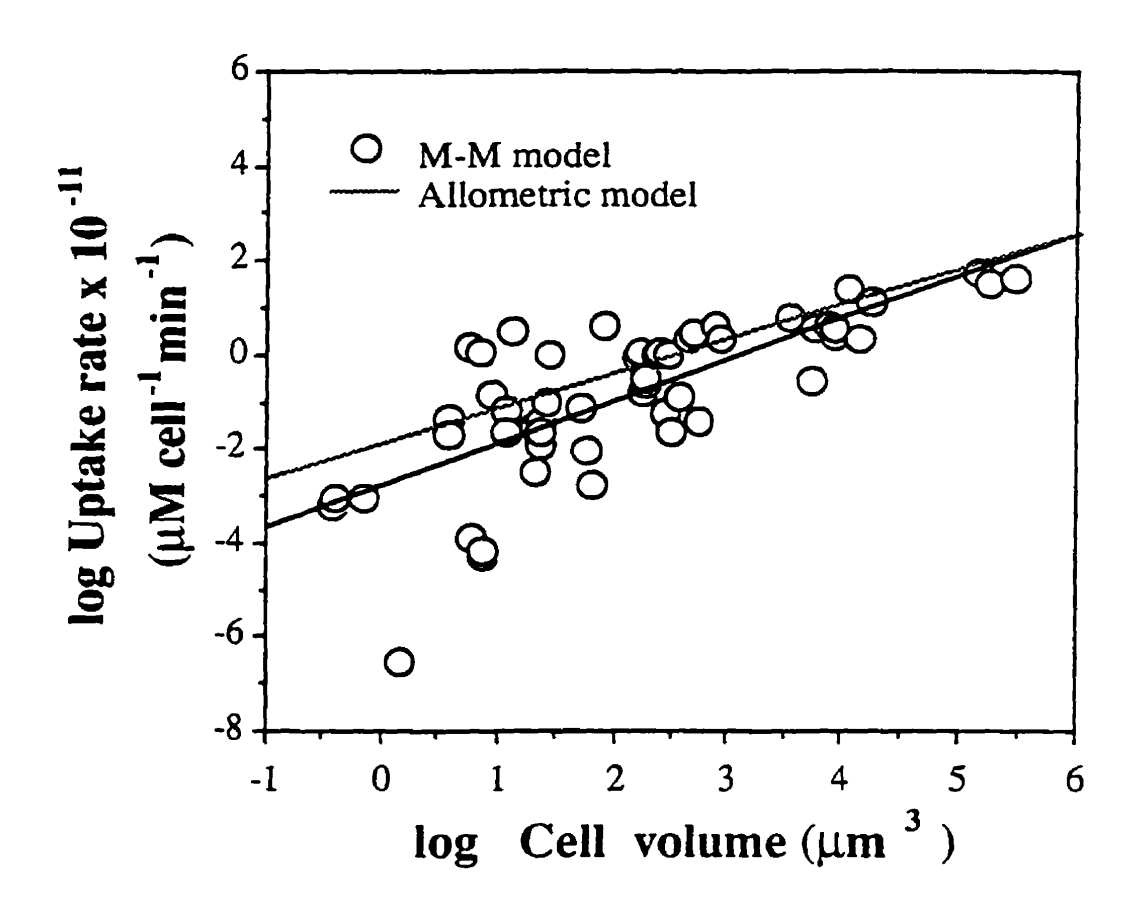


Fig. 8. Comparison of predictions by the allometric compartment model and the Michaelis-Menten-type enzyme function for P uptake by algae with data from the literature (References: Button et al. 1973; Chisholm and Stross 1975; Currie and Kalff 1984; Fuhs et al. 1972; Gotham and Rhee 1981; Holm and Armstrong 1981; Lean and Nalewajko 1976; Kennedy 1984; Kilham et al. 1977; Morgan 1976; Nalewajko and Lean 1978; Rhee 1973; Senft et al. 1981; Smith and Kalff 1982; Tilman and Kilham 1976).

biphasic over the time span of incubation. Thus the pattern of PO_4 uptake indicates that the radioactivity may be accumulated in two compartments: the first may be a "metabolic" compartment, while the second seems to be a "structural" compartment. Such a distinction has been made by many authors treating zooplankton (reviewed in Wen et al. 1994) and other algal species (JeanJean 1976; Chisholm and Stross 1976a,b; Tomas 1979). A similar description has been applied to the absorption of $\mathrm{NH_4}^+$ by N-limited marine algae (Conway et al. 1976; Goldman and Glibert 1982; Parslow et al. 1985) and of silicate by Si-limited marine diatoms (Davis et al. 1978; Harrison et al. 1989). However, others have treated P uptake by algae as monophasic (Perry 1976; Tilman and Kilman 1976; Perry and Eppley 1981, and Harrison 1983) or triphasic (Rivkin and Swift 1982). However, the choice of a model to describe the uptake phases depends on the quality of the data, although others have given a functional interpretation to the ubiquitous choice of compartment models (Boxenbaum et al. 1974).

After reviewing the literature data on PO₄ uptake by marine algae, Harrison et al. (1989) identified a two-phase uptake process: the initial rapid uptake (surge uptake) fills an internal pool, and stops when the pool is full; subsequently, slower uptake (internally controlled uptake) delivers nutrients for cell metabolism and this uptake is terminated when cell quota is reached. In a comprehensive investigation of the P transport system in the green alga Scenedesmus quadricauda, Jansson (1993) also found two separate uptake

systems: an initial rapid uptake (high-affinity system, HA) and a subsequent slower uptake (low-affinity system, LA). The HA system binds P to the cells, and is especially important in P deficiency, while the LA system maintains the fixed internal P and transforms exchangeable to nonexchangeable phosphorus. Both systems are closely coupled so P is transferred from HA to LA. The same characteristics of uptake kinetics have been reported for a bacterium Escherichia coli (Rosenberg 1987) and a eucaryotic fungus Neurospora crassa (Burns and Beever 1979). These findings add further support to the claim that a two-compartment theory describes P transport mechanisms in a wide range of organisms.

The most striking feature of our data is the size dependence of PO_4 uptake rates. The exponent of the power equation relating uptake rates to algal volume was near 0.75, which is consistent with most studies (Peters 1983). Although Friebele et al. (1978) found an exponent of 0.22 (r^2 =0.51, n = 11, p < 0.05) for an estuarine phytoplankton population, both studies are consistent in indicating that PO_4 uptake capacity of small algae is much higher than that of large ones per unit volume. This size-dependent difference in nutrient uptake was also widely reported in other aquatic ecosystems (Berman 1983; 1985). The ubiquity of the 0.75 exponent demonstrates a general allometric pattern for the uptake of PO_4 by freshwater algae. Our overall scaling of PO_4 uptake to algal size further support the contention that small cells are generally better at acquiring ambient phosphate (Smith and Kalff 1983; Suttle

et al 1988) than are large algae, and demonstrates that this applies over a much broader range in algal size than in previous studies.

Our data showed a substantial variability among experiments in the measurement of uptake kinetics. This interexperimental variation is not uncommon, because many environmental factors, such as irradiance, light quality and temperature, can affect PO₄ uptake rates (Cembella et al. 1984). Furthermore, although these cultures were said to be axenic by the supplier and although cultures that showed bacterial contamination in plate tests were discarded, it is likely that modest levels of bacterial contamination increased rates of P uptake and excretion in some runs, increasing the observed variation.

A two-compartment excretion model (eqn. 4) is adequate to characterize P elimination for most algal species studied. Although some deviations were found, they did not influence the general kinetic patterns greatly. The purpose of our study was to scale the compartmental rate parameters to algal cell size and to establish predictive models, we therefore constructed the compartmental model to include as many compartments as possible to increase "information content" and predictive power of the model. On the other hand, we want the compartmental model to include as few compartments as possible because the variance of the prediction for each additional compartment increases as the number of compartments increases. In addition, the cost of data collection and model maintenance increases with the number of compartments. In our prior

study of P fluxes through cladocerans (Wen et al. 1994), a two-compartment model seemed a good compromise between these two conflicting objectives. This conclusion seems valid for algal models too.

Since literature does not offer any comparable data on algal PO₄ excretion rates, the validity of our P loss estimation remains uncertain. It is possible that our rates of PO₄ release by algae may be overestimated because bacterial contamination could have increased both PO₄ uptake and excretion rates (Rigler 1956; Currie and Kalff 1984). The wide variability in P excretion rates within and among species could be attributed to species difference or to the short-term responses to any environmental variations. For example, physical damage to the algal cells by the filtration might increase the release of intracellular P (Lean and Nalewajko 1976). At least, the similarity of uptake and release rates in this study suggests that the excretion rates are not impossibly high.

Our results showed that about half of the PO₄ taken up was excreted, whereas Kuenzler (1970) found that about 20% of fixed P was returned to the aquatic environment by a marine alga, suggesting that freshwater algae may release more P than marine species. Our excretion results clearly demonstrate that size is a fundamental factor for the P kinetics. Similar allometric relations between physiological and morphological properties have been widely reported for other organisms (Peters 1983).

Net PO₄ uptake rate could be an index of nutrient status of the biota.

Unfortunately very few experimentally derived net P uptake rates have been reported for algae. In this study, the net PO₄ uptake rates by algae were comparable to those obtained by others from freshwater algae (Lean and Nalewajko 1976; Nalewajko and Lean 1978; Stiller et al. 1978). However, our use of Lean and Nalewajko's (1976) ³²P partitioning data between algae and PO₄ compartments to estimate the external P concentration in the culture medium introduces uncertainty in the estimation of net P uptake rates.

Comparison of the predictions made by two models (Fig. 8) shows that the net PO4 uptake rates estimated by our allometric compartment model were about one order magnitude higher than those calculated from M-M kinetic parameters in the small size range, although variation in the data is large relative to the difference in the prediction. A discrepancy of this size could be due to different species acclimatization and experimental conditions in addition to model differences. The size-specific difference in algal PO_4 uptake rates has been noted in previous studies (Smith and Kalff 1982). In the M-M model, V_{max} basically estimates the maximum rate of assimilation of inorganic phosphate into organic compounds, while K_{m} is a measure of affinity for phosphate uptake and $V_{\text{max}}/K_{\text{m}}$ ratio quantifies the efficiency of uptake at low phosphate concentrations. All these kinetic parameters are a function of external substrate concentration, and the proportion of their variances explained by changes in cell volume were relatively low (45-62%). In contrast, in our allometric compartment model, the flux parameters are all scaled to

algal cell volume and the variances attributed to cell volume were relatively high (88-89%). Any size dependent properties will be reflected by the model parameters. This implies that our allometric model could be a candidate for the replacement of M-M model because size is a fundamental factor influencing the biochemical composition, growth and metabolism of all organisms (Peters 1983), and an allometric model implicitly addresses all these factors.

In the present study, the PO₄ uptake rates exceeded the excretion rates for all the algal species examined, so algae can be sustained by PO_4 alone and cannot be net sources of P. This result implies that algal excretion was of limited importance in heterotrophic remineralization. It is highly likely that algae keep a large proportion of the PO₄ taken up. This finding is congruent with the data from other reports. Other studies have also failed to demonstrate a net PO₄ release in cultured phytoplankton (Lean and Nalewajko 1976; Perry 1976; Burmaster and Chisholm 1979) and in field investigations (Perry 1976; Harrison 1983, Istvánovics and Herodek 1995). However, direct extrapolation of our models to the field populations may introduce errors. Firstly, our experiments were conducted in the laboratory, so the experimental conditions may not exactly simulate natural ones modifying the physiological and biological responses of the algae. Secondly, because only a few species and a limited size range of algae were used in our studies, many biological influences on the uptake and excretion rates may have been ignored. Thus we caution against direct extrapolation of our results to the field.

The present study provides a framework from which to develop models for material

flux. Perhaps these models may be extended to other nutrients and algae simply by changing the appropriate parameter values. More research is therefore needed to determine the generality of models like these for a greater variety of organisms, nutrients and growth rates, and to elucidate the additional ecological, physiological and biological factors contributing to this size dependence of P flux in algae, thereby improving the predictive capabilities of these models.

Acknowledgments

We wish to thank Drs. J. Kalff, J. Rasmussen, N. Price and W. K. Dodds for their helpful suggestions and critical comments on the manuscript. This work was supported by the Natural Sciences and Engineering Research Council of Canada (NSERC), Fonds pour la Formation de Chercheurs et l'Aide à la Recherche (FCAR) and the Faculty of Graduate Studies of McGill University. Y.H.W. was a recipient of an FCAR scholarship from the Québec government.

References

- Auer, M. T., and R. P. Canale. 1982. Ecological studies and mathematical modeling of Cladophora in Lake Huron: 2. Phosphorus uptake kinetics. J. Great Lakes Res. 8: 84-92.
- Bentzen, E., and W. D. Taylor. 1991. Estimating Michaelis-Menten parameters and lake water phosphate by the Rigler bioassay: importance of fitting technique, plankton size and substrate range. Can J. Fish. Aquat. Sci. 48:73-83.
- Bentzen, E., W. D. Taylor, and E. S. Millard. 1992. The importance of dissolved organic phosphorus to phosphorus uptake by limnetic plankton. Limnol. Oceanogr. 37: 217-231.
- Berman, T. 1983. Phosphorus uptake by microplankton in estuarine and coastal shelf waters near Sapelo Island, Georgia, U. S. A. Estuaries 7:98-101.
- Berman, T. 1985. Uptake of [32P] orthophosphate by algae and bacteria in lake Kinneret.

 J. Plank. Res. 7:71-84.
- Boxenbaum, H. G., S. Riegelman, and R. M. Elashoff. 1974. Statistical estimations in pharmacokinetics. J. Pharmacokinet. Biopharm. 2: 123-148.
- Brown, E. J., and J. F. Koonce. 1978. Kinetics of phosphate uptake by aquatic microorganisms: deviations from a simple Michaelis-Menten equation. Limnol. Oceanogr. 23: 27-34.
- Burmaster, D. E., and S. W. Chisholm. 1979. A comparison of two methods for measuring phosphate uptake by Monochrysis lutheri Droop grown in continuous

- culture. J. Exp. Mar. Biol. Ecol. 39: 187-202.
- Burns, D. J. W., and R. E. Beever. 1979. Mechanisms controlling the two phosphate uptake systems in Neurospora crassa. J. Bacteriol. 139-204.
- Button, D. K., S. S. Dunker, and M. L. Morse. 1973. Continuous culture of <u>Rhodotorula</u> rubra: kinetics of phosphate-arsenate uptake, inhibition, and phosphate-limited growth. J. Bacteriol. 113: 599-611.
- Cembella, A. D., N. J. Anita, and P. J. Harrison. 1984. The utilization of inorganic and organic phosphorus compounds as nutrients by eukaryotic microalgae: A multidisciplinary perspective: Part I. CRC Crit. Rev. Microbiol. 10: 317-391.
- Chisholm, S. W., and R. G. Stross. 1975. Light/dark phased cell division in <u>Euglena</u> gracilis (Euglenophyceae) in PO₄-limited continuous culture. J. Phycol. 11: 367-373.
- Chisholm, S. W., and R. G. Stross. 1976a,b. Phosphate uptake kinetics in <u>Euglena gracilis</u> (Euglenophyceae) grown in light/dark cycles. I. Synchronized batch cultures. II. Phased PO₄-limited cultures. J. Phycol. 12: 210-217: 217-222.
- Conway, H. L., P. J. Harrison, and C. O. Davis. 1976. Marine diatoms grown in chemostats under silicate or ammonium limitation. 2. Transient response of Skeletonema costatum to a single addition of the limiting nutrient. Mar. Biol. 35: 187-199.
- Currie, D. J. 1982. Estimating Michaelis-Menten parameters: bias, variance and experimental design. Biometrics 38: 907-919.
- Currie, D. J., and J. Kalff. 1984. A comparison of the abilities of freshwater algae and

- bacteria to acquire and retain phosphorus. Limnol. Oceanogr. 29: 298-310.
- Davis, C. O., N. F. Breitner, and P. J. Harrison. 1978. Continuous culture of marine diatoms under silicon limitation. 3. A model of Si-limited diatom growth. Limnol. Oceanogr. 23: 41-52.
- Dixon, W. J. 1988. BMDP Software Manual. Berkeley: University of California Press.
- Dodds, W. K. 1995. Availability, uptake and regeneration of phosphate in mesocosm with varied levels of P deficiency. Hydrobiologia 297: 1-9.
- Friebele, E. S., D. L. Correll, and M. Faust. 1978. Relationship between phytoplankton cell size and the rate of orthophosphate uptake: In situ observations of an estuarine population. Mar. Biol. 45: 39-52.
- Fuhs, G. W., S. D. Demmerle, E. Canelli, and M. Chen. 1972. Characterization of phosphorus-limited algae. Spec. Symp. Amer. Soc. Limnol. Oceanogr. 1: 113-132.
- Goldman, J. C., and P. M. Glibert. 1982. Comparative rapid ammonium uptake by four species of marine phytoplankton. Limnol. Oceanogr. 27: 814-827.
- Gotham, I. J., and G-Y., Rhee. 1981. Comparative kinetic studies of phosphate-limited growth and phosphate uptake in phytoplankton in continous culture. J. Phycol. 17: 257-265.
- Harrison, P. J., J. S. Parslow, and H. L. Conway. 1989. Determination of nutrient kinetic parameters: a comparison of methods. Mar. Ecol. Prog. Ser. 52: 301-312.
- Harrison, W. G. 1983. Uptake and recycling of soluble reactive phosphorus by marine microplankton. Mar. Ecol. Prog. Ser. 10: 127-135.
- Holm, H. D., and D. E. Armstrong. 1981. Role of nutrient limitation and competition in

- controlling the populations of <u>Asterionella formosa</u> and <u>Microcystis aeruginosa</u> in semi-continuous culture. Limnol. Oceanogr. 26: 622-634.
- Istvánovics, V., and S. Herodek. 1995. Estimation of net uptake and leakage rates of orthophosphate from ³²P-uptake kinetics by a linear force-flow model. Limnol. Oceanogr. 40: 17-32.
- Jansson, M. 1993. Uptake, exchange, and excretion of orthophosphate in phosphatestarved <u>Scenedesmus quadricauda</u> and <u>Pseudomonas</u> K7. Limnol. Oceanogr. 38: 1162-1178.
- JeanJean, R. 1976. The effect of metabolic poisons on ATP level and on active phosphate uptake in Chlorella pyrenoidsoa. Physiol. Pl. 37: 107-110.
- Kennedy, K. C. 1984. The influence of cell size and the colonial habit on phytoplankton growth and nutrient uptake kinetics: a critical evaluation using a phylogentically related series of volvocene green algae. M. Sc. dissertation. The University of Texas at Arlington, Arlington, Texas.
- Kilham, S. S., C. L. Kott, and D. Tilman. 1977. Phosphate and silicate kinetics for the Lake Michigan diatom Diatoma elongatum. J. Great Lakes Res. 3: 93-99.
- Kuenzler, E. J. 1970. Dissolved organic phosphorus excretion by marine phytoplankton.

 J. Phycol. 6: 7-13.
- Lean, D. R. S. 1973. Phosphorus dynamics in lake water. Science 179: 678-680.
- Lean, D. R. S., and C. Nalewajko. 1976. Phosphate exchange and organic phosphorus excretion by freshwater algae. J. Fish. Res. Board Can. 33: 1312-1323.
- Li, W. K. W. 1982. Consideration in errors in estimating kinetic parameters based on

- Michaelis-Menten formalism in microbial ecology. Limnol. Oceanogr. 28: 185-190.
- Menzel, D. W., and N. Corwin. 1965. The measurement of total phosphorus in seawater based on the liberation of organically bound fractions by persulfate oxidation.

 Limnol. Oceanogr. 10: 280-282.
- Morgan, K. C. 1976. Studies on the Autecology of the Freshwater Algal Flagellate,

 <u>Cryptomonas erosa</u> Skuja. Ph.D. Thesis. McGill University, Montreal, 211 pp.
- Nalewajko, C., and D. R. S. Lean. 1978. Phosphorus kinetics-algal growth relationships in batch cultures. Mitt. Int. Ver. Limnol. 21: 184-192.
- Nürnberg, G. K., and R. H. Peters. 19842. Biological availability of soluble reactive phosphorus in anoxic and oxic freshwater. Can. J. Fish. Aquat. Sci. 41: 757-765.
- Parslow, J. S., P. J. Harrison, and P. A. Thompson. 1985. Interpreting rapid changes in the uptake kinetics of the marine diatom <u>Thalassiosira pseudonana</u> (Hustedt). J. Exp. Mar. Biol. Ecol. 91: 53-64.
- Perry, M. J. 1976. Phosphate utilization by an oceanic diatom in phosphorus-limited chemostat culture and in oligotrophic waters of the central North Pacific. Limnol. Oceanogr. 21: 88-107.
- Perry, M. J., and R. W. Eppley. 1981. Phosphate uptake by phytoplankton in the central North Pacific Ocean. Deep-sea Res. 28: 39-49.
- Peters, R. H. 1983. The Ecological Implications of Body Size. Cambridge Univ. Press.
- Rhee, G-Yull. 1973. A continuous culture study of phosphate uptake, growth rate and polyphosphate in <u>Scenedesmus</u> sp. J. Phycol. 9: 495-506.
- Rigler, F. H. 1956. A tracer study of the phosphorus cycle in lake water. Ecology 37:

- Rivkin, R. B., and E. Swift. 1982. Phosphate uptake by the oceanic dinoflagellate

 Pyrocystis noctiluca. J. Phycol. 18: 113-120.
- Rosenberg, H. 1987. Phosphate transport in prokaryotes. p 205-246. In B. P. Rosen and S. Silver [eds]. Ion transport in prokaryotes. Academic.
- SAS Institute Inc. 1983. SAS/STAT User's Guild. Release 6.03 ed. Cary, NC:SAS Institute.
- Senft II, W. H., R. A. Hunchberger, and K. E. Roberts. 1981. Temperature dependence of growth and phosphorus uptake in two species of <u>Volvox</u> (Volvocales, Chlorophyta). J. Phycol. 17: 323-329.
- Shuter, B. J. 1978. Size dependence of phosphorus and nitrogen subsistence quotas in unicellular microorganisms. Limnol. Oceanogr. 23: 1256-1263.
- Smith, R. E. H., and J. Kalff. 1982. Size-dependent phosphorus uptake kinetics and cell quota in phytoplankton. J. Phycol. 18: 275-284.
- Stiller, M., M. Edelstein, H. Volohonsky, and C. Serruya. 1978. Validity of ³²P kinetic experiments in algae. Verh. Internat. Verein. Limnol. 20: 75-81.
- Strickland, J.D.H., and T. R. Parsons. 1968. A practical handbook of seawater analysis.

 2nd ed. Bull. Fish. Res. Board Can. 167.
- Suttle, C. A., J. G. Stockner, K. S. Shortreed, and P. J. Harrison. 1988. Time-courses of size-fractionated phosphate uptake: are larger cells better competitors for pulses of phosphate than smaller cells? Oecologia 74:571-576.
- Suttle, C. A., W. P. Cochlar, and J. G. Stockner. 1991. Size-dependent ammonium and

- phosphate uptake, and N:P supply ratios in an oligotrophic lake. Can. J. Fish. Aquat. Sci. 48:1226-1234.
- Suttle, C. A., P. J. Harrison. 1988. Ammonium and phosphate uptake kinetics of size-fractionated plankton from an oligotrophic freshwater lake. J. Plankton Res. 10:133-149.
- Tarapchak, S. J., and L. R. Herche. 1986. Phosphate uptake by microorganisms in lake water: deviations from simple Michaelis-Menten kinetics. Can. J. Fish. Aquat. Sci. 43: 319-328.
- Tilman, D., and S. S. Kilham. 1976. Phosphate and silicate growth and uptake kinetics of the diatoms <u>Asterionella formosa</u> and <u>Cyclotella meneghiniana</u> in batch and semicontinuous culture. J. Phycol. 12: 375-383.
- Tomas, C. R. 1979. Olisthodiscus luteus (Chrysophyceae). III. Uptake and utilization of nitrogen and phosphorus. J. Phycol. 15: 5-12.
- Vézina, A. F. 1986. Body size and mass flow in freshwater plankton: models and tests.

 J. Plankton Res. 8: 939-956.
- Wen, Y. H., A. Vézina, and R. H. Peters. 1994. Phosphorus fluxes in limnetic cladocerans: coupling of allometry and compartmental analysis. Can. J. Fish. Aquat. Sci. 51: 1055-1064.
- Zar, J. H. 1984. Biostatistical Analysis. Prentice-Hall, Englewood Cliffs, New Jersey.

CHAPTER II

Phosphorus fluxes in limnetic cladocerans:

The coupling of allometry and compartmental analysis*

^{*} Published in Canadian Journal of Fisheries and Aquatic Sciences (51: 1055-1064, 1994).

A size-dependent two-compartmental model was developed for estimation of ³²P turnover and fluxes by limnetic cladocerans in steady state. After feeding on radioactively labelled food, uniformly labelled animals were fed unlabelled cells and the time course of release of tracer followed. Rates of turnover and size-specific fluxes were subsequently fitted to a twocompartment model. The model predicted that steady state turnover and sizespecific fluxes for ³²P excretion declined as body weight and that the exponent of weight did not significantly differ from -0.25, suggesting the relationships between total P turnover or flux rates and body size in cladocerans follow the same allometry observed for other organisms and other metabolic activities. However, rate constants for intercompartmental exchanges declined faster than weight-1/4, indicating that their turnover and flux declined much faster with increasing body size than would be expected from general allometry. Sizespecific ingestion and assimilation rates of ³²P by cladocerans decreased with increasing body size with a slope of the allometric function similar to -0.25.

The need for a realistic, general model to quantify phosphorus (P) fluxes in zooplankton has often been stressed (Rigler 1973; Vézina 1986) and several models have been proposed for various zooplankton species (Peters and Rigler 1973; Peters 1975; Taylor and Lean 1981; Taylor 1984). These studies have found applications in simulation models of nutrient regeneration (Ikeda et al. 1982; Ejsmont-Karabin 1984; Olsen and Østgaard 1985), in comparing the role of P cycling by different organisms (Ganf and Blazka 1974; Nakashima and Leggett 1980; James and Salonen 1991), and in describing P fluxes through living organisms (Lehman 1980; den Oude and Gulati 1988). However, the formulation of a more general model has been hindered by the limited flux data for many species.

One limitation of existing models is their inability to predict the dynamics of P turnover and flux in aquatic animals. Although radiotracer techniques have been used to study the P cycle in aquatic ecosystems for decades, there has been little use of compartmental kinetics to analyze P turnover and fluxes. The rather comprehensive model of Peters and Rigler (1973) is essentially a one-compartmental analysis of internal tracer loss. Shipley and Clark (1972), Conover and Francis (1973) and Lampert and Gabriel (1984) cautioned that considering an animal as a single, instantaneously mixed compartment might cause considerable errors in assessment of material flow in biological systems. Perhaps for this reason, the Peters and Rigler model overestimates P excretion rates for small animals (Peters and Rigler 1973) and in oligotrophic waters

(Olson and Østgaard 1985). Moreover, although the Peters and Rigler model incorporated the effects of temperature, food level and body size on P release, it was generated from data for only a single species, <u>Daphnia rosea</u>, and therefore covered a limited size range. Perhaps because of these restrictions, its description of the effect of size on excretion rate is anomalous: instead of the expected body weight exponent of -0.25 (Peters 1983), the allometric slope was -0.38, which suggests that size-specific excretion rates fall much more rapidly with size than expected. This model needs further development and refinement.

Lampert and Gabriel (1984) suggested that a two-compartment, open, reversible system is a more appropriate model of ¹⁴C dynamics in <u>Daphnia</u>. In the present paper, we extend this model to treat P turnover and fluxes in limnetic cladocerans of different size. The model parameters were determined by laboratory studies of ³²P kinetics and analyzed by both compartmental modelling and allometric parameterization. We further tested an <u>a priori</u> expectation that the exponents of the allometric equations relating P fluxes to body size should approximate -0.25 (Peters 1983). Our general premise is that all processes of material fluxes in aquatic organisms can be fitted to a single model, provided that the model's fundamental parameters can be described as functions of characteristics of the organisms, especially body size, and their environment, such as food level and water temperature.

The two-compartment model

The conceptual model (Fig. 1, symbols and abbreviations as in Table 1) is a slight modification of the two-compartment configuration used by Lampert (1975) and Lampert and Gabriel (1984) to quantify 14 C turnover in Daphnia. In the model, 32 P is conceptualized to be distributed between two kinetically, but not necessarily anatomically, identifiable compartments inside the animal: a small, rapidly turning over "metabolic" compartment or pool (Q_a) and a large, slowly turning over "structural" pool (Q_b). We assumed that 32 P enters the metabolic pool by assimilation through the gut (Martinez et al. 1995), and that irreversible P loss occurs from the metabolic pool through excretion. The two pools are open in the sense that Q_a interchanges with Q_b . The rates of change of 32 P in each pool was established by algebraic summation of rates of acquisition and loss of tracer, which is mathematically described for pool a as:

$$dQ_{a}/dt = F_{ao} + F_{ab} - F_{ba} - F_{oa}$$

$$= F_{ao} + k_{ab}Q_{b} - Q_{a}(k_{ba} + k_{oa})$$
 (1)

and for pool b as:
$$dQ_b/dt = F_{ba} - F_{ab} = k_{ba}Q_a - k_{ab}Q_b$$
 (2)

At apparent dynamic equilibrium,

$$dQ_a/dt = dQ_b/dt = 0 (3)$$

The rate constants (k_{ab}, k_{ba}, k_{oa}) were calculated by numerical integration of simultaneous differential equations (1) and (2) and fitted to time courses of 32 P release.

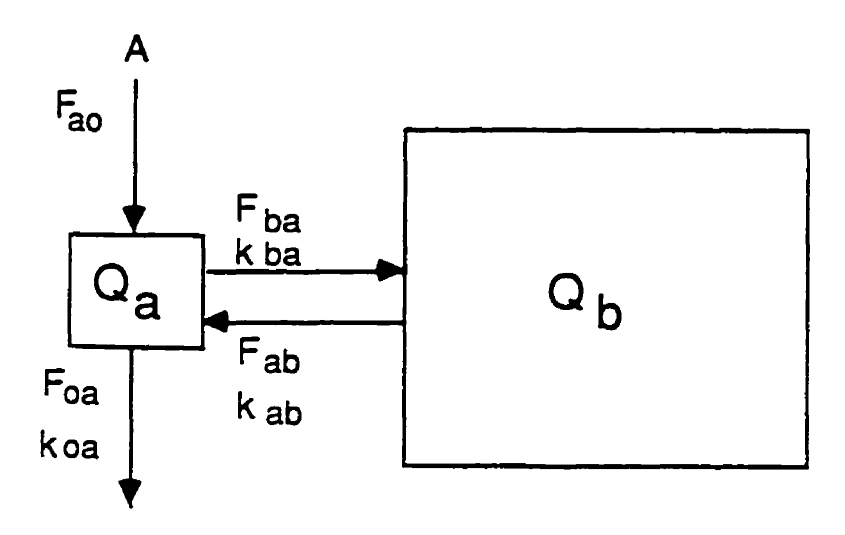


Fig. 1. Diagrammatic representation of the two-compartment model of ^{32}P kinetics in cladocerans. ^{32}P is introduced to the metabolic compartment (Q_a) through the animals's diet at a constant rate F_{ao} . ^{32}P accumulating in the structural compartment (Q_b) is described by a rate constant (k_{ba}) or a rate F_{ba} . Through recycling, ^{32}P returns from Q_b to Q_a with a rate constant of k_{ab} or a flux rate F_{ab} . A certain amount of ^{32}P is removed from Q_a through excretion with a rate constant (k_{oa}) or a rate of F_{oa} .

Table 1. List of major symbols used, and their meanings and dimensions.

Symbol	Parameter description
A	Assimilation, µg mg h ⁻¹
A _a ; A _b	Coefficients (intercepts) in double exponential expansion, CPM min ⁻¹
AE	Assimilation efficiency, dimensionless
b	Exponent in allometric equations, dimensionless
F _{ab} ; F _{ba}	Flux rates of P from pool b to pool a and from pool a to pool b,
	μg mg h ⁻¹
Fao	Rate of transfer of P from environment to compartment a, µg mg h-1
F_{oa}	Rate of transfer of P from compartment a to the environment, $\mu g \ mg \ h^{-1}$
I	Ingestion rate, µg mg h ⁻¹
k _a ; k _b	Fractional turnover rate of P transfer from compartment a and b, min-1
k_{ab} ; k_{ba} ; k_{oa}	Fractional turnover rate of P from compartment b to compartment a; from
	compartment a to compartment b; from compartment a to the environment.
	min ⁻¹
$Q_a; Q_b$	Pool size of compartment a and b, µg
w	Animal body dry weight, mg

In the modelling processes, we further specified that the rate constants (k) and flux parameters (F_{ab} , F_{ba} , F_{oa}) are power functions of body size (W) such that

Rate parameters
$$(k \text{ or } F) = aW^b$$
 (4)

In all cases, flux rates represent mass specific fluxes and have the units of μg P $mg^{-1}\ h^{-1}$.

Materials and Methods

Animal culture, sizing and body P determinations - Six species of cladocerans (Daphnia magna, D. pulex, D. galeata, Simocephalus vetulus, Ceriodaphnia quadrangula and Bosmina longirostris) were kept in separate aquaria with dechlorinated Montreal tap water on a 14h:10h light/dark cycle. The water temperature was maintained at approximately 20°C. Stock animals were fed ad libitum with "green water" from a goldfish tank (Peters 1987a). The animals used in the experiments were sized under a dissecting microscope fitted with an ocular micrometer. Length (L, mm) was taken as the distance from the anterior margin of the head to the base of the tail spine. Dry body weight (W, mg) of the large species was obtained by drying 10-25 sorted animals of different sizes at 60°C for 24 h, cooling them in a desiccator, and weighing them individually to the nearest 0.1 µg on a Cahn Electro balance. The dry body weight of small individuals was determined for each species by

weighing a group of similarly sized animals (within 0.01 mm). Animal body P content was measured with the ascorbic acid modification of the molybdenum blue technique (Strickland and Parsons 1968), after persulfate oxidation of the organically bound P (Menzel and Corwin 1965). All measurements of body P were made in duplicate.

Radioactivity counting - Cerenkov counting was used to measure total radioactivity of the samples. Because this counting is conducted without scintillation fluor (Wang et al. 1975; Haney et al. 1986), the technique has the advantages of rapid sample preparation, reduced cost and reduced chemical quenching. Before counting, animals were digested overnight in a tissue solubilizer at 60°C, and then transferred to plastic scintillation vials. Counts were made with an LKB Wallac liquid scintillation counter for 10 min. All samples were counted in triplicate to a reliable error (95% confidence level) of ±5%. In sample preparation, all glassware and plasticware was soaked in acid overnight to remove all radioactivity, washed with P-free detergent, and rinsed three times with deionized, distilled water. All solutions were prepared with deionized-distilled water. All reagents were of reagent grade or better and checked for possible P contamination.

Isotope-labelling of yeast - Log-phase yeast, <u>Rhodotorula glutinis</u>, grown in Downing and Peters' (1980) culture medium, were placed in carrier-free medium containing approximately 50 KBq of ³²P-PO₄ (New England Nuclear), and incubated at room temperature for over 24 h to incorporate the tracer.

During exposure, the uniformity of labelling of the yeast was checked by comparing the specific activity of a labile cell fraction to that of the whole cells. The labile cell fraction was obtained by centrifuging the labelling yeast cells, resuspending them in 100 mL of ice-cold 10% (w/w) trichloroacetic acid (TCA) for 10 min and centrifuging them again to collect the supernatant. Samples of the supernatant and whole radioactive culture were then assayed for radioactivity by a liquid scintillation counter in five replicates; other subsamples were chemically analyzed for total phosphorus.

P ingestion - We determined the ingestion rates of ³²P labelled yeast cells by different sized cladocerans with the technique of Rigler (1971). From 50 to 300 animals, depending on size, were allowed to feed for 30 - 60 min in a feeding chamber containing 500-1000 mL of non-radioactive yeast suspension at a concentration of 10⁵ cells mL⁻¹. Burns and Rigler (1967) indicated that Daphnia reached maximum feeding rates at this concentration. McMahon (1965) and Geller (1975) reported that a prefeeding time of 30 min was needed for adaptation to food concentration and quality. The feeding period before labelling also allowed animals to acclimatize to the test conditions and minimized differences in initial gut fullness. After the initial feeding period, an equal volume of ³²P-labelled yeast suspension at the same concentration as the non-radioactive cells was added to the chamber and gently mixed with the non-radioactive suspension. At 2 to 15 min intervals, 3 to 5 individual animals were quickly removed from the feeding chamber, anaesthetized in carbonated

water, rinsed thoroughly in distilled water, transferred to plastic scintillation vials, and immediately measured for radioactivity. Uptake curves were established by plotting radioactivity in animals as a function of feeding time. To delimit the ingestion phase in the uptake curves, we applied the STEPWISE procedure (SAS Institute Inc., 1983) to fit the data to a quadratic regression:

$$y = a_1 + b_1 x + b_2 x^2 (5)$$

where y is animal body radioactivity and x is feeding time. The first inflection point was taken to indicate the onset of defecation of unassimilated tracer. Since in the initial stage of the radioactive feeding, the radioactivity of the animal body should increase linearly with time (Rigler 1971), we expected that the slope (b_1) of the linear term (x) would be significantly different from 0, but the slope (b_2) of the quadratic term (x^2) would be not significant. We tested this a priori expectation by adding each time point sequentially to the regression equation until b_2 became significant, which indicates a curvilinear change resulting from egestion of radioactive food (Rigler 1971). The linear slope (b_1) was taken as tracer uptake rate (cpm mg⁻¹ min⁻¹) and converted to P ingestion rates (µg mg⁻¹ min⁻¹) on multiplication by the specific activity (cpm a_2) of the yeast P.

P release - Isotope release measurements were performed in 21-mL gelfiltration columns (Pharmacia Fine Chemicals), which had been modified to flow-through chambers by fitting each end with Pharmacia flow adapters with 75 µm Nitex screens to retain the animals in the columns. Groups of 5 to 25 animals of similar size, which had been fed labelled yeast cells at 10⁵ cells mL⁻¹ for 7-10 days (Peters and Rigler 1973), were gently introduced to the column to allow adaptation to the experimental conditions. A suspension of 10⁵ radioactive yeast cells mL⁻¹ was pumped into the top of each column by a Buchler peristaltic pump at 1 mL min⁻¹. After 30-60 min, an identical concentration of non-radioactive yeast culture was pumped in at 5 mL min⁻¹ for 5 min to replace all radioactive suspension in the column and to allow animals to begin to clear their guts of undigested radioactive cells. Because flow is laminar in these columns, 5 min was sufficient to flush the entire column, as confirmed by experiments with dye. The flow rates were then reduced to 1 mL min⁻¹, the eluant was collected at 5 min intervals for 8 to 24 h by an LKB automatic fraction collector, and the radioactivity of subsamples of each fraction was determined.

³²P release rate was estimated from the time course of radioactivity in the eluant. Since samples collected in the first 5 to 15 min were likely contaminated by radioactive faeces, depending on body size, the first 5 to 15 min samples were discarded in the estimation. As a result, ³²P release is intended to represent excretion only. To determine the ³²P turnover rate constant in each fully labelled compartment over time, we first fitted the tracer data to a double exponential function:

$$A_{t} = A_{a} \exp(-k_{a}t) + A_{b} \exp(-k_{b}t)$$
 (6)

All curve fitting was conducted by the 3R routine of the BMDP package. This program allows direct iterative estimation of non-linear parameters using the efficient algorithm of the Newton-Raphson procedure (Dixon 1988). The adequacy of the model fit was assessed by the residual sum of squares (RSS), the asymptotic standard deviations of the parameters, and the homoscedasticity of the residuals with time. This approach to fitting compartmental models is much more direct, convenient and powerful than the traditional curve peeling of the graphical method (Riggs 1963). Estimates for the components (k and A) of exponential decay curves emerge directly from the Newton-Raphson fitting procedure, so there is no need to subtract the asymptote from the curve (Conover and Francis 1973). The computer program provides the asymptotic standard deviation, which is essential for statistical comparisons.

We used both fractional turnover and P flux to represent ³²P loss from a pool. Fractional rate of loss is calculated as a proportion of the P content of the pool lost per unit of time and is expressed per min. For P flux, the loss was expressed in absolute units (µg min⁻¹). The two rates are related by:

fractional turnover rate = P flux rate / P content of the pool (7)

The fractional rates of turnover from pool a to pool b (k_{ba}) and from the metabolic pool to the outside (k_{oa}) were estimated after normalization of equation (6) using the techniques described by Shipley and Clark (1972). Because the intercompartmental turnover rate (k_{ab}) cannot be determined

accurately, it was calculated by solving the differential equation (2) at steady state:

$$k_{ab} = k_{ba} \times Q_a / Q_b \tag{8}$$

The relative pool sizes of compartments Q_a and Q_b were computed from the exponents and time-zero intercepts of the double exponential expression of ^{32}P loss (equation 6) by the method of Conover (1961). The absolute sizes of each pool were then calculated by multiplying the total body P content by the relative pool size. P flux was estimated as the product of the absolute pool size of the donor pool and its corresponding fractional turnover rate.

P assimilation - To explore P metabolism in cladocerans further, we estimated 32 P assimilation rates as model-derived influx rates (F_{ao}). For comparison with the rates of 32 P assimilation, 32 P ingestion rates for these experimental animals were calculated from the experimentally determined size-specific ingestion rate functions. Assimilation efficiency was then calculated as assimilation rates/ingestion rates x 100 (Peters 1984). Both assimilation rates and efficiencies were analyzed as a function of size.

Allometric statistics - We estimated the slopes and intercepts of all allometric relationships by least-squares linear regression of log-transformed data. The strengths of the relationships were determined by the coefficients of determination (r^2) , standard errors of the regression $(S_{y,x})$ and by visual inspection of the data plots. The homogeneity of the allometric lines was tested with an F-test and the null hypothesis (b = -0.25) was tested with a Student

t-test. For all statistical comparisons, p < 0.05 was considered to represent a significant difference.

Results and Discussion

Body dry weight and P content

The allometric relation between body dry weight (W, mg) and body length (L, mm) for all species studied is best described as

$$W = 0.013L^{2.14\pm0.12} \quad (r^2 = 0.85, S_{y,x} = 0.55, n = 54, p < 0.01)$$
(9)

where 0.12 is the standard error of the slope. Both the allometric scaling factor (2.14) and the constant (0.013) in the above power function agree well with those reported by Burns (1969), Porter et al. (1982) and Lynch et al. (1986) for freshwater cladocerans. There is also a significant power function between dry body weight (W, mg) and body P content (P, µg), which can be quantitatively described by the equation:

$$P = 13.18W^{1.02\pm0.03}$$
 ($r^2 = 0.98$, $S_{y,x} = 0.20$, $n = 28$, $p < 0.01$). (10)

On average, individual body P content was 1.26% of its dry body weight, which is also similar to published values (Vijverberg and Frank 1976; Peters 1983; Behrendt 1990; Andersen and Henssen 1991).

Homogeneity of yeast labelling

 $^{32}\mathrm{P}$ incorporation by the yeast cells reached an equilibrium about 72 h after

inoculation (Table 2). The efficiency of label uptake became highest on the 3rd and 4th day of culture, when 98 to 100% of ^{32}P was bound in yeast cells. There was no significant difference in radioactivity between these two days (t test, n=5, p > 0.05), indicating that 3-4 days was long enough to achieve homogeneous labelling, which is consistent with the yeast labelling time of other studies (Peters and Rigler 1973). After 96 h radiolabelling, 2.7×10^5 CPM was equivalent to 1 µg of the yeast-TP.

P ingestion

The time course uptake of ³²P from labelled yeast cells by cladocerans differed considerably among species (Fig. 2). Nevertheless, in all species, the uptake of radioactivity was almost linear over the first 5-60 min after introduction of the radioactive food suspension. This may reflect constant rates of feeding as the animals consumed radioactive food. Thereafter, the rates of accumulation became less rapid, probably reflecting the simultaneous processes of defecation and excretion. There are no clear inflection points in the uptake curves, so gut passage time could not be estimated adequately. A similar difficulty was encountered by Muck and Lampert (1984) in their studies of Daphnia feeding on ¹⁴C-labelled algae. This gradual transition between ingestion and assimilation may be attributed primarily to the inter-individual variability in feeding activity and assimilation efficiency, and to high assimilation efficiency when cladocerans eat P-limited food (Olsen and Østgaad

1985).

Although highly variable, size-specific P ingestion rates (I, µg mg⁻¹ h⁻¹) show a strong tendency to decrease with increasing body size (Fig. 3) and can be described by the following power model:

$$I = 0.035W^{-0.24(\pm 0.09)} (r^2 = 0.39, S_{y,x} = 0.19, n = 13, p < 0.01)$$
 (11)

The exponent of -0.24 is not significantly different from -0.25 (t test, p> 0.05), implying that the ingestion rates have the same body size dependence as other metabolic rates for other animals (Peters 1983).

P release

³²P activity of cladoceran excreta declined rapidly when the animals were placed in unlabelled yeast suspension. The initial 5-15 min changes were excluded since they included the defecated label. The subsequent loss of radioactivity was exponential (Fig. 4). In 1-5 min, the excreta radioactivities were reduced to 20-30% of the initial values. Thereafter changes in release rates of the isotope became gradually smaller and more linear. There was pronounced variability in the release curves both among individuals (Fig. 4) and among species (Table 3). This variation is common in labelled excretion experiments (Marshall and Orr 1955) and probably reflects experimental stresses on the animals.

Based on the fit to the data, for most experiments, ³²P activity-time

Table 2. The time course of specific activity of TCA extractable fraction (TCSA, CPM), total specific activity of the yeast suspension (TSA, CPM), TCSA/TSA (%), total phosphorus (TP, μ g) and total radioactivity (TA, CPM) of the yeast cells (n = 5).

Labelling	TCSA		TSA		%	TP		TA	
time (h)	Mean	SD	Mean	SD	-	Mean	SD	Mean	SD
48	0.298	0.026	0.319	0.028	93.23	0.186	0.006	53161	3783
72	0.324	0.010	0.328	0.021	98.81	0.184	0.004	54080	2886
96	0.301	0.008	0.299	0.011	100.64	0.188	0.003	50217	1473

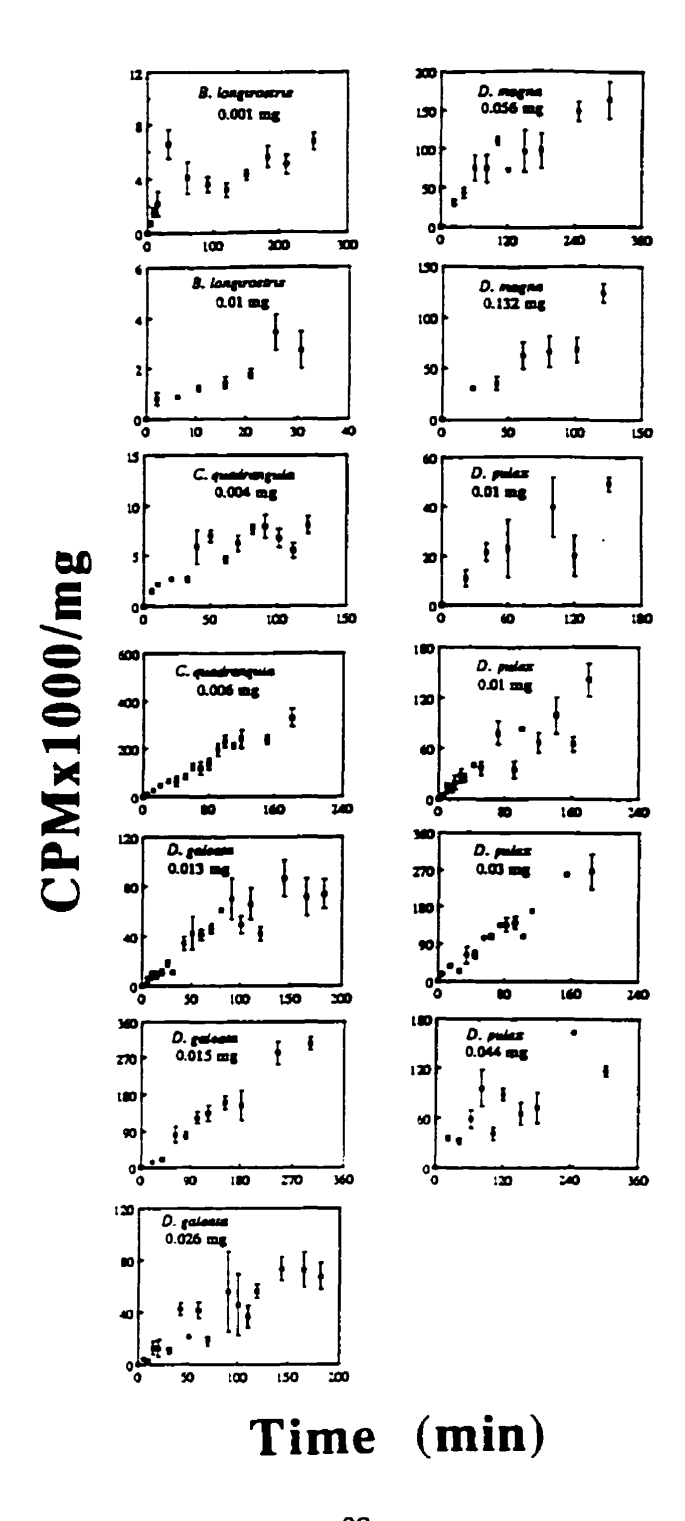


Fig. 2. Changes (mean ± SD) of body ³²P activity in individual groups of cladocerans after transfer from non-radioactive to radioactive yeast suspension.

relations conformed to a simple two-compartment model (Fig. 4). For others (mainly <u>D</u>. <u>magna</u>, and some <u>C</u>. <u>quadrangula</u> and <u>D</u>. <u>pulex</u>), a higher order compartmental model seems to fit better. The coefficients (time zero intercept) and exponents (fractional rate constants) of the exponential function fitted to all curves for ³²P loss (Table 3) showed significant variations among different sizes and species of cladocerans. The fractional turnover rates of pool a (k_a) varied 6-fold and those of pool b (k_b) varied 21-fold. There was a clear trend for small individuals to have large fractional turnover rates for pool a $(b=-0.46, r^2=0.73, S_{y,x}=0.16, n=14, P<0.01)$. There was a similar trend for pool b, but the power function was not significant $(b=-0.27, r^2=0.15, S_{y,x}=0.36, n=14, p>0.05)$. This lack of significance reflects the high variations of the second exponents, possibly related to the small values of the rate constants in the large compartments.

The relative pool sizes of both exchangeable compartments (% Q_a and % Q_b) varied only slightly among species (Table 3) ranging between 1 and 5% for pool a. The relative dimensions of both pools are independent of body size (for pools a and b: $r^2 = 0.06$, $S_{x,y} = 1.42$, n = 14, p > 0.05).

The values of k_{ba} were 18-87 times bigger than those of k_{ab} and both parameters varied over an order of magnitude. The fractional turnover rates for excretion were intermediate between k_{ab} and k_{ba} and varied over 10 times as well. The fractional rate constants for the conversion between two pools (k_{ab} and k_{ba}) and for the excretion from the first pool (k_{oa}) declined with increasing

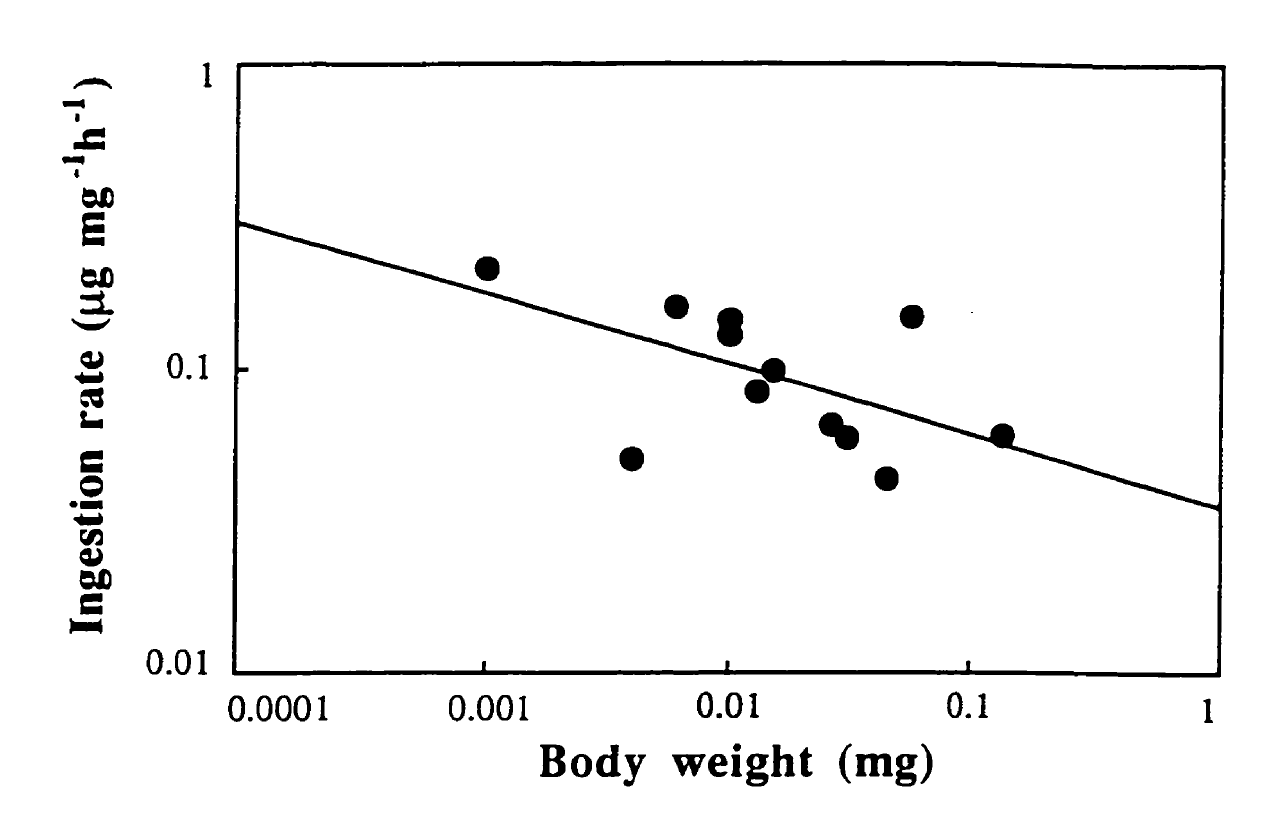


Fig. 3. The allometric relations describing the size dependence of P ingestion rate in cladocerans feeding on a radio-labelled yeast suspension.

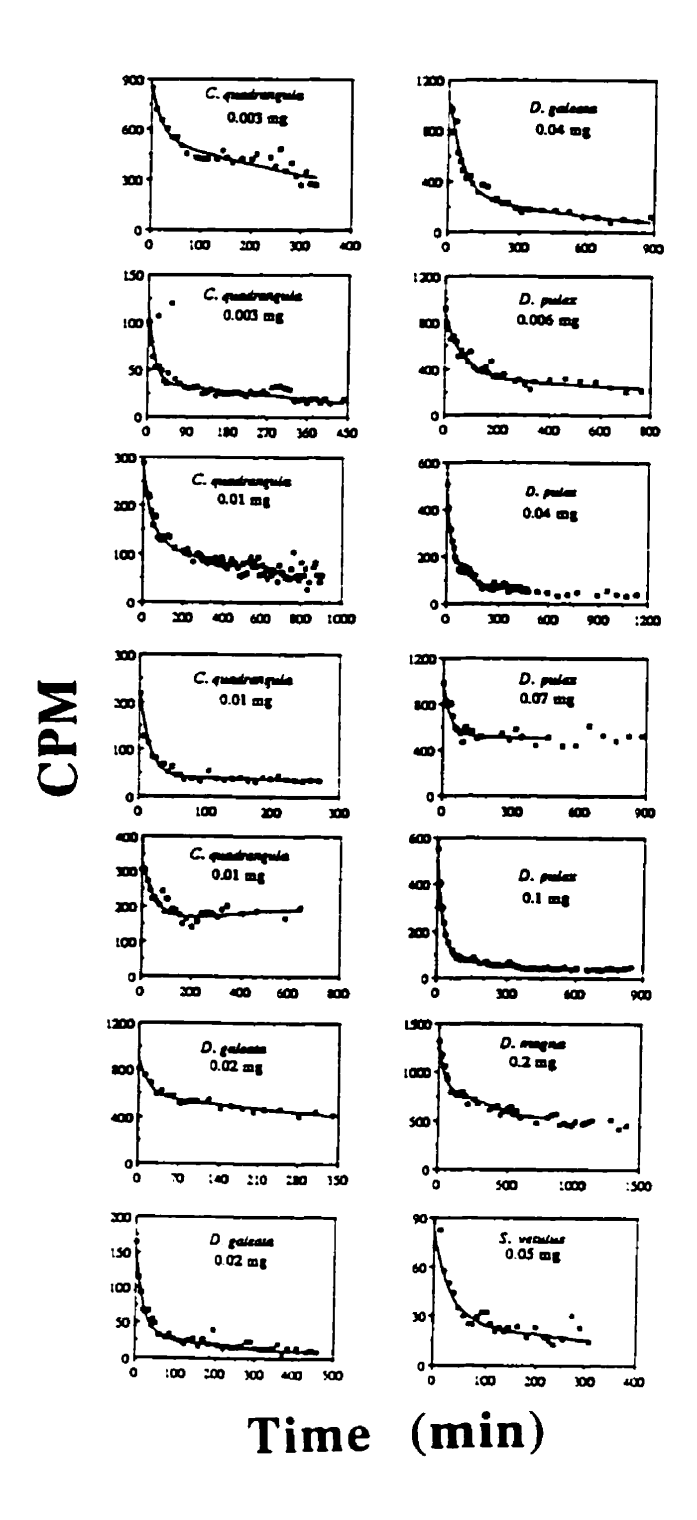


Fig. 4. Experimentally observed (dots) and model-fitted (solid line) time-course curves of ³²P excreted by initially fully labelled individual groups of cladocerans feeding on nonradioactive food at various time-intervals.

Table 3. Values (mean±SD) of model parameters deduced from computer-curve fitting a double exponential equation to excreted ³²P activity data and the relative pool sizes of two compartments in the different species of cladocerans studied. N is the number of runs.

Species	N	Mean	Aa	Ka	A _b	К _b	%Qa	%Qb
		dry	CPM	min ⁻¹	CPM	min ⁻¹	%	%
		weight	min ⁻¹		min ⁻¹			
		(mg)						
D. magna	1	0.2	570.79	0.0167	767.67	0.0010	4.35	95.65
S. vetulus	1	0.05	55.38	0.0358	280.21	0.0021	1.24	98.86
D. galeata	3	0.027	363.64	0.0482	621.50	0.0019	2.18	97.82
		±0.009	±185.00	±0.0197	±218.82	±0.0010	±0.51	±0.51
D. pulex	4	0.054	377.72	0.0495	292.47	0.0011	3.28	96.72
		±0.035	±233.55	±0.0318	±166.00	±0.0005	±1.44	±1.44
C. quadrangula	5	0.007	197.81	0.0911	159.57	0.0029	3.26	96.74
		±0.003	±115.77	±0.0082	±197.58	±0.0024	±0.93	±0.93

body size (Fig. 5) and can be described by the following power functions (n = 14):

$$k_{ab} = 0.00004W^{-0.66 \pm 0.26}$$
 ($r^2 = 0.35$, $S_{v,x} = 0.52$, $p < 0.05$) (12)

$$k_{ba} = 0.0024W^{-0.54\pm0.18}$$
 ($r^2 = 0.44$, $S_{y,x} = 0.35$, $p < 0.05$) (13)

$$k_{oa} = 0.0011W^{-0.31\pm0.08}$$
 (r² = 0.56, S_{v,x} = 0.16, p < 0.01) (14)

The exponent (-0.31) for k_{oa} does not significantly differ from theoretical expectation for b-1 = -0.25 (t test, n = 14, p> 0.05). Similar exponents have been determined experimentally for many metabolic activities of zooplankton (Peters 1983, 1987b). However, the exponents of kab and kba were significantly less than expected, so these rate constants decrease much faster with body size than does excretion (t test, n = 14, p < 0.01).

Both intercompartmental flux rates and excretion rates decreased with increasing body size (Fig. 6), and can be reflected by the following equations (n = 14):

$$F_{ba} = F_{ab} = 0.049W^{-0.52\pm0.23} (r^2 = 0.31, S_{y,x} = 0.46, p < 0.05)$$
 (15)

$$F_{oa} = 0.021W^{-0.30\pm0.11}$$
 $(r^2 = 0.28, S_{y,x} = 0.25, p < 0.05)$ (16)

The exponent (-0.30) of the allometric equation for F_{oa} did not significantly differ from -0.25 (t test, n=14, P> 0.05), indicating that this flux rate followed the same trend as other physiological rates of routine metabolism with respect to relation to body size. The exponents of F_{ba} and F_{ab} are, however, significantly lower than -0.25 (t test, p < 0.01), suggesting that these flux rates decrease much faster with body size than release rates.

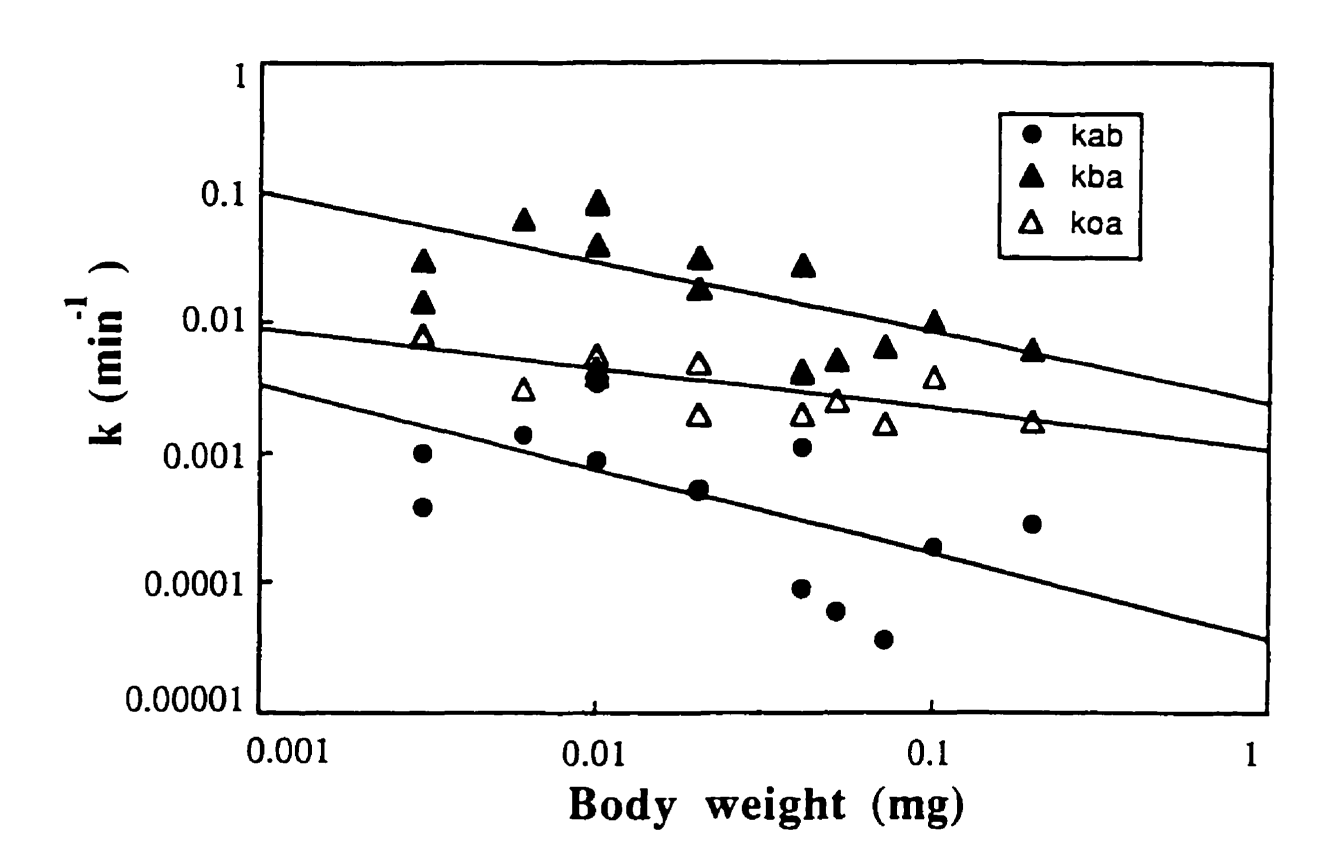


Fig. 5. The allometric relations describing the size dependence of intercompartmental release and fractional turnover rates.

P assimilation

Our model assumes that assimilation rates (F_{ao}) are equal to excretion rate (F_{oa}) in steady state (Eq. 2). The slope of the power function for ^{32}P size-specific assimilation rates would therefore be close to -0.25, as expected, and the assimilation efficiencies can be then derived by the power equation:

$$A/I = 0.021 \text{ W}^{-0.30}/0.035 \text{ W}^{-0.24} = 0.60 \text{ W}^{-0.06}$$
 (17)

Because the exponent (-0.06) is very close to zero, cladoceran P assimilation rates appear to be above 60% (66-85%) of ³²P ingestion and independent of body size.

General Discussion

Compartmental modelling of P fluxes

Our results demonstrate that P fluxes in cladocerans could be modelled with a two-compartmental system (Fig. 6). This is consistent with Lampert and Gabriel (1984), who also found that the ¹⁴C dynamics in <u>Daphnia</u> followed a two-compartment model. However, we further found that for some cladocerans, a model of more than two pools could better describe the tracer dynamics. This finding may account partially for the large variance in most estimated model parameters. As Shipley and Clark (1972) pointed out, combining three-, four-, or more compartments into a working model with only two compartments may introduce errors.

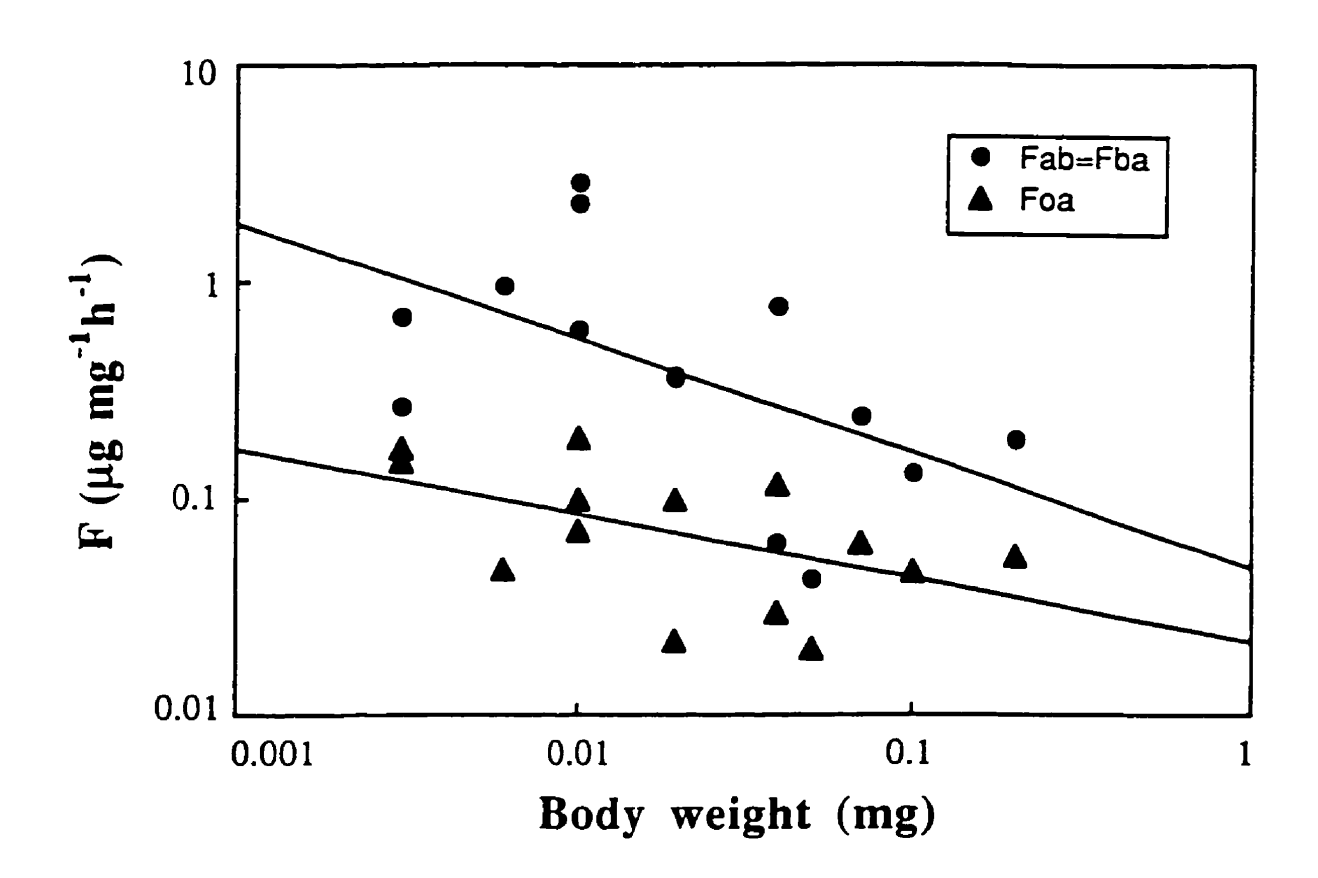


Fig. 6. The allometric relations describing the size-dependence of intercompartmental exchange and exit flux rates.

We demonstrated that in all the cladocerans investigated, the relative pool size of rapidly exchanging pools was much smaller than the slowly exchanging pools, agreeing with previous results for zooplankton labelled with ³²P (Conover 1961; Peters and Rigler 1973) and ¹⁴C (Brandl and Fernando 1975; Lampert 1975; Lampert and Gabriel 1984).

There are strong allometries in P release by cladocerans. Smaller species have higher rates per unit body size than large ones. The slope of the regression describing relations between body size and release rates (-0.30±0.11) did not significantly differ from the theoretical expectations of -0.25, which suggests that the allometry of P release in cladocerans is similar to those for other metabolic activities. Our exponent is somewhat higher than that of Peters and Rigler (1973) for <u>Daphnia</u> (-0.38), but lower than that recorded by Ejsmont-Karabin (1984) for Cladocera (-0.23) and that for freshwater zooplankton (-0.16) reported by Gutel'makher (1977). These disagreements with the literature values may be due to the experimental protocols that involved different food P levels, zooplankton species, and number of compartments analyzed.

The two compartmental models can only provide an approximate fit to the complex metabolic and structural processes that underlie tracer kinetics. Thus, one could always fit more compartments, if the data are sufficiently numerous. However, given the quality of available data, models involving more than two or three compartments are rarely justified. The surprisingly steep allometric

slopes describing intercompartmental exchanges may reflect an adjustment in fitting multi-compartmental processes to a two-compartment model. In other words, the anomalously steep exponents for the exchange rates between the compartments may reflect the net effect of second or higher order exchanges involving several interacting compartments.

Our model provides a new quantitative insight into P release in cladocerans. A crude comparison shows that the excretion rates of P we measured fall in the lower range of literature values (Table 4). Our rates are very close to those of Rigler (1961); Barlow and Bishop (1965), LaRow (1971), Peters and Lean (1973) and Olsen and Østgaard (1985). Although our rates refer to total P, and not just to biologically available PO₄, Peters and Lean (1973) showed that most of the P excreted by <u>Daphnia</u> was PO₄ (90%) and even soluble organic forms may be available. Our relatively low P excretion rates probably reflect the use of P-starved yeast as food. Other possible sources of underestimation inherent to the technique employed could be responsible: P sinks via growth, reproduction and ecdysis (Peters and Rigler 1973) were not measured. Other comparisons are difficult to make because literature estimates of P release rate are highly variable (Peters 1987b), and often reflect methodological and environmental influences. All of the following affect zooplankton excretion rates to some extent: re-uptake of excreta by animals (Ganf and Blazka 1974; Takahashi and Ikeda 1975; Blazka et al. 1982) and by epizootics living on the zooplankton (Rigler 1961; Peters and Lean 1973);

starvation (Takahashi and Ikeda 1975); injury (Mullin et al. 1975; Ikeda et al. 1982); reproductive stage (Scavia and McFarland 1982); size of the experimental animals (Johannes 1964; Ikeda et al. 1982; Peters 1983; Ejsmont-Karabin 1984); incomplete labelling of animals (Peters and Rigler 1973; Peters 1975); and quantity and quality of the diet (Scavia and Gardner 1982; Lehman and Naumoski 1985; Olsen and Østgaard 1985; Sterner 1990). Further studies are required to examine the contributions of these potential sources of error to the variability of ³²P release rates.

The validity of the feeding and flux allometries

Few workers have attempted to estimate cladoceran P ingestion rates by a radiotracer technique as we did, so its validity should be examined. Because our results show that the estimated ingestion rates are sufficient to sustain excretion, an indirect test is possible by comparing our ingestion rates with others in the literature. Reported ingestion rates (reviewed in Chow-Fraser and Sprules 1992) are generally similar to those we measured, which also fall within the range predicted by the empirical model of Peters and Downing (1984) for cladocerans. Because their model was based on a large number of literature values, this consistency supports our data for both ingestion and excretion. We also showed that ingestion in cladocerans is a size-dependent process, with the specific rates decreasing with body size at a rate constant close to -0.25, again in good agreement with general trends (Peters 1983,

Table 4. Comparison of size-specific P release rates of limnetic zooplankton measured by different techniques. W = body dry weight (μg); T = temperature (^{0}C); RR = release rate (μg P mg⁻¹ h⁻¹); M = method of measurement; na = data not available.

Species	W	Т	RR	M	Investigator
D. magna	250	20-22	0.032	Radiotracer	Rigler (1961)
D. pulex	21	10-25	0.927	Radiotracer	Whittaker (1961)
Cladocera	0.9	5-20	0.085-0.190	Chemical	Barlow and Bishop
					(1965)
D. rosea	13.4	20-22	0.08	Radiotracer	Peters and Lean (1973)
D. galeata	1-10	20	0.30-1.10	Radiotracer	Peters (1975)
Zooplankton	4-12	15	0.04-0.08	Chemical	LaRow (1971)
<u>Daphnia</u> spp.	na	10-20	0.16-0.39	Chemical	LaRow et al. (1975)
D. pulex	20	20	0.15-0.21	Chemical	Lehman (1980)
Zooplankton	10-70	20	0.32-0.80	Modelling	Bartell (1981)
<u>Daphnia</u> spp.	10-48	15-16	0.05-1.5	Chemical	Olsen and Østgaard
					(1985)
Zooplankton	1-5	18-20	0.17	Chemical	den Oude and Gulati
					(1988)
D. longispina	2->55	na	0.23-1.06	Radiotracer	James and Salonen
			0.14-0.7	Modelling	(1991)
Cladocera	3-200	20	0.02-0.19	Radiotracer	Present study

1984). Consequently our equation provides information about P flux that seems both physiologically meaningful and quantitatively reliable.

Our estimates of phosphorus assimilation efficiency seem typical for zooplankton if somewhat high. Lampert (1987) indicated that the assimilation efficiencies of Daphnia species varied nearly 10-fold (10.5-100%) in the literature, depending on the food concentration and quality, temperature, nutritional state and physiological condition of the animals. Schindler (1971) found similar variation in assimilation efficiencies for D. longispina feeding on different foods. Our calculated P assimilation efficiencies are at the high end of the range reported by Rigler (1961) for D. magna (40%), Haney (1971) for D. galeata medotae and D. rosea (60%), Peters and Rigler (1973) for D. rosea (0-100%), James and Salonen (1991) for Daphnia sp. (52.6-63.3%) and Taylor and Lean (1991) for lake zooplankton (21-63%), but are comparable to those by Marshall and Orr (1955) for Calanus spp. (15-99%) and Berner (1962) for Temora longicornis (50-98%). Our values may be higher because the yeast were grown in P limited cultures to increase assimilation of the label; Olsen and Østgaard (1985) have noted that when food P is in low supply, P assimilation is high and P release is low. Our estimates seem more reliable than previous ones because our values fall in the range of those measured for various food items and are less variable. It is clear that compartmental analysis can provide fairly good estimates for assimilation rates for cladocerans.

Our two-compartment model also allows a quantitative assessment of the

effects of non-uniform labelling and of compartment numbers on the cladoceran P excretion rates (Table 5). To evaluate the effect of incomplete labelling, the model of Fig. 1. and Equations 1 and 2 with their parameters set by the allometric equations 11-14 and 17 were used to estimate the distribution of the tracer in compartments A and B. After 1, 5, 10, 30, 50 and 100 h of "feeding" on radioactive food, these model animals were no longer given labelled diet to simulate the dynamics of ³²P excretion, and to estimate P excretion rate. Excretion rate was estimated as the product of pool size a and excretion rate constant (kna). Pool size a, the amount of phosphorus in compartment A at time t, was calculated as 0.0126W*Q $_a$ /(Q $_a$ +Q $_b$), where Q $_a$ and Q $_b$ are the amount of tracer in compartment a and b, W is animal dry weight in mg and 0.0126 is the proportion of P in cladocerans. The results (Table 5) clearly indicate that the further the animals depart from equilibrium of tracer and tracee atoms between 31P and 32P (the shorter the incubation time), the larger the overestimation of excretion rates (5 to 19 times between 1 and 100 h radioactive labelling). It is also apparent that the larger the animal, the longer time is required for isotopic equilibrium with the P source. We also estimated the one-compartmental P excretion rates. We fitted one compartment model to the excretion data derived from the model with two compartments, and extrapolated the regression line to t = 0 at which point the intercept represents the loss rate of P from the single compartment (Peters and Rigler 1973). As shown in Table 5, treating a two-compartment system as though it consisted

Table 5. The results of a simulation to show the effects of incubation time and number of compartments on the cladoceran P excretion rates (µg mg⁻¹ h⁻¹).

Number of	Incubation	Body size (mg)				
compartments	time (h)	0.001	0.01	0.1	1	
	1	1.31	1.64	1.33	0.77	
	5	0.47	0.46	0.62	0.59	
2	10	0.36	0.28	0.35	0.43	
	30	0.29	0.16	0.14	0.19	
	50	0.27	0.13	0.10	0.12	
	100	0.26	0.11	0.07	0.07	
	1	5.67	3.40	1.70	0.83	
	5	2.28	2.42	1.63	0.83	
1	10	1.37	1.64	1.45	0.82	
	30	0.68	0.73	0.88	0.73	
	50	0.52	0.50	0.62	0.62	
	100	0.51	0.49	0.58	0.60	

only of one compartment may result in an overestimation up to 1 order of magnitude, depending on the animal size and labelling time.

Acknowledgements

We thank Drs. W. D. Taylor, J. Kalff, N. Price and J. Rasmussen for their helpful comments and suggestions to improve the manuscript. The Natural Sciences and Engineering Research Council of Canada (NSERC), Fonds pour la Formation de Chercheurs et l'Aide à la Recherche (FCAR), and the Graduate Faculty of McGill University provided financial support.

References

- Andersen, T., and D. O. Hensen. 1991. Carbon, nitrogen, and phosphorus content of freshwater zooplankton. Limnol. Oceanogr. 36: 807-814.
- Barlow, J. P., and J. W. Bishop. 1965. Phosphate regeneration by zooplankton in Cayuga Lake. Limnol. Oceanogr. (Supp.). 10: R15-R24.
- Bartell, S. M. 1981. Potential impact of size-selective planktivory on phosphorus release by zooplankton. Hydrobiologia 80: 139-145.
- Behrendt, H. 1990. The chemical composition of phytoplankton and zooplankton in an eutrophic shallow lake. Arch. Hydrobiol. 118: 129-145.
- Berner, A. 1962. Feeding and respiration in the copepod <u>Temora longicornis</u> (Müller). J. Mar. Biol. Ass. U.K. 42: 625-640.
- Blazka, P., Z. Brandl and L. Prochazkova. 1982. Oxygen consumption and ammonia and phosphate excretion in pond zooplankton. Limnol.

 Oceanogr. 27: 294-303.
- Brandl, Z., and C. H. Fernando. 1975. Investigations on the feeding of carnivorous cyclopoids. Verh. Internat. Verein. Limnol. 19: 2959-2965.
- Burns, C. W. 1969. Relation between filtering rate, temperature and body size in four species of <u>Daphnia</u>. Limnol. Oceanogr. 14: 693-700.
- Burns, C. W., and F. H. Rigler. 1967. Comparison of filtering rates of <u>Daphnia</u>

 <u>rosea</u> in lake water and in suspension of yeast. Limnol. Oceanogr. 12:
 492-502.

- Chow-Fraser, P., and W. G. Sprules. 1992. Type-3 functional response in limnetic suspension-feeders, as demonstrated by in situ grazing rates.

 Hydrobiologia 232: 175-191.
- Conover, R. J. 1961. The turnover time of phosphorus by <u>Calanus</u> finmarchicus. J. Mar. Biol. Assoc. U.K. 41: 484-488.
- Conover, R. J., and V. Francis. 1973. The use of radioactive isotopes to measure the transfer of materials in aquatic food chains. Mar. Biol. 18: 272-283.
- den Oude, P. J., and R. D. Gulati. 1988. Phosphorus and nitrogen excretion rates of zooplankton from the eutrophic Loosdrecht lakes, with notes on other P sources for phytoplankton requirements. Hydrobiologia 169: 379-390.
- Dixon, W. J. 1988. BMDP Software Manual. Berkeley: University of California Press.
- Downing, J. A., and R. H. Peters. 1980. The effect of body size and food concentration on the in situ filtering rate of <u>Sida crystallina</u>. Limnol. Oceanogr. 25: 883-895.
- Ejsmont-Karabin, J. L. 1984. Phosphorus and nitrogen excretion by lake zooplankton (rotifers and crustaceans) in relationship to individual body weights of the animal, ambient temperature and presence or absence of food. Ekol. Polska. 32: 3-42.
- Ganf, G. and P. Blazka. 1974. Oxygen uptake, ammonia and phosphate

- excretion by zooplankton of a shallow equatorial lake (Lake George, Uganda). Limnol. Oceanogr. 19: 313-324.
- Geller, W. 1975. Die Nahrungsaufnahme von <u>Daphnia pulex</u> in Abhangigkeit von der Futterkonzentration, der Temperature, der Korpergrosse und dem Hungerzustand der Tiere. Arch. Hydrobiol. (Suppl.), 48: 47-107.
- Gutel'makher, B. L. 1977. Quantitative assessment of the importance of zooplankton in phosphorus cycle in a lake. Zh. obshch. Biol. 38: 914-923.
- Haney, J. F. 1971. An in situ method for the measurement of zooplankton grazing rates. Limnol. Oceanogr. 16: 970-977.
- Haney, J. F., M. Brauer, and G. Nurnberg. 1986. Feeding and egestion rates of individual zooplankton using Cerenkov counting. Hydrobiologia 141: 165-174.
- Ikeda, T., E. Hing Fay, S. A. Hutchinson and G. M. Bato. 1982. Ammonia and inorganic phosphate excretion by zooplankton from inshore water of the Great Barrier Reef. I. Relationship between excretion rates and body size. Austr. J. Mar. Freshw. Res. 33: 55-70.
- James, M. R., and K. Salonen. 1991. Zooplankton-phytoplankton interactions and their importance in the phosphorus cycle of a polyhumic lake. Arch. Hydrobiol. 123: 37-51.
- Johannes, R. E. 1964. Phosphorus excretion and body size in marine animals:

 Microzooplankton and nutrient regeneration. Science 146: 923-924.
- Lampert, W. 1975. A tracer study of the carbon turnover of <u>Daphnia pulex</u>.

- Verh. Internat. Verein. Limnol. 19: 2913-2921.
- Lampert, W. 1987. Feeding and nutrition in <u>Daphnia</u>. In Peters, R. H., and R. de Bernardi (Eds). <u>Daphnia</u>. Mem. Ist. Ital. Idrobiol. 45: 143-192.
- Lampert, W. and W. Gabriel. 1984. Tracer kinetics in <u>Daphnia</u>: an improved two-compartment model and experimental test. Archiv. Hydrobiol. 100: 1-20.
- LaRow, E. J. 1971. Secondary production of predatory zooplankton. U.S. IBP EDFB Memo report #71-118. 44p.
- LaRow, E. J., J. W. Wilkinson and K. D. Kumar. 1975. The effect of food concentration and temperature on respiration and excretion in herbivorous zooplankton. Verh. Internat. Verein Limnol. 19: 966-973.
- Lehman, J. T. 1980. Release and cycling of nutrients between planktonic algae and herbivores. Limnol. Oceanogr. 25: 620-632.
- Lehman, J. T., and T. Naumoski. 1985. Content and turnover rates of phosphorus in <u>Daphnia pulex</u>: Effect of food quality. Hydrobiologia 128: 119-125.
- Lynch, M., L. J. Weider, and W. Lampert. 1986. Measurement of the carbon balance in <u>Daphnia</u>. Limnol. Oceanogr. 31: 17-33.
- Martinez, C. P., O. F. R. van Tongeren, and R. D. Gulati. 1995. Estimation of phosphorus metabolic rates of Daphnia galeata using a three compartment model. J. Plank. Res. 17: 1325-1335.
- McMahon, J. W. 1965. Some physical factors influencing the feeding behavior

- of Daphnia magna Straus. Can. J. Zool. 43: 603-611.
- Menzel, D. W., and N. Corwin. 1965. The measurement of total phosphorus in seawater based on the liberation of organically bound fractions by persulfate oxidation. Limnol. Oceanogr. 10: 280-282.
- Muck, P., and W. Lampert. 1984. An experimental study on the importance of food concentrations for the relative abundance of calanoid copepods and cladocerans. I. Comparative feeding studies with <u>Eudiaptomus gracilis</u> and <u>Daphnia longispina</u>. Arch. Hydrobiol. Suppl. 66: 157-179.
- Mullin, M. M., M. J. Perry, E. H. Renger and P. M. Evans. 1975. Nutrient regeneration by oceanic zooplankton: a comparison of methods. Mar. Sci. Comm. 1: 1-13.
- Nakashima, B. S., and W. C. Leggett. 1980. The role of fishes in the regulation of phosphorus availability in lakes. Can. J. Fish. Aquat. Sci. 37: 1540-1549.
- Olsen, Y., and K. Østgaard. 1985. Estimating release rates of phosphorus from zooplankton: Model and experimental verification. Limnol. Oceanogr. 30: 844-85
- Peters, R. H. 1975. Phosphorus regeneration by natural populations of limnetic zooplankton. Verh. Internat. Verein. Limnol. 19: 273-279.
- Peters, R. H. 1983. Ecological implications of body size. Cambridge University

 Press, Cambridge.
- Peters, R. H. 1984. Methods for the study of feeding, filtering and assimilation

- by zooplankton. p. 336-412. In Downing, J. A., and F. H. Rigler (eds.).

 A manual on methods for the assessment of secondary productivity in fresh waters. IBP Handbook no. 17. Blackwell.
- Peters, R. H. 1987a. <u>Daphnia</u> culture. In Peters, R. H. and R. de Bernardi (Eds.), Daphnia. Mem. Ist. Ital. Idrobiol. 45: 483-495.
- Peters, R. H. 1987b. Metabolism in <u>Daphnia</u>. In Peters, R. H. and R. de Bernardi (Eds.), <u>Daphnia</u>. Mem. Ist. Ital. Idrobiol. 45: 193-243.
- Peters, R. H., and J. A. Downing. 1984. Empirical analysis of zooplankton filtering and feeding rates. Limnol. Oceanogr. 29: 763-784.
- Peters, R. H., and D. R. S. Lean. 1973. The characterization of soluble phosphorus released by limnetic zooplankton. Limnol. Oceanogr. 18: 270-279.
- Peters, R. H., and F. H. Rigler. 1973. Phosphorus release by <u>Daphnia</u>. Limnol. Oceanogr. 18: 821-839.
- Porter, K. G., J. Gerritsen, and J. D. Orcutt Jr. 1982. The effect of food concentration on swimming patterns, feeding behaviour, ingestion, assimilation and respiration by <u>Daphnia</u>. Limnol. Oceanogr. 27: 935-949.
- Riggs, D. S. 1963. The mathematical approach to physiological problems.

 Waverly Press, Inc. Baltimore, USA.
- Rigler, F. H. 1961. The uptake and release of inorganic phosphorus by <u>Daphnia</u> magna (Straus). Limnol. Oceanogr. 6: 165-174.
- Rigler, F. H. 1971. Methods for measuring the assimilation of food by

- zooplankton. P 264-270. In Edmondson, W. T., and G. G. Winberg (eds.).

 A Manual for the Assessment of Secondary Productivity in Freshwaters.

 IBP Handbook No. 17. Oxford: Blackwell.
- Rigler, F. H. 1973. A dynamic view of the phosphorus cycle in lakes. p. 539-572. In Griffith, E. J., A. Beeton, J. M. Spencer, and D. T. Spencer (eds.).

 Environmental Phosphorus Handbook. Wiley NY.
- SAS Institute Inc. 1983. SAS/STAT User's Guide. Release 6.03 edition. Cary, NC: SAS Institute.
- Scavia, D., and W. S. Gardner. 1982. Kinetics of nitrogen and phosphorus release in varying food supplies by <u>Daphinia magna</u>. Hydrobiologia 96: 105-111.
- Scavia, D., and M. J. McFarland. 1982. Phosphorus release patterns and the effects of reproductive stage and ecdysis in Daphnia magna. Can. J. Fish. Aquat. Sci. 39: 1310-1314.
- Schindler, J. E. 1971. Food quality and zooplankton nutrition. J. Anim. Ecol. 40: 589-595.
- Shipley, R. A., and R. E. Clark. 1972. Tracer methods for in vivo kinetics. New York: Academic Press.
- Sterner, R. W. 1990. The ratio of nitrogen to phosphorus resupplied by herbivores: zooplankton and the algal competitive arena. Am. Nat. 136: 209-229.
- Strickland, J. D. H., and T. R. Parsons. 1968. A practical handbook of seawater

- analysis. 2nd ed. Bull. Fish. Res. Board Can. 167.
- Takahashi, M., and T. Ikeda. 1975. Excretion of ammonia and inorganic phosphorus by Euphasia pacifica and Metridia pacifica at different concentrations of phytoplankton. J. Fish. Res. Boad Can. 32: 2189-2195.
- Taylor, W. D. 1984. Phosphorus flux through epilimnetic zooplankton from Lake Ontario: Relationship with body size and significance to phytoplankton. Can. J. Fish. Aquat. Sci. 41: 1702-1712.
- Taylor, W. D., and D. R. S. Lean. 1981. Radiotracer experiments on phosphorus uptake and release by limnetic microzooplankton. Can. J. Fish. Aquat. Sci. 38: 1316-1321.
- Taylor, W. D., and D. R. S. Lean. 1991. Phosphorus pool sizes and fluxes in the epilimnion of a mesotrophic lake. Can. J. Fish. Aquat. Sci. 48: 1293-1301.
- Vézina, A. F. 1986. Body size and mass flow in freshwater plankton: models and tests. J. Plankton Res. 8: 939-956.
- Vijverberg, J., and T. H. Frank. 1976. The chemical composition and energy contents of copepods and cladocerans in relation to body size. Freshw. Biol. 6: 333-345.
- Wang, C. H., D. L. Willis, and W. D. Loveland. 1975. Radiotracer methodology in the biological, environmental and physical sciences. Prentice-Hall.
- Whittaker, R. E. 1961. Experiments with radiophosphorus tracer in aquarium ecosystems. Ecol. Monogr. 31: 157-188.

CHAPTER III

Quantitative Structure-Pharmacokinetic Relationships for Organic Toxicant Fluxes in <u>Chlorella pyrenoidosa</u>*

^{*} Submitted to Environmental Toxicology and Chemistry.

Abstract

The rate constants and flux rates of uptake, elimination and intercompartmental transfers of 22 14C-labelled organic compounds by the alga-Chlorella pyrenoidosa were quantified in short-term laboratory experiments. The pharmacokinetic fluxes of all toxicants were satisfactorily described by a two-compartment open model. Bioconcentration factors, rate constants and flux rates of uptake and those from the "structural pool" to the "metabolic pool" were positively correlated with the octanol/water partition coefficient (K_{ow}) . However, those of elimination and those from the "metabolic pool" to "structural pool" were negatively related to Kow. Molecular weight, parachor, connectivity index and boiling point, melting point and log aqueous solubility were all good correlates of rate constants and flux rates of uptake, elimination and intercompartmental transfers. In contrast, chemical density had no significant effect. Among all the structural variables studied, K_{ow} always gave good predictions. These quantitative structure-pharmacokinetic relations may be used to predict the rate constants of organic toxicants, and the possible pharmacokinetic flux rates by phytoplankton when aqueous concentration of organic toxicants are near their solubilities.

Introduction

The primary goal of a Quantitative Structure-Pharmacokinetic Relationship (QSPR) or Quantitative Structure-Activity Relationship (QSAR) is to establish a mathematical model to predict certain biological activity measurements from some structural parameters of a series of related chemical compounds. Such relationships are well established in pharmacology to predict the flux rates of medicinal drugs determined from pharmacokinetic modelling (Seydel and Schaper 1982). QSPRs provide powerful research tools for mapping and understanding adverse effects of chemicals and for predicting the biological activities of additional yet untested compounds. QSPRs offer great advantages in risk assessment and new drug discovery. However, the potential of this rational approach to assess the environmental hazards of organic toxicants has been exploited less in toxicology.

The model structure of QSPRs needs two types of state variables for each test molecule: the biological activity (e.g., uptake, elimination and intercompartmental exchanges) derived from pharmacokinetic analysis of concentration-time functions and one or more predictor variables describing chemical structure. The leading structural descriptors are the physicochemical properties of the molecules, including hydrophobic, electronic and steric parameters (Chu 1979). These properties determine the mode of interaction with the biosystem and the extent of toxicity. Hydrophobicity is related to the

possibility that a parent drug or toxicant will reach the site of action; electronic factors can influence the degree of ionization of the chemicals and the rate of uptake; and steric factors affect the intramolecular and intermolecular hindrance to reaction or binding. All three factors are involved in the reaction or interaction of toxicant with the receptor. The most frequently used physicochemical properties or chemical descriptors are n-octanol-water partition coefficient (K_{ow}) and aqueous solubility $(S, Mailhot \ and \ Peters \ 1988)$. For chemicals acting by the same mechanism, the potency of a specified biological activity exerted by these compounds can often be predicted by a single QSPR equation.

The objective of the present research was to develop general QSPR models to predict uptake, elimination and intercompartmental exchange rates of 22 structurally diverse organic chemicals by the alga <u>Chlorella pyrenoidosa</u>. The biological parameters describing uptake, elimination and intercompartmental exchange rates were determined by a two-compartment kinetic analysis of fluxes measured with radiolabled organic chemicals. All rate parameters were then correlated with the structural descriptors to establish QSPRs to describe and predict the relationships between pharmacokinetic flux rates and toxicant structure.

We selected <u>C</u>. <u>pyrenoidosa</u> as the sentinel organism because this species is a dominant phytoplankter in freshwaters, can be readily cultured in the laboratory, and has been frequently used in toxicological investigations

(Hermens 1986). The 22 organic toxicants were chosen because they are priority contaminants that require regulation.

Materials and Methods

Reagents and Labware

The 22 ¹⁴C-labelled organic compounds comprised important environmental toxicants and covered a wide range of structures (Table 1). Table 1 also gives source, purity and specific activity of these radiochemicals. These compounds were all reagent-grade and were used without further purification. Dimethyl sulfoxide (DMSO), toluene, acetone, or the unlabelled form of the same chemical was used as the vehicle to dissolve the radiochemical and dilute it to proper concentration. Exposure concentrations of all toxicants were at or below their reported aqueous solubility. None of the chemicals had any observable effects on the growth of alga. Radioactivity was assessed by liquid scintillation counting (LKB Wallac 1215 RackBeta liquid scintillation spectrometer) with quench correction by external standardization using a calibration curve made from ¹⁴C-spiked samples. Scintillation cocktails (Ready Micro) were purchased from Beckman Canada (Mississauga, Ontario).

All other reagents used in this study were of analytical grade or better.

Deionized water was used to prepare stock solutions and culture medium. To minimize any contamination, all tracer experiments was carried out in

Table 1. Test compounds

Compound	Symbol	Supplier	Purity	Specific activity (mCi/mmol)	
Acetone	AC	Sigma	>98%	2.7	
n-Butanol	BUT	Sigma	>98%	7.84	
Acetophenone	ACP	Sigma	>98%	17.57	
Benzoic acid	BZA	NEN	>99%	29.4	
Chloroform	CHL	Pathfinder	98%	13.9	
Benzene	BEN	Sigma	>99%	10.0	
Toluene	TOL	Chemsyn	>98%	2.16	
Atrazine	ATR	Amersham	99%	25	
Chlorobenzene	CB	Sigma	>98%	12.07	
Bromobenzene	BB	Sigma	94%	9.8	
1,2-dichlorobenzene	1,2-DCB	Sigma	>98%	10.7	
1,4-dichlorobenzene	1,4-DCB	Sigma	>99%	6.8	
2-methylnaphthalene	2MN	Sigma	>98%	8.92	
Benzene hexachloride	ВН	Amersham	97%	62	
1,2,4-trichlorobenzene	TCB	Sigma	>98%	12.8	
Anthracene	ANT	Amersham	98%	15.1	
1,2,3,4-Tetrachlorobenzene	TTB	Sigma	>99%	13.5	
4,4'-DDE	DDE	Sigma	>95%	12.7	
4,4'-DDT	DDT	Sigma	>95%	11.8	
Pentachlorobenzene	PTCB	Sigma	>99%	19.2	
Hexachlorobenzene	нсв	Pathfinder	98%	13.49	
2,2',4,4',5,5'-hexachlorobiphenyl	PCB	Sigma	>98%	12.6	

borosilicate containers with stoppers. All labware were soaked in Dekasol (ICN Radiochemicals) for 10 hours, in cleaning solution (ICN Biomedicals, Inc.) overnight, and then rigorously rinsed three times with deionized water before use. All culture medium and associated tubing were sterilized by autoclaving. Operations that might result in contamination by airborne particles were performed in a laminar flow hood with negative pressure of filtered air.

Test Organisms and Culture Conditions

The test alga was the unicellular, nonmotile, freshwater green alga Chlorella pyrenoidosa with an average cell volume of 13.9 µm³. The original culture was obtained from Carolina Biological Supply Company. Subsequent cultures were grown in cotton-stoppered 500-mL Pyrex flasks with the modified Woods Hole MBI growth media (Nichols 1979). Each unialgal culture was maintained in suspension by constant bubbling with a continuous stream of air passed through sterile cotton. The culture was incubated at a constant temperature (24±1 °C) and illuminated from above at 400 foot-candles by fluorescent light (General Electric cool-white) on a 16:8 h light/dark cycle. Stock culture was transferred to fresh medium every 4-7 days. Cells were counted with a Spencer bright line haemocytometer at the start of each experiment. Axenicity of the culture was periodically monitored by plating 1-ml aliquots of stock onto nutrient agar and incubating the plates along with the cultures. Contaminated cultures were discarded.

Uptake experiments

Algal cells in exponential growth (about 7 days old) were used for the uptake experiments because they are less variable in cell size. Because algal biomass may influence the magnitude of uptake rates (Richer and Peters 1993), the cultures were diluted with sterile stock solution to obtain a cell concentration of approximately 10⁵ - 10⁶ cells/L. Uptake rate per cell was not influenced by cell density over this range. Depending on the total radioactivity, 10-40 µl of radioactive tracer solution was added to each of the four 50-ml aliquots of algal suspension in Pyrex flasks. The flasks were closed with glass stoppers to minimize evaporation of the tracer. Flasks were continually agitated on a shaker table (100 rpm) to avoid algal setting within the flasks. and maintained at the same temperature and light conditions as the stock cultures. During the 8-h uptake experiment, two 1-ml aliquots were withdrawn from each of the six flasks at fixed time intervals from 5 min to 2 h, and placed in borosilicate glass minivials. After adding 5-ml Ready Micro, the total radioactive counts of the tracer in the flask were determined. Simultaneously, two 1-ml subsamples were also withdrawn, placed in two separate microcentrifuge tubes, and centrifuged at 6,500 rpm (6700 g) for 4 min. A 0.5ml sample of supernatant was transferred into a borosilicate glass scintillation minivial with 5-ml Ready Micro to determine the radioactivity of the tracer within the water. The remainder was vortexed vigorously to resuspend the pellet and also placed in a second scintillation vial with 5-ml Ready Micro and

counted for radioactivity. The amount of radioactivity associated with the cells was estimated by $Y = A_t - 2A_s$, where Y is the activity of the algal pellet, A_t the total activity, A_s the activity of the supernatant. A similar procedure was followed with two control flasks containing isotope but no algae. Each sample received 5-ml of counting fluor (Ready Micro) and was counted in a liquid scintillation counter for 4 min. Because the water concentrations of the compound under study decreased during the exposure, probably resulting from sorption to the flasks, evaporation and operational losses, the decline in the total radioactivity was estimated from the experimental and control vials. Any loss in the time course of sampling in comparison to the total counts should be due to the abiotic processes. Therefore, in the biouptake estimation, this abiotic loss should be corrected for the total radioactivity of each time-course sample.

Elimination experiments

During the exponential growth phase, 50-ml of algal culture was transferred to 125-ml flasks and 10 to 40-µl of the tracer was added. The alga was incubated in the radioactive solution until the uptake had reached a plateau. After removal from the culture medium, the algal density was adjusted to 10^4 - 10^5 cells ml⁻¹ using unlabelled culture medium. Then 30-ml of labelled algal culture were placed in a 21-ml gel-filtration column (Pharmacia Fine Chemicals). A glass microfibre filter (3 µm pore size) was placed on the lower flow adaptor to retain algae in the column, but to leave

water flow unimpeded. Uncontaminated culture medium was pumped into the chamber through the top adaptor at approximately 100 ml h⁻¹ to maintain a constant water level in the column. At 5-min time intervals, the eluent was collected by a Pharmacia LKB FRA 100 fraction collector. One ml from each collected fraction was placed in a scintillation minimial and 5 ml of Ready Micro (LKB) scintillation cocktail was added. The samples were counted for 4 min in the liquid scintillation spectrometer.

Pharmacokinetic modelling

Uptake

For all the chemical compounds tested, the resulting radioactivity was plotted against sampling time. The uptake rate constants for the time-course data were estimated by fitting the observed tracer incorporation to a two-compartment uptake model:

$$A_t = A_1 [1-\exp(-b_1t)] + A_2 [1-\exp(-b_2t)]$$
 (1)

where A_t is the radioactivity measured at time t, A_1 and A_2 are the maximal activity incorporated in the two compartments (structural and metabolic pools), and b_1 and b_2 are uptake rate constants (per min). The first compartment, which is small and turns over rapidly, is usually considered a "metabolic pool" and the second, which is large and turns over more slowly, is considered a "structural pool", although both terms are only terms of convenience since the

pools do not necessarily correspond to any observable division of cell parts. The coefficient of the first compartment (b_1) was used as the uptake rate constant (k_{01}) to estimate the tracer uptake rate $(F_{01}, \mu mol ind^{-1} min^{-1})$ by:

$$\mathbf{F}_{01} = [\Pi \times \mathbf{k}_{01}]$$
 (2)

where [I] is the concentration of the contaminant in the medium (µmol mL⁻¹). The rational for this estimation is based on the assumption that the rate of tracer uptake is proportional to the actual contaminant concentration in the medium, [I], which can be calculated by the formula:

$$[I] = I_{o}/S \tag{3}$$

where I_0 is the initial radioactivity of the culture medium (DPM mL⁻¹) and S is the specific activity of contaminant.

Elimination

The elimination curves were constructed from time course of radioactivities of the washout. A first-order two-compartment open model (Fig. 1) was fit to the isotope release data:

$$C_t = C_1 \exp(-k_1 t) + C_2 \exp(-k_2 t)$$
 (4)

where C_t is the total radioactivity of the washout; C_1 is the radioactivity in compartment 1 (the metabolic compartment); C_2 is the radioactivity in compartment 2 (the structural compartment); k_1 and k_2 are the rate constants of loss for two compartments. The rate constants for transfer between the two compartments (k_{12} and k_{21}), and for excretion (k_{10}) were estimated from the

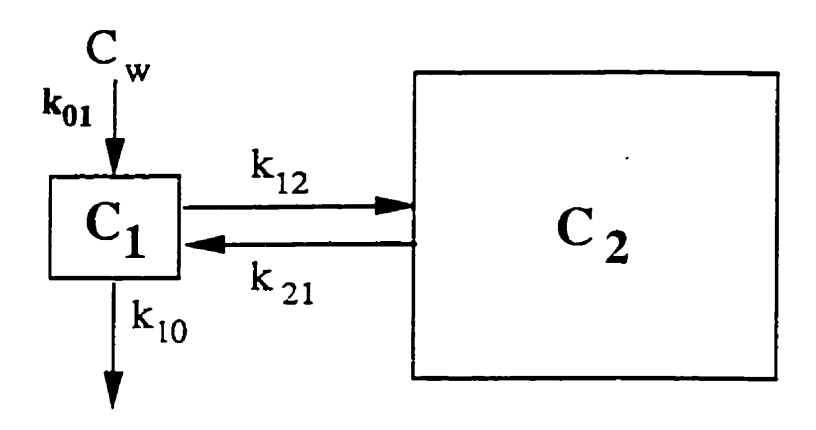


Fig. 1. Schematic representation of two-compartment model. C_1 and C_2 are the compartment size of the two compartments. k_{01} is the uptake rate constants, k_{10} the elimination rate constant, k_{12} and k_{21} the intercompartmental exchanges.

equations of Spacie and Hamelink (1982):

$$k_{21} = (C_1k_2 + C_2k_1)/(C_1 + C_2)$$
 (5)

$$k_{10} = k_1 k_2 / k_{21} \tag{6}$$

$$\mathbf{k}_{12} = \mathbf{k}_1 + \mathbf{k}_2 - \mathbf{k}_{21} - \mathbf{k}_{10} \tag{7}$$

The rate of bioaccunulation of a contaminant by the algal cell can be estimated from the balance between uptake and elimination rates by the following equation:

$$A = dC_R/dt = k_{01} C_W - k_{10} C_R$$
 (8)

where C_B is the concentration of contaminant in the algal cell, C_W concentration in the water and t is time (min).

The concentration of contaminant in the algal cell can be estimated by integrating equation (8), therefore

$$C_B = C_W(k_{01}/k_{10}) [1 - \exp(-k_{10}t)]$$
 (9)

The bioconcentration factor (BCF) was calculated by following Cocherham and Shane (1994):

BCF =
$$(b_1/(k_1 \times k_2))x(k_{12} + k_{21})$$
 (10)

Intercompartmental fluxes

The compartmental influx and efflux rates were estimated by multiplying the compartment size by the corresponding rate constant. The compartment size was calculated as a product of relative pool size and total body burden of the toxicants, the latter of which was derived from the asymptotic radioactivity of the time course uptake curves.

Curve fitting

For both uptake and excretion data analyses, the sampling times (independent variable) were assumed to be error-free. The kinetic constants estimated by fitting the data to the model are reported as mean \pm asymptotic standard error. Uptake data were fitted to eqn (1) with the Marquardt least square fit of nonlinear regression by NLIN procedure of the Statistical Analysis System (SAS Institute 1983). The overall goodness of fit was evaluated by an F-test, by the coefficient of determination r^2 and by the standard error of the regression $(S_{y,x})$. Eqn 4 was fitted to the tracer elimination data using the 3R program of the Biomedical Statistics Package (BMDP, Dixon 1988). The adequacy of model was assessed as that which achieves the minimal residual mean square, the smallest scatter of the actual data points around the fitted function and by the plot of residuals against the regressor (t). An F-test was used to select the most appropriate number of compartments (Boxenbaum et al. 1974).

QSPR analysis and statistics

Eight physicochemical parameters (Table 2) that are frequently used in the QSAR literature were obtained from previous studies (Mailhot 1987, Mailhot and Peters 1988 and 1991). Log K_{ow} is the logarithm of the octanol-water

Table 2. Structural parameters of the tested chemical compounds. P_{ow} is the partition coefficient, S is aqueous solubility (mol L⁻¹), CI is the connectivity index, PA is parachor, MW is molecular weight, MP is melting point (°C), BP is boiling point (°C), and D is density (g cm⁻³).

Chemical	log P _{ow}	log S	CI	PA	MW	MP	BD	D
AC	0.23	infin.	1.54	161.5	58.08	-95	56.01	0.7899
BUT	0.87	4.88	2.41	203.8	74.12	-90	117.7	0.81
ACP	1.62	3.74	3.01	293.8	120.14	19	202	1.03
BZA	1.87	-1.65	3.01	175	122	122	249	1.32
CHL	1.94	-1.15	1.73	190	119	-64	62	1.49
BEN	2.09	-1.67	2	207.1	78.08	5.5	80.1	0.8787
TOL	2.57	2.87	2.89	246.2	92.1	95	110.7	0.87
ATR	2.69	-3.84	5.71	456	216	174		1.55
CB	2.88	-2.40	2.411	244.4	112.56	-45.3	132	1.1064
BB	2.97	2.65		259.7	157.02	-31	156	1.52
1,2-DCB	3.44	-3.10	2.827	285.2	147.01	-17.2	179.8	1.3048
1,4-DCB	3.44	-3.30	2.821	279.5	147.01	53.4	173.7	1.533
2-MN	3.99	1.41			142.2	34.39	241	1.029
BH	4.06	-4.70	5.46	479	291	112	323	1.87
TCB	4.08	-3.83	3.238	324.8	180.97	17	213.3	1.4542
ANT	4.49	-6.45	4.81	410	178	216	340	1.25
TTB	5.05	-4.76	3.661	364.3	215.9	47.3	254	
DDE	5.59	-1.83			318	88	189	1.832
DDT	5.7	-7.68	7.01	663	353	109		1.55
PTCB	5.79	-5.46	4.077	403.9	250.35	84.8	276.5	1.8342
HCB	6.53	-7.36	4.5	443.4	284.86	229	324	1.569
PCB	7.08	-7.98	6.56	618	361	103		1.56

partition coefficient and expresses the lipophilic character of the molecules. Log S is the logarithm of the solubility expressing the mass of a chemical contained in an aqueous solution which is in equilibrium with an excess of the chemical. The molecular connectivity index (CI) is a measure of the strength of the chemical structure in terms of number of bonds per atom. Parachor (PA) is a combined function representing the surface tension, density and molecular weight of the chemical. Molecular weight (MW) is the atomic weight of all the atoms in a molecule. Density (D) is the concentration of the chemical in mass per unit of volume. Boiling point (BP) is the temperature at which the vapor pressure in a liquid equals the atmospheric pressure, and melting point (MP) is the temperature at which a solid substance becomes a liquid.

The correlation matrix for these structural parameters for these chemicals is given in Table 3. A high collinearity (p < 0.01) was detected in most cases. However, only slight significant correlations (0.01>p>0.05) were found between MP and D, and between BP and D. Among all the structural properties, log K_{ow} always correlates well with other parameters.

QSPRs were established by simple linear regression analysis. If chemicals do not have the same mode of action on pharmacokinetic parameters, the correlation coefficients derived from each class of compounds will differ, indicating different types of interaction between the toxicants and organisms. The intercept of the regression function demonstrates the activity of a class of chemicals for a biological species. Variations in regression coefficients imply

Table 3. Matrix of the correlation coefficients. All correlation coefficients are statistically significant (p < 0.05, n = 19 to 22). P_{ow} is the partition coefficient, S is aqueous solubility (mol L^{-1}), CI is the connectivity index, PA is parachor, MW is molecular weight, MP is melting point (°C), BP is boiling point (°C), and D is density (g cm⁻³).

	log P _{ow}	log S	CI	PA	MW	MP	BD
log Pow	1			-			
log S	0.777	1					
CI	0.739	0.699	1				
PA	0.822	0.740	0.968	1			
MW	0.884	0.732	0.915	0.952	1		
MP	0.626	0.614	0.715	0.631	0.606	1	
BD	0.729	0.622	0.946	0.867	0.719	0.812	1
D	0.691	0.629	0.631	0.619	0.798	0.474	0.548

differences in the contributions of a chemical's structural properties to the pharmacokinetic action (Mendza and Klein 1990). The regression relationships were assessed by the standard error of the estimate $(S_{y,x})$, a test of null-hypothesis (F-test), and the amount of explained variance (r^2) . The predicted vs. the observed values were plotted to identify any systematic errors in the prediction.

Multivariate regression analysis was employed to seek better correlations between pharmacokinetic parameters and physicochemical properties. Only those structural variables with low collinearity ($r^2 < 0.40$) were used in the same QSPR model. The SAS stepwise, forward, multiple linear regression program was used to delete variables with nonsignificant partial F-values.

All statistical analyses were performed using SAS (SAS Institute 1985). The Corr option of the RSQUARE procedure was used to detect collinearity between structural parameters. The significance of linear correlation coefficients was determined from a table of critical values in Zar (1984). The strength of the relationship was further evaluated by r^2 and $S_{y,x}$. Slopes of the regression lines were determined to be significant by comparison to zero (Student's t test). In all cases, p < 0.05 was set as the critical level of significance.

Results

Pharmacokinetics

Uptake

Chlorella accumulated most toxicants rapidly and approached plateau concentrations 0.5 to 3 h after exposure began (data not shown). A period of relatively slow uptake followed. For pentachlorobenzene and 1,2,4-trichlorobenzene, no obvious steady state level was reached during the experiment.

The time course uptake data was adequately described by a two-compartment accumulation model (Table 4). The proportion of variance explained by the model ranged from 89 to 100%. The uptake rate constants of the first compartment varied by eight orders of magnitude. However, the uptake rate constants of the second compartment varied much less, over about three orders of magnitude.

Elimination

Inspection of the elimination data indicates that <u>Chlorella</u> cleared the contaminants very slowly as indicated by the decline in the radioactivity of the washout (data not shown). Most accumulated radioactivity was retained in the cell over the 8-hr time frame of elimination experiments. The statistical

Table 4. Biphasic uptake constants and model-fitting statistics for C. pyrenoidosa.

Chemical	D Cells mL ⁻¹	A ₁ DPM mL ⁻¹	b ₁ min ⁻¹	A ₂ DPM mL ⁻¹	b ₂ min ⁻¹	F	r ²	S _{y,x}
AC	489000	0.38	0.000317	4.27	0.075	704.8	0.997	0.23
BUT	381000	2.503	0.0022	31.89	0.0022	277.9	0.992	4.62
ACP	381000	34.00	0.105	24.464	0.0058	326.8	0.993	17.65
BZA	489000	10.40	0.49	14.23	0.04	100.0	0.997	0.46
CHL	554000	10.39	0.22	8.589	0.0036	1130.4	0.999	7.25
BEN	554000	8.023	3.591	7.129	0.018	270.8	0.991	64.18
TOL	489000	1.47	0.45	2.00	0.045	538.0	0.996	0.22
ATR	300000	19.00	3.01	11.065	0.02	1021.9	0.998	5.51
CB	606000	0.37	0.12	15.73	0.094	587.4	0.997	0.91
BB	515000	7.00	1.143	23.00	0.002	2317.8	0.999	0.98
1,2-DCB	505000	201.73	9.77	296.09	0.022	905.5	0.997	24.36
1,4-DCB	381000	199.66	21.364	82.75	0.027	1479.6	0.998	11.83
2-MN	515000	114.32	10.56	115.16	0.125	3193.5	0.999	0.73
BH	300000	156.10	20.00	118.00	0.18	6769.1	1	0.296
TCB	505000	410.40	142.30	55.64	0.44	19.3	0.892	50.65
ANT	554000	237.78	130.59	130.27	0.13	2102.8	0.999	13.33
TTB	300000	184.01	232.40	78.89	0.48	11523.7	1	4.037
DDE	606000	117.30	498.00	145.62	0.283	1625.9	0.999	2.28
DDT	606000	154.00	242.60	120.17	0.155	1472.7	0.999	5.16
PTCB	463000	47.12	868.00	62.34	0.729	19.4	0.893	58.02
HCB	463000	377.45	1146.60	363.00	0.83	6805.8	1	1.86
PCB	463000	422.66	2665.80	486.52	0.90	3135.7	0.999	12.11

goodness of fit tests indicated that radioactivity-time curve for each chemical was adequately characterized by the two-compartment elimination model. Table 5 shows that the observed and model predicted values for the two compartment model were consistent in most cases as indicated by the small residual mean square (RMS). The elimination rate constants varied three-fold for both compartments.

Kow based QSPRs

Rate constants

Rate constants of uptake and intercompartmental exchange increased with increasing $\log K_{ow}$, while that of elimination decreased with increasing $\log K_{ow}$ (Fig. 2). These QSPRs for rate constants can be reflected by the following equations (n= 22, p < 0.01):

 $\log k_{01} = 0.68(\pm\ 0.07) \log K_{ow} - 2.67(\pm\ 0.293) \quad r^2 = 0.81, \ S_{y,x} = 0.62, \ F = 86.6$ $\log k_{10} = -0.33(\pm\ 0.08) \log K_{ow} - 1.77(\pm\ 0.08) \quad r^2 = 0.47, \ S_{y,x} = 0.66, \ F = 17.7$ $\log k_{12} = 0.35(\pm\ 0.04) \log K_{ow} - 2.81(\pm\ 0.16) \quad r^2 = 0.80, \ S_{y,x} = 0.33, \ F = 79.5$ $\log k_{21} = 0.34(\pm\ 0.05) \log K_{ow} - 2.77(\pm\ 0.19) \quad r^2 = 0.71, \ S_{y,x} = 0.41, \ F = 48.5$ For the rate constants of intercompartmental exchanges, the regression lines almost overlapped, indicating their slopes and intercept are similar in relation to log K_{ow} . However, the slope of the rate constants for uptake rises much faster with log K_{ow} than do for those for intercompartmental exchanges.

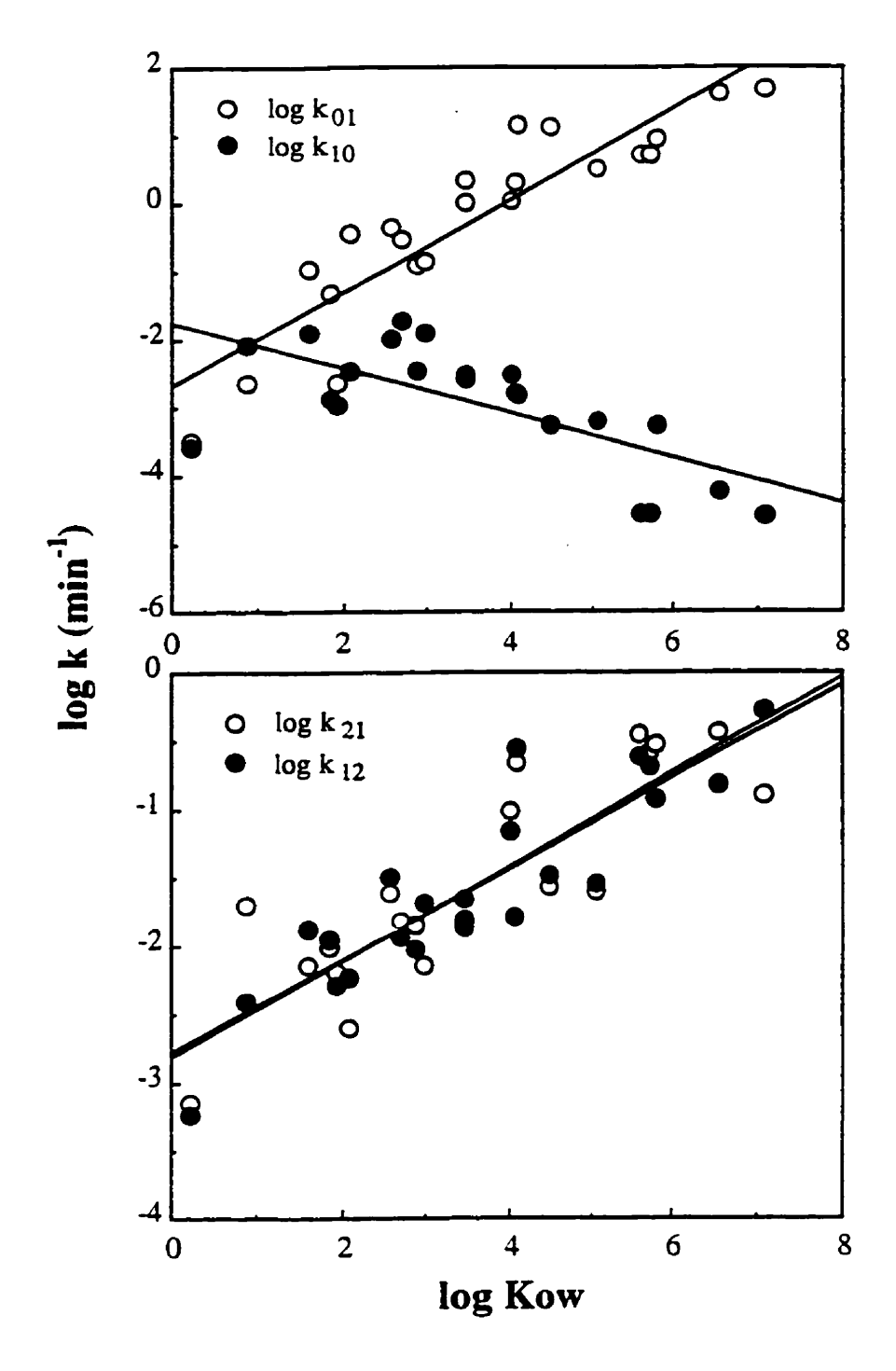


Fig. 2. The relationships between rate constants of uptake (k_{01}) , elimination (k_{10}) , and intercompartmental exchanges $(k_{12} \text{ and } k_{21})$ of organic chemicals and octanol-water partition coefficient (k_{0w}) in <u>C. pyrenoidosa</u>.

Table 5. <u>C. pyrenoidosa</u> cell density (D), biexponential excretion constants and model-fitting statistics for 22 organic compounds.

Chemical	D Cells mL ⁻¹	C ₁ DPM mL ⁻¹	k ₁ min ⁻¹	C ₂ DPM mL ⁻¹	k ₂ min ⁻¹	RMS	df
AC	456000	217.9	0.0012	164.28	0.000013	0.0012	57
BUT	311000	43.03	0.0315	4.416	0.00001	0.0028	51
ACP	351000	490.4	0.0317	216.22	0.000496	0.0153	56
BZA	600000	573.1	0.0213	594.7	0.000682	0.0023	62
CHL	646000	982	0.0114	717.6	0.000467	0.0301	56
BEN	774000	138.5	0.0116	99.2	0.00047	0.0030	57
TOL	616000	385.5	0.0645	303.86	0.000476	0.0021	60
ATR	575000	1953.9	0.044	396.9	0.00048	0.0029	56
СВ	650000	157.9	0.0268	72.87	0.00012	0.0068	62
BB	760000	57.02	0.04	40.0	0.000638	0.0045	56
1,2-DCB	433000	2064	0.0253	2511	0.00176	0.0041	57
1,4-DCB	959000	154.4	0.0397	176.5	0.0024	0.0054	56
2-MN	840000	89.61	0.168	62.14	0.0012	0.0015	62
ВН	606000	60.57	0.034	52.68	0.00158	0.0060	56
TCB	600000	978.2	0.4959	1213.2	0.00281	0.0006	62
ANT	849000	160.6	0.06	195.5	0.0029	0.0182	56
TTB	636000	84.2	0.054	93.0	0.0032	0.0275	56
DDE	519000	644.6	0.587	442.5	0.00314	0.0042	54
DDT	618000	45.8	0.464	35.79	0.00414	0.0111	57
PTCB	908000	209.59	0.409	83.7	0.00352	0.0040	56
НСВ	973000	233.8	0.513	98.9	0.0047	0.0031	54
PCB	766000	40.39	0.647	166.4	0.0081	0.0021	56

Uptake rate constants (k_{01}) varied from 3.2×10^{-4} to $48.6 \, \mathrm{min^{-1}}$; the elimination rates (k_{10}) ranged between 2.6×10^{-5} and $1.8 \times 10^{-2} \, \mathrm{min^{-1}}$; the intercompartmental transfer rates varied between 5.9×10^{-4} and $0.5 \, \mathrm{min^{-1}}$ for flux from the metabolic pool to the structural pool (k_{12}) and between 7.1×10^{-4} and $0.4 \, \mathrm{min^{-1}}$ for flux from the structural pool to the metabolic pool (k_{21}) .

Relative pool sizes

The relative pool size (%) of the metabolic compartment decreased significantly with increasing log K_{ow} (log $C_1(\%)$ = -0.04(± 0.01) log K_{ow} + 0.21(± 0.02), r^2 = 0.42, $S_{y,x}$ = 0.08, F = 36.5, p < 0.01). In contrast, the relative pool size of the structural compartment increased with increasing log K_{ow} (log $C_1(\%)$ = 0.04(± 0.01) log K_{ow} + 0.79(± 0.06), r^2 = 0.42, $S_{y,x}$ = 0.08, F = 36.5, p < 0.01).

Flux rates

Flux rates of uptake and forward intercompartmental exchanges (F_{12}) increased with increasing log K_{ow} , whereas the reverse relationship was detected for elimination (F_{10}) and backward intercompartmental exchange (F_{21}) rates (F_{10}). The relationships between these fluxes ($x10^{-14}$ µmol cell⁻¹ min⁻¹) and K_{ow} are best expressed by the following QSPRs (n=22, p<0.01): log $F_{01}=0.98(\pm 0.38)$ log $K_{ow}+1.44(\pm 0.38)$ r² = 0.84, $S_{y,x}=0.80$, F=105.7 log $F_{10}=-0.92(\pm 0.12)$ log $K_{ow}+0.88(\pm 0.49)$ r² = 0.74, $S_{y,x}=1.03$, F=56.5

 $\log F_{12} = -0.26(\pm 0.08) \log K_{ow} - 0.12(\pm 0.32) \quad r^2 = 0.35, S_{y,x} = 0.66, F = 10.6$ $\log F_{21} = 0.46(\pm 0.10) \log K_{ow} - 0.72(\pm 0.41) \quad r^2 = 0.50, S_{y,x} = 0.86, F = 19.9$

The effect of log K_{ow} on the uptake rate (F_{01}) is greater than its effect on the backward intercompartmental exchange (F_{21}) . The slope of the elimination (F_{10}) relation is more negative than that for the forward intercompartmental exchanges (F_{12}) . In terms of intercepts, uptake and elimination rates are the highest, and two intercompartmental exchange rates the lowest. The two intercompartmental exchange rates increasingly diverge as log K_{ow} increases.

Bioconcentration

<u>Chlorella pyrenoidosa</u> accumulated lipophilic organics very rapidly from the water. The rate of accumulation was close to the uptake rate, and can be adequately predicted by the following equation:

 $\log A = 0.98(\pm 0.10) \log K_{ow} + 1.43(\pm 0.38)$ $r^2 = 0.84$, $S_{y,x} = 0.80$, F = 105.7 Both slope and intercept were not statistically different from those for uptake (t test, p > 0.05).

Validation of the K_{ow} based accumulation model

The validity of K_{ow} in the prediction of accumulation rates of organic contaminants by algae can be made by comparing the predictions with experimental data on contaminant concentration in the algal cell (Fig. 4) calculated from Equation (9). Most of the predicted values were in a close

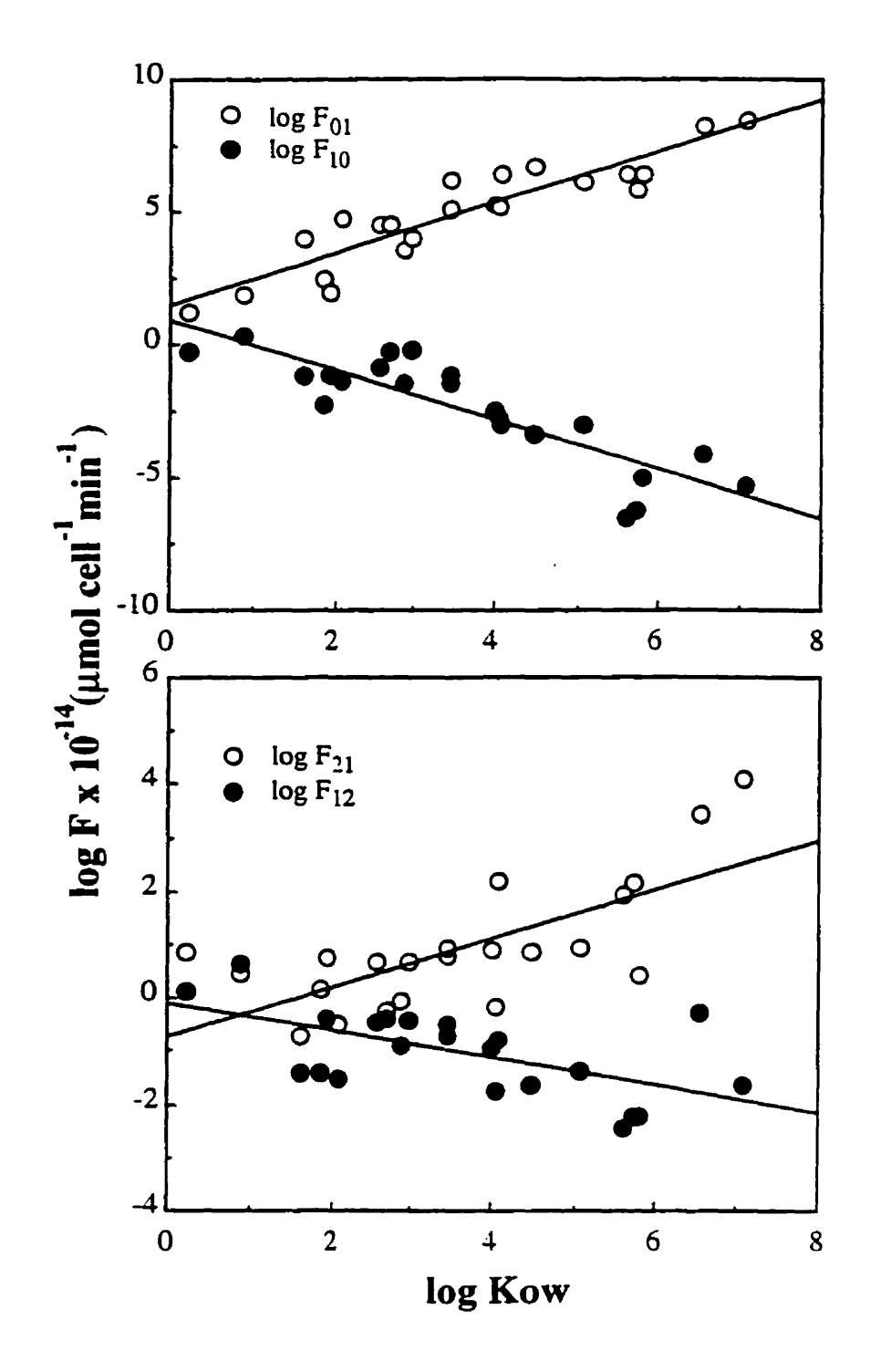


Fig. 3. The relationships between flux rates of uptake (F_{01}) , elimination (F_{10}) , and intercompartmental exchanges $(F_{12} \text{ and } F_{21})$ of organic chemicals and octanol-water partition coefficient (K_{ow}) in \underline{C} . pyrenoidosa.

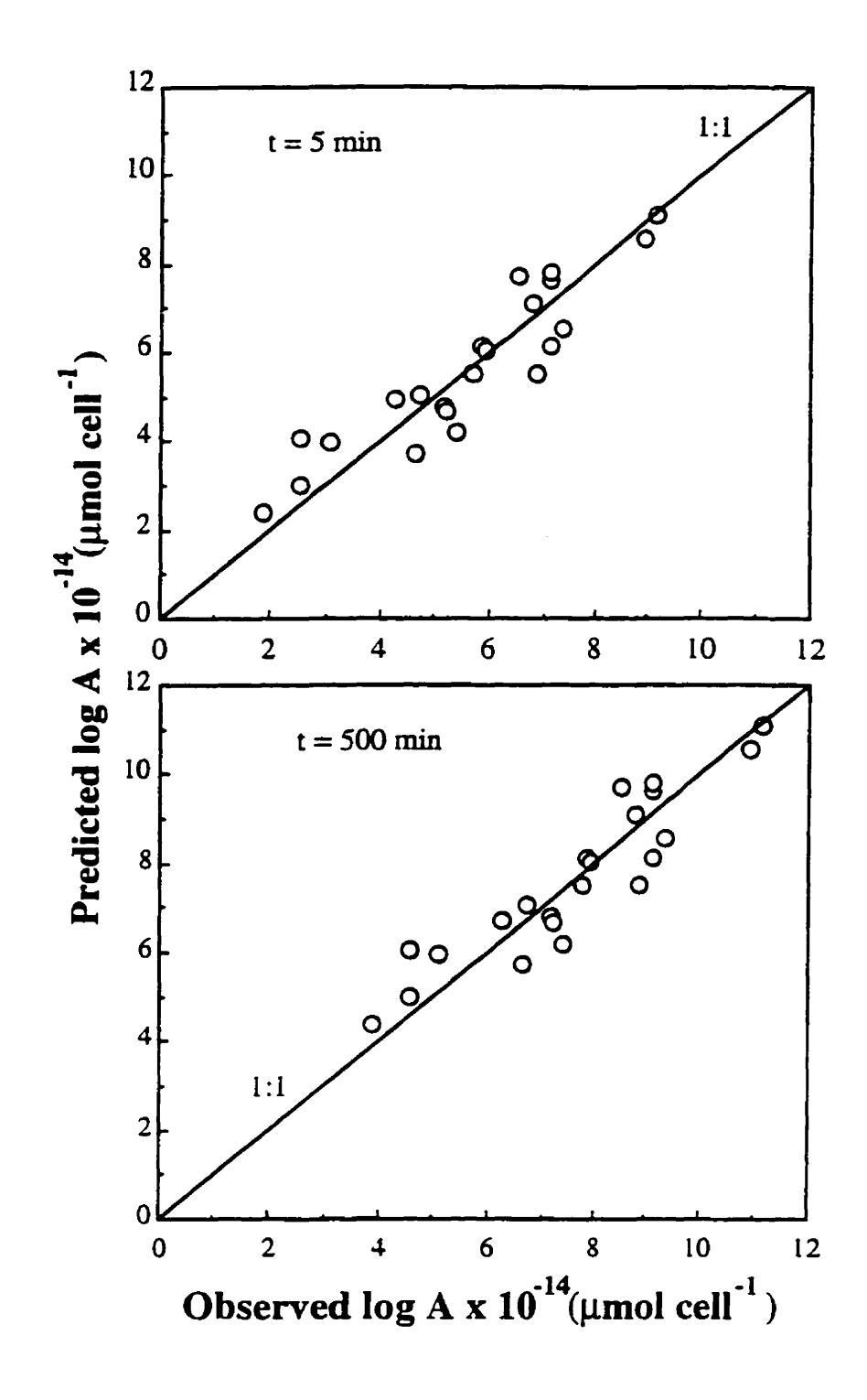


Fig. 4. Comparison of predicted and experimentally-determined concentration of contaminant in the agal cell.

agreement with the experimentally determined values. Some dots are always above or below the line, but on an average were within a factor of one or two of the experimental data.

Bioconcentration Factors

Bioconcentration factors (BCF) varied over six orders of magnitude in Chlorella. BCF was lowest in n-butanol (1.6) and highest in hexachlorobenzene (2.4x10⁶). The mean BCF was about $2.2x10^5$. Bioconcentration factors (BCF) increased with increasing log K_{ow} (Fig. 5) and can be expressed by the equation:

log BCF =
$$0.87(\pm 0.08)$$
 log K_{ow} - $0.22(\pm 0.26)$ $r^2 = 0.85$, $S_{v,x} = 0.68$, $F = 115.0$

Other structure-based QSPRs

Simple regression analysis revealed that, in addition to K_{ow} , BP, $\log S$, MW, PA and MP are also significant predictors of uptake rate constants (k_{01}) . K_{ow} , MW and $\log S$ are the best correlates of elimination rate constants $(k_{10}, Table 6)$. Other parameters, although significant, gave relatively poor correlations $(r^2 < 50\%)$. The intercompartmental exchange rate constants were significantly correlated to $\log K_{ow}$, MW and PA. The remaining parameters explained <50% variance.

Uptake (F_{01}) , elimination (F_{10}) and accumulation (A) rates (Table 7) are significantly related to K_{ow} , MW and PA. In addition, log S is also a good

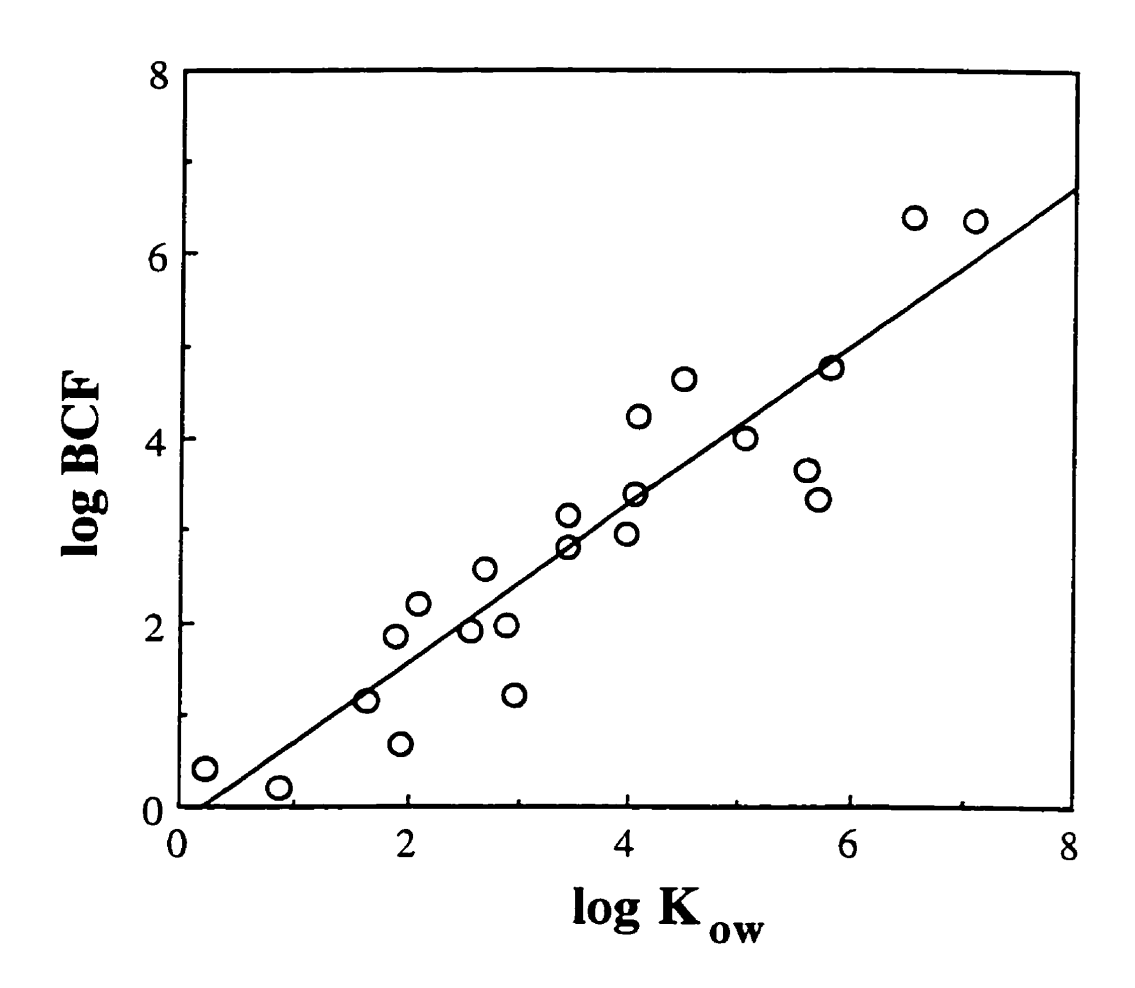


Fig. 5. The relationships between bioconcentration factors (BCF) of organic chemicals and octanol-water partition coefficient (K_{ow}) in \underline{C} . pyrenoidosa.

Table 6. Simple regression equations relating BCF and rate constants of \underline{C} . pyrenoidosa to other chemical structural properties. N is the number of data points, $S_{y,x}$ is the root of the mean square error of the regression, and the standard deviation of the coefficient is given in parentheses. All regressions are highly significant (P < 0.001).

Models	N	$S_{y,x}$	r ²	F				
Bioconcentration factor								
$\log BCF = 2.12(\pm 0.26) - 0.37(\pm 0.06) \log S$	21	0.98	0.68	39.9				
$\log BCF = -0.17(\pm 0.60) + 0.01(\pm 0.00) BP$	19	1.06	0.62	27.6				
$\log BCF = 0.27(\pm 0.56) + 0.01(\pm 0.00) MW$	22	1.15	0.58	27.4				
$\log BCF = -0.22(\pm 0.75) + 0.019(\pm 0.00) PA$	20	1.28	0.52	19.7				
$\log BCF = 2.18(\pm 0.31) + 0.01(\pm 0.00) MP$	22	1.23	0.51	20.9				
Uptake	•							
$\log k_{01} = -2.68(\pm 0.54) + 0.01(\pm 0.00) BP$	19	0.96	0.56	21.5				
$\log k_{01} = -0.65(\pm 0.22) - 0.23(\pm 0.05) \log S$	21	0.84	0.54	22.5				
$\log k_{01} = -2.26(\pm 0.47) + 0.01(\pm 0.00) \text{ MW}$	22	0.97	0.54	23.4				
$\log k_{01} = -2.76(\pm 0.59) + 0.01(\pm 0.00) PA$	20	1.02	0.53	20.1				
$\log k_{01} = -0.81(\pm 0.25) + 0.01(\pm 0.00) MP$	22	1.00	0.50	20.4				
Excretio	n							
$\log k_{10} = -1.70(\pm 0.31) - 0.01(\pm 0.00) \text{ MW}$	22	0.64	0.51	20.5				
$\log k_{10} = -2.51(\pm 0.17) + 0.17(\pm 0.04) \log S$	21	0.65	0.50	19.1				
Intercompartmental exchange rates								
$\log k_{12} = -2.68(\pm 0.22) + 0.01(\pm 0.00) \text{ MW}$	22	0.45	0.61	31.7				
$\log k_{12} = -2.88(\pm 0.28) + 0.01(\pm 0.00) \text{ PA}$	22	0.48	0.55	22.4				
$\log k_{21} = -2.65(\pm 0.24) + 0.01(\pm 0.00) \text{ MW}$	22	0.50	0.55	24.5				

Table 7. Simple regression equations relating flux parameters of \underline{C} . $\underline{pyrenoidosa}$ to other chemical structural properties. N is the number of data points, $S_{y,x}$ is the root of the mean square error of the regression, and the standard deviation of the coefficient is given in parentheses. All regressions are highly significant (P < 0.001).

Models	N	S _{y,x}	r ²	F
Uptake				
$\log F_{01} = 2.05(\pm 0.65) + 0.02(\pm 0.00) \text{ MW}$	22	1.34	0.55	24.5
$\log F_{01} = 1.37(\pm 0.83) + 0.01(\pm 0.00) PA$	20	1.42	0.53	20.7
$\log F_{01} = 4.29(\pm 0.34) - 0.34(\pm 0.08) \log S$	21	1.31	0.50	19.3
Excretion				
$\log F_{10} = 0.90(\pm 0.52) - 0.02(\pm 0.00) MW$	22	1.08	0.72	50.1
$\log F_{10} = 1.17(\pm 0.68) - 0.01(\pm 0.00) PA$	20	1.16	0.62	29.0
$\log F_{10} = 0.64(\pm 0.77) - 0.81(\pm 0.19) \text{ CI}$	19	1.31	0.51	17.9
Accumulation	ı			
$\log F = 2.04(\pm 0.65) + 0.02(\pm 0.00) MW$	22	1.35	0.55	24.5
$\log F = 1.36(\pm 0.83) + 0.01(\pm 0.00) PA$	20	1.42	0.53	20.7
$\log F = 4.29(\pm 0.34) - 0.34(\pm 0.08) \log S$	21	1.31	0.50	19.3

predictor of uptake and accumulation rates, so is CI for elimination rates. However, none of the structural parameters resulted in $r^2 > 0.50$ for intercompartmental transfers.

There were significant linear relationships between the BCFs of 22 organic contaminants and seven other structure variables (p< 0.05). The best equations were obtained when BCFs were associated with log K_{ow} , log S, BP, MW, PA and MP (Table 6) which explained >50% variance. The remaining structural parameters explained less variance or were non-significant.

Step-wise regression analysis did not increase the overall correlations between pharmacokinetic parameters. No multivariate combination of structural properties significantly improved the regression.

Discussion

Pharmacokinetic Fluxes

In this study, the accumulation of most organic contaminants by algae was very quick: high toxicant burdens were reached within 0.5 to 3 h. This is consistent with other reports for chlorinated hydrocarbons. Mailhot (1987) found that the uptake of DDT and tetrachlorobenzene by <u>Selenastrum capricornutum</u> reached an asymptote in 1 to 3 hrs. Harding and Phillips (1978), and Richer and Peters (1993) also reported that the time to equilibrium for PCBs were within 0.5 to 2 h for marine algae and freshwater plankton

assemblages, respectively, depending on species and biomass. The uptake rates observed are comparable to the values obtained by Sodergren (1968, 1971) for Chlorella species.

Several factors have been demonstrated to affect the uptake of organic xenobiotics in algae (Skoglund and Swackhamer 1994; Stange and Swackhamer 1994). The major chemical factors are hydrophobicity, solubility, and the molecular configuration of the compound. The main biological factors include the growth phase, species size, surface area, the lipid content and composition of the algae. This factors can act singly or in combination.

The rate of elimination of the compounds under study was inversely proportional to $\log K_{ow}$, implying that the major rate controlling factor for the elimination is lipophilicity and aqueous solubility. As lipophilicity increases or aqueous solubility decreases, the affinity of the compound for lipids increases, and its affinity for the surrounding medium decrease, resulting in extremely slow elimination rates for high K_{ow} compounds. We also found a similar dependence of elimination rates on K_{ow} for these hydrophobic organic chemicals in <u>Daphnia magna</u> (Wen and Peters 1986). However, literature data on the relationship between elimination and lipophilicity of organic compounds for algae are relatively rare, and consequently the validity of our findings needs further confirmation.

Bioconcentration Factors

Bioconcentration factor (BCF) is basically the ratio of the chemical concentration in the algae at steady state to the chemical concentration in the exposure water. It has been widely used to estimate the propensity of a chemical to bioaccumulate in the living organisms and is a useful parameter in decision making by regulators and risk accessors regarding the allowable toxicant concentration in the water. In the toxicological literature, most BCFs are estimated as the ratio between the uptake to depuration rate constants of the first order, single compartment model. Our estimated BCFs from the two compartment model for Chlorella compared favorably with those reported in the literature (Table 8). Mailhot (1987) experimentally showed that, in S. capricornutum, the bioconcentration factors varied between 6.9 and 56000 for nine organic compounds which were included in our study. Harding and Phillips (1978) reported the BCFs of 2,4,5,2',5'-pentachlorobiphenyl for 11 marine algal species ranged from 1.23x10⁴ to 2.4x 10⁶. Swackhamer and Skoglund (1991) compiled literature values of BCFs for a variety of hydrophobic organic compounds taken up by different species of phytoplankton and found considerable heterogeneity for different compounds, and for different species, and even among species for the same compound. BCFs ranged from 1.2 X10⁴ to 8.0x10⁴ for DDT, while BCFs varied between 18 and 10⁶ for PCBs. Urey et al. (1976) found that tetrachloro- and hexachlorobiphenyl isomers were concentrated by dead C. pyrenoidosa cells by a factor of 6000 to 15000.

Table 8. Comparisons of relationships between BCFs and physical-chemical properties of the chemicals for limnoplankton.

Equation	n	r ²	Species	Reference
$\log BCF = 0.36 \log K_{ow} + 2.1$	7	0.81	S. capricornutum	Mailhot (1987)
$\log BCF = 0.46 \log K_{ow} + 2.36$	8	0.83	S. capricornutum	Casserly et al. (1983)
$\log BCF = 0.68 \log K_{ow} + 0.16$	41	0.81	Chlorella	Geyer et al. (1984)
$\log BCF = 0.7 \log K_{ow} - 0.26$	8	0.93	<u>Scenedesmus</u>	Ellgehausen et al.
$\log BCF = 0.78 \log K_{ow} + 3.4$	40	0.84	<u>Scenedesmus</u>	Swackhamer & Skoglund (1991)
$\log BCF = 0.87 \log K_{ow} - 0.22$	22	0.85	C. pyrenoidosa	This study

QSPR models

Our QSPR equations from simple linear regression are of interest in terms of their utility for prediction. All the pharmacokinetic flux parameters are a function of an appropriate molecular descriptor. However, the r^2 values in our QSPRs may indicate that employing single structural descriptors may not be fully sufficient for accurate prediction of pharmacokinetic phenomena. This is because most biological systems are complex and mechanisms of action are not well understood. It is unlikely that only a few structural parameters will suffice to predict contaminant kinetics accurately. Reliable models with better predictive utility will need a wider range of physicochemical parameters and environmental factors. These parameters should be combined into a model with multivariate chemical and biological descriptions to construct a reliable QSPR model. However, the success of this technique depends on two conditions: the sample size (here, number of chemical compounds) should be large, and the structural descriptors should be independent of each other. Because of the intercorrelations among our eight structural parameters (Table 3), we could not assess their relative importance by simple multiple regression analysis. Hence, these data should be integrated with other relevant information to achieve sound predictive capabilities.

Our data showed that the bioconcentration factors can be reliably predicted from K_{ow} , BP, MW, log S, PA and MP for <u>Chlorella</u>. Among all the predictors, K_{ow} gave the highest correlations, indicating chemical hydrophobicity is the

principal driving force of bioconcentration. Several previous studies reported the similar relations between log BCF and log K_{ow} (Table 7). It is interesting to note that, in all of the equations, the slopes are less than the hypothetical expectation of one (Mackay 1982), possibly indicating a lack of equilibrium among the compounds with highest K_{ow} 's.

Our models can not be applied to chemicals with K_{ow} 's outside the range of this study. Chemicals with high K_{ow} 's could not reach the level as would be predicted from its lipophilicity for there is a lack of proportional relationship between BCF and K_{ow} at high K_{ow} 's (Stange and Swackhamer 1994). This deviation from the expected BCF- K_{ow} relationship has been observed for a wide range of algal species. Swackhamer and Skoglund (1991) reported a strong relation between log BCF and log K_{ow} for 40 PCB congeners in axenic cultures of Scenedesmus sp., but for congeners with log $K_{ow} > 7$, there was no direct relationship between BCFs and K_{ow} , demonstrating that for superhydrophobic chemicals, log BCFs are independent of their log K_{ow} 's. This phenomenon was attributed to the lack of equilibrium conditions in cultures that were actively growing or the membrane permeation resistance caused by molecular size (Stange and Swackhamer 1994). These deviations may influence the predictability of the QSPR models.

Other physical-chemical properties have been also shown to be able to predict the BCFs. Mailhot (1987) indicated that the BCF of hydrocarbon by <u>S</u>. capricornutum correlated significantly with the HPLC capacity factor,

parachor, molar volume (the volume occupied by a mole), connectivity, and solubility. Geyer et al. (1981) showed significant relationship between water solubility of the chemicals and their bioconcentrations by alga <u>Chlorella</u> sp.. Richer and Peters (1993) reported that BCFs of 2,2',4,4',5,5'-hexachlorobiphenyl by plankton (primarily phytoplankton) could be predicted from log capacity ratio (k'), log biomass and absorbance at 440 nm.

Our data indicated that both uptake and elimination rate constants of the tested chemicals were also described well by log octanol/water partition coefficients and aqueous solubilities in Chlorella. These derived relationships demonstrated that K_{ow} and solubility have practical utility in the prediction of their bioconcentration rates by algae. These findings are similar to those of other studies (Mailhot 1987). This commonness of QSPRs could be explained by the passive uptake process of these toxicants by algae. When xenobiotics are transported across water and lipid phases alternatively, the thermodynamic processes which are governed by the concentration or fugacity gradient between the phases provide the free energy to power the mass transfer of these compounds. Thus the lipophilicity of the compound, the area and type of cell surface available for diffusion, and type of lipids in the organism may affect the penetration processes. Our results suggest a possibility to extrapolate these QSPR relations to different chemicals or organisms. Furthermore, the significance of the equations also depends on the quality of measurements of the pharmacokinetic parameters. This requires good experimental design and

the standardization of the pharmacokinetic tests.

Acknowledgments

We wish to thank Drs. J. Kalff, J. Rasmussen, N. Price for their comments and discussion of the manuscript, and M. Peters and D. Klimuk for their fine laboratory assistance. This work was financially supported by the Natural Sciences and Engineering Research Council of Canada (NSERC) and Fonds pour la Formation de Chercheurs et l'Aide à la Recherche (FCAR). Y.H.W. was a recipient of an FCAR scholarship from the Québec government.

References

- Boxenbaum, H. G., S. Riegelman, and R. M. Elashoff. 1974. Statistical estimations in pharmacokinetics. J. Pharmacokin. Biopharm. 2: 123-148.
- Casserly, D. M., E. M. Davis, T. D. Downs, and R. K. Guthrie. 1983. Sorption of organics by <u>Selenastrum capricornutum</u>. Water Res. 17: 1591-1594.
- Chu, K. C. 1979. The quantitative analysis of structure-activity relationships.

 In M. E. Wolff, Ed. The Basis of Medicinal Chemistry, 4th Ed. John Wiley, N.Y.
- Cockerham, L. G., and B. S. Shane. 1994. Basic Environmental Toxicology.

 CRC Press, Boca Raton, FL. 627 p.
- Dixon, W. J. 1988. BMDP Software Manual. Berkeley: University of California Press.
- Ellgehausen, H., J. A. Guth, and H. O. Esser. 1980. Factors determining the bioaccumulation potential of pesticides in the individual compartments of aquatic food chains. Ecotoxicol. Environ. Saf. 4: 134-157.
- Geyer, H., R. Viswanathan, D. Freitag, and F. Korte. 1981. Relationship between water solubility of organic chemicals and their bioaccumulation by the alga <u>Chlorella</u>. Chemosphere 10: 1307-1313.
- Harding, L. W., and J. H. Philips. 1978. Polychlorinated biphenyl (PCB) uptake by marine phytoplankton. Mar. Biol. 49: 103-111.
- Hermens, J. L. 1986. Quantitative structure-activity relationships in aquatic

- toxicology. Pestic. Sci. 17:287-296.
- Mackay, D. 1982. Correlation of bioconcentration factors. Environ. Sci. Technol. 16: 274-278.
- Mailhot, H. 1987. Prediction of algal bioaccumulation and uptake rate of nine organic compounds by ten physicochemical properties. Environ. Sci. Technol. 21: 1009-1013.
- Mailhot, H., and R. H. Peters. 1988. Empirical relationships between the 1-octanol/water partition coefficient and nine physicochemical properties.

 Environ. Sci. Technol. 22: 1479-1488.
- Mailhot, H., and R. H. Peters. 1991. Short-term sorption of chlorinated benzenes by concentrated seston. Verh. Internat. Verein. Limnol. 24: 2302-2306.
- Neely, W., D. Branson, and G. Blau. 1974. Partition coefficient to measure bioconcentration potential of organic chemicals in fish. Environ. Sci. Technol. 8: 1113-1115.
- Nendza, M., and W. Klein. 1990. Comparative QSAR study on freshwater and estuarine toxicity. Aquat. Toxicol.17: 63-74.
- Nichols, H. W. 1979. Growth media-freshwater. In: J. R. Stein (ed.). Handbook of Phycological Methods. Cambridge University Press, Cambridge.
- Richer, G., and R. H. Peters. 1993. Determinants of the short-term dynamics of PCB uptake by plankton. Environ. Toxicol. Chem. 12: 207-218.
- SAS Institute Inc. 1983. SAS/STAT User's Guide. Release 6.03 ed. Cary, NC:

SAS Institute.

- Seydel, J. K., and K.-J. Schaper. 1982. Quantitative structure-pharmacokinetic relationship and drug design. Pharmac. Ther. 15: 131-182.
- Skoglund, R. S., and D. L. Swackhamer. 1994. Processes affecting the uptake and fate of hydrophobic organic contaminants by phytoplankton. In L. A. Baker, ed., Environmental Chemistry of Lakes and Reservoirs. ACS Advances in Chemistry Series, Lewis, Chelsea, MI. pp 559-574.
- Sodergren, A. 1968. Uptake and accumulation of C¹⁴-DDT by <u>Chlorella</u> sp. (Chlorophyceae). Oikos 19: 126-138.
- Sodergren, A. 1971. Accumulation and distribution of chlorinated hydrocarbons in cultures of <u>Chlorella pyrenoidosa</u> (Chlorophyceae). Oikos 22: 215-220.
- Stange, K, and D. L. Swackhamer. 1994. Factors affecting phytoplankton species-specific differences in accumulation of 40 polychlorinated biphenyls (PCBs). Environ. Toxicol. Chem. 11: 1849-1860.
- Swackhamer, D. L., and R. S. Skoglund. 1991. The role of phytoplankton in the partitioning of hydrophobic organic contaminants in water. In R. Baker, ed., Organic Substances and Sediments in Water. Lewis, Chelsea, MI, pp 91-105.
- Urey, J. C., J. C. Kricher, and J. M. Boylan. 1976. Bioconcentration of four pure PCB isomers by <u>Chlorella pyrenoidosa</u>. Bull. Environ. Contam. Toxicol. 16: 81-xx.
- Wen, Y. H., and R. H. Peters. 1996. Structural dependency of pharmacokinetic

fluxes of organic toxicants by <u>Daphnia magna</u>, with comparisons of the QSPRs of <u>Daphnia</u> and the alga <u>Chlorella pyrenoidosa</u> (to be submitted).

Zar, J. H. 1984. Biostatistical Analysis. 2nd ed. Prentice-Hall, Inc., Englewood Cliffs, N.J.

CHAPTER IV

Structural Dependency of Pharmacokinetic Fluxes
of Organic Toxicants by Crustacean <u>Daphnia magna</u>,
With Comparisons of the QSPRs of <u>Daphnia</u> and of the
Alga <u>Chlorella pyrenoidosa</u>*

* Submitted to Environmental Toxicology and Chemistry

Abstract

The rate constants and flux rates of uptake (via water and food). elimination and intercompartmental transfers of 22 14C-labelled organic compounds by the microcrustacean Daphnia magna were determined as quantitative structure-pharmacokinetic relationships (QSPRs). pharmacokinetic parameters were significantly correlated to the octanol-water partition coefficient (Kow). Bioconcentration factors, uptake (from water and from food) and rates of intercompartmental exchange from "structural" to "metabolic" pools were directly related to log Kow. In contrast, the rates of elimination and intercompartmental exchanges from "metabolic" to "structural" pools were inversely related to log Kow. Other structural factors, including molecular weight, parachor, connectivity index, and boiling point, produced models similar to those based on $\log K_{ow}$, while aqueous solubility behaved as the inverse of $\log K_{ow}$.

Comparisons of pharmacokinetic parameters between <u>Daphnia</u> and <u>Chlorella</u> demonstrated that, although all kinetic parameters displayed similar patterns, the relative magnitude of corresponding parameters differed significantly between the two species. These dissimilarities should be taken into consideration if these QSPRs are applied to predict the pharmacokinetic fluxes of organic toxicants by lake plankton.

Introduction

Hazardous organic chemical compounds have been introduced into the aquatic environment for decades and in considerable amounts (Cockerham and Shane 1994). Most of these chemicals are toxic, persistent, and of major environmental concern. These chemicals have high chemical stability, and due to their lipophilicity, can accumulate to high concentrations in aquatic organisms relative to the concentrations in their environment. The potential of these chemicals to bioconcentrate depends on the relative magnitude of two kinetic processes, uptake and depuration, which may be determined by first order pharmacokinetic models. Although pharmacokinetic modeling has been widely used to study the toxicant dynamics in aquatic organisms, most such models were developed from few chemical or biological species. Consequently the predictive reliability of these models are largely uncertain when applied in risk assessments.

Much attention has already been paid to the chemical-specific and organism-specific pharmacokinetics of organic toxicants in modern ecotoxicology. By conducting interspecies extrapolation for a diverse, structurally different chemicals, some general trends appeared: taxonomically related biological species tend to have comparable pharmacokinetic behavior (Rice and Sikka 1973; Smith et al. 1990). These results are promising because inter-species and inter-compound extrapolation of the pharmacokinetics of

chemicals is a challenging, yet essential task for quantitative risk assessment of environmental toxicants. However, large-scale pharmacokinetic extrapolation has been hampered by the shortage of data on the kinetic fluxes of taxonomically different organisms when exposed to a variety of chemical compounds.

In a previous study (Wen and Peters 1986), we demonstrated that quantitative structure-pharmacokinetic relationships (QSPRs) provide good empirical relations between physico-chemical parameters and pharmacokinetic effects of a series of organic chemicals for the alga <u>Chlorella pyrenoidosa</u>. If such QSPRs are estimated for <u>Daphnia magna</u> for the same group of chemicals under identical conditions, the analysis will allow one to compare the flux rates in representatives of phytoplankton and zooplankton, autotrophs and heterotrophs.

The objective of this study was to obtain more insight into the pharmacokinetic fluxes of 22 ¹⁴C-labeled organic toxicants by microcrustacean <u>Daphnia magna</u>. The rate constants and flux rates of uptake, depuration and intercompartmental exchanges were determined by a two compartment pharmacokinetic model. In this paper, we further compare QSPRs in <u>C. pyrenoidosa</u> and <u>D. magna</u>, and discuss the differences between two species on the basis of differences in bioconcentration patterns of the organisms and lipophilicity of the compounds.

Materials and Methods

Organisms

Microcrustacean <u>Daphnia magna</u> was chosen as model species because of its cosmopolitan distribution and importance in aquatic food webs. In addition, it is readily available and easily cultured. Consequently this species is extensively used in toxicological studies, and there is a large data base on the toxicity of a variety of environmental chemicals to this species (Hermens 1986).

Stock cultures of <u>D</u>. <u>magna</u> were obtained from Environmental Biology Annex I, University of Guelph, and continuous cultures were maintained in the laboratory for many years. Both stock and experimental animals were grown in 4-L aquaria with standard reconstituted water at constant temperature (20 °C). The animals were maintained at 18-h light and 6-h dark cycle, and fed daily with "green water" from a goldfish tank (Peters 1988) with a dense growth of green algae dominated by <u>Scenedesmus</u> sp.. The aquarium was cleaned and water was changed weekly.

Chemicals

Twenty two ¹⁴C-radiolabeled organic chemicals were used in the <u>Daphnia</u> QSPR experiments. Their sources, purities, specific activities, the major structural parameters encoded in their chemical molecular formula, preparative and analytical procedures were presented in Wen and Peters

(1996). The model used to describe the uptake, elimination and intercompartmental exchanges of these chemicals is presented in Fig. 1.

Uptake

Aqueous uptake

Because D. magna reproduced continuously during the experimentation, only large, mature adults were selected for the tests. About 200 daphnids of similar size (body lengths between 2.6 - 3.2 mm) selected visually from the stock cultures were transferred by a hand net into each of a series of small flasks containing 250 mL aerated standard reconstituted water (APHA 1989). The flasks were covered with glass stoppers to minimize evaporation of the chemical and to help maintain a constant isotope concentration. Static exposure was conducted at 20 °C with a photoperiod of 16 hr light and 8 hr dark. The uptake experiment was started by adding the isotope to the flask. At the specific time intervals, 10 individuals were retrieved from the flask, rinsed with distilled water three times, blotted-dry on a tissue, and then placed into 7 mL scintillation glass vials with 5 mL Ready Protein solubilizer and fluor (Beckman Canada, Mississauga, Ontario, Canada). Their radioactivity was determined by liquid scintillation counter after solubilization overnight. At each sampling time, two 1-mL water samples (without daphnids) were also taken from each flask to measure the total radioactivity of the culture medium. Aqueous concentration of each isotope was estimated from measured radioactivity and its specific activity.

Controls were conducted by placing daphnids in reconstituted water with no chemical. The behavior of the experimental animals was routinely noted to ensure that the chemical concentration was not toxic. If there was any sign of poisoning, the experiment was repeated at a lower concentration.

Dietary uptake

"Green water" was chosen as the food source for daphnids. Prior to the uptake experiment, aliquots of "green water" were radiolabelled with each isotope for over 24 h in a shaker. The uptake rates of the isotope in the "green water" by <u>D</u>. magna was determined with the tracer incorporation technique (Peters 1984). About 200 animals of similar size were allowed to prefeed for 30 min in a static feeding chamber containing 150 mL of non-radioactive "green water" to allow animals to acclimatize to the food and the test conditions. After the initial feeding period, an equal volume of tracer-labelled "green water" was added to the chamber and gently mixed. To minimize the loss of the compound from the solution by volatilization, no aeration was provided. At ten predetermined time intervals from 5 min to 2 h, 10 individual animals were quickly removed from the feeding chamber with a small hand net, rinsed three times in reconstituted water, blotted-dry, transferred to a 7 ml-glass scintillation vial with 5 ml Ready Protein cocktail, solubilized overnight and

then quantified for ¹⁴C activity by scintillation spectrometry. Uptake curves were established by plotting radioactivity in the animals as a function of feeding time. At each sampling time, two 1-mL water samples (without daphnids) were also transferred from the feeding chamber and measured for total radioactivity.

Elimination

Isotope elimination rates were measured in the gel-filtration column (Pharmacia Fine Chemicals), which had been modified to flow-through chambers by fitting each end with Pharmacia flow adapters with 75 µm Nitex screens to retain the animals in the columns. About 200 animals of similar size, which had been previously fed labelled "green water" overnight, were gently introduced to the column. Labelled "green water" was subsequently added into the column to allow animals to adapt to the experimental conditions. After 30 min of prefeeding, non-radioactive "green water" was pumped into the top of each column by a Buchler peristaltic pump at 3 mL min⁻¹ for 10 min to replace all radioactive suspension in the column and to allow animals to begin to clear their guts of undigested radioactive cells. The unlabelled "green water" was aerated to maintain an adequate dissolved oxygen level. Because flow is laminar in these columns, 10 min was sufficient to flush the entire column, as confirmed by experiments with dye. The flow rates were then reduced to 1 mL min⁻¹, the eluent was collected at 5 min

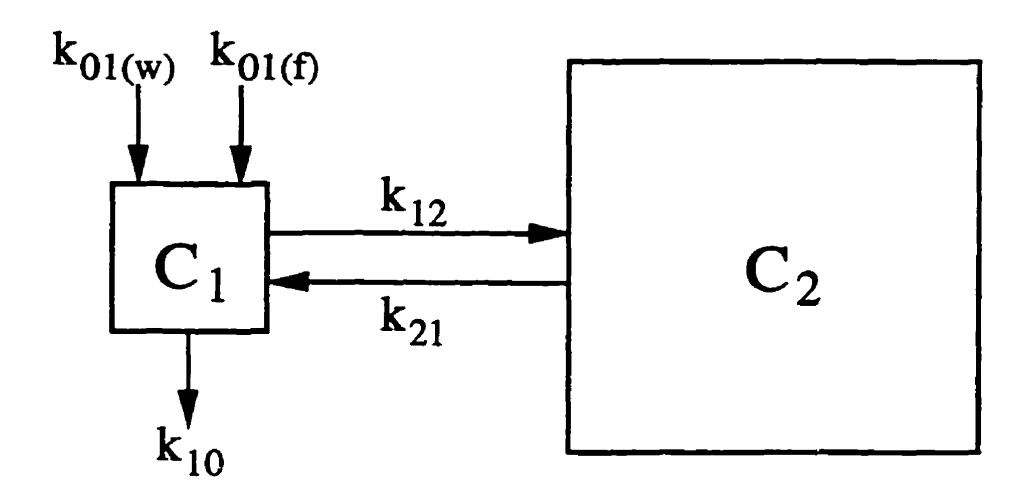


Fig. 1. Schematic representation of two-compartment model for <u>Daphnia</u> pharmacokinetics. C_1 and C_2 are the compartment size of the two compartments. $k_{01(w)}$ and $k_{01(f)}$ are the rate constants of uptake from water and food, respectively, k_{10} the elimination rate constant, k_{12} and k_{21} the intercompartmental exchanges.

intervals for 6 to 9 h by a fraction collector (Pharmacia LKB FRA 100). One mL of subsample from each fraction was transferred to a 7 mL-glass scintillation vial with 5 mL Ready Micro scintillator fluid, and immediately measured for radioactivity. Release curves were established by plotting the radioactivity in the eluent as a function of feeding time. Since samples collected in the first 5 to 25 min were likely contaminated by radioactive faeces, depending on the isotope, they were discarded in the estimation. As a result, the tracer release was intended to represent true elimination only.

Results

Pharmacokinetic parameters

Uptake

<u>Daphnia</u> took up toxicants very rapidly and usually reached nearly asymptotic concentrations 0.2 to 3 h after the beginning of exposure (data not shown). Thereafter there was a phase of relatively slow increase. For some compounds, such as hexachlorobenzene and 2,2',4,4',5,5-hexachlorobiphenyl, no apparent steady state was achieved during the experiment.

A two-compartment uptake model provided a satisfactory fit to the

observed concentration of the test compounds (Tables 1 and 2). The proportion of variances explained by the model ranged from 87 to 100%. The uptake rate constants of the first compartment varied by four orders of magnitude for uptake from food (Table 1) and those for uptake from water by three orders of magnitude (Table 2). The uptake rate constants of the second compartment for both uptake routes varied by four orders of magnitude.

Elimination

Most of the <u>Daphnia</u> eliminated organic contaminant relatively fast within the first 1 to 3 h and then the rate of elimination became much slow (data not shown). Only small amount (less than half) of the accumulated radioactivity was lost over the 8 h of the elimination experiments. Statistical tests for goodness of fit indicated that radioactivity-time curve for each chemical was satisfactorily described by a two-compartment elimination model. Table 3 show that the observed and model predicted values for the two compartment model parameters were consistent in most cases as indicated by the small residual mean square (RMS). The elimination rate constants varied three-fold for the first compartments and four-fold for the second compartments.

Table 1. Pharmacokinetic model parameters and model-fitting statistics for \underline{D} . \underline{magna} exposed to radiolabelled green water (n = 10).

Chemical	A ₁ DPM mL ⁻¹	b ₁ min ⁻¹	A ₂ DPM mL ⁻¹	b ₂ min ⁻¹	F	r ²	S _{y,x}
AC	1.16	0.00129	2.841	0.00021	631.8	0.998	0.21
BUT	2.44	0.00456	1.28	0.0012	1207.7	0.998	0.16
ACP	1.57	0.0189	0.83	0.0083	401.3	0.994	0.21
BZA	1.697	0.0105	8.961	0.00013	172.3	0.987	5.29
CHL	2.029	0.0148	70.99	0.001	76.6	0.970	0.88
BEN	6.93	0.0239	30.38	0.0021	2070.7	0.999	1.14
TOL	1.964	0.294	2.872	0.0065	2972.5	0.999	0.11
ATR	3.36	0.1261	25.06	0.0069	243.4	0.990	1.95
CB	1.751	0.132	0.794	0.00966	5051.7	1	0.054
BB	1.879	0.7527	13.495	0.0026	2283.9	0.999	0.089
1,2-DCB	2.422	0.374	7.895	0.0055	203.5	0.989	0.77
1,4-DCB	7.4	0.362	13.59	0.01	588.8	0.996	0.998
2-MN	12.31	0.864	11.3	0.0085	3193.5	0.999	0.27
BH	54.98	2.8	52.44	0.028	716.9	0.994	3.32
TCB	3.15	0.521	6.6	0.01	2037.4	0.999	0.26
ANT	127.73	6.1	136.45	0.031	3773.8	0.998	8.01
TTB	23.15	3.05	55.48	0.03	918.5	0.997	0.23
DDE	26.9	0.324	78.63	0.035	486.3	0.997	0.39
DDT	33.62	3.238	67.56	0.072	461.2	0.995	1.04
PTCB	123.41	13.857	77.27	0.157	1194.8	0.998	0.81
HCB	40.44	28.6	289.37	0.28	110.8	0.987	3.0
PCB	50.09	32.21	66.72	0.382	15.1	0.866	68.62

Table 2. Pharmacokinetic model parameters and model-fitting statistics for \underline{D} . \underline{magna} feeding on radiolabelled water (n = 10).

Chemical	A ₁ DPM mL ⁻¹	b ₁ min ⁻¹	$f A_2$ DPM mL $^{-1}$	b ₂ min ⁻¹	F	t ²	S _{y,x}
AC	0.133	0.045	0.42	0.0034	942.8	0.996	0.27
BUT	0.1955	0.0367	9.94	0.00087	3109.1	0.999	0.084
ACP	2.799	0.596	2.277	0.0019	3441.1	1	3.54
BZA	1.822	0.4768	0.969	0.021	20537.6	1	0.03
CHL	3.17	0.6699	11.49	0.0071	51.9	0.957	2.30
BEN	198.19	0.0065	77.997	0.00093	473.6	0.997	8.77
TOL	1.851	2.48	0.935	0.013	17900.0	1	0.032
ATR	2.423	0.7	1.88	0.024	19130.4	1	0.05
CB	2.319	6.816	4.167	0.0024	357.5	0.994	0.32
BB	2.337	1.5431	1.968	0.011	3405.5	0.999	0.1
1,2-DCB	6.04	7.627	77.15	0.0031	338.4	0.993	3.32
1,4-DCB	2.222	1.22	8.348	0.00091	4156.47	0.999	0.1
2-MN	3.87	4.56	2.74	0.035	3217.2	0.998	0.47
BH	2.32	2.3	6.85	0.39	619.9	0.996	0.36
TCB	92	23.1	71.88	0.01	964.6	0.998	0.03
ANT	254.31	4.9	74.64	0.125	426.5	0.997	14.1
TTB	5.704	16.8	87.76	0.14	314.6	0.993	6.64
DDE	7.328	42.39	11.03	0.1	776.9	0.997	0.88
DDT	71.073	35.239	212.698	0.18	1970.2	0.998	4.9
PTCB	18	0.152	1.2	0.01	3473.5	0.999	0.09
нсв	74.7	239.66	102.24	0.82	384.9	0.994	0.07
PCB	62.76	327.6	512.23	0.81	1630.1	0.999	15.9

Table 3. Biexponential excretion constants and model-fitting statistics for <u>D. magna.</u>

Chemical	C ₁ DPM mL ⁻¹	k ₁ min ⁻¹	C ₂ DPM mL ⁻¹	k ₂ min ⁻¹	RMS	df
AC	3.423	0.0045	3.118	0.000031	0.0045	59
BUT	2.811	0.0028	4.953	0.000085	0.0025	61
ACP	38.43	0.0169	35.06	0.000124	0.0061	64
BZA	41.58	0.0096	36.54	0.000249	0.0050	62
CHL	305.26	0.0187	83.2	0.00024	0.0120	59
BEN	48.58	0.0196	3.424	0.000034	0.0050	62
TOL	19.45	0.0585	33.91	0.00007	0.0037	62
ATR	502.8	0.0374	78.4	0.000311	0.0049	57
CB	55.0	0.0121	43.01	0.000445	0.0045	60
BB	264.7	0.0177	44.26	0.00017	0.0046	62
1,2-DCB	190.0	0.0636	63.06	0.000873	0.0122	61
1,4-DCB	35.2	0.0552	50.96	0.00101	0.0025	59
2-MN	59.68	0.037	40.53	0.00064	0.0025	60
вн	38.31	0.0596	43.03	0.000462	0.0042	59
TCB	597.0	0.0622	30.27	0.000136	0.0286	63
ANT	37.89	0.0632	44.47	0.00099	0.0066	60
TTB	139.9	0.0577	35.64	0.000762	0.0030	61
DDE	943.1	0.0737	329.0	0.00012	0.0040	61
DDT	215.9	0.0659	43.6	0.00058	0.0159	61
PTCB	109.7	0.0807	64.05	0.0021	0.0042	57
HCB	93.3	0.0616	46.8	0.00165	0.0042	60
PCB	1337.6	0.612	604.5	0.001929	0.0047	60

Kow based QSPRs

Uptake

The average uptake rate constants from water and from food were both of the same magnitude (Fig. 1). The uptake rate constants varied from 1.29×10^{-4} to 3.22 min^{-1} for uptake via food and 3.67×10^{-3} to 4.24 min^{-1} for uptake via water. Both rate constants for uptake from water and from food increased with increasing log K_{ow} (Fig. 1) as expressed by the following equations (n = 22, P < 0.01):

 $\log k_{01} \text{ (food)} = 0.62(\pm 0.05) \log K_{ow} - 3.69(\pm 0.22) \quad R^2 = 0.87, \, S_{y,x} = 0.45, \, F = 132.7$

 $\log k_{01}$ (water) = 0.46(±0.07) $\log K_{ow}$ - 2.61(±0.30) R^2 = 0.66, $S_{y,x}$ = 0.62, F = 39.2

The slope of the uptake from water is shallower than that from food (t test, p < 0.01), indicating that uptake from food increased with K_{ow} much faster than uptake from water. The intercept of the uptake from food is much more negative than that from water (t test, p < 0.01), suggesting uptake rate constants from water were higher than those from food at lower K_{ow} . With increasing K_{ow} , the two regression lines merged, demonstrating that, on average, both rate constants had similar values.

Average concentration of contaminant was 44.37×10^{-9} mmol mL⁻¹ with a range between 1.91 and 194.94×10^{-9} mmol mL⁻¹ for aqueous uptake

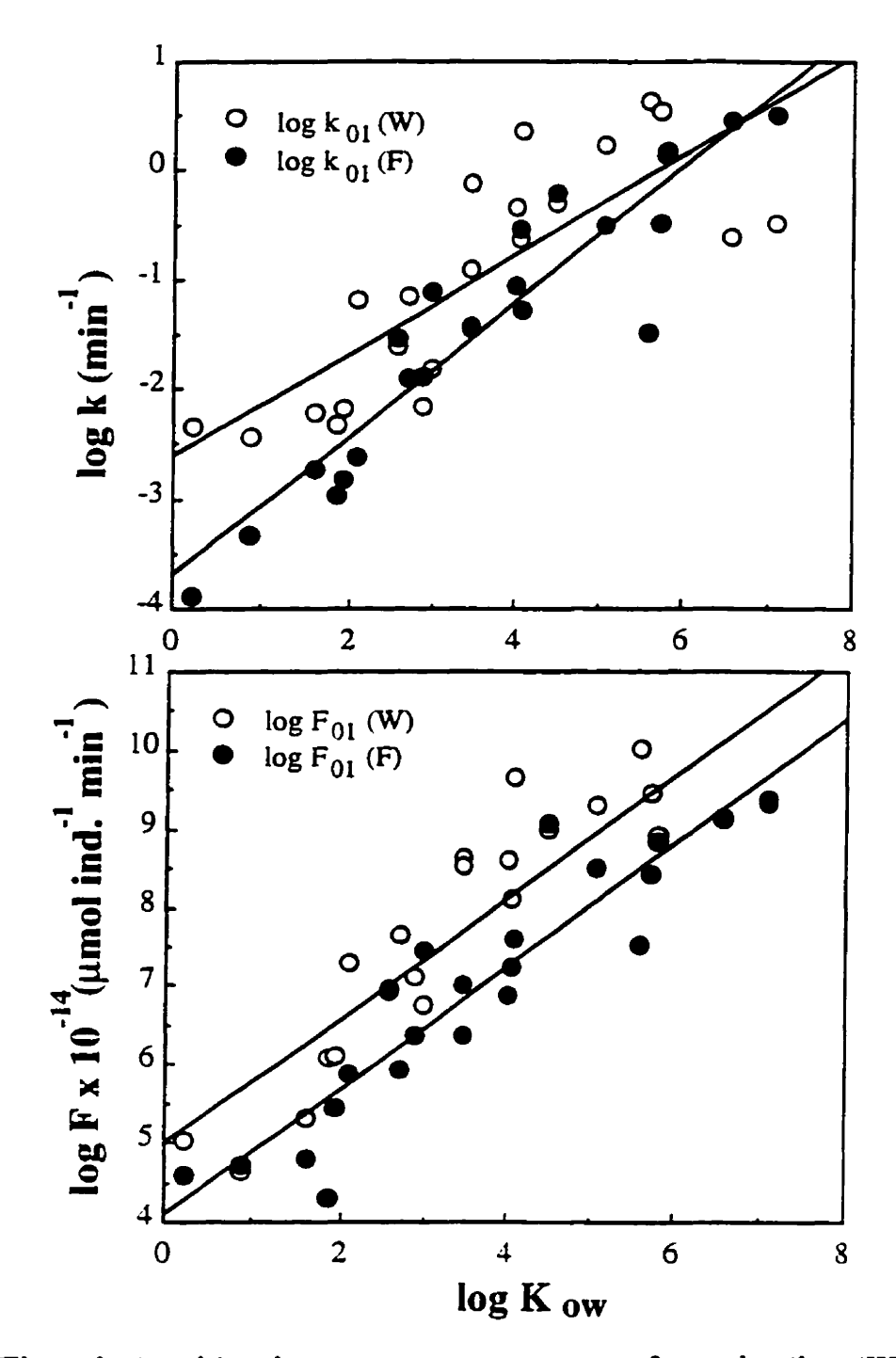


Fig. 1. The relationships between rate constants of uptake $(k_{01} (W))$: uptake from water; $k_{01} (F)$: uptake from food), and flux rates of uptake $(F_{01} (W))$: uptake from water; $F_{01} (F)$: uptake from food) of organic chemicals and their octanol-water partition coefficient (k_{ow}) in \underline{D} . \underline{magna} .

experiment, and 134.66×10^{-9} mmol mL⁻¹ with a range between 1.19 and 630.09×10^{-9} mmol mL⁻¹ for dietary uptake experiment. Uptake rates from water and from food had similar slopes in relation to log K_{ow} , and the intercept differed by about one order of magnitude (Fig. 1). The relationships are best represented by the following QSPR equations (n = 22, P < 0.01):

$$\log F_{01} \text{ (food)} = 0.79(\pm 0.07) \log K_{ow} + 4.10(\pm 0.29) \quad R^2 = 0.85, S_{y,x} = 0.62,$$

$$F = 115.5$$

$$\log F_{01} \text{ (water)} = 0.78 (\pm 0.09) \log K_{ow} - 5.00 (\pm 0.35) \quad R^2 = 0.80, S_{y,x} = 0.74,$$

$$F = 78.4$$

The uptake rates varied from 2.0×10^{-10} to 2.4×10^{-5} µmol ind⁻¹ min⁻¹ for uptake via food and 4.4×10^{-10} to 1.04×10^{-4} µmol ind⁻¹ min⁻¹ for uptake via water. After standardizing the effect of contaminant concentrations of the medium in the two uptake experiments, it is obvious that <u>Daphnia</u> took up organic chemicals at about the same rate from water and from food.

Elimination and intercompartmental exchanges

The two rate constants for intercompartmental exchanges increased with increasing log K_{ow} with similar slopes, but the intercepts for intercompartmental rate constants differed about two orders of magnitude. In contrast, the rate constants for elimination decreased with increasing log K_{ow} (Fig. 2). The relationship between K_{ow} and rate constant of uptake, elimination or intercompartmental exchanges was indicated by following relations (n = 22,

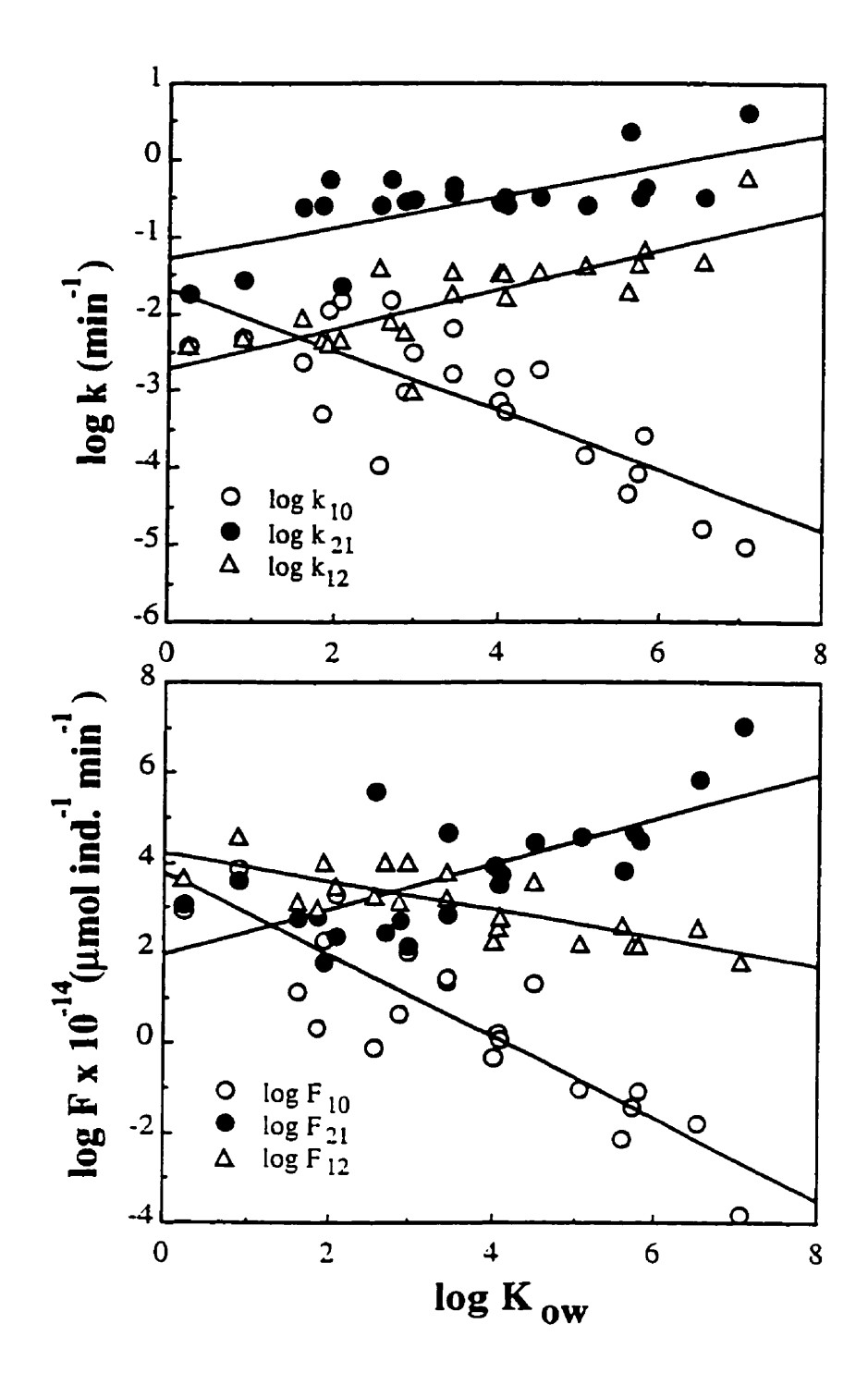


Fig. 2. The relationships between rate constants and flux rates of elimination $(k_{10},\,F_{10})$ and intercompartmental exchanges $(k_{12},\,k_{21},\,F_{12},\,F_{21})$ of organic chemicals and their octanol-water partition coefficient (K_{ow}) in \underline{D} . \underline{magna} .

P < 0.01):

$$\label{eq:k10} \begin{split} \log \, k_{10} &= \text{-}0.39(\pm\,0.07)\,\log\, K_{ow} \,\text{-}\,1.71(\pm\,0.28) \quad R^2 = 0.60,\, S_{y,x} = 0.60,\, F = 30.2 \\ \log \, k_{12} &= 0.25(\pm\,0.04)\,\log\, K_{ow} \,\text{-}\,2.71(\pm\,0.18) \quad R^2 = 0.62,\, S_{y,x} = 0.37,\, F = 32.7 \\ \log \, k_{21} &= 0.20(\pm\,0.05)\,\log\, K_{ow} \,\text{-}\,1.29(\pm\,0.19) \quad R^2 = 0.48,\, S_{y,x} = 0.40,\, F = 18.6 \end{split}$$
 The elimination rate constants (k₁₀) varied from 9.0x10⁻⁶ to 1.5x10⁻² min⁻¹. The intercompartmental transfer rate constants varied between 9.4x10⁻⁴ and 0.58 min1⁻¹ for K₁₂ and between 0.02 and 4.1 min⁻¹ for K₂₁.

The relative pool size (%) of the metabolic compartment declined with the increasing K_{ow} , while the relative pool size of the structural compartment increased with increasing K_{ow} . The relationships between relative pool size and log K_{ow} can be described by the following equations:

$$\log C_1(\%) = -0.08(\pm 0.02) \log K_{ow} + 0.43(\pm 0.05) \quad R^2 = 0.42, \, S_{y,x} = 0.18, \, F = 51.5$$

$$\log C_2(\%) = 0.08(\pm 0.02) \log K_{ow} + 0.43(\pm 0.07) \quad R^2 = 0.42, \, S_{y,x} = 0.18, \, F = 10.8$$

For forward intercompartmental exchange (F_{12}) and elimination rate (F_{01}) , the slopes of the regression line are negative. These rates decrease with increasing log K_{ow} (Fig. 2). In contrast, the backward intercompartmental exchange rate (F_{21}) increased with increasing K_{ow} . The slope of the forward intercompartmental exchange was shallower than that of elimination, implying that elimination rates dropped faster than that of forward internal flux with the increasing K_{ow} . The relationship between K_{ow} and rates of uptake, elimination or intercompartmental exchanges was described by the following QSPRs (n = 22, P < 0.01):

log F_{10} = -0.91(± 0.12) log K_{ow} + 3.78(± 0.46) R^2 = 0.76, $S_{y,x}$ = 0.97, F = 62.5 log F_{12} = -0.31(± 0.06) log K_{ow} + 4.19(± 0.23) R^2 = 0.60, $S_{y,x}$ = 0.49, F = 29.8 log F_{21} = 0.50(± 0.11) log K_{ow} + 1.95(± 0.46) R^2 = 0.50, $S_{y,x}$ = 0.96, F = 19.6 The elimination rates (F_{10}) ranged between 1.4x10⁻¹⁸ and 6.9x10⁻¹¹ µmol ind⁻¹ min⁻¹. The intercompartmental transfer rates varied between 6.3x10⁻¹³ and 3.7x10⁻¹⁰ µmol ind⁻¹ min⁻¹ for forward intercompartmental exchange (F_{12}) and between 6.3x10⁻¹³ and 1.1x10⁻⁷ µmol ind⁻¹ min⁻¹ for backward intercompartmental exchange (F_{21}).

Bioaccumulation

<u>Daphina magna</u> accumulated contaminants very quickly both from water and from food. The rates of accumulation from both pathways showed significant dependence on chemical's $\log K_{ow}$. The predictive equation can be reflected by the same equation:

$$\log A_{\text{food}} = \log A_{\text{water}} = 0.78(\pm 0.09) \log K_{\text{ow}} + 5.99(\pm 0.36)$$

 $R^2 = 0.80, S_{y,x} = 0.74, F = 78.3$

Both slopes for accumulation from water and from food do not differ significantly from those of the corresponding uptake rates, indicating the uptake is the dominant process in the bioaccumulation of organic contaminants. The intercept of the accumulation from food is not significantly different from that the of the uptake as well. However, the intercept of the accumulation from water is significantly lower than that of uptake, suggesting

elimination played a significant role in this accumulation processes of organic contaminants.

Bioconcentration Factors

Bioconcentration factors (BCF) varied by 5 orders of magnitude in <u>Daphnia</u>, being lowest in n-Butanol (4.8), and highest in 4,4'-DDT (3.3x10⁵). The average BCF of <u>Daphnia</u> was around 4.5 x 10^4 . Simple regression analysis revealed that log K_{ow} was a significant structural correlate of BCFs (Fig. 3), and can be expressed by the equation below (n = 22, P < 0.01):

$$\log \mathrm{BCF} = 0.73(\pm~0.06) \log~\mathrm{K_{ow}} + 0.71(\pm~0.25) \quad \mathrm{R}^2 = 0.87, \, \mathrm{S_{y,x}} = 0.54, \, \mathrm{F} = 131.7$$

Other structure-based QSPRs

Overall K_{ow} was the best correlate of each of the rate constants, flux rates and BCF. However, a number of the QSPRs could be built using other structural parameters. For BCFs, the second best equation was obtained when BCFs were regressed against MW (Table 4). The next best variables were PA, BP and log S. The remaining structural parameters explained less than 50% total variance.

In addition to K_{ow} , many structural parameters, PA, MW, BP, CI and log S were significant correlates of the uptake rate constants (k_{01}) from food (Table 4). In contrast, the uptake rate constants from water were strongly related

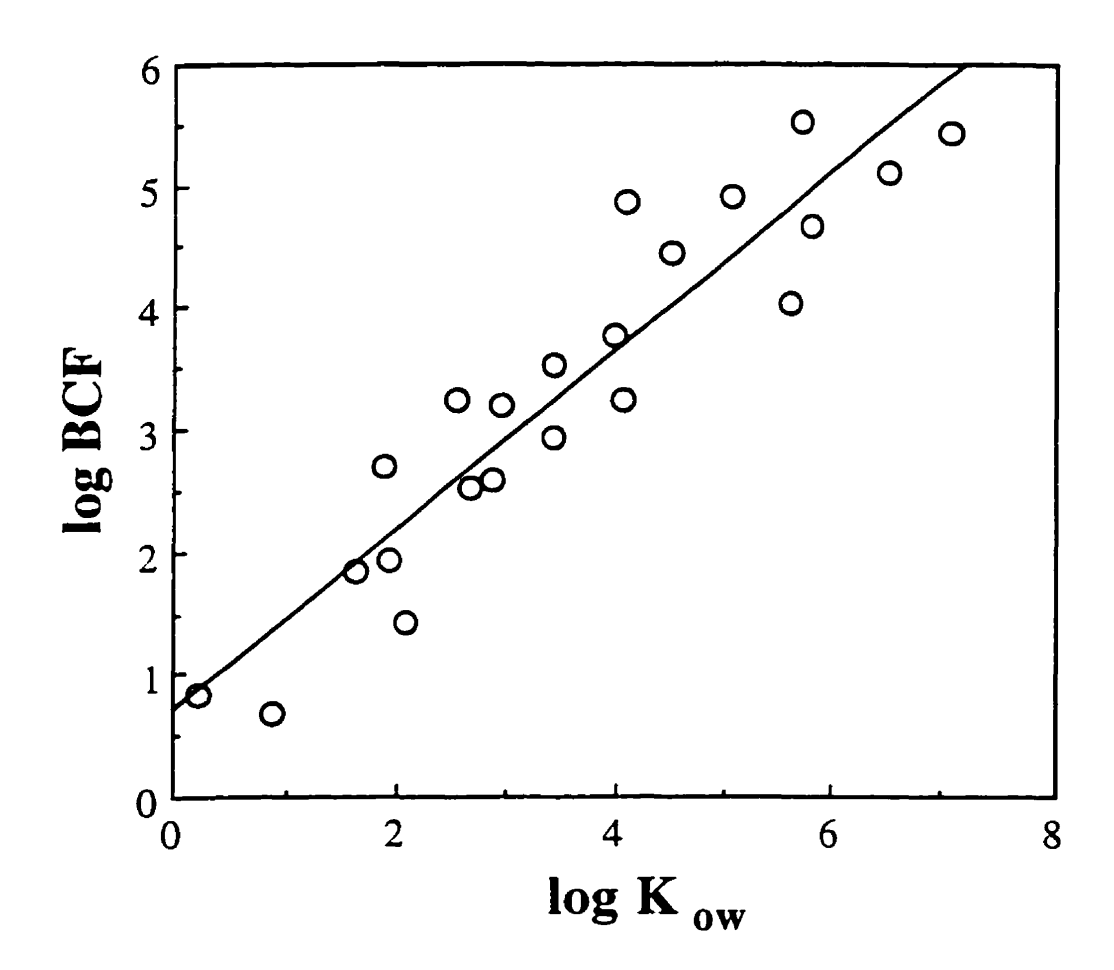


Fig. 3. The relationship between bioconcentration factors (BCF) of organic chemicals and their octanol-water partition coefficient (K_{ow}) in \underline{D} . \underline{magna} .

Table 4. Simple regression equations relating BCF and rate constants of \underline{D} . \underline{magna} to chemical structural properties. N is the number of data points, $S_{y,x}$ is the root of the mean square error of the regression, and the standard deviation of the coefficient is given in parentheses. All regressions are highly significant (P < 0.001).

Models	N	S _{y,x}	r ²	F			
Bioconcentration factor							
$\log BCF = 1.06(\pm 0.44) + 0.01(\pm 0.00) MW$	22	0.91	0.63	33.3			
$\log BCF = 0.59(\pm 0.59) + 0.01(\pm 0.00) PA$	20	1.00	0.58	24.3			
$\log BCF = 0.93(\pm 0.53) + 0.01(\pm 0.00) BP$	19	1.15	0.55	20.9			
log BCF = $2.81(\pm 0.25) - 0.26(\pm 0.06) \log S$	21	0.95	0.54	22.2			
Uptake from v	vater						
$\log K_{01} = -2.44(\pm 0.36) + 0.01(\pm 0.00) \text{ MW}$	22	0.75	0.51	20.8			
Uptake from	food						
$\log K_{01} = -3.85(\pm 0.48) + 0.01(\pm 0.00) PA$	20	0.83	0.61	28.2			
$\log K_{01} = -3.35(\pm 0.39) + 0.01(\pm 0.08) \text{ MW}$	22	0.80	0.60	29.7			
$\log K_{01} = -3.64(\pm 0.45) + 0.01(\pm 0.00) BP$	19	0.79	0.60	25.1			
$\log K_{01} = -3.69(\pm 0.54) + 0.60(\pm 0.14) \text{ CI}$	19	0.93	0.53	19.3			
$\log K_{01} = -1.88(\pm 0.21) - 0.22(\pm 0.05) \log S$	21	0.80	0.52	20.8			
Intercompartmental exchanges							
$log K_{12} = -2.88(\pm 0.25) + 0.01(\pm 0.00) PA$	20	0.43	0.54	21.0			
$\log K_{21} = -2.12(\pm 0.36) + 1.16(\pm 0.26) D$	21	0.40	0.52	20.1			

only to K_{ow} and MW. Other parameters, although significant, gave poorer relationships ($r^2 < 0.50$). However, with the exception of K_{ow} , no structural parameters were related to the elimination rate constants with $r^2 > 0.50$.

The flux rates behaved dissimilarly in relation to structural properties (Table 5). Uptake rates via water can be predicted from $\log K_{ow}$, $\log S$, MW and PA, while the uptake rates via food could be estimated by $\log K_{ow}$, MW, PA, BP, and $\log S$. The elimination rates were significantly related to $\log K_{ow}$, MW and PA with r^2 above 0.5. In contrast, no structural parameters other than K_{ow} showed high regressions ($r^2 > 0.50$) to intercompartmental exchange rates.

Multivariate regression analysis did not significantly improve the overall relation between pharmacokinetic flux rates and structural properties. No additional variable reached the level of significance (p > 0.05).

Inter-specific comparison of pharmacokinetic parameters

On average, <u>Daphnia</u> has a smaller uptake rate constant (k_{01}) than <u>Chlorella</u>. There was a clear shift in relative magnitude of uptake rate constants in <u>Chlorella</u> and <u>Daphnia</u> (Fig. 4) as indicated by the distribution of data points around the 1:1 line. When the rate constant from the water (log k_{01}) of <u>Chlorella</u> is less than -2, <u>Daphnia</u> k_{01} exceeds <u>Chlorella</u> k_{01} ; otherwise <u>Daphnia</u> k_{01} is less than <u>Chlorella</u> k_{01} . This suggests that, <u>Chlorella</u> usually

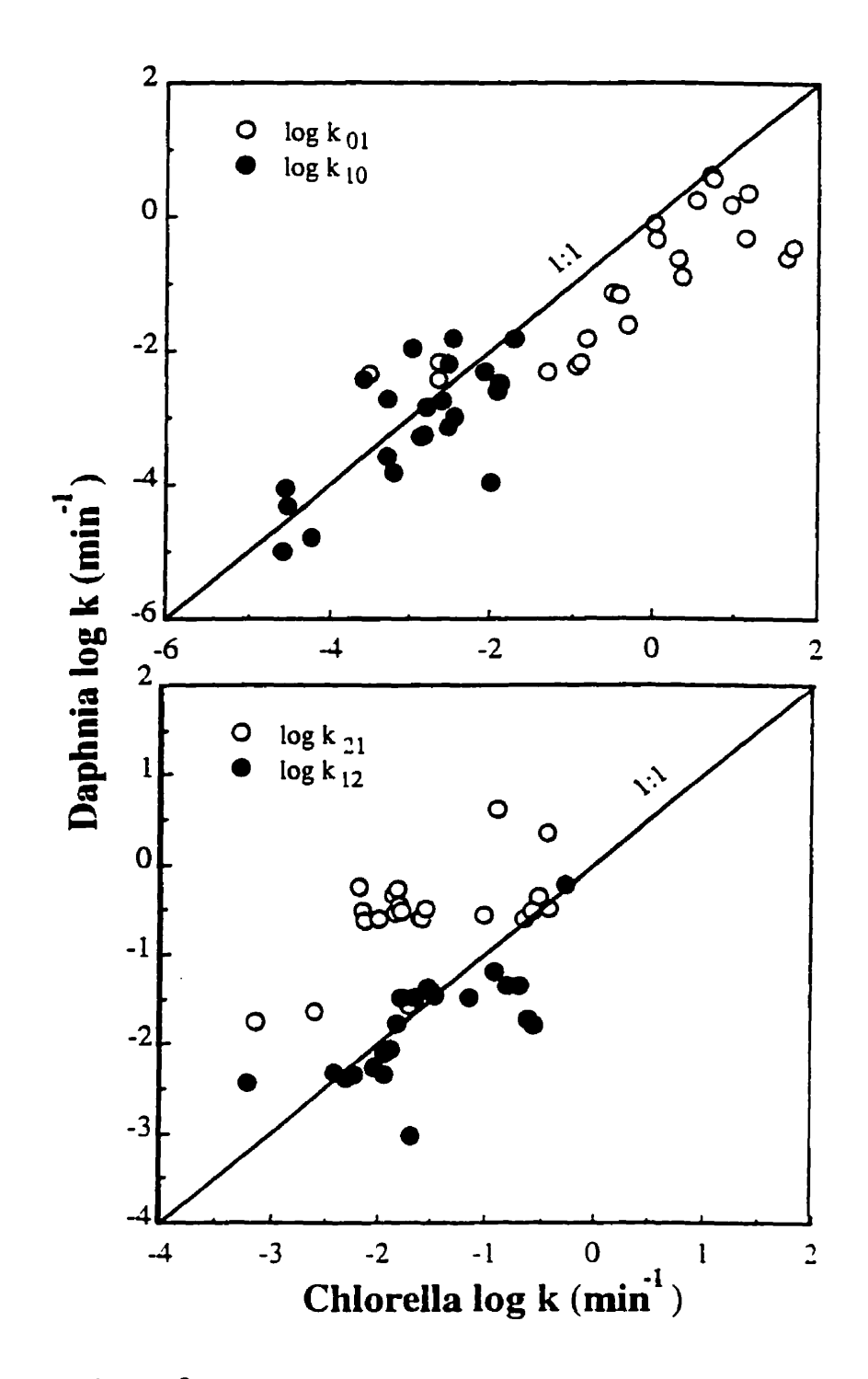


Fig. 4. Comparison of rate constants of aqueous uptake (k_{01}) , elimination (k_{10}) and intercompartmental exchanges $(k_{12},\,k_{21})$ of organic chemicals between \underline{C} . pyrenoidosa and \underline{D} . magna.

Table 5. Simple regression equations relating pharmacokinetic flux parameters of \underline{D} . \underline{magna} to chemical structural properties. N is the number of data points, $S_{y,x}$ is the root of the mean square error of the regression, and the standard deviation of the coefficient is given in parentheses. All regressions are highly significant (P < 0.001).

Models	N	$S_{y,x}$	r^2	F
Uptake from water				
$\log F_{01} = 7.18(\pm 0.27) - 0.30(\pm 0.06) \log S$	21	1.02	0.57	25.5
$\log F_{01} = 5.41(\pm 0.53) + 0.01(\pm 0.00) \text{ MW}$	22	1.10	0.56	25.0
$log F_{01} = 4.99(\pm 0.68) + 0.01(\pm 0.00) PA$	20	1.16	0.50	18.0
Uptake from food				
$\log F_{01} = 4.60(\pm 0.52) + 0.01(\pm 0.00) \text{ MW}$	22	1.08	0.55	24.8
$\log F_{01} = 4.05(\pm 0.67) + 0.01(\pm 0.00) PA$	22	1.15	0.54	21.2
$\log F_{01} = -3.64(\pm 0.45) + 0.01(\pm 0.00) BP$	19	0.79	0.60	25.1
$\log F_{01} = 6.34(\pm 0.29) - 0.28(\pm 0.06) \log S$	21	1.10	0.50	19.3
Elimination				
$\log F_{10} = 3.56(\pm 0.58) - 0.02(\pm 0.00) \text{ MW}$	22	1.19	0.63	34.4
$\log F_{10} = 3.85(\pm 0.81) - 0.01(\pm 0.00) PA$	20	1.39	0.50	17.7
Accumulation from water				
$log A = 8.18(\pm 0.27) - 0.30(\pm 0.06) log S$	21	1.02	0.57	25.5
$\log A = 6.41(\pm 0.53) + 0.01(\pm 0.00) MW$	22	1.10	0.56	25.0
$\log A = 5.99(\pm 0.68) + 0.01(\pm 0.00) PA$	20	1.16	0.50	18.0
Accumulation from food				
$\log A = 8.18(\pm 0.27) - 0.30(\pm 0.06) \log S$	21	1.02	0.57	25.5
$\log A = 6.40(\pm 0.53) + 0.01(\pm 0.00) \text{ MW}$	22	1.10	0.56	25.0
$\log A = 5.98(\pm 0.68) + 0.01(\pm 0.00) PA$	20	1.16	0.50	18.0

takes up contaminants from the water faster than <u>Daphnia</u>. The elimination rate constants (Fig. 4) were, in contrast, distributed close to 1:1 line, suggesting that two rate constants were similar in magnitude. Rate constants of most forward intercompartmental exchanges (Fig. 4) were at or below 1:1 line, suggesting that <u>Chlorella</u> forward rate constants were higher than, or at least equal to those of <u>Daphnia</u>. The rate constants of the backward intercompartmental exchanges were, however, at or above the 1:1 line, indicating that <u>Daphnia</u>'s backward intercompartmental exchange rate constants were usually greater than those of <u>Chlorella</u>.

Flux rates of uptake, elimination and intercompartmental exchanges in the <u>Daphnia-Chlorella</u> plot (Fig. 5) showed different patterns compared to their rate constants. All the data points were above the 1:1 line, implying that <u>Daphnia</u> flux rates were always higher than those of <u>Chlorella</u>.

The 1:1 line intersects the data in the plot of <u>Daphnia</u> BCF vs. <u>Chlorella</u> BCF (Fig. 6), demonstrating that BCFs are of different quantity between two species. Although for most chemicals, <u>Daphnia</u> have a higher values of BCFs than those of <u>Chlorella</u>, on average, <u>Chlorella</u> had a higher value of BCF than <u>Daphnia</u>, because the positive residuals (mean = 33812.9, n = 14) in Fig. 6 are smaller than the negative ones (mean = 554217.5, n = 8).

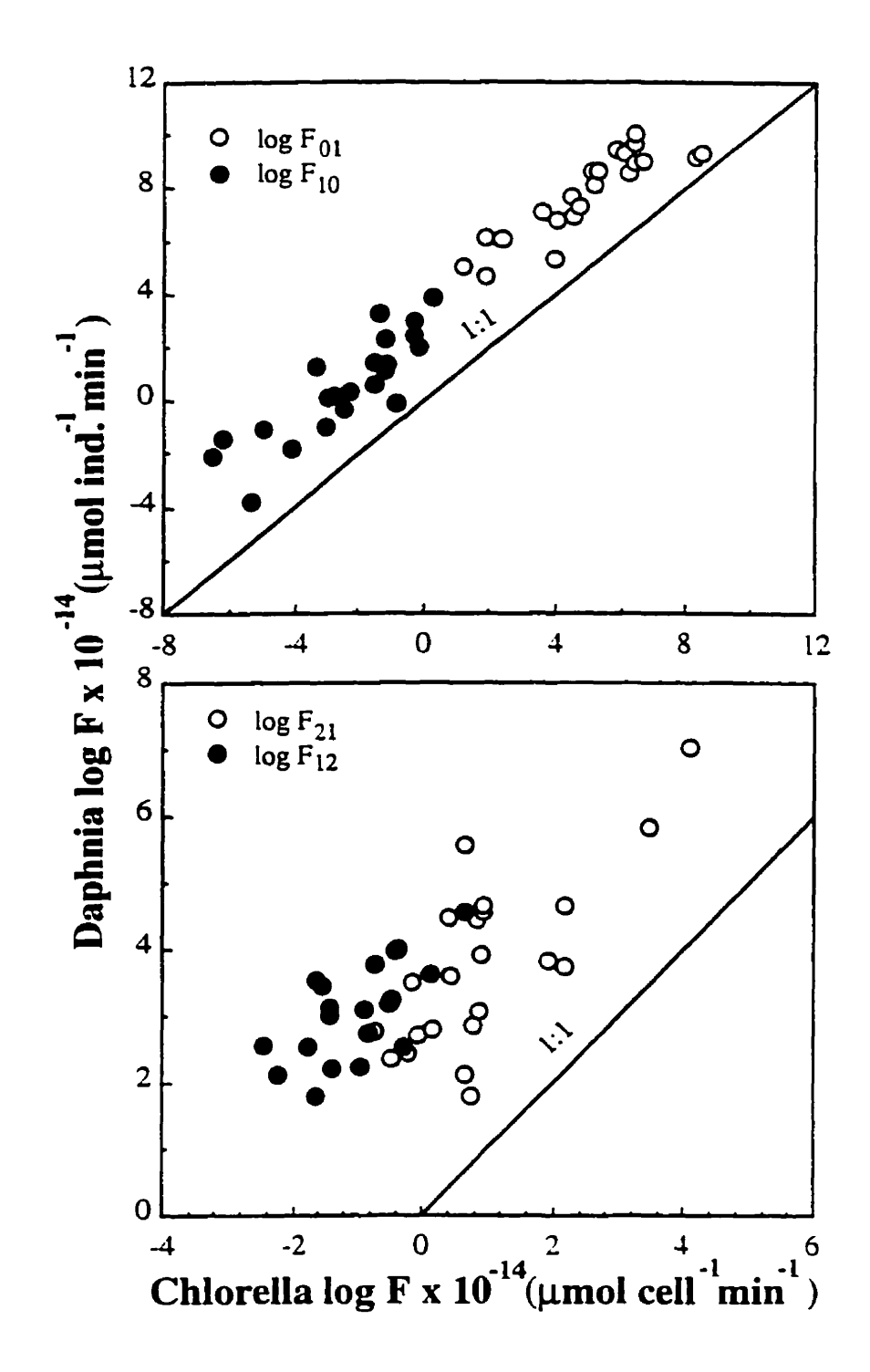


Fig. 5. Comparison of flux rates of aqueous uptake (F_{01}) , elimination (F_{10}) and intercompartmental exchanges (F_{12}, F_{21}) of organic chemicals between \underline{C} . pyrenoidosa and \underline{D} . magna.

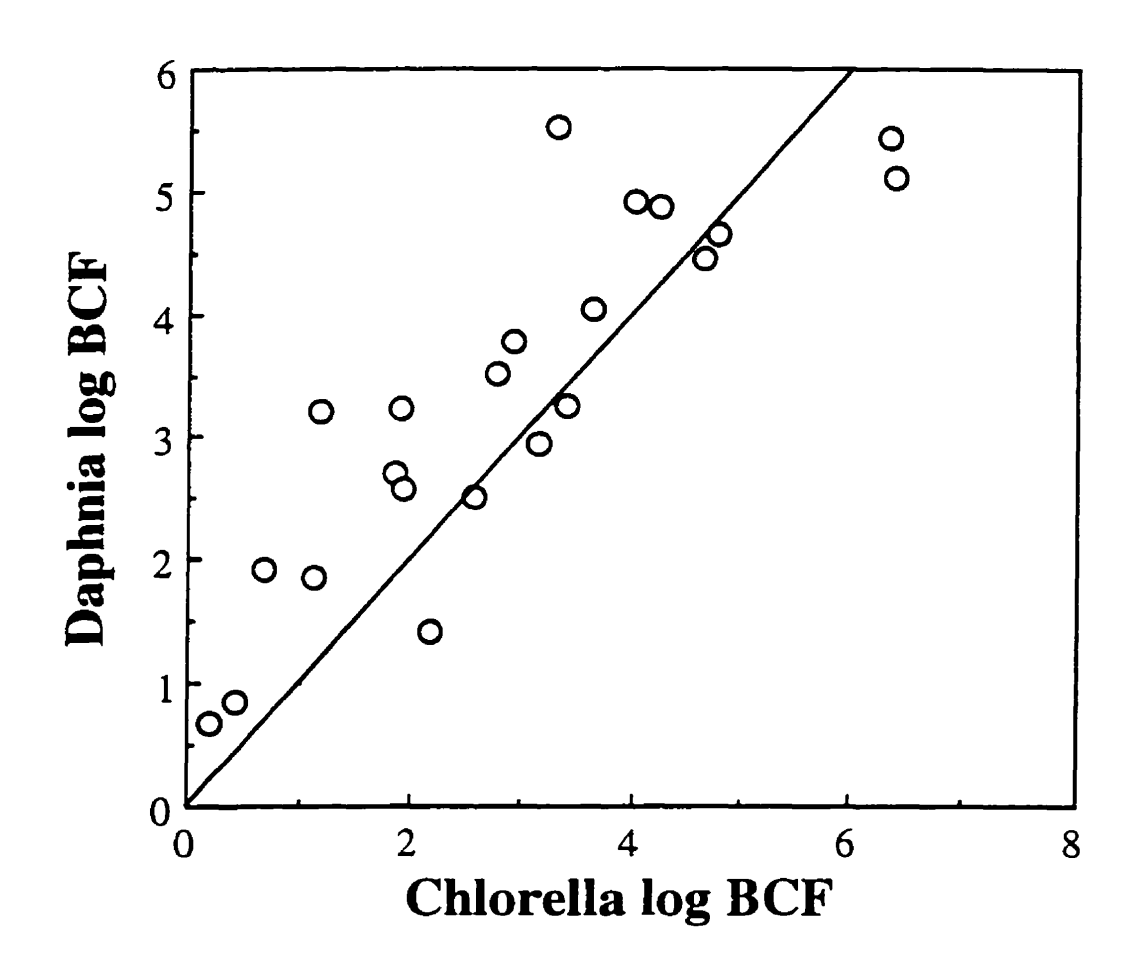


Fig. 6. Comparison of bioconcentration factors of organic chemicals between \underline{C} . pyrenoidosa and \underline{D} . magna.

Discussion

Pharmacokinetic parameters

The uptake kinetics of 22 organic compounds by <u>D</u>. <u>magna</u> varied substantially for uptake both via water and via food. Such variations were also encountered in other studies on uptake of persistent hydrophobic chemicals by fish (Loonen et al. 1994). Unfortunately the uptake rates of organic chemicals by <u>D</u>. <u>magna</u> are rare in the literature, so a quantitative comparison of our findings with others is impossible. Interestingly we found that <u>D</u>. <u>magna</u> accumulates organic chemicals as fast from water as from food. This has not been previously reported for <u>D</u>. <u>magna</u>.

Understanding the relative contribution of food and water as uptake vectors is a very important aspect in the examination and prediction of the bioavailability of a toxicant to an animal species. However, there is a contradiction in the current literature concerning the relative importance of uptake pathways for aquatic organisms. Some studies indicated that direct uptake of hydrophobic contaminants from food dominates over uptake from water (Bruggeman et al. 1981, Rhead and Perkins 1984), whereas other studies demonstrated that bioaccumulation of organic xenobiotics occurs predominantly via uptake from water (Neely et al. 1974; Southworth et al 1979). To date, experimental data pertaining to the relative importance of the two uptake pathways is lacking for daphnids. Our data indicated that, for all lipophilics

daphnid bioconcentration. Although the uptake rate from water was about four times higher than uptake rate from food, the aqueous concentration of the contaminant in the experiments on uptake from water was about three times higher than that in the uptake from food experiment. After taking this difference into consideration, the overall flux rates between two pathways are not much different. This result seems contradictory to expectation from the field. In the field, bioaccumulation causes the food to have much higher contaminant concentration than the water. Consequently the food may represent a more significant source than water. However, this need not be the case in the laboratory where the aqueous concentration may vary considerably. Because the kinetic flux of contaminant is pool size dependent, any difference in the aqueous concentration can cause large difference in the flux rates. Our result seems reasonable because the uptake of contaminants by Daphnia not only occur directly from the diet intake, but also from the passive transport. Because Daphnia pass a large quantity of water through their appendages to collect food, direct uptake from passive diffusion across the body surface could become an important route as the chemicals establish an equilibrium between body and water very rapidly (Connell 1990).

tested, the water and food are both important sources of organic compound for

The first order, two-compartment model satisfactorily described the elimination of organic toxicants by <u>Daphnia</u>. This biphasic nature of clearance has been also noted in earthworms (Belfroid et al 1994), gastropods (Thybaud

and Caquet 1991), and fish (de Wolf et al. 1994). However, for some toxicants, the RMS were relatively high, indicating that, in reality, more internal compartments were involved in the actual accumulation processes of organic chemicals. The "anomalous" exponents of intercompartmental exchanges and the apparent unbalance of the fluxes may also represent points of "slippage" as the models generate values that may be "fit to error" and inconsistent among the experiments, resulting in low intercept and low slope. Our measured elimination rates were several orders of magnitude lower than the uptake rates. This is consistent with other studies on persistent organic compounds (Landrum 1988; Evans and Landrum 1989; de Voogt et al. 1991).

Bioconcentration Factors

Direct comparisons of our laboratory-determined BCF data for all the chemicals with other studies are impossible due to the scarcity of the literature data. Some possible comparisons indicate that our measured value of 2.7×10^5 for 2,2',4,4',5,5'-Hexachlorobiphenyl is generally higher than the field studies. Evans (1991) reported BCFs between a low of 4.5×10^4 and a high of 12×10^4 for 2,2',4,4',5,5'-Hexachlorobiphenyl in \underline{D} . magna. Oliver and Niimi (1988) reported a BCF of 4.4×10^4 for this PCB congener for all plankton in Lake Ontario. Sanders and Chandler (1972) reported that \underline{D} . magna accumulated total body concentrations of PCB (1254) 48000 times greater than those in water. This discrepancy could be caused by the concentration and period exposure, and the

presence of other chemicals, which have been demonstrated to exercise physical and physiological influences on bioconcentration of the aquatic organisms (Landrum 1988).

The relationship between BCFs and K_{ow} from our study is consistent with those of others (Table 6). In the literature, the slopes of the BCF- K_{ow} relations varied between 0.66 and 0.90, and intercepts between -1.32 and -0.05. Both slope and intercept detected in present study lie in the higher range of these studies. These differences may be the results of interspecies and intercompound responses, but too little information is available to make such comparisons among studies.

Although our data demonstrated a highly significant linear correlation between BCFs and K_{ow} , it should be cautious to extrapolate this relationship to the K_{ow} range beyond the present study. For compounds with K_{ow} greater than 7, a loss of proportionality has been reported in fish (Gobas et al. 1989) and in phytoplankton (Stange and Swackhamer 1994). The possible causes for this nonlinearity in the BCF- K_{ow} function include insufficient exposure times, reduced bioavailability, differences in membrane permeation and lipid-water partitioning (Gobas et al. 1987).

Structure-pharmacokinetic relationships

Our data on uptake of toxicants by $\underline{Daphnia}$ demonstrated that both uptake rate constants and uptake rates are positive functions of K_{ow} , suggesting

Table 6. Comparisons of relationships between BCFs and physical-chemical properties of the chemicals for <u>Daphnia</u>.

Equation	n	r ²	Species	Reference
$\log BCF = 0.66 \log K_{ow} - 0.05$	6	0.81	D. magna	Eastmond et al.
log BCF = $0.75 \log K_{ow} - 0.44$	7	0.85	D. pulex	Southworth et al. (1978a)
$\log BCF = 0.82 \log K_{ow} - 1.15$	3	0.99	D. pulex	Southworth et al. (1978b)
$\log BCF = 0.87 \log K_{ow} - 0.22$	22	0.85	D. magna	This study
$\log BCF = 0.90 \log K_{ow} - 1.32$	22	0.96	D. pulex	Hawker and Connell (1986)

relative lipophilicity is an excellent predictor describing these metabolic processes in animals. Since the larger the $K_{\rm ow}$, the greater is the lipophilicity of a chemical, our finding agrees with current theory. Chu (1979) indicates that $K_{\rm ow}$ reflects the transport of chemical by serum-binding or receptor-binding factors. Our result is also consistent with other studies. De Bruijn and Hermens (1991) found a strong correlation between log $K_{\rm ow}$ and uptake and elimination rate constants for 12 organophosphorus compounds in guppies (Poecilia reticulata). Lohner and Collins (1987) showed that the uptake rate constants of six organochlorines were highly correlated with their $K_{\rm ow}$ values for midge larvae.

Our results indicated that elimination of organic chemicals was inversely related to the compound's lipophilicity. This structure-kinetic relation also agrees with previous studies (Konemann and Van Leeuwen 1980; Landrum 1988; Gobas et al. 1986; de Voogt et al. 1991). However, K_{ow} explained a relatively smaller portion of the variance in the elimination rate constants and flux rates than that of other pharmacokinetic parameters. This anomaly has been frequently reported in fish and explained by the biotransformation of the toxicants. de Wolf et al. (1993) reported that, in the guppy, the elimination rate constants for two isomers of trichloroanilines were much higher than those expected from K_{ow} , and attributed this to the influence of biotransformation on the overall elimination rates of the compounds. In their measurements of uptake and elimination of DDE, benzo(a)pyrene and 2,4,5,2',4',5'-

hexachlorobiphenyl by the amphipod <u>Pontoporeia boyi</u> and the mysid <u>Mysis relicta</u>, Evans and Landrum (1989) found a similar discrepancy for elimination rate constants. Both species were very efficient at eliminating some of these compounds. Because no metabolites were checked in our study, the role of biotransformation in the elimination of these toxicants by <u>Daphnia</u> is uncertain.

The utility of lipophilicity as a predictor for contaminant accumulation was evaluated by the plot of predicted from K_{ow} vs observed values experimentally derived from the first order kinetics. The predicted rates of accumulation (both from water and from food) were reasonably in good agreement with the corresponding experimental data (Figs. 7 and 8), indicating that K_{ow} would provide a quantitative measure of flux rates of organic contaminants by $\underline{Daphnia}$. However, there are still some degree of discrepancy between predicted and measured values, demonstrating that K_{ow} as a sole predictor could introduce some residual errors. Therefore QSPR models should be validated, whenever possible, to increase their predictability and our confidence in toxicological assessment.

Interspecies comparison of QSPRs

There may be a tendency for bioconcentration factors to increase faster with K_{ow} in <u>Chlorella</u> than in <u>Daphnia</u>. For chemicals with low log K_{ow} , <u>Daphnia</u>

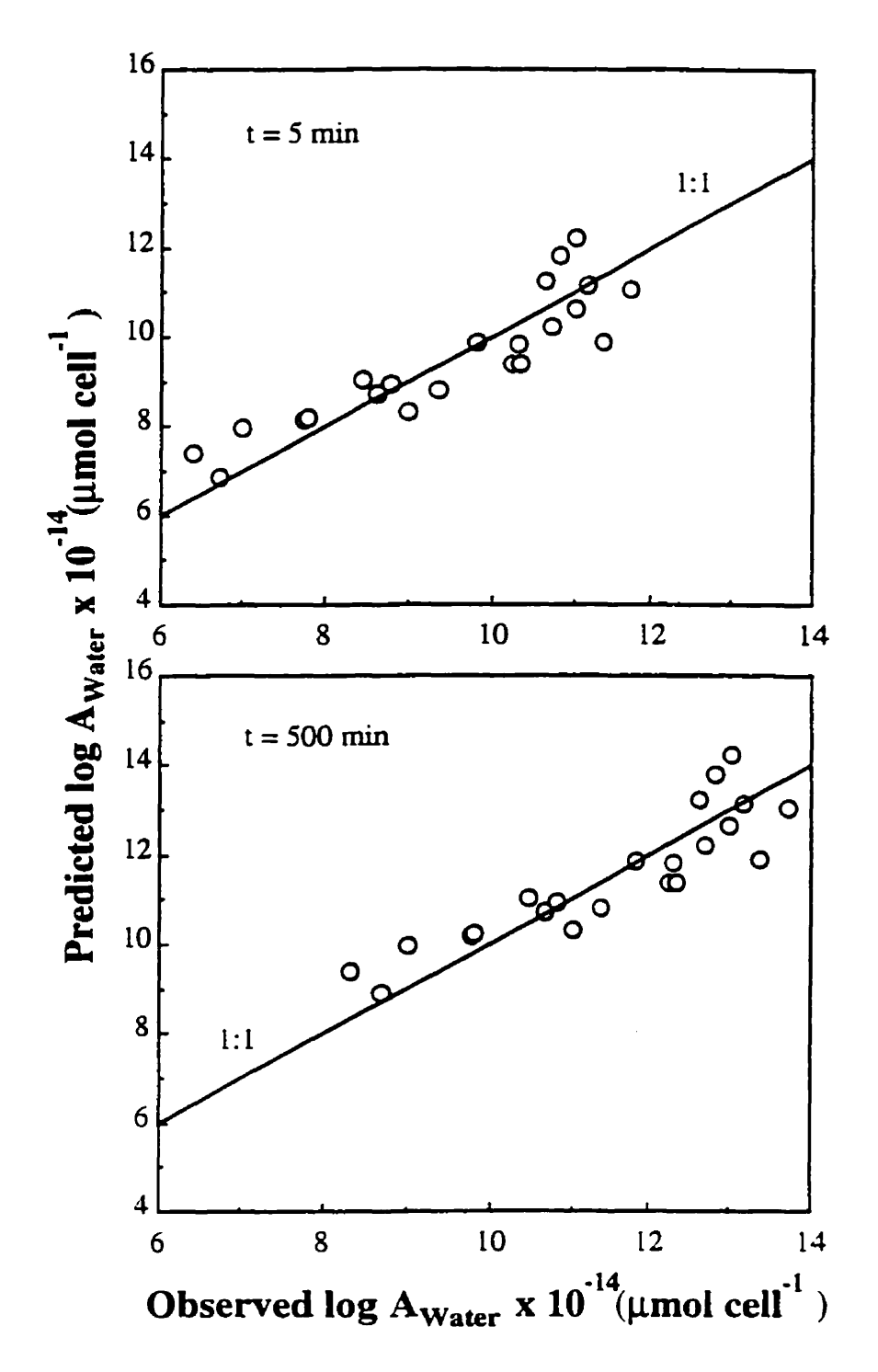


Fig. 7. Logarithms (base 10) of observed vs predicted accumulation from water (μ mol ind⁻¹) of various organic chemicals in <u>D</u>. <u>magna</u>. The solid line represents the ideal fit.

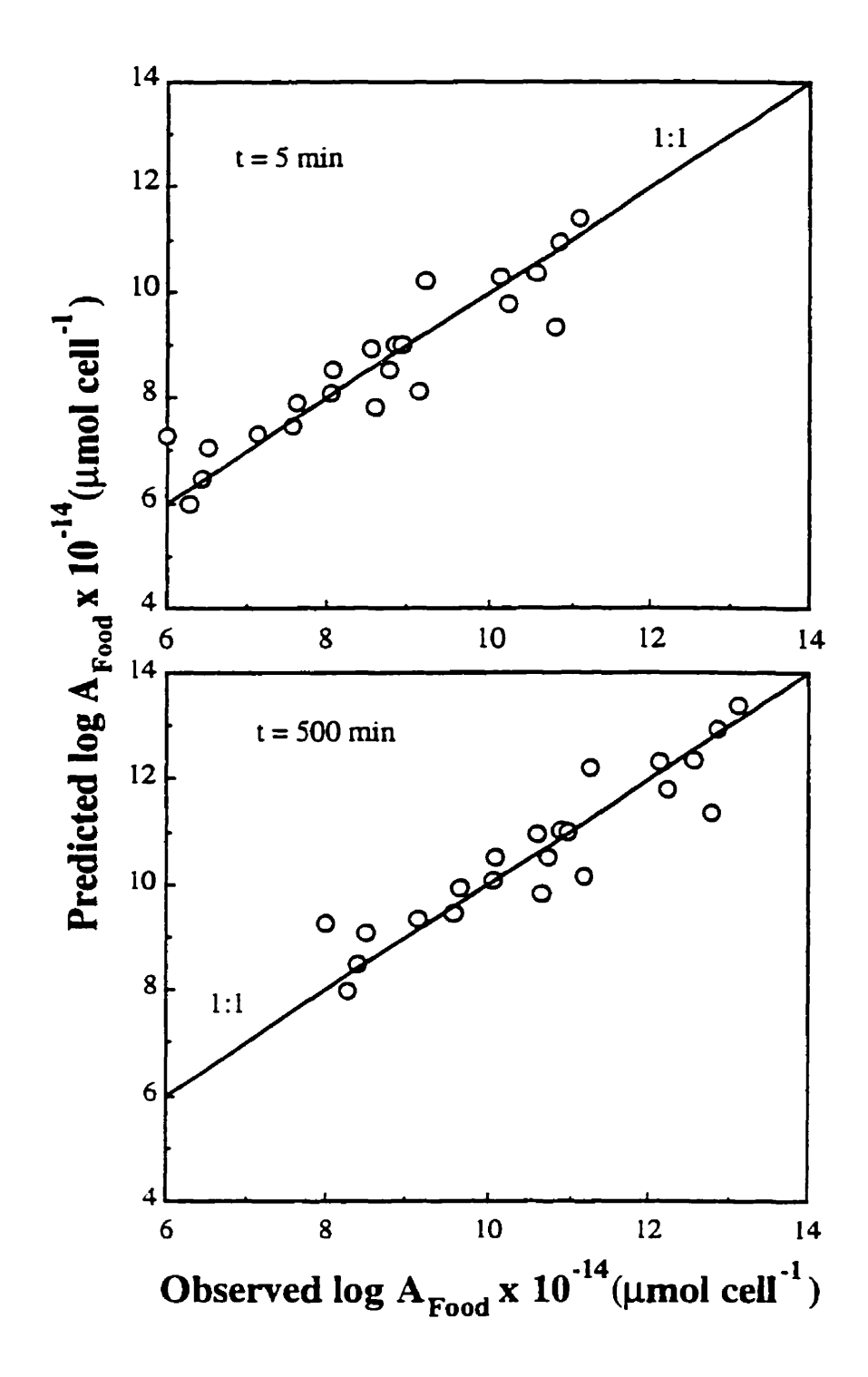


Fig. 8. Logarithms (base 10) of observed vs predicted accumulation from food (µmol ind⁻¹) of various organic chemicals in <u>D</u>. <u>magna</u>. The solid line represents the ideal fit.

have higher BCF values than <u>Chlorella</u>. However, for chemicals with high log P_{ow} , <u>Chlorella</u> have higher BCF values than <u>Daphnia</u>. This differences could be caused by the interaction between physiological and kinetic properties, such as the surface to volume ratio of the organisms and kinetics of association of chemicals to lipids. Gobas et al. (1986) argued that chemicals once taken up, have to pass through a series of membranes. Since most hydrophobic compounds are transported from the ambient water to the organism's lipid pool by passive diffusion, the relative surface area (S:V) can considerably influence the transfer rates. Because <u>Chlorella</u> has a much greater surface to volume ratio than <u>Daphnia</u> (Fig. 9), <u>Chlorella</u> may have relatively high diffusion rate and membrane permeability for highly lipophilic chemicals.

The rate constants of uptake by <u>Chlorella</u> were larger than those of <u>Daphnia</u>, while those of elimination were similar for both species. These kinetic patterns suggest that <u>Chlorella</u> have higher bioconcentration potential than <u>Daphnia</u>. Our BCFs data indicated this tendency. Rice and Sikka (1973) also found an inverse relationship between BCFs and cell size in marine algae. It is apparent that this difference in BCF between <u>Chlorella</u> and <u>Daphnia</u> may represent a size effect.

All the flux rates of toxicants of <u>Daphnia</u> were higher than those of <u>Chlorella</u>. These flux patterns are consistent with expectations. Because <u>Daphnia</u> have much bigger body size than <u>Chlorella</u> (Fig. 9), and consequently bigger the compartment size, <u>Daphnia</u> should have high flux rates per

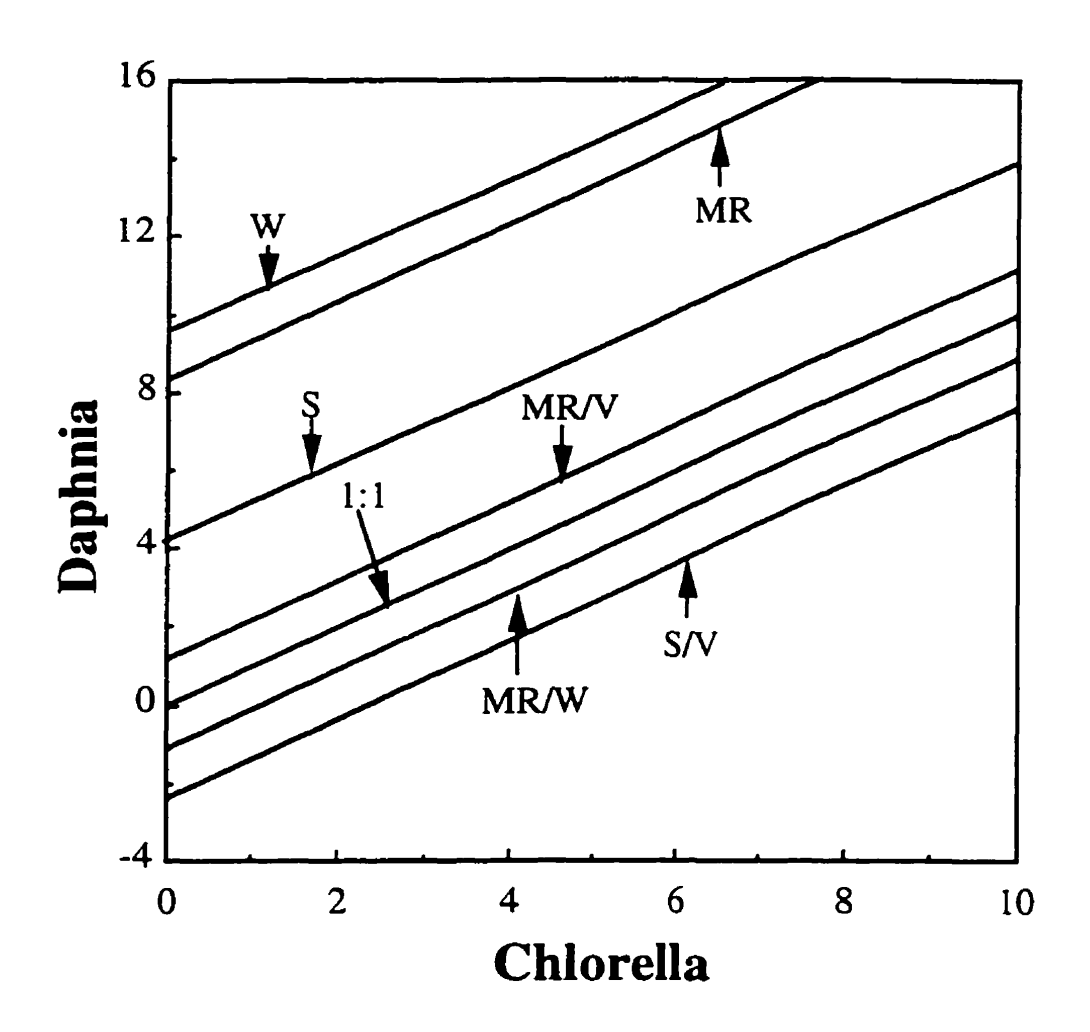


Fig. 9. Comparison of weight (W), surface area (S), surface area/volume ratio (S/V), metabolic rates (MR), metabolic rate/volume (MR/V), and metabolic rate/weight (MR/W) between <u>Chlorella</u> and <u>Daphnia</u>. The average cell volume of the <u>Chlorella</u> is 13.9 µm³ and the average length of the <u>Daphnia</u> is 3.0 mm.

individual (Peters 1983). This accordance indicates that our model predictions match those of general allometry. Whereas the dissimilar pattern of the intercompartmental exchanges between two species may indicate a flexibility of the fits of the data to the model, rather than underlying biological differences.

It is of interest to further examine the slopes of the QSPR equations for both species. K_{ow} had positive slopes between 0.20 and 0.98, and negative slopes between -0.92 and -0.26. Log S generally had negative slopes with values between -0.37 and -0.22, and no statistical difference were detected for most slopes. The slopes of other structural variables, BP, MP, MW and PA, were all close to 0.01 and varied slightly.

The close resemblance of the slopes in most QSPR models between alga and daphnid is somewhat surprising. The effect of structural configuration of the chemical molecules on the pharmacokinetic properties is similar for both biological species. The parallel slopes may indicate a uniform interaction mode between chemicals and biosystems. The close similarity of these QSPR models for two biological species provides a means of predicting the pharmacokinetic fluxes of a non-tested compound by using K_{ow} within the range of validity (K_{ow} less than 7) in the QSPR model.

Acknowledgments

The authors thank Drs. J. Kalff, J. Rasmussen, N. Price for their useful comments on the manuscript and Miss D. Klimuk for her able laboratory assistance. We thank the Natural Sciences and Engineering Research Council of Canada (NSERC) and Fonds pour la Formation de Chercheurs et l'Aide à la Recherche (FCAR) for their financial support. Y.H.W. was a recipient of an FCAR scholarship from the Québec government.

References

- APHA. 1989. Standard Methods for the Examination of Water and Waste Water, 17th ed. American Public Health Association: Washington.
- Banse, K. 1976. Rates of growth, respiration and photosynthesis of unicellular algae as related to cell size a review. J. Phycol. 12: 135-140.
- Belfroid, A., M. Sikkenk, W. Seinen, K. V. Gestel, and J. Hermens. 1994. The toxicokinetic behavior of chlorobenzenes in earthworm (Eisenia Andrei) experiments in soil. Environ. Toxicol. Chem. 13:93-99.
- Bruggeman, W. A., L. B. J. M. Martron, D. Kooiman, and O. Hutzinger. 1981.

 Accumulation and elimination kinetics of di-, tri- and tetra chlorobiphenyls by goldfish after dietary and aqueous exposure.

 Chemosphere 8: 811-832.
- Chu, K. C. 1979. The quantitative analysis of structure-activity relationships.

 In M. E. Wolff, Ed. The Basis of Medicinal Chemistry, 4th Ed. John Wiley, N.Y.
- Cockerham, L. G., and B. S. Shane. 1994. Basic Environmental Toxicology.

 CRC Press, Boca Raton, FL. 627 p.
- Connell, D. W. 1990. Bioaccumulation of Xenobiotic Compounds. CRC Press, Inc. Boca Raton, Fl. 219p.
- Dawson, T. J., and A. J. Hurlbert. 1970. Standard metabolism, body temperature, and surface areas of Australian marsupials. Am. J. Physiol.

- 218: 1233-1238.
- De Bruijn, J. L. M. Hermens. 1991. Uptake and elimination kinetics of organophosphorus pesticides in the guppy (<u>Poecilia reticulata</u>): correlation with the octanol/water partition coefficient. Environ. Toxicol. Chem. 10: 791-804.
- de Voogt, P., B. van Hattum, P. Leonards, J. C. Klamer, and H. Govers. 1991.

 Bioconcentration of polycyclic heteroaromatic hydrocarbons in the guppy

 (Poecilia reticulata). Aquat. Toxicol. 20: 169-194.
- de Wolf, W., W. Seinen, and J. L. M. Hermens. 1993. Biotransformation and toxicokinetics of trichloroanilines in fish in relation to their hydrophobicity. Arch. Environ. Contam. Toxicol. 25: 110-117.
- de Wolf, W., E. S. E. Yedema, W. Seinen, and J. L. M. Hermens. 1994.

 Bioconcentration kinetics of chlorinated anilines in guppy, <u>Poecilia</u>

 <u>reticulata</u>. Chemosphere 28: 159-167.
- Dixon, W. J. 1988. BMDP software manual. University of California Press, Berkeley, Calif.
- Eastmond, D. A., G. M. Booth, and M. L. Lee. 1984. Toxicity, accumulation and elimination of polycyclic aromatic sulphur heterocycles in <u>D. magna</u>.

 Arch. Environ. Contam. Toxicol. 13: 105-111.
- Evans, H. E. 1991. The influence of water column dissolved organic carbon on the uptake of 2,2',4,4',5,5'-hexachlorobiphenyl (PCB 153) by <u>Daphnia</u> magna. In R. Baker, ed., Organic substances and Sediments in Water,

- Vol. 3. Lewis, Chelsea, MI, pp 95-109.
- Evans, M. S., and P. F. Landrum. 1989. Toxicokinetics of DDE, benzo(a)pyrene, and 2,2',4,4',5,5'-hexachlorobiphenyl in <u>Pontoporeia hoyi</u> and <u>Mysis relicta</u>. J. Great Lakes Res. 15: 589-600.
- Gobas, F. A. P. C., K. E. Clark, W. Y. Shiu and D. Mackay. 1989.

 Bioconcentration of polybrominated benzenes and biphenyls and related super-hydrophobic chemicals in fish: role of bioavailability and elimination into the faeces. Environ. Toxicol. Chem. 8: 231-247.
- Gobas, F. A. P. C., W. Y. Shiu and D. Mackay. 1987. Factors determining partitioning of hydrophobic organic chemicals in aquatic organisms. In K. L. E. Kaiser, ed., QSAR in Environmental Toxicology II. D. Reidel Publishing Co., Dordrecht, Netherlands, pp. 107-123.
- Gobas, F. A. P. C., A. Opperhuizen, O. Hutzinger. (1986). Bioconcentration of hydrophobic chemicals in fish: relationship with membrane permeation. Environ. Toxicol. Chem. 5: 637-646.
- Hawker, D. W., and D. W. Connell. 1986. Bioconcentration of lipophilic compounds by some aquatic organisms. Ecotoxicol. Environ. Saf. 11: 184-197.
- Hermens, J. L. 1986. Quantitative structure-activity relationships in aquatic toxicology. Pestic. Sci. 17:287-296.
- Konemann, H., and K. Van Leeuwen. 1980. Toxicokinetics in fish: accumulation and elimination of six chlorobenenes by guppies.

- Chemosphere 9: 3-19.
- Landrum, P. F. 1988. Toxicokinetics of organic xenobiotics in the amphipod,

 <u>Pontoporeia hovi</u>: role of physiological and environmental variables.

 Aquat. Toxicol. 12: 245-271.
- Lohner, T. W., and W. J. Collins. 1987. Determination of uptake rate constants for six organochlorines in midge larvae. Environ. Toxicol. Chem. 6: 137-146.
- Loonen, H., M. Tonkes, J. R. Parsons, H. A. J. Govers. 1994. Bioconcentration of polychlorinated dibenzo-p-dioxins and polychlorinated dibenzofurans in guppies after aqueous exposure to a complex PCDD/PCDF mixtures: relationship with molecular structure. Aquat. Toxicol. 30: 153-169.
- Neely, W., D. Branson, and G. Blau. 1974. Partition coefficient to measure bioconcentration potential of organic chemicals in fish. Environ. Sci. Technol. 8: 1113-1115.
- Nendza, M., and W. Klein. 1990. Comparative QSAR study on freshwater and estuarine toxicity. Aquat. Toxicol.17: 63-74.
- Niklas, K. J. 1994. Plant Allometry. The Scaling of Form and Process. The University of Chicago Press, Chicago, IL.
- Oliver, B. G., and A. J. Niimi. 1988. Trophodynamic analysis of polychlorinated biphenyl congeners and other chlorinated hydrocarbons in the Lake Ontario ecosystem. Environ. Sci. Technol. 22: 288-397.
- Pawlisz, A. V., and R. H. Peters. 1993. A radioactive tracer technique for the

- study of lethal body burdens of narcotic organic chemicals in <u>Daphnia</u> magna. Environ. Sci. Technol. 27: 2795-2800.
- Peters, R. H. 1983. Ecological Implications of Body Size. Cambridge University Press, Cambridge.
- Peters, R. H. 1984. Methods for the study of feeding, filtering and assimilation by zooplankton, p. 336-412. In J. A. Downing and F. H. Rigler [ed.] A manual on methods for the assessment of secondary productivity in fresh waters. IBP Handbook No. 17. Blackwell Scientific Publications Ltd., Oxford.
- Peters, R. H. 1987. <u>Daphnia</u> culture. In R. H. Peters and R. de Bernardi (ed).

 Daphnia. Mem. Ital. Idrobiol. 45: 483-495.
- Rhead, M. M., and J. M. Perkins. 1984. An evaluation of the relative importance of food and water as sources of <u>p,p</u>'-DDT to the goldfish, <u>Carassius auratus</u> (L.). Water Res. 18: 719-725.
- Rice, C. P., and H. C. Sikka. 1973. Uptake and metabolism of DDT by six species of marine algae. J. Agr. Food Chem. 21: 148-152.
- Robinson, W. R., R. H. Peters, and J. Zimmerman. 1983. The effects of body size and temperature on metabolic rate of organisms. Can. J. Zool. 61: 281-288.
- Sanders, H. O., and J. H. Chandler. 1972. Biological magnification of a polychlorinated biphenyl (Aroclor 1254) from water by aquatic invertebrates. Bull. Environ. Contam. Toxicol. 7: 257-xxx.

- SAS Institute Inc. 1983. SAS/STAT user's guide. Release 6.03 edition. SAS Institute Inc., Cary, N. C.
- Smith, A. D., A. Bharath, C. Mallard, D. Orr, L. S. McCarty, and G. W. Ozburn. 1990. Bioconcentration kinetics of some chlorinated benzenes and chlorinated phenols in American flagfish, <u>Jordanella floridae</u> (Goode and Bean). Chemosphere 20: 379-386.
- Southworth, G. R., B. R. Parkhurst, and J. J. Beauchamp. 1979. Accumulation of acridine from water, food, and sediment by the fathhead minnow, Pimephales promelas. Water, Air, Siol, Pollut. 12: 331-341.
- Stange, K, and D. L. Swackhamer. 1994. Factors affecting phytoplankton species-specific differences in accumulation of 40 polychlorinated biphenyls (PCBs). Environ. Toxicol. Chem. 11: 1849-1860.
- Thybaud, E., and T. Caquet. 1991. Uptake and elimination of lindane by

 Lymnaea palustris (Mollusca: Gastropoda): a pharmacokinetic approach.

 Ecotoxicol. Environ. Saf. 21: 365-376.
- Wen, Y. H., and R. H. Peters. 1996. Quantitative structure-pharmacokinetic relationships of organic toxicant fluxes by <u>Chlorella pyrenoidosa</u> (submitted).

CHAPTER V

General Conclusions

The primary goal of this thesis was to construct general models of pollutant fluxes by limnoplankton, which incorporated characteristics of the organism and the structure of the chemical. I used the two-compartmental pharmacokinetics as the basic model configuration, and body size or chemical structural properties as a descriptor to quantify the pollutant uptake, depuration and intercompartmental exchanges. The pollutants modelled were phosphorus (P) and 22 hazardous organic chemicals.

Current interests in pharmacokinetic compartment models have arisen because of a growing need to predict the time-course of pollutant concentrations in specific pools of interest, and because these models provide a basis for comparison of kinetic data between species. A compartment model defines an organism in terms of its kinetics and physiology, and can be parameterized by predictive descriptors. This leads to improved understanding of the uptake and release of pollutants and allows for prediction from some descriptors. I have demonstrated the utilities of these models by developing a series of equations which predict, as a function of time, the concentrations of the test pollutant in the algal cell or animal body. When these equations are combined with a basic understanding of the biochemical mechanisms responsible for toxicity, they can be employed to predict the fluxes and burdens of organic contaminants, especially the immediate fate of contaminants after a spill or below an outflow, and direct further research with other related chemicals once the models are fairly well validated with other representative

pollutants.

The use of any model involves the acceptance of some untested hypothesis. The reliability of any model depends on the degree to which that model simulates the systems being modeled, as well as the quantity and quality of the experimental data collected to determine the kinetic parameters of the model. Therefore we have to bring more philosophy into the pharmacokinetics. This need is being increasingly stated by both the scientific side, and also from those involved in the regulatory process. In chapter I, I reviewed some frequently used pharmacokinetic models, including compartment models, physiologically based pharmacokinetic models, non-compartment models, population based pharmacokinetic models, allometric pharmacokinetic models and quantitative structure-pharmacokinetic models. Such models involve a large number of physical, physicochemical, and biochemical parameters, each of which is subject to a certain degree of uncertainty and variability, depending on the precision and accuracy of the methods used for their determination. To provide a realistic description of pharmacokinetics of chemicals using a biologically motivated model, uncertainty, variability, and sensitivity analysis should be performed to increase the model's reliability. Chapter I was primarily concerned with the sensitivity analysis of pharmacokinetic parameters. The sensitivity analysis focuses on changes in model predictions due to changes in specific parameters, and consequently a measure of relative sensitivity can be used to identify those parameters contributing most to the

uncertainty in the prediction. The measure of relative sensitivity reflects the percentage change in the model output from its mean value. This information can be used to improve experimental designs in pharmacokinetic studies, and to achieve efficient resource allocation in risk assessment research.

Scaling is the process of utilizing structural and functional features of one system as a basis to predict those of another. Allometric pharmacokinetics signifies the interspecies scaling of the pharmacokinetic processes (i.e., uptake, distribution and clearance). This approach is empirical, primarily utilizing relationships between body size and physiological or pharmacokinetic parameters, and based on the assumption that pharmacokinetic parameters vary in a regular manner across species, and that pharmacokinetic processes can be described as a power function of the body size. After validation, these allometric pharmacokinetic models can be, to a limited extent, applied to interspecies scaling of pharmacokinetic parameters of the chemicals for untested species.

In Chapters II and III, I have developed allometric pharmacokinetic models to describe uptake and release of the prime limiting nutrient, phosphorus (P), by limnoplankton. For algae, the uptake of P was measured based on the disappearance of radioactivity of ³²P from filtrate over a sufficient period of time, while the release rate of P was estimated from the appearance of ³²P in label-free water washing over fully labelled cells. In zooplankton, the rate of uptake was calculated from rate constants based on the radioactivity of

animals feeding on a suspension of ³²P labelled yeast cells over a suitable period of time, whereas the release rate was estimated by the excretion of ³²P by animals which had been fed on radiolabelled yeast. The parameters of uptake and release were then estimated by compartmental analysis, and scaled to cell volume or animal size. The experimental results clearly demonstrated that all pharmacokinetic parameters of P varied predictably with cell volume across phytoplanktonic species or body mass across cladoceran species. The slopes of the rate constant for uptake and release did not significantly differ from theoretical expectation b = -0.25 for both algae and cladocerans. However, those of the rate constants for intercompartmental exchanges differed significantly between two group of organisms. For algae, the slopes of the allometric equations were not significantly different from -0.25, whereas for cladocerans, the slopes of two intercompartmental transfers were significantly less than expected value (-0.25). Therefore these rate constants decrease much faster with body size than the theoretical expectation. The flux rates showed the similar allometric scaling patterns to the rate constants.

Another powerful technique for the estimation of pharmacokinetic parameters is quantitative structure-pharmacokinetic relationship (QSPR). This approach relates the rates of pharmacokinetic fluxes to the structure or to physicochemical properties of xenobiotic compound and provide models for prediction and interpretation of the pharmacokinetic activity of the pollutants.

After the allometric pharmacokinetic models for P were established, I

further searched for possible dependence of pharmacokinetic parameters on chemical structure. I used 22 organic compounds of different structural characteristics (acetone, acetophenone, anthracene, atrazine, benzene, benzene hexachloride, benzoic acid, bromobenzene, n-butanol, chlorobenzene, chloroform, 4, 4'-DDE, 4, 4'-DDT, 1, 2-Dichlorobenzene, 1, 4-Dichlorobenzene, hexachlorobenzene, 2,2',4,4'5,5'-hexachlorobiphenyl, 2-methylnaphthalene, pentachlorobenzene, 1, 2, 3, 4-tritrachloroethane, toluene and 1, 2, 4trichlorobenzene) to study their uptake and release by Chlorella pyrenoidosa and Daphnia magna. Correlations were then sought among turnover coefficients or flux rates and a physical-chemical property (octanol/water partition coefficient (kow), aqueous solubility, connectivity index, parachor, molecular weight, melting point, density, boiling point). From these correlations, I established quantitative structure-pharmacokinetic relationships (QSPRs) capable of predicting the rates of uptake, excretion and intercompartmental exchange of contaminants by plankton.

Our experimental results demonstrated that among eight structural parameters examined, K_{ow} is always a good physicochemical descriptor of pharmacokinetic activities. Bioconcentration factors, rate constants and flux rates of uptake and intercompartmental exchanges from compartment 2 to compartment 1 were positively correlated with the octanol/water partition coefficient (K_{ow}) . However, those of elimination and intercompartmental transfers from compartment 1 to compartment 2 were negatively related to

 K_{ow} . Other physicochemical parameters, such as molecular weight (MW), parachor (PA), connectivity index (CI) and boiling point (BP) and melting point (MP) showed similar model actions as K_{ow} , while aqueous solubility (log S) behaved as the reverse of K_{ow} . Comparisons of pharmacokinetic parameters between <u>Daphnia</u> and <u>Chlorella</u> demonstrated that, although all kinetic parameters displayed similar patterns, the relative magnitudes of each corresponding parameters were significantly different between two species.

Our finding that K_{ow} is a good predictor of pharmacokinetic parameters has clear chemical meaning. As partitioning into the lipid phase (represented by octanol) increases, the uptake rate increases and elimination rate decreases, indicating that the partitioning of hydrophobic organic chemicals between the lipids of the organism and the dissolved aqueous phase is a thermodynamic process that is driven by the concentration or fugacity gradient between the phases. This thermodynamic lipid-partitioning mechanism has received wide support in experiments on a variety of biological and chemical species. Other structural parameters were also shown to be good predictors of pharmacokinetic parameters because the pharmacokinetic processes are controlled by a complex of factors which act singly or jointly. This is indicated by the significant collinearity between physicochemical properties of the chemicals and non-linear Kow-BCF relations. An understanding of the roles of these factors in the fate of the organic chemicals would be beneficial and would assist in determining the most accurate predictors for pharmacokinetic fluxes.

Further studies in the area of pharmacokinetic scaling and quantitative structure-pharmacokinetic relationships should concentrate on identifying and quantifying the mechanisms of uptake and depuration. To reach this goal, physiologically-based pharmacokinetic (PBPK) models are the promising tools which are increasingly used by toxicologists and risk assessors for the prediction of fluxes, distributions and toxicology of compounds from a combination of physical-chemical generalizations. These models should incorporate data on physiological parameters (especially using body size or body surface as a scaling factor), biochemical rate constants, and partition coefficients to describe the reactivity of specific chemicals within any tissue compartments of the organism and facilitate a "built-in" calculation of contaminant fluxes. These models can be further used for pharmacokinetic extrapolations from high dose to low dose and from any species.

APPENDIX I

Empirical Models of Phosphorus and

Nitrogen Excretion Rates by Zooplankton*

^{*} Published in Limnology and Oceanography (39: 1669-1680, 1994).

Acknowledgments

We thank Drs. J. Kalff, N. Price and J. Rasmussen for commenting on an early draft of this paper. We are also grateful to G. Cabana, G. Klein, R. Lehmann, A. Pawlisz, G. Scarborough, E. Tang, and K. Westcott for discussions and suggestions. Comments by Dr. S. Kilham and two anonymous referees improved the manuscript. Funds for this study was provided by the Natural Sciences and Engineering Research Council of Canada (NSERC) and the Ministry of Education of the Province of Québec (FCAR). This paper is a contribution to the Limnology Research Centre of McGill University (No. 350) and to the Groupe de Recherche Interuniversitaire en Limnologie et en Environnement Aquatique (G.R.I.L.).

Abstract

Although rates of P and N excretion by zooplankton have important implications for nutrient cycling in aquatic ecosystems, the literature offers few quantitative general models of these processes. In this paper, data collected from published studies were used to construct potentially predictive models of P and N excretion rates by zooplankton from freshwater and marine habitats. Excretion rates of N and P are strongly correlated ($r^2 = 0.88$) and consequently each predicts the other best. Respiration rate is also highly significantly correlated with P and N excretion rates and is the second best predictor. Although body size explained relatively less overall variability, the inclusion of temperature, container volume and experimental duration as independent variables in multiple regressions substantially improved the predictive power of models based on body size. The models can be corrected for taxonomic biases in zooplankton, but these were usually small. These models could provide both a basis for further empirical analysis of the determinants of zooplankton nutrient excretion and a means of predicting the fate of nutrients in aquatic ecosystems.

Introduction

Phosphorus (P) and nitrogen (N) excretion by zooplankton has attracted interest for decades since the magnitude of release rates is thought to influence the biomass and production of phytoplankton in both marine and freshwater ecosystems (Harris 1959; Hargrave and Geen 1968; Peters and Rigler 1973; Ganf and Blazka 1974; Kilham and Kilham 1984). Field and laboratory studies indicate that zooplankton regenerate enough P and N to provide up to 100% of the net daily nutrient requirements for phytoplankton production (Martin 1968; Ganf and Blazka 1974; James and Salonen 1991). The magnitude of this contribution depends on various environmental and biological factors, including temperature, salinity, light, oxygen concentration, crowding, food concentration and body size (Hargrave and Geen 1968; Peters and Rigler 1973; Ejsmont-Karabin 1984). As a consequence, literature estimates of excretion rates of P and N by zooplankton are quite variable (Peters 1972; 1987).

Although some quantitative models predicting zooplankton P and N excretion rates have been established (Peters and Rigler 1973; Ikeda et al. 1982; Ejsmont-Karabin 1984; Olsen and Østgaard 1985), most use only a single independent variable and leave considerable residual uncertainty. Peters (1987) compared some existing models for the rates of P and N excretion by marine and freshwater zooplankton, and found over ten fold differences among the allometric regression lines. This comparison shows that, although body size

has a large effect on release rates, other variables introduce considerable scatter. However, no general model quantifies the relative impacts of these potential variables.

The purpose of this study is to construct more comprehensive models which describe the rates of P and N excretion as general functions of several common factors for both marine and freshwater zooplankton, thus comparing the relative power of each candidate variable systematically over a wide range of literature values. The resulting models can be used both to predict P and N excretion rates by zooplankton under a variety of environmental conditions and to identify the most promising variables for further studies.

Methods

Data base - Data were collected from a survey of the Canadian Journal of Fisheries and Aquatic Sciences, Ecology, Freshwater Biology, Hydrobiologia, Journal of the Marine Biological Association of the United Kingdom, Limnology and Oceanography, Marine Biology and the Verhandlungen der Internationalen Vereinigung für Theoretische und Angewandte Limnologie published between 1960 and 1992. Simultaneous observations of zooplankton species, P and N excretion rates, respiration rate, animal body size, water temperature, container volume and experimental duration were taken from each reference. When possible, we used means reported in tables or text. If data were

presented as ranges, we took the midpoints, assuming the data points were normally distributed. Data expressed in different units were converted to those most frequently used in the literature by employing general conversion factors (Corner and Davies 1971; Peters and Downing 1984; Schneider 1990). Papers that reported only excretion rates have been omitted. In our data base, animal size (W) is expressed in μ g dry mass, P excretion rate (E_p) as μ g P/day, N excretion rate (E_N) in μ g N/day, oxygen uptake rate (R) in μ l O₂/day, temperature (T) in °Kelvin, container size (V) in ml and duration of experiment (D) in h. Taxonomic classification followed Omori and Ikeda (1984). A full listing of the data used in the analyses with their sources are available from the authors, or at a nominal charge from the Depository of Unpublished data, CISTI, National Research Council of Canada, Ottawa, Ont. K1A OS2, Canada.

Data analysis - Excretion rates, animal size and respiration rate were logtransformed (base 10) to meet the statistical requirements of normality and homoscedastic residual variance for least squares regressions. Simple and multiple least squares regression analyses fitted the data to the models:

$$log (E_P or E_N) = a + b log X$$

$$\log (E_p \text{ or } E_N) = a + b \log X + c T + d T^2 + f V + g D$$

where a-g are fitted constants, and X is one of the principal candidate predictors (W, R, E_P or E_N). Other variables are defined above. We did not transform temperature since the logarithms of biological rates are often effectively described as a linear function of temperature (Peters and Downing

1984). The quadratic term for temperature was introduced to allow the possibility of other nonlinearities in the response. Interaction terms between independent variables were not introduced into the models to minimize their complexity and fitting errors. For simple linear regression analysis, general linear models were used (SAS Institute Inc. 1983). To obtain multiple predictive equations, we used the SAS stepwise, forward, multiple linear regression program to delete variables with non-significant partial F-values (P > 0.05) in the basic model. The fit of the models was evaluated by the coefficient determination (r^2), the standard error of the estimate ($S_{y,x}$) and F-statistics (Zar 1984).

The effects of taxonomic affiliations of the zooplankton on the excretion relationships were examined as the mean residuals (predicted - observed P or N excretion rate) for each taxon. A null hypothesis that the residual mean does not significantly differ from zero was tested using a t-test.

Results

Description of the data base - The data set comprised 740 measurements of zooplankton excretion rates representing 23 marine and 5 freshwater studies (Table 1). These included wide ranges in taxonomy, representing 7 phyla (Cnidaria, Ctenophora, Mollusca, Annelida, Arthropoda, Chaetognatha and

Table 1. Mean \pm SD of log E_p (phosphorus excretion rates, µg/day), log E_N (nitrogen excretion rates, µg/day), log R (respiration rates, µl O₂/day), log W (body size, µg dry weight), T (water temperature, °K), V (container volume, ml) and D (duration of experiment, h) for the whole data set and for Crustacea. Sample sizes are in parentheses. CNI is Cnidaria; MOL, Mollusca; ART, Arthropoda; CHA, Chaetognatha; OTH, Others; BRA, Branchiopoda; COP, Copepoda, and MAL, Malacostraca.

	log E _P	log E _N	log R	log W	т	V_	D
All	-0.57±0.81	0.66±0.97	2.19±0.99	2.57±1.44	288.2±9.7	325.3±584.9	14.8±15.1
phyla	(462)	(574)	(257)	(740)	(740)	(740)	(740)
CNI	-0.12±0.06	1.70±0.77	2.97±0.65	3.97±0.73	296.9±7.2	653.1±516.1	5.1±5.6
	(2)	(51)	(49)	(51)	(51)	(51)	(51)
MOL	-0.17±0.99	0.97±0.97	2.25±0.93	3.92±0.88	279.5±10.9	493.9±558.9	11.5±10.3
	(6)	(23)	(20)	(23)	(23)	(23)	(23)
ART	-0.84±0.63	0.31±0.89	1.73±0.91	2.18±1.43	285.9±8.9	302.3±604.4	17.9±16.2
	(339)	(349)	(146)	(515)	(515)	(515)	(515)
СНА	0.001±0.58	0.87±0.61	1.89±0.51	2.78±0.52	296.5±3.4	103.1±144.9	7.3±9.4
	(92)	(106)	(2)	(106)	(106)	(106)	(106)
отн	0.84±1.20	1.57±0.89	2.86±0.60	4.25±1.17	289.6±11.5	654.8±770.9	10.1±9.1
	(23)	(45)	(40)	(45)	(45)	(45)	(45)
All Crust acea	-0.84±0.63 (339)	0.31±0.89 (349)	1.73±0.91 (146)	2.18±1.43 (515)	285.9±8.9 (515)	302.3±604.4 (515)	17.9±16.2 (515)
BRA	-0.98±0.48	-1.51±0.19	0.56±0.19	0.85±0.38	289.2±4.5	203.1±605.3	38.3±6.9
	(163)	(10)	(6)	(163)	(163)	(163)	(163)
СОР	-0.76±0.55	-0.03±0.54	1.21±0.58	2.26±0.78	287.4±9.6	272.8±521.9	6.5±7.0
	(145)	(232)	(69)	(235)	(235)	(235)	(235)
MAL	-0.48±1.23	1.20±0.77	2.34±0.78	3.85±1.50	278.3±7.81	499.8±709.0	12.5±11.0
	(31)	(107)	(71)	(117)	(117)	(117)	(117)

Data sources: Bamstedt (1983), Bamstedt and Tande (1985), Barlow and Bishop (1965), Beers (1964), Biggs (1977), Biggs (1982), Butler et al. 1969, Butler et al. (1970), Conover and Corner (1968), Ejsmont-Karabin (1984), Ganf and Blazka (1974), Harris (1959), Ikeda et al. 1982, Ikeda and Bruce (1986), Ikeda and Hing Fay (1981), Ikeda and Mitchell (1982), Ikeda and Skjodal (1989), Kremer (1977), Kremer et al. (1986), LaRow (1971), Mayzaud (1973), Mayzaud and Dallot (1973), Peters (1972), Quetin et al. (1980), Smith and Whitledge (1977), Szyper (1981), Taguchi and Ishii (1972) and Verity (1985).

Chordata), and in geography, from polar (Bamstedt and Tande 1985, Biggs 1982, Ikeda and Bruce 1986, Ikeda and Hing Fay 1981, Ikeda and Mitchell 1982, Ikeda and Skoldahl 1989), boreal and temperate waters (Bamstedt 1985, Butler et al. 1969, Butler et al. 1970, Conover and Corner 1968, Ejsmont-Karabin 1984, Ganf and Blazka 1974, Harris 1959, Kremer 1977, LaRow 1971, Mayzaud 1973, Mayzaud and Dallot 1973, Peters 1972, Taguchi and Ishii 1972), to subtropical and tropical waters (Biggs 1977, Ikeda et al. 1982, Kremer et al. 1986, Quetin et al. 1980, Szyper 1981, Verity 1985) and upwellings (Smith and Whitledge 1977).

As not all variables were available for all studies, the number of observations varied among variables (Table 1) and models (Tables 3-5). Nevertheless each variable covered a broad range. For the whole data set, experimental temperature varied from -1.8 to 30 °C; animal body size ranged over 7 orders of magnitude, and rates of P excretion, N excretion and respiration varied over 6, 4 and 6 orders of magnitude, respectively. Container volume varied between 4 and 4000 ml and incubation period from 1 to 40 h. For crustaceans, the magnitude of variation for each variable was similar to that of the total data set (Table 1).

The correlation matrix (Table 2) shows that metabolic rates (E_P , E_N and R) and body size were strongly intercorrelated. P excretion rate was also strongly correlated with temperature and the duration of the experiment, but not with container size. None of the experimental variables (T, V and D) was

Table 2. Correlation matrix of variables used in the analyses. $log E_p$ is phosphorus excretion rate; $log E_N$, nitrogen excretion rates; log W, dry body weight; log R, respiration rate; T, water temperature; V, container volume; D, duration of the experiment. NS represents p > 0.05; *: p < 0.05; and ***: p < 0.0001.

	log E _P	log E _N	log W	log R	Т	T^2	v	D
log E _p	1							
$\logE_N^{}$	0.94***	1						
log W	0.79***	0.85***	1					
log R	0.90***	0.94***	0.81***	1				
T	0.17*	0.08 NS	0.39***	0.38***	1			
T^2	0.15*	0.08 NS	0.38***	0.37***	1.00***	1		
v	0.05	0.07 NS	0.27***	0.26***	0.25***	0.24***	1	
	NS							
D	0.24***	0.01 NS	0.43***	0.25***	0.16***	0.17***	0.00NS	1

significantly correlated with N excretion rates, but all were correlated with both respiration rate and body size. Temperature was also significantly correlated with container volume and experiment duration, but container volume and experimental duration were not related. The predictor variables with high collinearity (r > 0.7) were not used in the same regression model.

Regression models - For the entire data set, N excretion rate was the best univariate correlate of P release rate, and P excretion rate was the strongest correlate of N excretion rate (Fig. 1). Each independent variable explained 88% of the variance (Tables 3). The average N:P atomic ratio was 16.5, with a range between 1.2 and 324 (n = 296). The second most powerful single correlate of zooplankton P and N excretion rates was respiration rate (Fig. 2), which accounted for 82 and 87% of the variances (Table 3), respectively. The mean O:N atomic ratio was 24.0 and varied from 0.6 to 235 (n = 255); the mean O:P atomic ratio was 213, and the ratio varied between 4.4 and 1481 (n = 76). Body size was also a significant correlate of P and N excretion rates (Fig. 3), accounting for 63 and 72% of their variances (Table 3), respectively.

Of the remaining variables, temperature and experiment duration were also significantly correlated to zooplankton P excretion rate in bivariate correlations (p < 0.01), but container size was not (p > 0.05). However, temperature and experimental duration explained little of the total variances (Table 2). None of these variables made significant contributions in bivariate regression models of N excretion (p > 0.05). Logarithmic transformation of

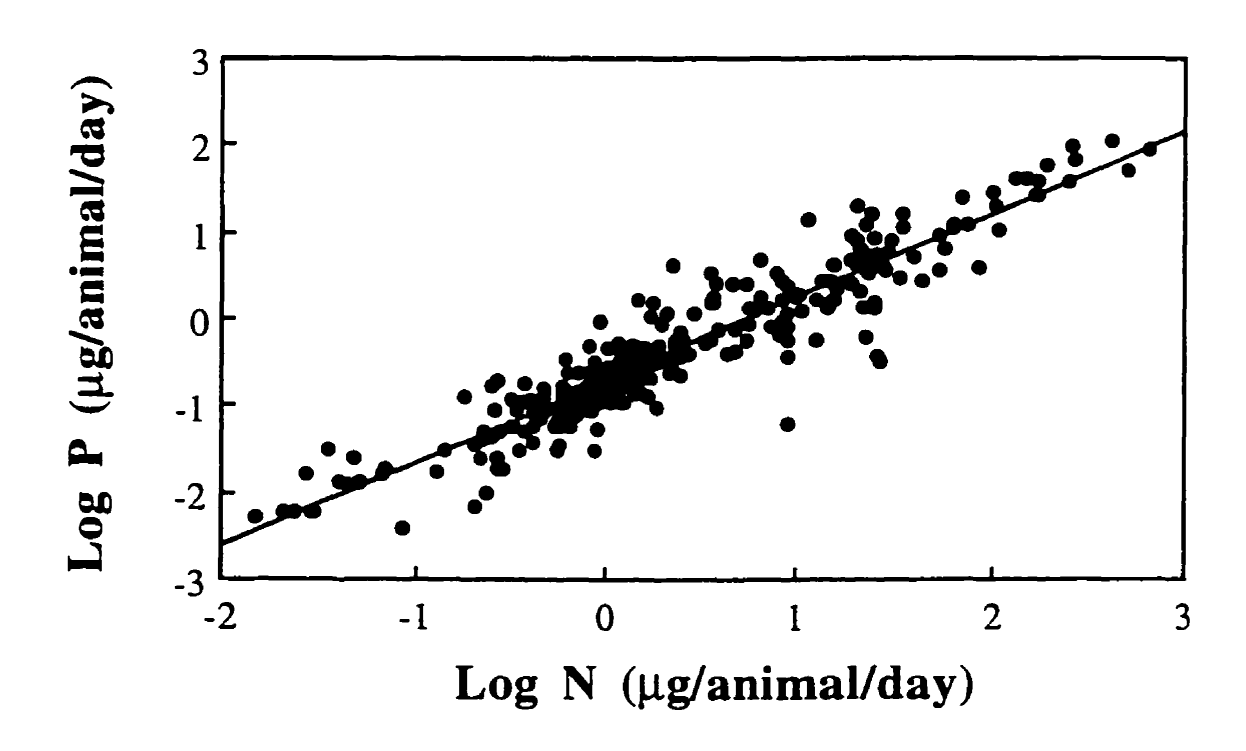


Fig. 1. The relationship between P excretion rates and N excretion rates in freshwater and marine zooplankton.

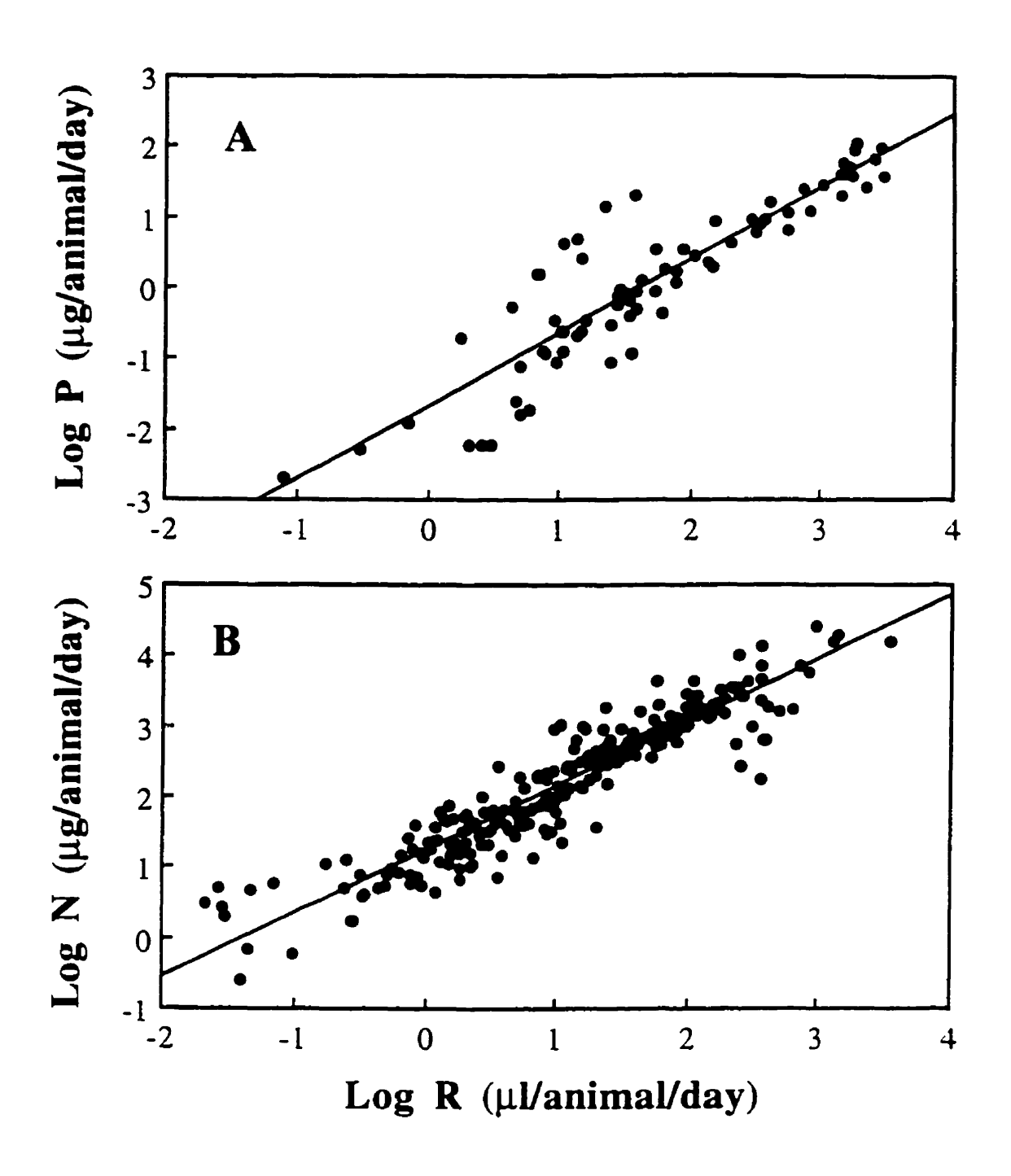


Fig. 2. The relationship between (A) P excretion rates or (B) N excretion rates and respiration rates in freshwater and marine zooplankton.

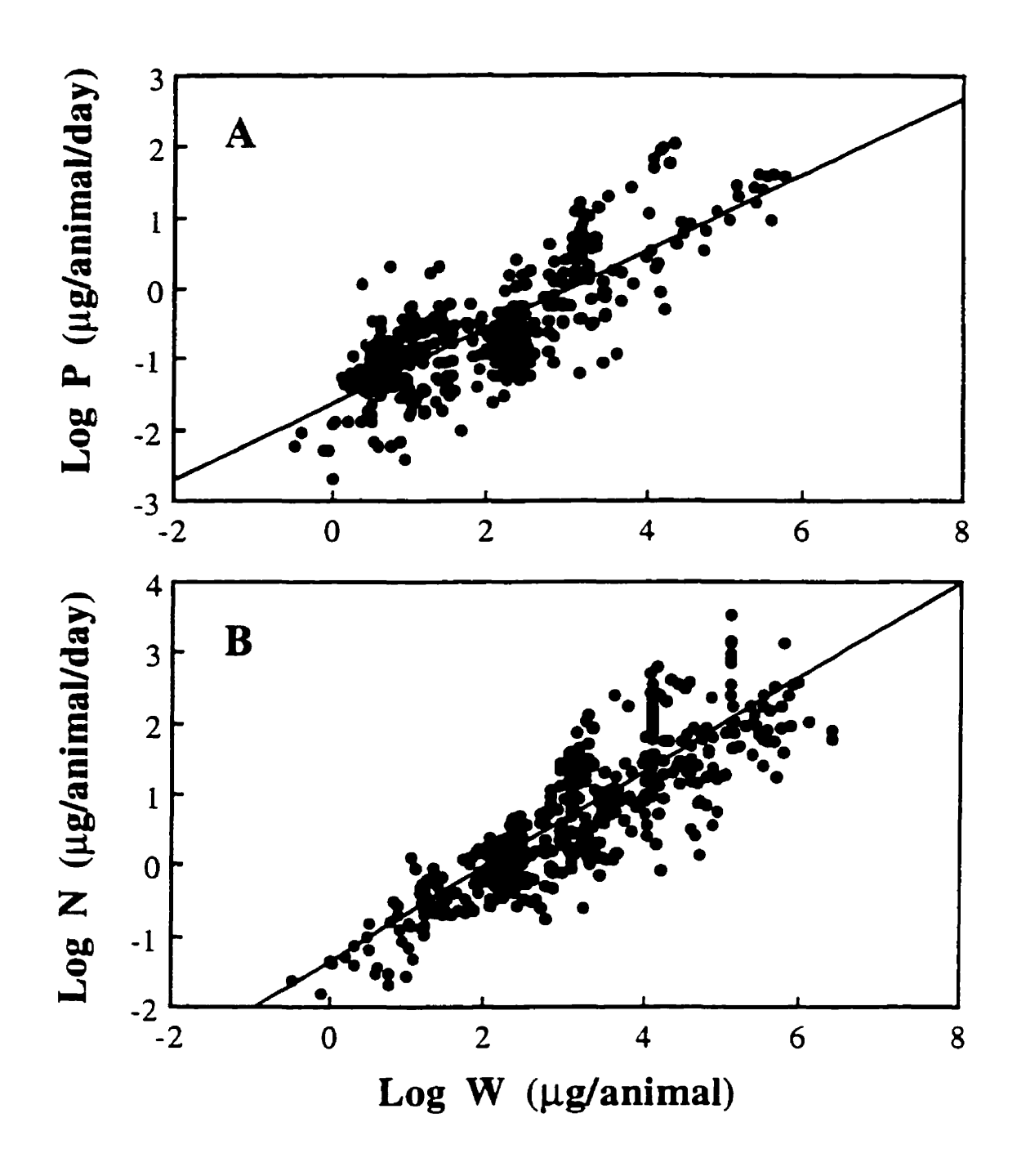


Fig. 3. The relationship between (A) P excretion rates or (B) N excretion rates and animal body size in freshwater and marine zooplankton.

Table 3. Simple regression equations relating zooplankton P or N excretion rates (E_P or E_N , $\mu g/day$) to excretion rate of another element, respiration rate (R, μl O₂/day) and body size (W, μg). N is the number of data points, $S_{y,x}$ is the root of the mean square error of the regression, and the standard deviation of the coefficient is given in parentheses. All regressions are highly significant (P < 0.001).

Models	N	S _{y,x}	r ²	F
P excretion				
$\log E_{\rm p} = -0.72(\pm 0.02) \\ + 0.96(\pm 0.02) \log E_{\rm N}$	296	0.31	0.88	2114
$\log E_{\rm p} = -1.69(\pm 0.12) \\ + 1.03(\pm 0.06) \log R$	76	0.51	0.82	330
$\log E_{\rm P} = -1.65(\pm 0.04) + 0.54(\pm 0.02) \log W$	462	0.49	0.63	787
N excretion				
$\log E_{N} = 0.71(\pm 0.02) + 0.92(\pm 0.02) \log E_{P}$	296	0.31	0.88	2114
$\log E_{N} = -1.07(\pm 0.06) + 0.97(\pm 0.02) \log R$	255	0.35	0.87	1747
$\log E_{N} = -1.38(\pm 0.06)$ + 0.67(\pm 0.02) $\log W$	574	0.51	0.72	1500

these variables did not improve their explanatory power.

In most cases, multiple regression models (Table 4) explained substantially more variance than the bivariate models. The most powerful multivariate models were based on metabolic rates (E_P, E_N and R) and explained similar proportions of the variances (88-90%). Body size-based models were less effective in predicting P and N excretion rates so relatively large fractions of variance remained unexplained in both cases. The addition of temperature and experimental duration as independent variables to the multiple regressions improved the predictive power of the models (71-84%).

Because much of the literature focuses on crustacean zooplankton, multiple regression models were also established for the class Crustacea (Table 5). These models generally explained similar proportions of the total variance in $\log E_P$ or E_N as those for the total data set. However, the slopes of the equations differ slightly from those in the whole data set, with the exception of the respiration-based model for crustacean P excretion. In all of these models, body size, respiration rate and excretion rate of other element explained most of the variations in P and N excretion rates (48-86%).

Effect of taxonomy - To estimate how much taxonomy affected P and N excretion rates, we first grouped zooplankton by phylum: Cnidaria (CNI), Mollusca (MOL), Arthropoda (ART), Chaetognatha (CHA) and Others (OTH). Other phyla were grouped together because preliminary multiple regressions using dummy variables (Gujarati 1988) showed that ctenophores, annelids and

Table 4. Multivariate regression equations for predicting total zooplankton P or N excretion rates (log E_p or log E_N , $\mu g/day$) from body size (W, μg), excretion rate of other element, respiration rate (R, μ l O_2/day), temperature (°K), container volume (V, ml) and experimental duration (D, h). N is the number of data points; Model r^2 is the cumulative square of the multiple correlation coefficient; F_p is partial F values.

	Models	N	S _{y,x}	Model r ²	F _p	p
	P excretion					
1	$\log E_{\mathbf{p}} = -8.77(\pm 0.91) \\ + 0.69(\pm 0.02) \log W \\ + 0.02 T \\ + 0.02 D$	462	0.44	0.63 0.67 0.71	93 983 55 109	<0.0001 <0.0001 <0.0001 <0.0001
2	$\log E_{\mathbf{P}} = 6.41(\pm 1.82) \\ + 1.05(\pm 0.04) \log R \\ - 0.03(\pm 0.01) T \\ - 0.04(\pm 0.01) D$	76	0.39	0.82 0.87 0.90	12 584 17 52	0.0008 <0.0001 <0.0001 <0.0001
3	$\begin{array}{l} \log E_{\rm P} = 0.93(\pm 0.28) \\ + 0.95(0.02) \log E_{\rm N} \\ - 0.00002 \ {\rm T}^2 \end{array}$	296	0.29	0.88 0.89	11 2319 35	0.0011 <0.0001 <0.0001
	N excretion					
4	log E _N = -9.36(±0.57) + 0.79(±0.01) log W + 0.03 T - 0.02 D	574	0.51	0.72 0.83 0.84	267 3005 198 42	<0.0001 <0.0001 <0.0001 <0.0001
5	$\log E_{N} = -1.06(\pm 0.06) + 0.99(\pm 0.02) \log R - 0.0001 V$	255	0.35	0.87 0.88	360 1719 7	<0.0001 <0.0001 0.0116
6	$\begin{array}{l} \log E_{N} = 55.57(\pm 19.85) \\ + 0.91(\pm 0.02) \log E_{P} \\ - 0.39(\pm 0.14) T \\ + 0.001 T^{2} \\ - 0.0001 V \end{array}$	296	0.29	0.88 0.89 0.89 0.89	8 2006 8 8 5	0.0055 <0.0001 0.0050 0.0041 0.0258

Table 5. As Table 4, but for crustacean zooplankton.

	Models	N	S _{y,x}	Model r ²	F _p	p
	P excretion					
1	$\log E_{p} = -5.28(\pm 1.19) + 0.61(\pm 0.03) \log W + 0.01 T + 0.02 D$	339	0.38	0.48 0.62 0.63	20 396 7 136	<0.0001 <0.0001 0.0077 <0.0001
2	$\log E_{\rm P} = 4.39(\pm 1.34) \\ + 1.12(\pm 0.08) \log R \\ - 0.00007 T^{2} \\ - 0.06(\pm 0.01) D$	50	0.37	0.69 0.86 0.89	11 214 16 71	0.0020 <0.0001 0.0003 <0.0001
3	$\begin{array}{l} \log E_{\rm P} = 2.29(\pm 0.55) \\ + 0.88(0.03) \log E_{\rm N} \\ - 0.00004 \ {\rm T}^2 \\ - 0.009(\pm 0.003) \ {\rm D} \end{array}$	173	0.26	0.86 0.87 0.88	18 656 31 7	<0.0001 <0.0001 <0.0001 0.01001
	N excretion					
4	$\log E_{N} = -3.47(\pm 0.43) + 0.74(\pm 0.02) \log W + 0.00002 T^{2} - 0.02(0.003) D$	349	0.32	0.83 0.86 0.87	65 1462 23 34	<0.0001 <0.0001 <0.0001 <0.0001
5	$\log E_{N} = -0.94(\pm 0.08) + 0.96(\pm 0.04) \log R - 0.008(\pm 0.003) D$	144	0.37	0.83 0.84	122 717 6	<0.0001 <0.0001 0.0155
6	$\log E_{N} = 0.62(\pm 0.03) + 0.86(\pm 0.03) \log E_{P} - 0.00005(\pm 0.00003) V$	173	0.26	0.86 0.86	470 9 9 5 5	<0.0001 <0.0001 0.0219

tunicates behaved similarly in the regressions for P and N excretion rates, and the data for these were few. We also compared the effects of taxonomy on P and N excretion rates across three subclasses of Crustacea: Malacostraca (MAL), Branchiopoda (BRA) and Copepoda (COP).

The variability of the multivariate model predictions for both phylum and class levels were assessed by examining the differences between observed and predicted P and N excretion rates. Most of the residual means (Tables 6 and 7) showed no significant departures from 0 (T test, p > 0.05), indicating the fitted models can be used to predict P and N excretion rates for these taxa. Significant differences were detected for some taxa (Table 6 and 7) and rates, especially among the crustacean regressions (Table 7). This lack of fit suggests some systematic error would result when the general equations are applied to these specific taxa. To avoid this bias, predictions for these groups can be adjusted by adding the mean residuals for the taxa to the predicted values from the general models.

Discussion

The main goal of this work is to establish empirical models to predict P and N excretion rates by zooplankton from some more easily measurable variables. Judging from the variance explained, the excretion rate of one element is the best predictor of the excretion rate of another. This result supports the

Table 6. Residual means \pm SD around the multivariate equations in Table 4 for total zooplankton. Each residual mean was tested for difference from 0 using a T-test. * p < 0.05; ** p < 0.01. Sample sizes are in parentheses. CIN is Cnidaria; MOL, Mollusca; ART, Arthropoda; CHA, Chaetognatha; OTH, Others.

	CNI	MOL	ART	CHA	ОТН
	· · · · · · · · · · · · · · · · · · ·	Phosphorus exci	etion		
Eq. 4.1.	-0.539±0.276	-0.483±0.448	-0.018±0.392	0.084±0.422	0.097±0.853
	(2)	(6)	(339)	(92)	(23)
Eq. 4.2.	-0.031	-0.036±0.277	-0.016±0.389	0.053	0.054±0.412
	(1)	(5)	(51)	(1)	(18)
Eq. 4.3.	0.221±0.036	-0.016±0.327	-0.022±0.266	0.012±0.337	0.101±0.278
	(2)	(6)	(173)	(92)	(23)
		Nitrogen excreti	on		
Eq. 4.4.	0.025±0.407	-0.095±0.429	-0.05 ^{**} ±0.336	0.195 ^{**} ±0.272	-0.049±0.699
	(51)	(23)	(349)	(106)	(45)
Eq. 4.5.	-0.061±0.238	-0.120±0.396	0.005±0.370	0.948±0.636	0.070±0.264
	(49)	(20)	(144)	(2)	(40)
Eq. 4.6.	-0.235°±0.021	-0.037±0.398 (6)	-0.021±0.263 (173)	0.036±0.324 (92)	0.043±0.229 (23)

Table 7. As Table 6, but for the multivariate equations in Table 5 for crustaceans. BRA is Branchiopoda; COP, Copepoda, and MAL, Malacostraca.

	BRA	COP	MAL					
	Phosphorus excretion							
Eq. 5.1.	0.022±0.357 (163)	-0.006±0.417 (145)	-0.086±0.325 (31)					
Eq. 5.2.	-0.336**±0.132	0.115±0.395 (30)	-0.096±0.191 (15)					
Eq. 5.3.	$0.188^{\circ}_{\pm}0.210$ (10)	-0.018±0.258 (142)	0.029 ± 0.249 (21)					
	Nitrogen	excretion						
Eq. 5.4.	-6.152±0.240 (10)	0.002±0.293 (232)	0.010±0.380 (107)					
Eq. 5.5.	-0.910 **±0.162 (6)	0.145 ^{**} ±0.325 (69)	-0.066±0.277 (69)					
Eq. 5.6.	-0.326 ^{**} ±0.183 (10)	0.002±0.242 (142)	0.142°±0.285 (21)					

contention that elemental excretions in zooplankton are quantitatively tightly linked, and the strong relationships with respiration suggest control by total metabolism. As a consequence, the P and N excretion rates are highly correlated (Fig. 1).

The mean N/P atomic ratio agrees with previous studies. In their seasonal study of total phosphorus and nitrogen excretion by Calanus finmarchicus and C. helgolandicus, Bulter et al. (1970) observed that N/P atomic ratio was 11.0 in spring and 14.6 in winter. Bamstedt (1985) found that the N/P ratios of zooplankton excreta in Swedish coastal waters ranged between 3.2 and 46.3. Omori and Ikeda (1984) compiled literature data and found that N/P ratios varied between 7.0 and 19. The much large variations around the ratio that we found may result from the feeding history and/or physical damage of the test zooplankton. Ikeda (1977) and Ikeda and Skjoldal (1989) demonstrated that phosphate excretion declined much faster than ammonia excretion in fooddepleted zooplankton; and Mullin et al. (1975) and Ikeda et al. (1982) recorded unusually high phosphate release rates from damaged zooplankton. Recently, the observations and models of Sterner (1990), Sterner et al. 1992 and Urabe (1993) have demonstrated that zooplankton taxonomy and N/P ratio of the diet significantly alter the excreted N/P values. Other factors, such as sex, animal size and experimental methodology, may also modify zooplankton P and N excretion rates (Omori and Ikeda 1984).

Recently, Kilham (1990) emphasized that nutrient stoichiometry should

receive much greater consideration in limnological studies and that the variation in N/P ratio of zooplankton excreta could be ecologically important. Sterner et al. (1990, 1992) indicate that the stoichiometric ratio of N to P determines the growth rate and community structure of phytoplankton. If the N/P ratio of zooplankton-regenerated nutrients is high, the phytoplankton should shift towards P limitation. In contrast, low N/P ratios could lead phytoplankton toward N limitation. These shifts in P and N limitation might consequently change phytoplankton species composition and succession (Smith 1983). This hypothesis of stoichiometric dependence has received field support (Elser et al. 1988, 1993; Moegenburg and Vanni 1991; Urabe 1993). Since our data were compiled from diverse zooplankton species, the observed range in excretory N/P ratio suggests that different herbivores may have substantial indirect effects on the community structure of the surrounding phytoplankton. However, because ratios compound errors in the components, we are not prepared to speculate that the very wide range in N/P observed is necessarily ecologically relevant. More conservative estimates of the likely range in N/P may be generated as the 68% or 95% confidence limits for individual values of P excretion predicted by N excretion (i.e. x± 1SD or x± 2·SD, respectively). We use this relation because the slope is very close to unity so that one set of values will apply to all zooplankton. These simple calculations suggest N/P ranges of 18 to 77 for the 68% limits and 9 to 155 for 95% limits. Such variations are already large enough to substantially alter N/P

supply ratios in communities where zooplankton excretions constitute a major source of nutrients.

Respiration-based models displayed predictive powers similar to those of the excretion-based models. The scatter of the data points in the respiration-excretion regression lines indicates variations in the ratios of oxygen consumed to nitrogen (O/N) or phosphorus excreted (O/P), perhaps because of difference in the composition and biological availability of the substrates (Mayzaud 1973; Mayzaud and Conover 1988; Omori and Ikeda 1984). These models could also have important predictive implications. Since oxygen consumption is an inclusive index of metabolism for aerobic organisms, and since models have been established to predict respiration rates for many planktonic taxa (Peters 1983) and size classes (Ahrens and Peters 1981), our models can be combined with these relations to estimate total nutrient flux of aquatic communities, or their components.

Although models based on body size provide less predictive power than those based on excretion and respiration, they still explain a substantial portion of the total variance. As expected, the slopes of the P and N excretion-body size regressions in this study are close to 0.75 and are similar therefore to values for other metabolic relations in the literature (Peters 1983, Peters 1987, Peters and Rigler 1973, Ejsmont-Karabin 1984). These models may find application when flux rates (excretion and respiration) are not available. Because size can be estimated from preserved samples and applied to size

spectra, the allometric models compensate for weaker prediction by greater facility of use.

We caution against extending these regressions to microplankton, like rotifers, ciliates, flagellates or bacteria. Banse (1982) showed that rates of respiration and production of tiny metazoans are lower than expected and the lower performances of unicells (relative to metazoans of similar size) have been recognized for many decades (Hemmingsen 1960; Zeuthen 1947). If these regressions for mesozooplankton and macrozooplankton are to be extrapolated to microplankton, the respiration-based equations are likely the most conservative choice. However, even that choice requires extrapolations.

The effect of temperature on the zooplankton excretion rates in the body size relations is close to expectation. Temperature strongly affects the rates of zooplankton excretion (Hargrave and Geen 1968; Peters and Rigler 1973; Ejsmont-Karabin 1984; Ikeda 1985). The values of Q_{10} obtained in the literature usually range from 1 to 2.59 for P excretion rates and 0.87-2.74 for N excretion rates (Ejsmont-Karabin 1984). The Q_{10} 's in this survey were 1.6 for Ep and 2.0 for E_N . No meaningful Q_{10} can be calculated for equations using fluxes as predictors because much of the effect of temperature operates through the flux used as an independent variable.

In regressions based on fluxes, the coefficients of temperature (T), experimental duration (D) and container volume (V) reflect differential impacts of these factors on the predicted and predictor fluxes. For example, the

negative coefficients of T and D in Equation 4.2 imply that T and D affect E_P less than is R; and Equation 4.3 suggests that E_P is less affected by T than is E_N . These minor effects could reflect different sensitivities of these processes or of some confounding artifact. For example, if bacterial growth reduces apparent P release (Peters and Rigler 1973), then the greater insensitivity of E_P to T and D may reflect more bacterial uptake of excreted P when temperature is high or experiments are long.

Few studies address taxonomic differences in excretion rate. Jawed (1973) and Ikeda (1974) demonstrated that the mass-specific N excretion rates of gelatinous zooplankton (mainly cnidarians, ctenophores and salps) were about one order of magnitude lower than those of non-gelatinous zooplankton (mainly crustaceans) of the same size. This difference was confirmed by Schneider (1990), who compiled about 560 literature data on dry weight-specific ammonia excretion rates and found that in gelatinous zooplankton, 91% of the data were below 100 μmol NH₄-N/g/d, and 75% were below 50 μmol NH₄-N/g/d. In contrast, only a few data for non-gelatinous zooplankton were below 100 μmol NH₄-N/g/d, and none lower than 50 μmol NH₄-N/g/d. In this study, we found that the N excretion rates of arthropods were slightly, but significantly less than the average response expected from size (Table 6). Residuals around the size-based N excretion regressions for Chaetognatha were significantly positive. No significant taxonomic differences were identified among P excretion rates.

Our models also demonstrated significant taxonomic differences in the

rates P and N excretion by Crustacea (Table 7). Copepods usually fit the crustacean model predictions of excretion rate reasonably well, but they release more nitrogen per unit of respiration. In contrast, branchiopods (mainly cladocerans) tend to excrete more P per unit of N excreted, but less per unit of respiration. Branchiopods also tend to excrete less N per unit of P excreted or O₂ respired. This implies that Branchiopoda should release excreta with low N/P ratios; this should reduce P limitation and intensify N limitation. Copepod excreta will be higher in N/P and so intensify P limitation and reduce N limitation. These patterns do not support recent views on the relative quantities of P and N excreted by Cladocera and Copepoda in lakes. In their experimental and field studies, Elser et al. (1988) associated copepoddominated communities with N limitation, whereas cladoceran domination led to P limitation. Sterner et al. (1992) proposed a homeostatic hypothesis to account for this phenomenon: herbivorous zooplankton with a high ratio of N/P in their tissue (i.e., Copepoda, Andersen and Hessen 1991; Urabe 1993) should resupply nutrients at a relatively low N/P ratio compared to those with low body N/P (i.e. Cladocera). We have no explanation for the difference between our results and those of other studies, but because our analyses are based on such a large sample of the literature and of living zooplankton, we are unwilling to accept that the issue is resolved.

Additional residual variability presumably reflects other potentially relevant independent variables. For example, animal density has long been

suspected to influence the rates of P and N excretion. Satomi and Pomerov (1965) and Nival et al. (1974) recorded increased rates of excretion under overcrowding, but Hargrave and Geen (1968) found decreased rates under similar conditions. Since there is no consistent effect of animal density on excretion, general conclusions are difficult to make. The quantity of food available during the experiment may also affect excretion rates, since nonfeeding zooplankton generally release less nutrient. Peters and Rigler (1973) found a 2.5 fold difference in P excretion rates between starved and fed Daphnia. Similarly, Hargrave and Geen (1968) recorded 1.4 to 2.4 fold differences in P excretion rates for marine zooplankton, and Ejsmont-Karabin (1984) reported a difference of 1.9 times in P excretion rates and 2.2 times in N excretion rates between fed and unfed freshwater zooplankton. Kremer (1982) reported that starved gelatinous zooplankton released much less ammonia than fed animals. Food quality may also be an important limiting factor for zooplankton excretion rates. Lehman and Naumoski (1985) found a large difference between rates of P excretion for D. pulex fed algae with high and low P content. Olsen et al. (1986) found a strong dependency on the P/C ratio of the food particles of the P release rate of <u>Daphnia</u>, and Urabe (1993) indicated that the P release by pond zooplankton was affected by the N/P ratio of the food. Since the majority of the data we analyzed represent non-feeding animals, our mean excretion estimates are likely somewhat low, and the variation due to these other factors is likely minimized, thus maximizing the

apparent predictive power of metabolic rates and body size.

In conclusion, this survey of published data has yielded empirical models which can be used to predict P and N excretion rates by zooplankton. On the basis of the results presented above, the excretion-based and respiration-based models provide the highest predictive potential, followed by the body size-based models. We hope that our models can find application when quantitative predictions of zooplankton nutrient excretion rates are needed. We have also demonstrated some complexities in predicting excretion and some difficulties involved in developing general excretion models. As they stand, the models presented here do not fully explain the variations in zooplankton P and N excretion rates, so there is still considerable scope for extension and refinement.

References

- Andersen, T., and D. O. Hessen. 1991. Carbon, nitrogen, and phosphorus content of freshwater zooplankton. Limnol. Oceanogr. 36: 807-814.
- Ahrens, M. A., and R. H. Peters. 1991. Plankton community respiration: relationships with size distribution and lake trophy. Hydrobiologia 224: 77-87.
- Banse, K. 1982. Mass scaled rates of respiration and intrinsic growth in very small invertebrates. Mar. Ecol. Prog. ser. 9: 281-297.
- Barlow, J. P., and J. W. Bishop. 1965. Phosphate regeneration by zooplankton in Cayuga Lake. Limnol. Oceanogr. (Supp.). 10: R15-R24.
- Bamstedt, U. 1985. Seasonal excretion rates of macrozooplankton from the Swedish west coast. Limnol. Oceanogr. 30: 607-617.
- glacialis in arctic waters of the Barents Sea. Mar. Biol. 87: 259-266.
- Beers, J. R. 1964. Ammonia and inorganic phosphorus excretion by the planktonic chaetognath, <u>Sagitta hispida</u> Conant. J. Cons. perm. int. Explor. Mer 29: 123-129.
- Biggs, D. C. 1977. Respiration and ammonium excretion by open ocean gelatinous zooplankton. Limnol. Oceanogr. 22: 108-117.
- of the southern ocean. I. Ross Sea, austral summer 1977-1978. Polar

- Biol. 1: 55-67.
- Butler, E. I., E. D. S. Corner, and S. M. Marshall. 1969. On the nutrition and metabolism of zooplankton. VI. Feeding efficiency of <u>Calanus</u> in terms of nitrogen and phosphorus. J. mar. biol. Ass. U.K. 49: 977-1001.
- metabolism of zooplankton. VII. Seasonal survey of nitrogen and phosphorus excretion by <u>Calanus</u> in the Clyde area. J. mar. biol. Ass. U.K. **50**: 525-560.
- Conover, R. J., and E. D. S. Corner. 1968. Respiration and nitrogen excretion by some marine zooplankton in relation to their life cycle. J. mar. biol. Ass. U.K. 48: 49-75.
- Corner, E. D. S., and A. C. Davies. 1971. Plankton as a factor in the nitrogen and phosphorus cycles in the sea. Adv. Mar. Biol. 9: 101-204.
- Ejsmont-Karabin, J. L. 1984. Phosphorus and nitrogen excretion by lake zooplankton (rotifers and crustaceans) in relationship to individual body weights of the animal, ambient temperature and presence or absence of food. Ekol. Polska. 32: 3-42.
- Elser, J. J., M. M. Elser, N. A. MacKay, and S. R. Carpenter. 1988.

 Zooplankton-mediated transitions between N- and P-limited algal
 growth. Limnol. Oceanogr. 33: 1-14.
- zone of Castle Lake, California. J. Plankton Res. 15: 977-992.

- Ganf, G., and P. Blazka. 1974. Oxygen uptake, ammonia and phosphate excretion by zooplankton of a shallow equatorial lake (Lake George, Uganda). Limnol. Oceanogr. 19: 313-324.
- Gujarati, D. N. 1988. Basic econometrics. 2nd Edition. McGraw-Hill Book Co.
- Hargrave, B. T., and G. H. Geen. 1968. Phosphorus excretion by zooplankton. Limnol. Oceanogr. 13: 332-343.
- Harris, E. 1959. The nitrogen cycle in Long Island Sound. Bull. Bingham Oceanogr. Coll. 17: 31-65.
- Hemmingsen, A. M. 1960. Energy metabolism as related to body size and respiratory surfaces, and its evolution. Rep. Steno. Mem. Hosp. (Copenh.) 9: 1-110.
- Ikeda, T. 1974. Nutritional ecology of marine zooplankton. Mem. Fac. Fish. Hokkaido Univ. 22: 1-97.
- experimental measurements to the ecology of marine zooplankton. IV.

 Changes in respiration and excretion rates of boreal zooplankton species maintained under fed and starved conditions. Mar. Biol. 41: 241-252.
- body mass and temperature. Mar. Biol. 85: 1-11.
- -----, and B. Bruce. 1986. Metabolic activity and elemental composition of krill and other zooplankton from Prydz Bay, Antarctica, during early summer (November-December). Mar. Biol. 92: 545-555.

- -----, and E. Hing Fay. 1981. Metabolic activity of zooplankton from the Antarctic ocean. Aust. J. Mar. Freshwat. Res. 32: 921-930.
- phosphate excretion by krill and other antarctic zooplankton in relation to body size and chemical composition. Mar. Biol. 71: 283-298.
- -----, and H. R. Skjoldal. 1989. Metabolism and elemental composition of zooplankton from the Barents Sea during early Arctic summer. Mar. Biol. 100: 173-183.
- -----, E. Hing Fay, S. A. Hutchinson, and G. M. Boto. 1982. Ammonia and inorganic phosphate excretion by zooplankton from inshore water of the Great Barrier Reef. I. Relationship between excretion rates and body size. Austr. J. Mar. Freshw. Res. 33: 55-70.
- James, M. R., and K. Salonen. 1991. Zooplankton-phytoplankton interactions and their importance in the phosphorus cycle of a polyhumic lake. Arch. Hydrobiol. 123: 37-51.
- Jawed, M. 1973. Ammonia excretion by zooplankton and its significance to primary productivity during summer. Mar. Biol. 23: 115-120.
- Kilham, S. S. 1990. Relationship of phytoplankton and nutrients to stoichiometric measures, p. 403-414. In M. M. Tilzer and C. Serruya [eds.], Large lakes: Ecological structure and function. Springer.
- determining phytoplankton community structure, p. 7-27. In D. G.

- Meyers and J. R. Strickler [eds.], Trophic interactions within aquatic ecosystems. Westview, Boulder, Colo.
- Kremer, P. 1977. Respiration and excretion by the ctenophore Mnemiopsis leidyi. Mar. Biol. 44: 43-50.
- -----. 1982. Effect of food availability on the metabolism of the ctenopore

 Mnemiopsis leidyi. Mar. Biol. 71:149-156.
- -----, M. F. Canino, and R. W. Gilmer. 1986. Metabolism of epipelagic tropical ctenophores. Mar. Biol. 90: 403-412.
- LaRow, E. J. 1971. Secondary production of predatory zooplankton. U.S. IBP EDFB Memo report #71-118. 44p.
- Lehman, J. T., and T. Naumoski. 1985. Content and turnover rates of phosphorus in <u>Daphnia pulex</u>: Effect of food quality. Hydrobiologia 128: 119-125.
- Martin, J. H. 1968. Phytoplankton-zooplankton relationships in Narragansett Bay. III. Seasonal changes in zooplankton excretion rates in relation to phytoplankton abundance. Limnol. Oceanogr. 13: 63-71.
- Mayzaud, P. 1973. Respiration and nitrogen excretion of zooplankton. II.

 Studies of the metabolic characteristics of the starved animals. Mar.

 Biol. 21: 19-28.
- -----, and S. Dallot. 1973. Respiration et excrétion azotée du zooplancton. I.

 Evaluation des niveaux métaboliques de quelques espèces de

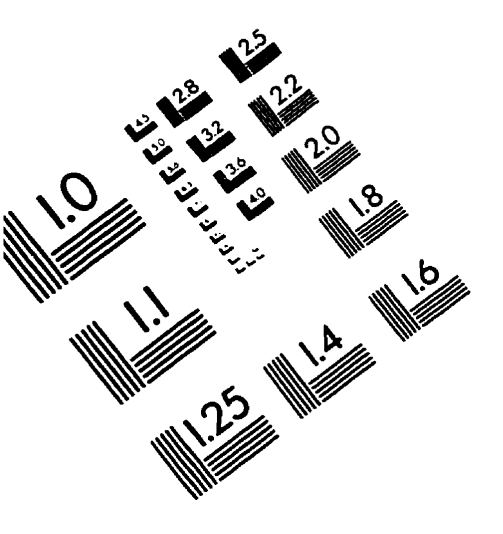
 Méditerranée occidentale. Mar. Biol. 19: 307-314.

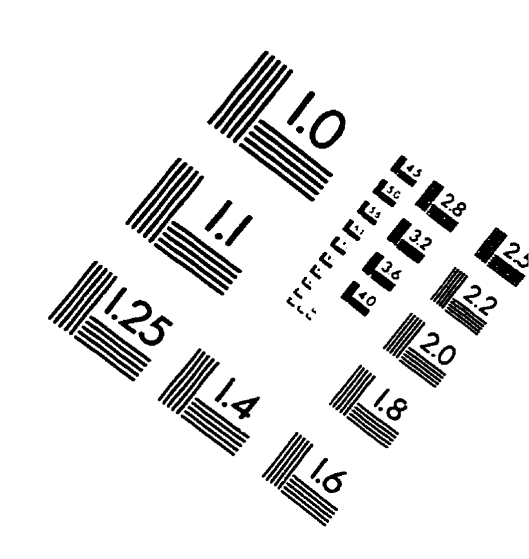
- zooplankton metabolism. Mar. Ecol. Prog. Ser. 45: 289-302.
- Mullin, M. M., M. J. Perry, E. H. Renger and P. M. Evans. 1975. Nutrient regeneration by oceanic zooplankton: a comparison of methods. Mar. Sci. Comm. 1: 1-13.
- Nival, P., G. Malara, R. Charra, I. Palazzoli, and S. Nival. 1974. Etude de la respiration et del'exrétion de quelques copépodes planktonique (Crustacea) dans la zone de remontée d'eau profonde des cotes Marocaines. J. Exp. Mar. Biol. Ecol. 15: 231-260.
- Olsen, Y., and K. Østgaad. 1985. Estimating release rates of phosphorus from zooplankton: Model and experimental verification. Limnol. Oceanogr. 30: 844-852.
- Olsen, Y., and others. 1986. Dependence of the rate of release of phosphorus by zooplankton on the P:C ratio in the food supply, as calculated by a recycling model. Limnol. Oceanogr. 31: 34-44.
- Omori, M., and T. Ikeda. 1984. Methods in marine zooplankton ecology. New York: John Wiley & Sons. 332 pp.
- Peters, R. H. 1972. Phosphorus release by zooplankton. Ph. D. thesis,
 University of Toronto. Toronto, Canada. 205 pp.
- ------ 1983. Ecological implications of body size. Cambridge University Press, Cambridge.
- -----. 1987. Metabolism in <u>Daphnia</u>. In Peters, R. H. and R. de Bernardi

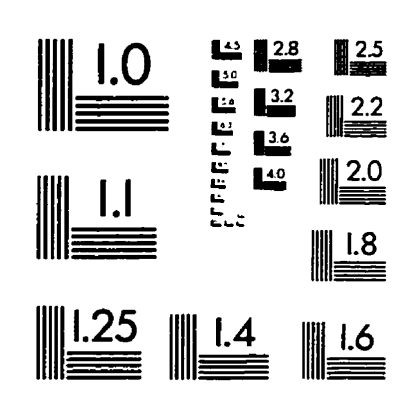
- (Eds.), Daphnia. Mem. Ist. Ital. Idrobiol. 45: 193-243.
- and feeding rates. Limnol. Oceanogr. 29: 763-784.
- Oceanogr. 18: 821-839.
- Quetin, L. B., R. M. Ross, and K. Uchio. 1980. Metabolic characteristics of midwater zooplankton: Ammonia excretion, O:N ratios, and the effect of starvation. Mar. Biol. 59: 201-209.
- SAS Institute Inc. 1983. SAS/STAT User's Guide. Release 6.03 edition, Cary, NC: SAS Institute.
- Satomi, M., and L. R. Pomeroy. 1965. Respiration and phosphorus excretion in some marine populations. Ecology 46:877-881.
- Schneider, G. 1990. A comparison of carbon based ammonia excretion rates between gelatinous and non-gelatinous zooplankton: implications and consequences. Mar. Biol. 106: 219-225.
- Smith, S. L., and T. E. Whitledge. 1977. The role of zooplankton in the regeneration of nitrogen in a coastal upwelling system off northwest Africa. Deep-Sea Res. 24: 49-56.
- Smith, V. H. 1983. Low nitrogen to phosphorus ratios favor dominance by bluegreen algae in lake phytoplankton. Science 211: 669-671.
- Sterner, R. W. 1990. The ratio of nitrogen to phosphorus resupplied by herbivores: zooplankton and the algal competitive arena. Am. Nat. 136:

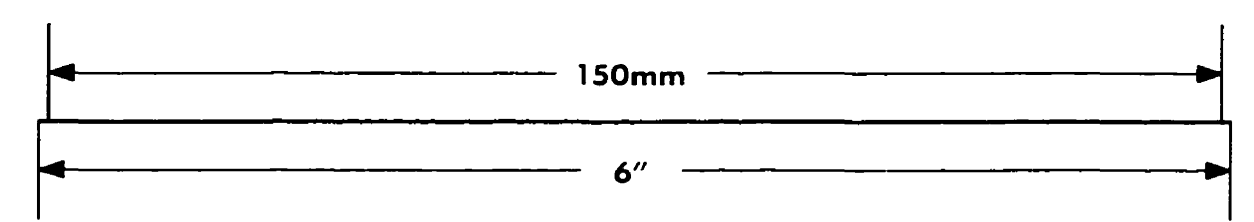
- among producers and consumers in food webs. Biogeochemistry 17: 49-67.
- Szyper, J. P. 1981. Short-term starvation effects on nitrogen and phosphorus excretion by the chaetognath <u>Sagitta enflata</u>. Estuar. Coat. Mar. Sci. 13: 691-700.
- Taguchi, S., and H. Hideki. 1972. Shipboard experiments on respiration, excretion, and grazing of <u>Calanus cristatus</u> and <u>C. plumchrus</u> (Copepoda) in the northern North Pacific. p. 419-431. In: Biological Oceanography of the northern North Pacific Ocean. Takenout, A. Y. (ed.), Idemitsu Shoten, Tokyo. 626p, 1972.
- Urabe, J. 1993. N and P cycling coupled by grazers' activities: food quality and nutrient release by zooplankton. Ecology 74: 2337-2350.
- Verity, P. G. 1985. Ammonia excretion rates of oceanic copepods and implications for estimates of primary production in the Sargasso sea. Biol. Oceanogr. 3: 249-283.
- Zar, J. H. 1984. Biostatistical analysis. Prentice-Hall, Englewood Cliffs, N. J. 718 pp.
- Zeuthen, E. 1947. Body size and metabolic rate in the animal kingdom with special regard to the marine microfauna. C. r. trav. lab. Carlsberg Ser. chim. 26: 17-161.

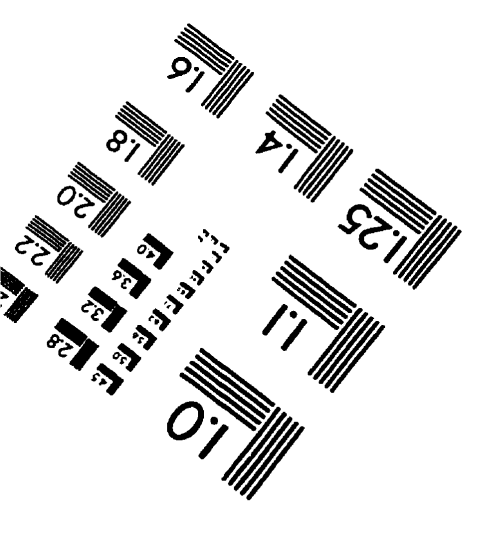
IMAGE EVALUATION TEST TARGET (QA-3)













© 1993, Applied Image, Inc., All Rights Reserved

